

**UNCLASSIFIED**

**AD\_ 4 5 8 2 5 6**

**DEFENSE DOCUMENTATION CENTER**

**FOR**

**SCIENTIFIC AND TECHNICAL INFORMATION**

**CAMERON STATION ALEXANDRIA, VIRGINIA**



**UNCLASSIFIED**

NOTICE: When government or other drawings, specifications or other data are used for any purpose other than in connection with a definitely related government procurement operation, the U. S. Government thereby incurs no responsibility, nor any obligation whatsoever; and the fact that the Government may have formulated, furnished, or in any way supplied the said drawings, specifications, or other data is not to be regarded by implication or otherwise as in any manner licensing the holder or any other person or corporation, or conveying any rights or permission to manufacture, use or sell any patented invention that may in any way be related thereto.

4 5 8 2 5 6

CATALOGED BY DDC

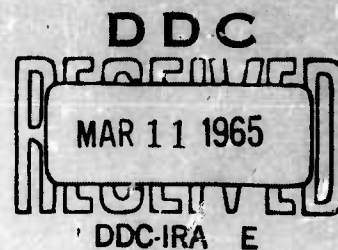
AS AD No. 458256

NOT AVAILABLE FOR REFERENCE USE  
AT DDC FIELD SERVICE COPY IS  
NOT AVAILABLE FOR FILING SALE

AGARDograph 83

# Manual on Aircraft Loads

JAMES TAYLOR  
F.R.Ae.S.



Pergamon Press



AGARDograph 83

*Manual on*  
**AIRCRAFT LOADS**



*Manual on*  
**AIRCRAFT LOADS**

by  
**JAMES TAYLOR**

*Published for and on behalf of*  
**ADVISORY GROUP FOR  
AERONAUTICAL RESEARCH AND DEVELOPMENT  
NORTH ATLANTIC TREATY ORGANIZATION**

by  
**PERGAMON PRESS**  
**OXFORD · LONDON · EDINBURGH · NEW YORK**  
**PARIS · FRANKFURT**

Pergamon Press Ltd., Headington Hill Hall, Oxford  
4 & 5 Fitzroy Square, London W.1  
Pergamon Press (Scotland) Ltd., 2 & 3 Teviot Place, Edinburgh 1  
Pergamon Press Inc., 122 East 55th St., New York 22, N.Y.  
Gauthier-Villars, 55 Quai des Grands-Augustins, Paris 6  
Pergamon Press GmbH, Kaiserstrasse 75, Frankfurt-am-Main

Copyright © 1965  
Pergamon Press Ltd

First edition 1965

Library of Congress Catalog Card No. 64-24959

PRINTED IN GREAT BRITAIN AT  
THE PITMAN PRESS, BATH

## PREFACE

THE preparation of this Manual was only possible through the co-operation of all the members of the Structures and Materials Panel of the Advisory Group for Aeronautical Research and Development of the North Atlantic Treaty Organization. I would like specially to thank Mr. R. V. Rhode, the Chairman, and Mr. A. van der Neut, the Vice-Chairman, for their guidance in the general planning of the work. Through the kind offices of the panel members I was permitted to consult the specialists in the various fields in any of the countries of N.A.T.O.

My task was greatly simplified by being supplied with copies of many research reports. These included about 500 published papers from U.S.A. and 500 from U.K. and a considerable amount of data prior to publication.

I made valuable use of the network of specialists throughout N.A.T.O. by having the technical content of every chapter checked by specialists in at least two countries. I am most grateful to all of them, but the individuals are too numerous to mention by name.

The whole of the manuscript has been read by Mr. W. Barrois and I am most grateful to him for his valuable comments on the technical content of the Manual as a whole. I would also like to thank Mr. G. H. Cooper for reading the whole of the manuscript and giving valuable comments on the presentation of each chapter.

I would like to thank Mr. W. A. P. Fisher for considerable technical analysis of the basic data on manoeuvre loads, much of which analysis was on extensive unpublished information from the Royal Aircraft Establishment.

I would like also to thank Mrs. Olive M. Watts for the typing of the original text of this Manual. Throughout the undertaking I have admired greatly her phenomenal accuracy.

*Paris,*  
*March 1964*

J. TAYLOR

## CONTENTS

FOREWORD	ix
1. INTRODUCTION	1
2. ATMOSPHERIC ENVIRONMENT	7
3. GROUND ENVIRONMENT	43
4. MANOEUVRES—THEORETICAL ANALYSIS OF MOTION IN STILL AIR	57
5. MEASURED SYMMETRICAL MANOEUVRES	85
6. MEASURED ASYMMETRICAL MANOEUVRES AND MOVEMENTS OF THE CONTROL SURFACES	133
7. GROUND LOADS	149
8. TEMPERATURE AND AIRSPEED IN FLIGHT	171
9. THEORETICAL ANALYSIS OF TURBULENCE	189
10. AIRCRAFT LOADS IN ATMOSPHERIC TURBULENCE	203
11. BUFFETING TURBULENCE	243
12. NOISE TURBULENCE	261
13. DESIGN PHILOSOPHY	279
NOTATION	333
REFERENCES	343

## FOREWORD

RICHARD V. RHODE

ALTHOUGH aeronautical technology has been under development for well over a half century, a well-ordered treatise on those aspects of aircraft loads which form the subject matter of this Manual is now appearing for the first time. An adequate discussion of all the reasons why such a work has not appeared in the past would probably be extensive and fruitless. A few words may, however, appropriately be said about why it is appearing now.

If these few words were to be summarized in one, that word would be "AGARD". The Advisory Group on Aeronautical Research and Development of the North Atlantic Treaty Organization is, in one of its aspects, a unique mechanism through which information on aeronautical technology can be assembled in orderly form within the N.A.T.O. nations and published. Mere mechanisms cannot, however, feel need and are not instruments of action. The Structures and Materials Panel of AGARD is such an instrument and it is to be credited with taking the action that was required to produce this Manual.

Requirements other than the existence of a mechanism and the initiation of action had to be satisfied before publication could be accomplished. The availability of a suitable person to perform the work was, of course, the most important of these requirements. James Taylor was unquestionably a most suitable choice. The Royal Aircraft Establishment of the United Kingdom is to be thanked for its cooperation in permitting Mr. Taylor to accept this assignment, and the Panel is to be congratulated that his services could be obtained.

It is to be hoped that this book may fulfill the expectations of its author and of the Structures and Materials Panel of AGARD.

**CHAPTER 1**  
**INTRODUCTION**

**CONTENTS**

1.1 Overall presentation	3
1.2 Environment	3
1.3 Manoeuvre loads	5
1.4 Turbulence	6
1.5 Design philosophy	6

## CHAPTER 1

### INTRODUCTION

#### 1.1 OVERALL PRESENTATION

Every body continues in a state of rest or of uniform motion in a straight line, unless acted upon by an external force. An aircraft is no exception to this rule and the environment in which it finds itself is the source of these external forces. So an essential part of any study of aircraft loads must be a study of its environment, which consists of the prepared ground of the runways and their environs for the ground loading conditions and the atmosphere for the flight loading conditions. This is the logical starting point to describe aircraft loads.

An important aspect of the "body" described above in Newton's first law of motion is that it shall be the whole body, and in the present case this includes the engine and the whole of its fuel from the start of the operation. This is not a convenient form in which to make a study of the loads as the loads that are of interest are those that are experienced by the aircraft including only the fuel that remains in it at the time. The range of the present investigation is for speeds up to  $M = 2.5$  and fortunately this means that the loads due to the rate at which the mass of fuel is emitted are small compared with the other loads and can be ignored. The scope of the work is restricted further by representing the engine loads by a thrust of known magnitude and direction and ignoring the local loads from the engine except in so far as they are instrumental in initiating other loads such as jet noise.

The Manual consists essentially of four parts

- (i) Environment
- (ii) Manoeuvres
- (iii) Turbulence
- (iv) Design philosophy

The environment is described in the first two chapters, one on the atmosphere and one on the ground. There are five chapters on manoeuvres, starting with one on the theoretical analysis and followed by four on measured values. The part on turbulence is in four chapters and is done the same way, the first on the theoretical analysis and the other three on measured values. The last part is a long chapter on design philosophy and gives a theoretical analysis of the procedure to be used to give a relationship between safety and the static and fatigue loads that are given in the rest of the Manual.

#### 1.2 ENVIRONMENT

The study of the environment must be restricted to a study of those parameters that can have a significant influence on the loads themselves. This

## MANUAL ON AIRCRAFT LOADS

inevitably introduces an anomaly, for to know which parameters are significant one should have some understanding of the loads and to know the cause of the loads one should know the appropriate parameter in the environment. It is for this reason that the normal procedure of determining any environment is first to measure the resulting loads on the aircraft, and then to assume some idealized form for the environment and decide which parameters are significant. Finally, an attempt is made to measure these parameters of the environment, calculate the corresponding loads on the aircraft and compare them with the measured loads.

This procedure is best explained by an illustration from the particular case of the normal acceleration experienced by an aircraft meeting an isolated gust. The total load on the aircraft is its mass times the normal acceleration, so that all that need be known is the mass and the acceleration. Some form of correlation is assumed to define the gust. If the work is being done for the one aircraft only, the actual form of the correlation has no effect whatsoever on any of the deduced loads, provided only that the system is linear: in this case the acceleration is measured, from which a gust is deduced using the formula of the correlation. Later in the procedure, possibly after manipulation such as adding numbers of gusts, the same formula is used in reverse to give accelerations again. In this case it would not matter at all if the actual relative velocity of the air bore no relationship to the one used in the calculation. If the measurements on one aircraft are to be used on another aircraft, errors will be introduced if the form used for the correlation is different for the two aircraft, but here again any parameter that is identical for the two aircraft can be given any value and need bear no relationship to actuality.

The same argument can be applied to any measurements. If the tool used for the measurements happens to have similar characteristics to those of the group of aircraft types for which the information will be used, considerable errors can be tolerated in the functions that are used to transfer the measurements to the basic parameters of the environment. Conversely if absolute measurements are made of the environment, great accuracy is needed in the transfer functions.

The first chapter on environment describes the atmosphere. There is a wealth of information on loads due to atmospheric turbulence, and there are sufficient data on direct measurements of the turbulence itself for an estimate to be made of the absolute value of the turbulence that is sufficiently accurate for the past information to be used for aircraft of completely new forms with some degree of confidence. Other characteristics of the atmosphere, such as temperature, density and pressure, are given on a macroscopic scale, but their local variations, which in particular may affect the aerodynamic heating of the aircraft, are not known with much certainty either from meteorological or from aircraft measurements.

There is a second chapter on environment describing the ground. The ground conditions have been measured as aircraft loads and also as the actual configuration of the ground itself. A special feature of this study of the environment is that an attempt was made to obtain an estimate of the absolute value of the environment, in this case the runway roughness, without first having studied the resulting loads. The investigation was extensive and

## INTRODUCTION

the roughness of a large number of runways is known accurately. Knowledge of loads on aircraft is nevertheless seriously limited by the realization that there might be other important dimensions of the runway that have not been measured; in addition there are inaccuracies in the transfer functions and an inability to give either the runway roughness or the combination of it and the transfer functions in an idealized linear form with much accuracy. This aspect is discussed in a subsequent chapter on ground loads.

### 1.3 MANOEUVRE LOADS

After discussing environment there is a second group of five chapters on manoeuvres. The first chapter gives the basic equations of motion for a rigid aircraft flying in a uniform and still atmosphere. Calculations are made of the load distribution over the whole aircraft, especially concentrating on the wing and tailplane loads. After the theoretical analysis there are chapters describing measurements of manoeuvres. The first is on symmetrical manoeuvres. Extensive operational data on normal accelerations of the centre of gravity are analysed to predict the frequency of occurrence of different accelerations for different classes of aircraft. It also includes the frequency of occurrence of forward velocities and the velocities at which the peak normal accelerations occur. The information available on tail loads is somewhat scanty and has been omitted.

The amount of data from asymmetrical manoeuvres is very limited, but the phenomena is so important for aircraft, in which gyroscopic loads are significant, that a chapter is included.

Ground loads are of a different character from air loads as the aerodynamic characteristics are relatively much less important than the structural ones, due to the low speeds. The landing conditions are described as the attitude, linear velocity and angular velocity of the aircraft at touchdown as these are more generally applicable to other aircraft than the normal acceleration which depends on the undercarriage performance and on the flexibility of the particular structures. The taxiing and take-off loads have to be described as normal accelerations and in consequence apply only to aircraft of the same general characteristics as those used for the measurements. In theory the taxiing loads could be calculated from the runway profile described under the ground environment, but in practice it is not possible to give sufficient details either for the environment or for the transfer functions of the aircraft to transfer accurately the environment into loads. A check is given on the transfer functions for the C.G. normal accelerations of one aircraft and for the normal accelerations at several positions on another aircraft when taxiing along nearly horizontal runways. Fair agreement is achieved, but it would not be so good were the roughness less homogeneous nor where there are steps or appreciable change of slope.

The last chapter on manoeuvres is on Mach number and temperatures. There is little direct information on the temperatures of an aircraft in flight, but the extensive information on the frequency of occurrence of, and times spent at, different velocities allows an indirect estimate to be made. This approach does not show up variations in temperature due to changes in the ambient temperature over lengths of a few hundred feet. The information



## MANUAL ON AIRCRAFT LOADS

available on these local temperature changes suggests that the structural temperature changes would be negligible but the data are so small that there is no certainty that they were typical.

### 1.4 TURBULENCE

As with manoeuvres the first chapter on turbulence gives the theoretical analysis. The turbulence is described in terms of its scale and the relative distribution of turbulence energy at different wavelengths. The characteristics of turbulence are substantially the same for all scales provided the contribution to the energy at wavelengths below about 1 cm is small so that viscous dissipation effects on the distribution at these wavelengths can be ignored. There are three main forms of turbulence, atmospheric, buffeting and noise. The atmospheric turbulence has a scale of the order of 1000 ft, buffeting of the order 10 ft or 100 ft, and noise of the order of 10 ft. In all cases the contribution to the energy at wavelengths below 1 cm is small. Thus the main features of turbulence for the whole range of scale of interest to aircraft can be expressed by the same model.

There is a separate chapter on the measured turbulence for each of atmospheric, buffeting and noise turbulence. As far as possible the empirical formulae, given in the theoretical analysis, are used as a basis, attention is drawn to departures from the formulae and a discussion made on the influence on the aircraft loads. The amount of data on the atmospheric loads is enormous, but that on the other two forms small. That on buffeting is particularly small, but it is described tentatively. One form that is becoming of increasing importance is buffeting produced by the wake of another aircraft. This may occur at low altitudes near congested aerodromes or at high altitudes during refuelling.

### 1.5 DESIGN PHILOSOPHY

The final chapter is on design philosophy and safety. An attempt is made to form a general appreciation of the loads that an aircraft encounters. In order to make full use of data on loads it is essential to recognize the interrelation of loads, strength and safety. On safety the discussion is centred on the frequency of occurrence of certain loads and the frequency of occurrence of strengths of parts, and is not concerned with the safety standards that should be called for in design. Design requirements are not formulated as they are not appropriate to this Manual.

## CHAPTER 2

### ATMOSPHERIC ENVIRONMENT

#### CONTENTS

2.1 Introduction	9
2.2 Quasi-static properties of the atmosphere	10
2.3 Large-scale dynamic properties of the atmosphere	12
2.4 Turbulence of the atmosphere—overall motion	15
2.5 Turbulence of the atmosphere—local motion within the turbulence	21
2.5.1 Turbulence measured at fixed points	21
2.5.2 Turbulence measured directly on aircraft	29
2.5.3 Comparison of measurements at fixed points and on aircraft	35
2.6 General conclusions on the structure of atmospheric turbulence	37
References	41

## CHAPTER 2

### ATMOSPHERIC ENVIRONMENT

#### 2.1 INTRODUCTION

The environment in which the aircraft operates is the source of all the loads that are applied to it. The complete system of loads includes those that are generated by the aircraft, but most of these, such as jet noise, are appreciably influenced by the environment. This influence emphasizes the vital importance of the environment. The environment is easy to define; it is the atmosphere up to some prescribed height and the prepared ground from which aircraft operate. However, it is not sufficient to say that the environment is known and that all its properties are required, for even with modern computing aids the task would be quite prohibitive to transform all the properties into aircraft loads. The procedure for correlation of environment properties into aircraft loads is one that cannot be transferred from the human operator to the machine, and the most important part of this is to know precisely which properties need to be known and also in what form the information should be presented. It is therefore a vital policy to obtain a clear understanding of the loads, deduce an idealized model for the environment properties, and then determine the environment characteristics in this form. This feature must be kept constantly in mind whatever loads are being considered.

The environment will be described in two parts, first the atmosphere in this chapter and then the airfields in Chapter 3. As the Manual is primarily concerned with speeds up to a Mach No. of 2.5, it is reasonable to suppose that the operating heights will be less than 100,000 ft; at such speeds the aircraft will normally have airbreathing engines and 100,000 ft is probably a little high, but for simplicity of presentation the "round number" is taken.

The properties of the atmosphere that are of major interest in the study of aircraft loads are its pressure and temperature from which can be calculated its density, viscosity and the speed of sound in it. The average values of these on a seasonal and geographical basis need to be known for every duty performed by aircraft. For certain duties more detail is required. The performance in landings and take-offs at high airfields is seriously affected by the local temperature and density at the airfield. At higher speeds kinetic heating has greater importance and local variations in temperature have more serious effects.

The movements of the atmosphere on both a large-scale and a small-scale are important. The overall velocities at different heights have an important influence on fuel consumption particularly at low aircraft speeds. Gradual changes of these velocities in any direction have a negligible loading effect. When the changes become sufficiently rapid they produce gust loads on the aircraft. At all aircraft speeds the transverse gusts are important, the loads

# MANUAL ON AIRCRAFT LOADS

that ensue depend on the motion of the atmosphere relative to itself and also on its effect on the motion of the aircraft. This chapter describes the motion of the atmosphere and Chapter 10 examines the ensuing aircraft loads. Head-on gusts (i.e. change in air velocity in the line of flight) produce much smaller loads, which are almost invariably negligible, but they significantly change, due to kinetic heating, the temperature of the air in contact with the aircraft surface. In this respect the effect on the aircraft depends so much on its heating properties that the phenomena is discussed in Chapter 8 on aircraft temperatures.

## 2.2 QUASI-STATIC PROPERTIES OF THE ATMOSPHERE

The important physical properties of the atmosphere that are of interest to the flight of aircraft are pressure and temperature. From these and a

Table 2.1. Atmospheric Temperatures ( $^{\circ}\text{C}$ ) in the Northern Hemisphere. Data Extracted from McNaughtan (1958)

Height		Latitude									
Pressure in lb/in <sup>2</sup>	Equivalent height in 1000's of ft	70° N		50° N		30° N		20° N		0°	
Mean temperatures of days in January and standard deviation between days											
0-160	100	-77	13	-61	11	-53	6	-56	5½	-63	5½
0-404	80	-75	12	-61	10	-59	5½	-63	5½	-65	5½
1-040	60	-66	8	-58	6½	-66	5	-77	5	-76	5
1-682	50	-61	6	-54	6	-64	4½	-71	3½	-73	3
2-721	40	-60	6	-55	6	-55	5	-57	3½	-54	2½
4-365	30	-57	4½	-51	4½	-40	4½	-35	4	-31	1½
6-754	20	-39	5½	-30	6½	-19	4	-13	3	-6	1½
10-107	10	-24	7	-15	8	+ 1	4	+ 7	2½	+ 10	1½
Mean temperatures of days in July and standard deviation between days											
0-160	100	-37	3½	-37	3½	-38	5½	-43	5½	-63	5½
0-404	80	-41	3½	-47	3½	-51	5½	-55	5½	-61	5½
1-040	60	-43	3½	-51	3½	-65	5	-69	5	-67	5½
1-682	50	-45	3	-51	3½	-66	4½	-71	3½	-71	3
2-721	40	-47	4½	-50	5½	-54	4½	-56	3½	-54	2
4-365	30	-43	5	-38	5	-31	4½	-31	3	-32	2
6-754	20	-29	4½	-13	4½	- 9	3½	- 9	2½	- 7	1½
10-107	10	- 4	4	+ 3	4	+10	3½	+11	2½	+ 9	1½

# ATMOSPHERIC ENVIRONMENT

knowledge of the properties of air it is possible to deduce the density, viscosity and the speed of sound. It is common practice to give heights in terms of the pressure and in such cases the properties are first obtained in terms of pressure and the I.C.A.O. altitude pressure relationship used to give the equivalent height.

The British Meteorological Office have collected temperature data from a large number of stations in the northern hemisphere and McNaughtan (1958) quotes an analysis of the data. The temperatures vary considerably due to latitude and longitude; that due to latitude is more regular and it is better to divide the data into latitude bands. The temperatures that were measured are taken to be typical for the day of the measurement and the scatter is estimated for other days at about the same time of year; the scatter due to longitude is automatically included. Broadly the data may be split up into winter conditions (January) and summer conditions (July). The mean temperatures and the standard deviation about the mean are given by McNaughtan for January days and July days for latitudes from the equator to 70° North and for heights up to 100,000 ft. These are given in Table 2.1 and Fig. 2.1 and for easy reference the I.C.A.O. pressures for the equivalent heights are also given. It is suggested by McNaughtan (1958) and also by Wilkinson (1951) that the temperature distributions may be assumed to be Normal. It is assumed further by McNaughtan that the soundings were made in a random manner in each latitude band. With these assumptions it is possible to deduce the relative frequency of occurrence of any temperature at any height and latitude. Within the accuracy of the data it is probably adequate to assume that the year is split up into 6 months like the January values and 6 months like the July ones. This will result in slightly conservative estimates of the extreme temperatures.

The values of density, speed of sound, and viscosity can be calculated from the following equations with the numerical values as quoted by McNaughtan.

$$\text{Density} = P/R_0 T \quad (2.1)$$

$$\text{Speed of sound} = C_0 (T/T_0)^{1/2} \quad (2.2)$$

$$\text{Viscosity} = \mu_0 (T/T_0)^{3/2} \cdot (T_0 + S_0)/(T + S_0) \quad (2.3)$$

where  $P$  = pressure

$T$  = absolute temperature (°K)

$= 273.16 + \text{temperature in } ^\circ\text{C}$

$T_0 = 288.16 \text{ } ^\circ\text{K}$

$R_0 = 95.984 \text{ ft lb/lb } ^\circ\text{K}$

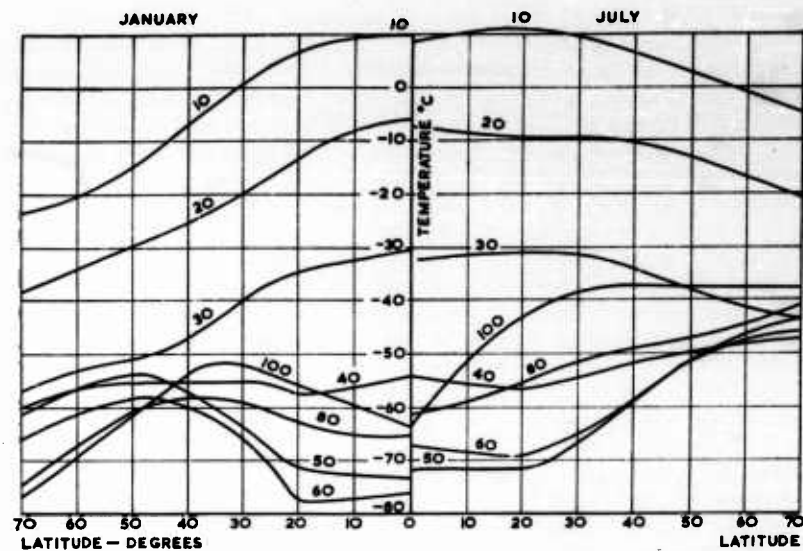
$C_0 = 1116.89 \text{ ft/sec}$

$\mu_0 = 3.719 \times 10^{-7} \text{ slugs/ft sec}$

$S_0 = 110.4$

All the information is from 10,000 ft to 100,000 ft. Below 10,000 ft the diurnal effects are large; also the local geographical conditions will have a large effect and generalized data are not very reliable. However, McNaughtan quotes maximum and minimum ground temperatures as given in

# MANUAL ON AIRCRAFT LOADS



MEAN TEMPERATURES °C AT ELEVATIONS QUOTED IN 1000'S OF FEET

HEIGHT IN 1000'S OF FEET	TABLE OF STANDARD DEVIATION BETWEEN DAYS.									
	JANUARY					JULY				
	LATITUDE					LATITUDE				
	70°	50°	30°	20°	0°	0°	20°	30°	50°	70°
100	13	11	6	5 1/2	5 1/2	5 1/2	5 1/2	5 1/2	3 1/2	3 1/2
80	12	10	5 1/2	5 1/2	5 1/2	5 1/2	5 1/2	5 1/2	3 1/2	3 1/2
60	8	6 1/2	5	5	5	5 1/2	5	5	3 1/2	3 1/2
50	6	6	4 1/2	3 1/2	3	3	3 1/2	4 1/2	3 1/2	3
40	6	6	5	3 1/2	2 1/2	2	3 1/2	4 1/2	5 1/2	4 1/2
30	4 1/2	4 1/2	4 1/2	4	1 1/2	2	3	4 1/2	5	5
20	5 1/2	6 1/2	4	3	1 1/2	1 1/2	2 1/2	3 1/2	4 1/2	4 1/2
10	7	8	4	2 1/2	1 1/2	1 1/2	2 1/2	3 1/2	4	4

Fig. 2.1. Atmospheric temperatures (°C) in northern hemisphere. Data extracted from McNaughtan (1958).

Table 2.2. These values are not comparable with those of Table 2.1 which are averages for each latitude whereas Table 2.2 is for specific places, chosen because of the severity of their ground temperatures.

## 2.3 LARGE-SCALE DYNAMIC PROPERTIES OF THE ATMOSPHERE

The temperature distribution that has been given for summer and winter conditions may be regarded as quasi-static, but it is associated with a large-scale wind system covering the whole of the earth's atmosphere. It consists mainly of warm air moving upwards and towards the poles and cold air moving downwards and towards the equator. On a macroscopic scale this system is predominantly stable and produces the trade winds and doldrums;

# ATMOSPHERIC ENVIRONMENT

*Table 2.2. Extremes of Ground Level Temperatures (°C). Data Extracted from McNaughtan (1958)*

<i>Place</i>	<i>Highest monthly mean of daily maxima</i>	<i>Place</i>	<i>Lowest monthly mean of daily minima</i>
Abadan	48	Barrow	-40
Baghdad	47	Chesterfield	-44
Basra	48	Churchill	-40
Biskra	45.6	Coppermine	-43
Dehibat	49	Dawson	-47
Gadames	50	Fort Good Hope	-48
Insalah	47.2	Fort Yukon	-50
Kayes	46.7	Hay River	-43.3
Lugh	47.2	Tanana	-44
Suakin	46.7		
Toggourt	47.2		

it has been known for centuries that these are remarkably constant for distances of hundreds of miles and heights up to 100 ft. The changes with height are more rapid and may be significant for vertical flight, but it is unlikely that aircraft with maximum speeds up to Mach No. 2.5 will ever fly at such rates of climb or descent that the changes of velocity with height will produce significant loads.

Advantage can be taken of the predominant winds in aircraft flight as in sailing ships but with two main differences. The flying height can be selected within limits to obtain optimum conditions, but the duration of the journey is far less than that of the ship and it is the average wind speed for that duration that is important. Thus the perturbations of the wind system achieve greater significance although allowance may be made for weather forecasts.

The temperature distribution, shown in Fig. 2.1, is roughly the same shape in the lower atmosphere (troposphere) at all latitudes and the temperature reduces with height up to a certain level (tropopause) which varies with latitude. The rate of drop of temperature with height (lapse rate) tends to be above 1.5°C to 2.5°C per 1000 ft. Provided the air is dry it is stable and only becomes neutrally stable at 3.0°C per 1000 ft. If the air is saturated with water vapour the air becomes less stable and the lapse rate for neutral stability reduces with temperature and can come down to 1.5°C per 1000 ft. Another way the stability can be reduced is by the air near the ground being heated, due to the sun's radiation on to the ground, and thus increasing the lapse rate locally. The major geographical features of the earth's surface influence the wind system and cause local instabilities to be set up in the atmosphere. The large-scale breakdown consists of cyclones, anti-cyclones, troughs and ridges that move over the earth's surface and change slightly in form in the process. Sheppard (1963) shows a typical "snapshot of the horizontal component of the large-scale turbulence at mid-troposphere; the major feature is a system of three long waves between the west of North

America and Central Russia". These meteorological data are used to predict wind speeds. Another type of large-scale disturbance that appreciably influences wind speeds is a jet stream. Such a system is of the order of half the size of cyclones and anticyclones.

Only in exhibition or demonstration flights is it possible to wait for favourable winds and the problem reduces to one of deciding whether a certain stage length can be attempted with a certain payload. There are so many variables involved and in such uncertain proportions that predictions of effective winds, other than by inference from the resultant aircraft behaviour, would be very inaccurate. All phases of aircraft flying are influenced by the human operators but perhaps none more than those which involve taking account of wind velocity. Here meteorologists and the aircrew are respectively the first and last in the chain, but between them are ground personnel of airlines, traffic control, customs, and the communications to the meteorologists, all of whom have an enormous effect in varying ways. It is evident that a knowledge of the wind velocities at any particular moment at a particular place can be of only little help in predicting all the velocities that will be met by the aircraft. The research involved in approaching the problem by first predicting the wind velocities at all possible relevant times, then predicting all the influences and finally determining the effective difference in wind velocity from that used in the flight plane would be enormous, quite apart from errors in prediction. The best approach is to do the research directly on the aircraft operations.

The effective stage lengths of particular routes depends on the mean winds and standard deviations for particular seasons and this is part of the operational duties of the particular airlines operating these routes. The interest as far as aircraft loads and safety are concerned lies in the departures from forecasted conditions rather than typical seasonal conditions. Wilkinson (1951) suggested that departures from wind speed forecasts are substantially Normal distributions. His data were for rather short periods at about 20,000 ft but they indicate that the standard deviation of the error was about 5 knots 5 hr after the forecast and increased linearly to 15 knots 24 hr after the forecast; it did not seem to matter whether the actual conditions at the time of the forecast or the predicted conditions for the future were used.

These values are from such limited data, and include only one aspect of the problem, that they cannot be used for determining design conditions, but they do indicate the order of wind variations to be expected. Recent publications have been made by Wilkinson (1953), Anon Institute of Navigation (1960) and Anon Institute of Navigation (1961) on the general problem of fuel reserves on airline operations; this covers, of necessity, a much wider field than just effective winds. The interest is almost entirely limited to the amount of fuel remaining at the end of the flight and particularly the rare occurrence of little fuel remaining. This cannot be offset by the occasions when there are large quantities remaining. Likewise extrapolation from the usual condition is of little value, except in so far as it gives an indication of what happens at the extremes. One feature worth taking into account by the airline operators is a comparison between large quantities remaining, presumably due to unexpected tail winds, and small quantities due to unexpected head winds; in any such examination care must be taken to correct



## ATMOSPHERIC ENVIRONMENT

the original numerical values to account for the tanks being unnecessarily full when tail winds are forecast. The interest lies in whether the flight path in emergency becomes more, or less, economical in fuel than simple prediction; for example, does a plane that arrives unexpectedly early have to wait a different time from one that arrives unexpectedly late, and does the pilot fly at increased or reduced speed to compensate for some of the error in time.

### 2.4 TURBULENCE OF THE ATMOSPHERE—OVERALL MOTION

The description of the atmosphere so far has been on a scale of hundreds of miles and the movements on the same scale. Whilst a meteorological phenomenon, such as a cyclone, is building up or at discontinuities, such as ridges or jet streams, there will be a smaller scale turbulence of the air. The typical dimensions of such turbulence would tend to be tens rather than hundreds of miles. The major physical characteristics of these areas of turbulence are examined by studying the following main causes of turbulence:

- (i) Surface radiation.
- (ii) Water vapour.
- (iii) Shape of earth's surface.

It is convenient to consider first the effect of surface radiation as it is one that can occur almost completely in isolation from the other effects, and also does not of itself precipitate a secondary system of turbulence. The mechanism of producing turbulence due to surface radiation is an interaction of gravity forces due to change of air temperature with height and wind forces due to change in horizontal velocity of the air with height. When there is no horizontal velocity the turbulence is one of free convection and the energy available is that due to gravity and is proportional to  $g(\Gamma - \gamma)/T$

where  $g$  = acceleration due to gravity

$\Gamma$  = lapse rate to give neutral equilibrium in dry air

$\gamma$  = actual lapse rate

$T$  = absolute temperature

When  $\Gamma$  is greater than  $\gamma$  the air tends to remain stationary and the system is termed Stable. When  $\Gamma$  is less than  $\gamma$  parcels of air tend to move up and the system is termed Unstable. If, however, there is a horizontal wind there is energy available to be turned into turbulence that is proportional to  $(\partial U / \partial Z)^2$

where  $U$  = mean wind speed at height  $Z$ .

The ratio of these two energies is called the Richardson number  $R_i$  and is given by

$$R_i = \{g(\Gamma - \gamma)/T\} / \left(\frac{\partial U}{\partial Z}\right)^2 \quad (2.4)$$

The absolute value of  $R_i$ , being a ratio, may be low due to the numerator being low (i.e. near neutral equilibrium) or due to the denominator being high (i.e. high wind shear). When  $R_i$  is low the wind shear turbulence

predominates, but as  $R_i$  increases there is a tendency for the wind shear turbulence to be damped by the buoyancy forces and for the air to become freely convective.

The order of the significant vertical dimensions can be estimated fairly readily for the buoyancy considerations. The direct effect of buoyancy, as opposed to its indirect influence on wind shear turbulence, will only produce appreciable turbulence in Unstable conditions. In the absence of water vapour, it is unlikely to reach very great heights although the diurnal heating will frequently produce dry thermals up to 5000 ft, but, of course, their intensity will fall rapidly with height. The horizontal extent of their influence will presumably be of the same order as the corresponding thermals containing water vapour (i.e. extending to a diameter equal to about half their height as will be mentioned later in this paragraph 2.4). This is the extent of influence of an individual source of the thermal, so that in reality the total extent will depend on the variation in ground temperature, but this should quickly lose its local identity for heights exceeding 100 ft. The wind shear turbulence will extend to a greater height than pure convection as it can be significant even in moderately stable conditions. Another indirect influence of stability is that the earth's boundary layer is about 100 ft thick in stable conditions but may increase to the order of 1000 ft in unstable conditions. Thus it is only necessary to have unstable conditions sufficiently high to increase the thickness of the boundary layer and this in turn will influence the wind shear to even greater heights. The extent to which radiation turbulence in dry air may be experienced can definitely reach 10,000 ft, and the horizontal extent must be of the same order as that for convection alone. The overall characteristics of turbulence associated with radiation seem to be that it can have moderate intensity which is likely to be reasonably uniform over horizontal distances of tens of miles, with few sharp discontinuities other than those that can be attributed directly to ground influences.

When water vapour is present in the atmosphere the convection situation changes considerably as the lapse rate for neutral stability is lower than that for dry air. Thus if part of the air near the ground contains water vapour, convection can be set up and Scorer (1957) has shown that the ascent takes the form of a cone starting from the ground, the initial volume of wet air mixing with the air on the sides of the cone as it rises. The horizontal diameter  $D$  of the cone at any place was found by Scorer to be approximately half the distance from the origin and P. M. Saunders (1961) obtained similar results. Ludlam and Scorer (1953) and P. M. Saunders (1961) regard typical large cumulus clouds as being an assemblage of a few thermals. Thus the scale even of single clouds is normally of the order of thousands of feet. Turbulence usually exists in the plane of or below cumulus clouds and is fairly similar to turbulence due to radiation in the absence of water vapour. It can have a moderate intensity which will frequently be uniform over horizontal distances of tens of miles.

The turbulence already described, no matter whether water vapour is present or not, is essentially one of a stream of air travelling more or less in straight lines and that stream containing turbulence that has been initiated by convection. The energy of the main stream is much greater than the

energy of turbulence. Many observers have noticed that the root mean square (r.m.s.) of the turbulence velocity is about 10 per cent of the mean stream velocity in neutral equilibrium conditions and about 3 per cent and 30 per cent respectively for stable and unstable conditions. So the energy of the turbulence varies from 0.1 to 10 per cent of the stream energy from stable to unstable conditions. In extremely stable conditions the turbulence is very low, so that even if its magnitude is increased several-fold by slight changes of direction of the main stream, the effect on aircraft loads will be small. In the unstable conditions the loads are already appreciable and any further extraction of energy from the main stream is important.

So far the energies being discussed are those due to velocity. Frequently there is a considerable amount of water vapour present and this greatly increases the total energy available. This energy may be extracted from the water vapour in relatively short times and result in violent storms. Whilst it may be said truthfully that any turbulence that may occur is convective, it is important to appreciate that it has occurred in two stages. The water has been raised as humid air by convection to form cumulus clouds at the height appropriate to the humidity and lapse rate of the air. Subsequently after energy has been concentrated in the clouds over a period of time, the equilibrium of the local system is disturbed. This usually occurs at the onset of precipitation, after which there is an increase in the ascent speeds resulting in the appearance of towers from the cumulus layer. Byers and Braham (1949) point out that the precipitation causes deep strong down draughts to appear, which spread out at the ground as cool squalls. This new system may itself develop into a persistent quasi steady one, in which case it becomes a cumulo-nimbus and leads to severe thunderstorms and hailstorms.

Ludlam (1963) describes a typical severe storm that occurred in Wokingham in southern England on 9th July, 1959. It was possible to examine this storm in considerable detail and make consistent estimates of stream speeds from radar measurements, aircraft observations of the cloud formations, hailstone measurements, including an examination of the internal structure of some retrieved hailstones. A model of this storm, taken from Ludlam's paper, is plotted in Fig. 2.2. It is thought to be representative of severe storms which have the following general characteristics. Air is taken into the storm at the front at a relative speed of about 30 ft/sec, the horizontal width over which it is taken in is about 10 miles and the height up to about 6000 ft. The air is then changed in direction and is accelerated up to the tropopause where it can reach a maximum velocity in the range of 150-300 ft/sec; the hailstones and increase in height of the tops of the cumulo-nimbus at Wokingham were consistent with speeds of about 130 ft/sec. The updraught has a fairly uniform cross-section of about 10 miles transverse to and 3000 to 6000 ft in the direction of the storm, although in severe vertical velocities the cross-section may be reduced with height; the changes in density and velocity with height are probably not vastly different from the values necessary for compatibility of (velocity  $\times$  density  $\times$  cross-section area) remaining constant. Behind this updraught which is stated by glider pilots to be smooth there is a flow of air that has entered the storm from behind and is forced down. Ludlam suggests that the maximum down-draught speeds will be comparable with the maximum updraught speeds and

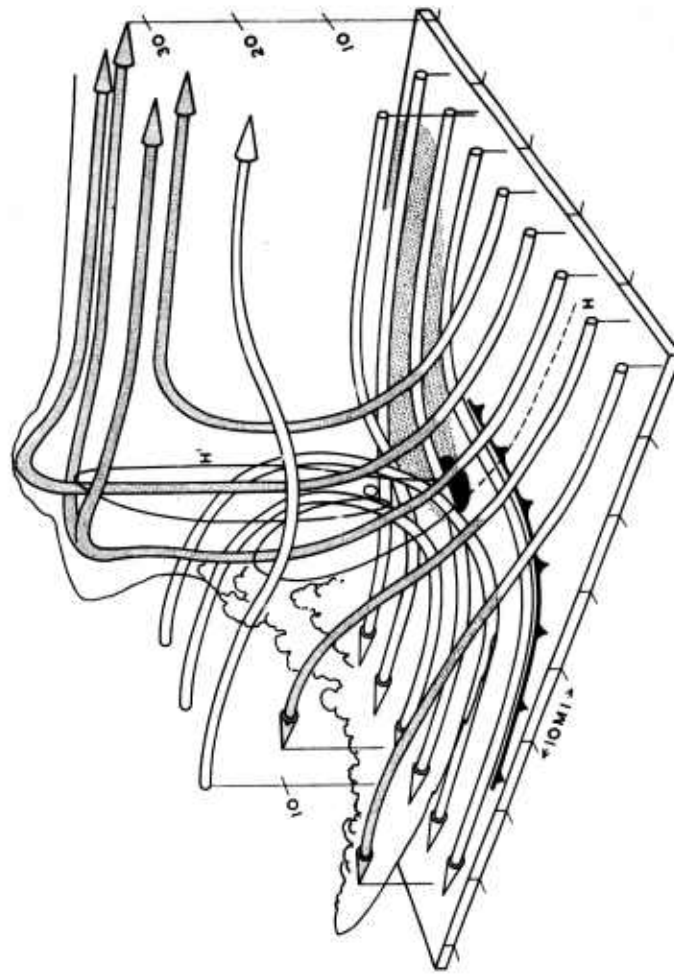


Fig. 2.2. Model of air flow in a severe storm cumulonimbus (constructed for the Wokingham hailstorm of 9 July 1959). Streamlines are drawn of the motion relative to the storm, which moves from left to right, and are shaded where condensation has occurred. A schematic outline is drawn of the anvil cloud and of a cumulus belt over the trailing edge of the squall front (marked on the ground as a cold front). Heights are marked in thousands of feet. HOH' is the path of a particle which becomes a precipitation element, falls ahead of the cloud tops on the storm flank, re-enters the updraught at O and grows into a large hailstone before again falling out (at H') and eventually reaching the ground in the black hail area. Rain reaches the ground in the stippled area farther forward and to the left of the direction of advance of the storm.

[Reproduced from "Air flow in Cumulonimbus" by F. H. Ludlam, Atmospheric Turbulence and its relation to Aircraft, H.M.S.O., 1963, with permission of the Controller of H.M.S.O.]

# ATMOSPHERIC ENVIRONMENT

will occur within a few thousand feet of the ground. He suggests that the turbulence in the borders of the updraught should be associated with a smaller-scale convection arising from local static instability rather than with eddies produced in the region of extreme shear; he points out that such convection can be seen in the well-known manna of the flanks of the anvil cloud. He suggests also that the air entering the downdraught, particularly in the lower troposphere, penetrates the convection surrounding the updraught and is broken down by it. Ludlam has suggested orally that the transition from maximum updraught to maximum downdraught might

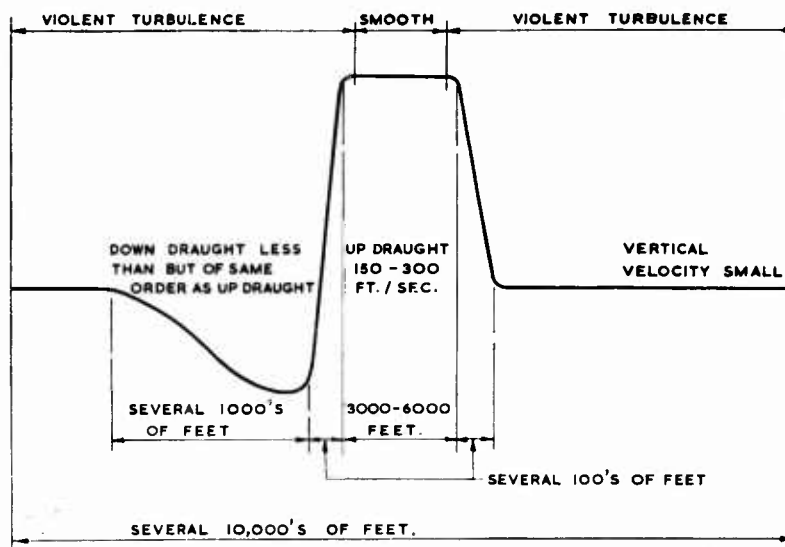


Fig. 2.3. Variation of mean vertical velocity in line of travel of a thunderstorm and a few thousand feet below tops of clouds. (Not to scale.)

occur within a distance of about 3000 ft, but Anne Burns suggested orally that the transition on leaving the updraught in any direction may be of the order of 300 ft. The distance to which the downdraught extends has not been estimated, but it is thought to be greater than for the updraught and the fall off in down velocity to the edge of the storm rather more gradual. A cross-section of a thunderstorm is shown diagrammatically in Fig. 2.3 which summarizes the position as far as an aircraft is concerned. The aircraft will encounter turbulence in front of the storm and behind the storm each of which has a varying vertical component of stream velocity. It will also encounter turbulence in the centre between the updraught and the downdraught and this too will have a varying vertical component of stream velocity. In addition there is one region of low turbulence in the steady upcurrent. The three regions of turbulence other than the low intensity one in the upcurrent probably have a considerable variation of intensity within them. In addition there are the three steps in vertical velocity of "up-down-

up" or "down-up-down" depending on whether the aircraft is entering the storm from the front of it or from behind. The gradient distances involved are such that there will be considerable attenuation of the normal accelerations of the aircraft due to the actual air velocities, but the duration of these lower accelerations will be longer and the accelerations will be additive to those due to the turbulence.

The storms that have been described are violent in the way they disturb the reasonably homogeneous turbulence due to radiation of heat from the earth's surface. There is the other less violent way in which the turbulence can be disturbed by the form of the earth's surface. Perhaps the simplest form to understand is that which occurs on moving from land to sea or any other large expanse of water. The effective thermal inertia of the two surfaces is markedly different and there may be the condition that air above one is stable whilst that above the other is unstable, but in addition there are the morning and evening breezes that occur at the interface. If there are cliffs these will result in local changes in direction of the main airstream and are easily noticed as gusts to an aircraft crossing low over a cliff; the main gust is not detectable as a gust to an instrument on a tower placed on top of the cliff, but merely as a change in direction of the whole stream. This serves as an illustration of the general problem of geographical turbulence.

Many observations have been made of the effect of ground contours on wind speeds. Morgans (1931) summarizes a lot of work done in the previous twenty years in connection with free flying balloons and sailplanes and in all cases he is concerned with the atmosphere in a stable state. Comparison work was done at Biville by Idrac (1923) on dunes of height 10 m and a plateau of 100 m, and he obtained similar results. In both cases the air was influenced to a height above the ridge of about four times the height of the plateau. Observations on mountains with a clearly defined top had suggested an influence up to 0.3 times the height above the top, but a mathematical solution by Pockels (1901) gave an influence up to four times the height above a ridge of infinite length; in Pockel's solution there is a vertical component of 5 per cent of the wind speed at three times the height above the ridge.

A number of observers have noticed that there is often a persistent vertical velocity above ridges; glider pilots take considerable advantage of this in the immediate neighbourhood of ridges and Scorer (1963) draws attention to the way air rises from the Owens Valley floor to about 14,000 ft whilst the mountain tops are only 6000 and 9000 ft above the valley floor. Scorer (1963) points out that some of these flows are unsteady, but he infers that the air was stable. Bannon (1963) suggests that turbulence in jet streams might be influenced by mountains. If there is an influence over a ridge up to four times its height, then it may be such as to act as a disturbing agent on the otherwise steady jet stream system. All this discussion is for stable conditions; for unstable conditions the influence on jet streams might be greater but less easy to separate from the condition that had caused the disturbance.

At levels near the ground the influence is more self-evident and in any study of turbulence below 1000 ft, particular care must be taken to take as full an account as possible of the ground effects.

2.5 TURBULENCE OF THE ATMOSPHERE—LOCAL MOTION  
WITHIN THE TURBULENCE

Many of the large-scale movements of the atmosphere produce negligible loads on an aircraft. As far as the aircraft is concerned it is flying relative to the whole volume of air in the large-scale movement which in turn is moving relative to the earth. Within these large volumes of atmospheric movements there is a smaller scale movement that is of significance to the aircraft. In this smaller scale turbulence water vapour may be present. The main difference between the presence and absence of water vapour is that the water vapour contains a considerable amount of energy that can be released and set up violent storms as described in paragraph 2.4. The turbulence varies in intensity throughout the storm, which is almost invariably associated with precipitation. It was suggested that both forms of turbulence in the absence of precipitation have much more uniform intensities and the error should not be great if they are grouped together in making the measurements. This has the advantage that special meteorological discrimination is unnecessary, and also a number of experiments have been done that are bounded in this way. G. I. Taylor (1938) has shown theoretically that for a turbulent airstream in a wind-tunnel that has an intensity that remains uniform with only random variations from the average, the mean energy at different wavelengths measured along the mean direction of the airstream is the same no matter whether the measuring point is fixed or has a velocity in the direction of the airstream. Lin (1953) has extended the work to include wind shears such as are present in the atmosphere, and shows that for sufficiently small wavelengths Taylor's hypothesis will hold rigorously. Experiments were made by the Cornell Laboratories (Anon ASTIA 1959a) to verify this at heights of about 400 ft. The results are discussed in paragraph 2.5.3 together with the extensive fixed point measurements of paragraph 2.5.1 and the extensive flight measurements of paragraph 2.5.2. For agreement to be achieved even if the wind shear effects are negligible, the intensity of the turbulence must remain steady for the duration of the test; in the fixed point measurements this means that the duration has to be sufficient for the wind run (velocity  $\times$  time) to include the wavelengths of interest and in the aeroplane measurements the line of flight must all be in the same type of turbulence. In addition the flights must be over reasonably uniform terrain, otherwise the additional energy due to change of the relative attitude of the aircraft to the stream may be an appreciable fraction of the energy from the turbulence. As far as the fixed point measurements are concerned, there may be a change of energy due to the turbulent stream being distorted by its close proximity to the terrain.

2.5.1. *Turbulence Measured at Fixed Points*

F. B. Smith (1961) did a series of experiments on a captive balloon cable between heights of 500 ft and 2000 ft (with a few between 2000 ft and 5000 ft) that represent this condition fairly well. No records were made when there was a risk of lightning or precipitation was heavy. There were, however, further limitations; light turbulence was not recorded as records were omitted when the atmosphere was very stable and also when the wind

# MANUAL ON AIRCRAFT LOADS

speed was below 1.5 m/sec. Also records were not taken at wind speeds in excess of 10 m/sec.

It is appropriate to consider the intensity of the turbulence to be the average energy per unit mass of air. This is equal to half the mean square of the velocity of the turbulence relative to the stream velocity. In Smith's experiments the interest is restricted to vertical velocities, so he measures the mean square of the vertical fluctuations relative to the mean vertical velocity for the duration of the run. The duration of each run is made to last long enough to allow a prediction to be made of the contributions of all wavelengths. Using Smith's breakdown between stable and unstable conditions, the distribution of r.m.s. of turbulent velocity for different stream speeds is given in Table 2.3.

Table 2.3. Comparison of Intensity of Turbulence and Stream Velocity Past a Fixed Point (Deduced from F. B. Smith (1961)).

## Stable Air—Number of Occurrences

r.m.s. of turbulence velocity ft/sec	Stream velocity in ft/sec					Total
	0-6.55	6.55-13.1	13.1-19.65	19.65-26.2	26.2-32.75	
0-1	1	0	1	4	3	9
1-2	1	3	5	11	6	26
2-3		2	2	6	4	14
3-4			2		1	3
4-5						

## Unstable Air—Number of Occurrences

r.m.s. of turbulence velocity ft/sec	Stream velocity in ft/sec					Total
	0-6.55	6.55-13.1	13.1-19.65	19.65-26.2	26.2-32.75	
0-1						0
1-2	1	1				2
2-3		5	6			11
3-4		4	3	3		10
4-5			2	1		3

Of the actual 78 recordings made by Smith, the individual runs in unstable conditions had a mean r.m.s. value of 3.04 ft/sec with a standard deviation about that mean of 0.90 ft/sec, and those in stable conditions had a mean r.m.s. value of 1.7 ft/sec with a standard deviation of 0.93 ft/sec. In the unstable conditions there is a tendency for turbulence to increase with stream velocity, but in the stable conditions there is no such tendency and it would be difficult to estimate the real tendency as the time that has been



# ATMOSPHERIC ENVIRONMENT

unrecorded because of low turbulence and low stream velocity may be quite different at the different stream velocities.

All the recorded occurrences are grouped together and shown in Fig. 2.4. For comparison a Normal distribution of the r.m.s. vertical velocity with mean zero and standard deviation 2.2 ft/sec is also shown. The difference between the actual distribution and the Normal distribution would not be

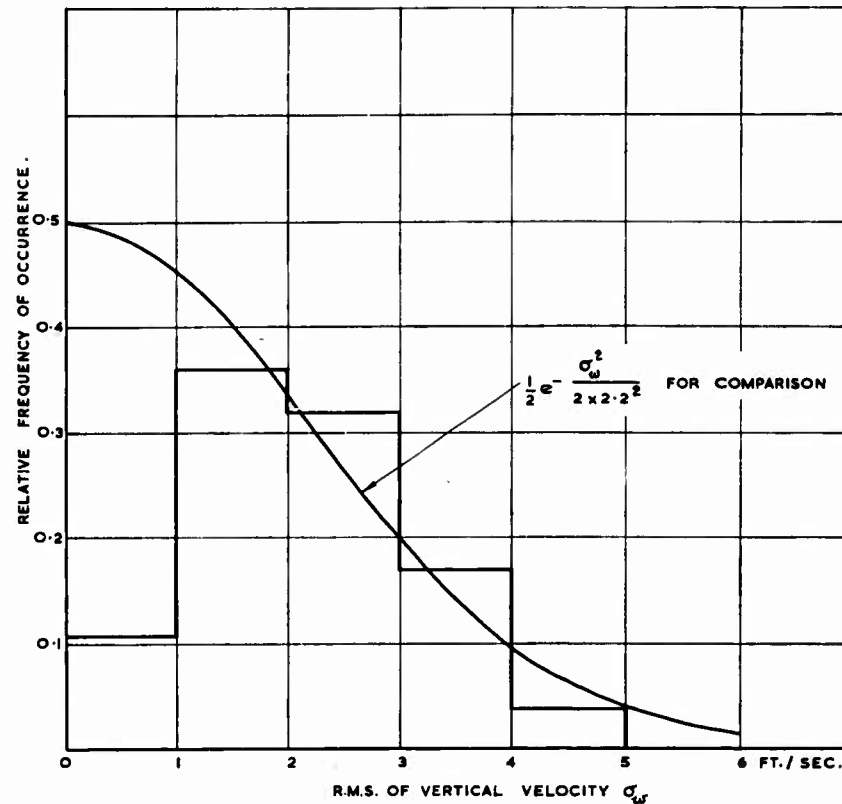
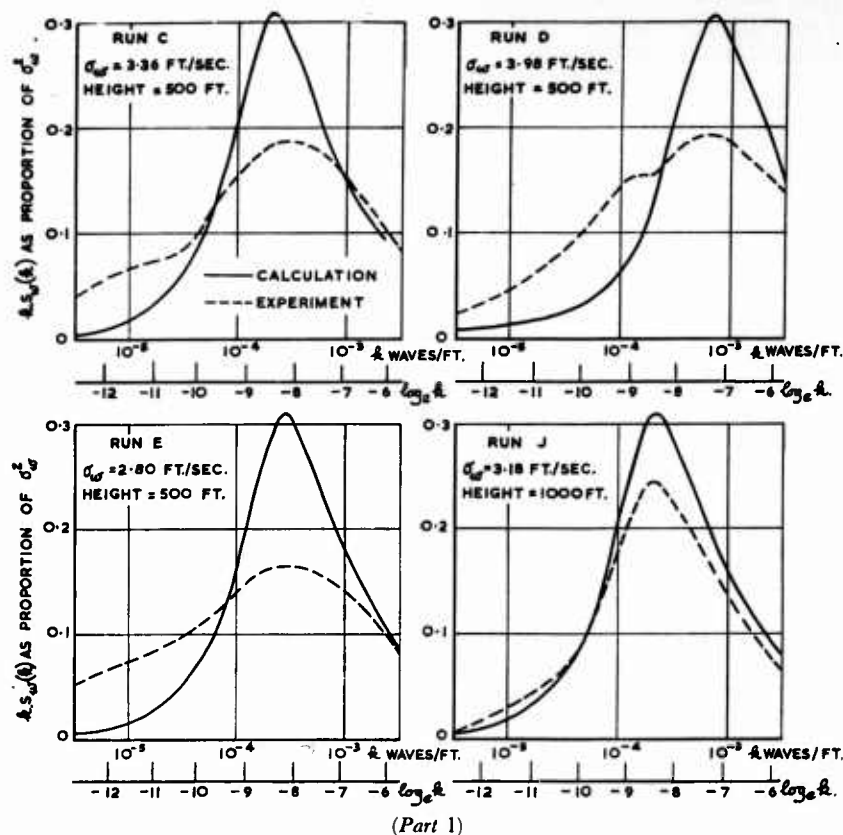


Fig. 2.4. Variation in intensity of vertical component of turbulence. Measurements by F. B. Smith (1961) on tethered balloon cables at heights of 500 to 5000 ft.

very great in total effect, as the contribution when the r.m.s. of the vertical velocity is less than 1 ft/sec is small in both cases; the contribution above 5 ft/sec in the Normal distribution would be significant, but this would tend to be avoided in the experiment by deliberately avoiding taking readings when the wind speed exceeded 10 m/sec.

The total energy of the turbulence in the stream is a good measure of its intensity, but the information is not sufficiently detailed for the determination of aircraft loads as the aircraft responds differently to disturbances of different

wavelengths. Thus it is necessary to determine the proportions of energy at different wavelengths. This has been done for a number of the runs by F. B. Smith (1961) at heights of 500, 1000 and 2000 ft. The results are



(Part 1)

Fig. 2.5. Distribution of energy of turbulence per unit mass of air  $\{\frac{1}{2}S_w(k)\}$  at different wavelengths  $(1/k)$ .

Measurements on balloon cables deduced from F. B. Smith (1961) and compared with

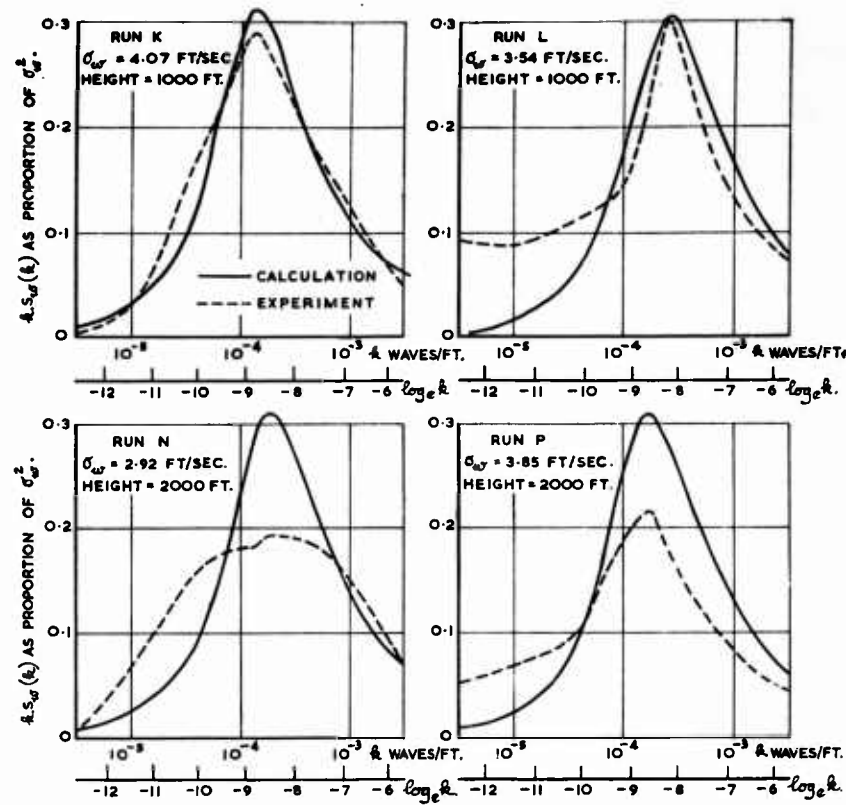
$$S_w(k) = 2L\sigma_w^2[1 + (8/3)(L_1k)^2]/[1 + (L_1k)^2]^{11/6}$$

where  $L_1 = 1.339(2\pi L)$ ;  $\sigma_w$  = r.m.s. vertical velocity.

$L$  is chosen so that calculated and experimental distributions have  $k \cdot S(k)$  a maximum at the same  $k$ .

shown in Fig. 2.5 omitting those runs in which Smith noticed that the intensity did not remain steady and one during which the intensity was very low. The abscissa is plotted as the logarithm of the inverse wavelength  $k$ , i.e. cycles per ft, and the ordinate as  $kS_w(k)/\sigma_w^2$  where  $S_w(k)$  is twice the energy density, with respect to  $k$ , per unit mass of air and  $\sigma_w^2$  is the mean square of the vertical component of the turbulence velocity. Twice the total energy

# ATMOSPHERIC ENVIRONMENT



(Part 2)

Fig. 2.5 (cont.). Distribution of energy of turbulence per unit mass of air  $\{\frac{1}{2}S_w(k)\}$  at different wavelengths  $(1/k)$ .

Measurements on balloon cables deduced from F. B. Smith (1961) and compared with

$$S_w(k) = 2L\sigma_w^2[1 + (8/3)(L_1k)^2]/[1 + (L_1k)^2]^{11/6}$$

where  $L_1 = 1.339 (2\pi L)$ ;  $\sigma_w$  = r.m.s. vertical velocity.

$L$  is chosen so that calculated and experimental distributions have  $k \cdot S(k)$  a maximum at the same  $k$ .

per unit mass of air equals the mean square of the turbulence velocity so that

$$\sigma_w^2 = \int_0^\infty S_w(k) dk = \int_{-\infty}^\infty kS_w(k) d(\log_e k) \quad (2.5)$$

Thus twice the total energy per unit mass of air is given by the area under the curve of  $kS_w(k)$  against  $\log_e k$  and the area under the curve of  $kS_w(k)/\sigma_w^2$

is unity. The contribution in any band of wavelengths is the area under that portion of the curve. It is suggested in Chapter 9 that within the range of wavelengths of these measurements the energy density of the vertical component of homogeneous and isotropic turbulence in a horizontal stream should be represented well by the formula (9.40), which is

$$S_w(k) = 2L\sigma_w^2[1 + (8/3)(L_1k)^2]/[1 + (L_1k)^2]^{11/6} \quad (2.6)$$

where  $L_1 = 1.339 (2\pi L)$

Each run is compared with this formula and  $L$  is chosen so that the theoretical curve of  $kS_w(k)$  has a maximum at the same wavelength as the experimental curve. In all cases the shapes of the experimental curves agree well with the theoretical curve for high inverse wavelengths but the measured contribution to the energy is generally a little lower than the prediction. This suggests that the major portion of the energy is distributed in the manner predicted but that there is a second distribution predominantly at lower inverse wavelengths. There is insufficient evidence to form an opinion about the characteristics of this second distribution.

In order that the turbulence velocities in the atmosphere may be transformed into loads on an aircraft it is also necessary to know the distribution of the turbulence velocities along the direction of the stream. This distribution may be determined in several ways, the most commonly used ones being the measurement of

- (i) the total time spent above each level of velocity,
- (ii) the number of times each level of velocity is crossed in one direction,
- (iii) the number of peak velocities exceeding each level of velocity.

The first method can be defined more rigorously but the other two are more directly transformable into loads. The crossings\* of levels of velocity of runs  $J, K, N, P$  of F. B. Smith (1961) are shown in Fig. 2.6 and are compared with a Normal distribution with a standard deviation equal to the r.m.s. of the vertical velocity. The absolute value of the number of crossings increases with the band of wavelengths over which the measurements are made. Unfortunately for energy density distributions appropriate to atmospheric turbulence the number approaches infinity as the band of inverse wavelengths approaches infinity, so that an arbitrary cut-off has to be made. These particular crossings were taken from a low-pass trace equivalent to a running average over 30 sec and wind speeds from 10 to 20 ft/sec, i.e. a running average over 300 to 600 ft. In all four cases the relative number of high velocities was greater than would be expected from a Normal distribution, although on runs  $N$  and  $P$  the difference was not significant.

If runs  $J$  and  $K$  happened to be made up of two or more patches of homogeneous turbulence of different intensity but each with a Normal distribution of crossings, the resultant distribution of crossings would have more high velocities than a single Normal distribution with the same standard deviation. Thus this evidence is not incompatible with the contention

\* The values were not given in the published paper and have been supplied privately.

# ATMOSPHERIC ENVIRONMENT

that homogeneous turbulence has a Normal distribution of crossings of velocities and that the atmosphere studied by F. B. Smith (1961) was made up of a number of patches of homogeneous turbulence. Rice (1944) has shown that a Normal distribution of crossings could arise from a Normal

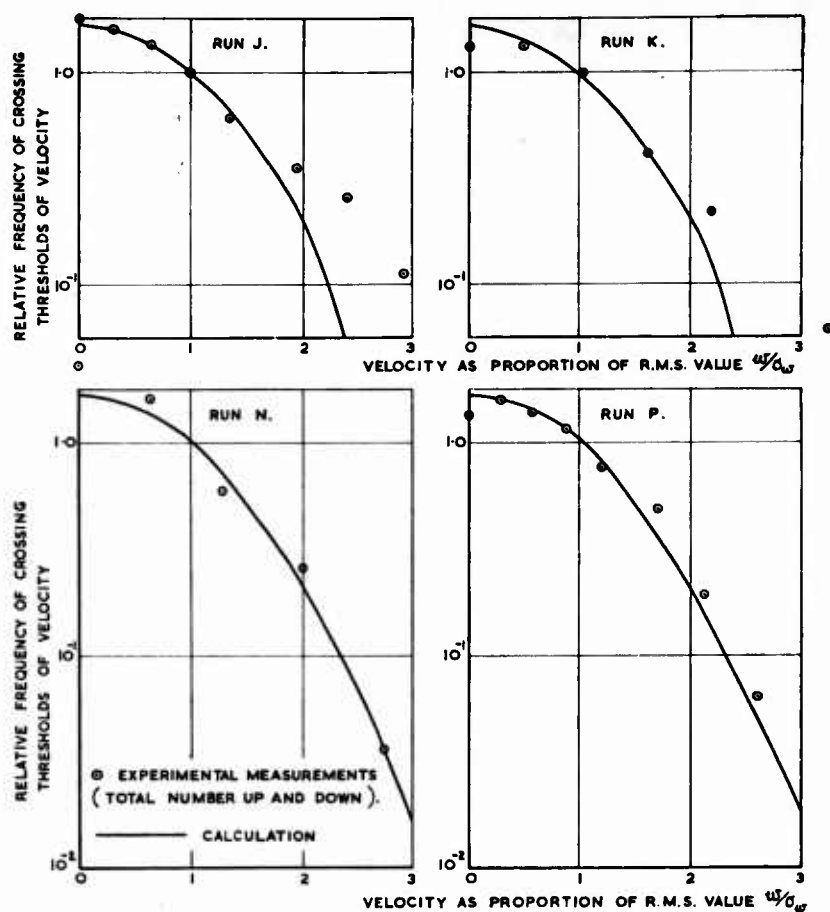


Fig. 2.6. Relative frequency of crossing different thresholds of vertical velocity.

Measurements from F. B. Smith (1961) are compared with normal distribution with same r.m.s. velocity and same number of crossings at a vertical velocity equal to the r.m.s. value.

distribution with the same standard deviation of time spent at different velocities, so for calculation purposes either a crossings or a time distribution may be used.

In addition to the measurements by F. B. Smith (1961) at 500, 1000 and

# MANUAL ON AIRCRAFT LOADS

2000 ft of distributions of the vertical component of turbulence energy at different wavelengths Panofsky and McCormick (1959) quote a number of measurements at heights from 4 ft to 300 ft. The theoretical distribution of  $S_w(k)$  that represented well Smith's results also represents well Panofsky and McCormick's. The range of heights of the combined results is large and gives an opportunity of checking the effect of height. Table 2.4 gives a summary of the data and includes

- (i)  $\sigma_w$  (r.m.s. vertical velocity),
- (ii) the wavelength ( $1/k$ ) at which  $kS_w(k)$  is a maximum, and the value of the constant  $L$  in the theoretical formula

$$S_w(k) = 2L\sigma_w^2[1 + (8/3)(L_1k)^2]/[1 + (L_1k)^2]^{11/4}$$

to give a maximum at the same value of  $k$ ,

- (iii) the parameter  $(\sigma_w/L^{1/3})$ .

Table 2.4. Measured Intensities of Turbulence and Scale of Turbulence at Fixed Points at Different Heights

Reference	Height ft	r.m.s. vertical velocity $\sigma_w$ ft/sec	Wavelength at which $kS_w(k)$ is a maximum ft	Scale of turbulence $L$ ft	$(\sigma_w/L^{1/3})$
Panofsky and McCormick (1959)					
<i>K</i>	4	1.02	15.6	3.3	0.684
<i>J</i>	6.6	0.91	29.1	6.2	0.496
<i>S</i> (Average of four)	10	1.82	48.1	10.2	0.839
<i>H</i>	26.2	3.06	153	32.4	0.960
<i>H</i>	26.2	1.18	920	19.5	0.438
<i>S_w</i> (Average of two)	30	1.55	650	13.8	0.646
<i>B</i> (Average of five)	300	3.98	1560	330	0.576
Smith, F. B. (1961)					
<i>C</i>	500	3.36	4620	980	0.339
<i>D</i>	500	3.98	1510	320	0.579
<i>E</i>	500	2.79	3680	780	0.304
<i>J</i>	1000	3.18	4620	980	0.320
<i>K</i>	1000	4.06	7830	1660	0.343
<i>L</i>	1000	3.54	4190	890	0.368
<i>N</i>	2000	2.92	5330	1150	0.279
<i>P</i>	2000	3.85	5940	1260	0.356

The wavelength at which  $kS_w(k)$  is a maximum is an indication of the scale of the turbulence and there is roughly half the energy each side of this wavelength. For the theoretical distribution of  $S_w(k)$  this wavelength is always  $4.722L$  so  $L$  too may be used as a measure of the scale of turbulence and

## ATMOSPHERIC ENVIRONMENT

$L$  is in fact usually called the scale of turbulence. At high values of inverse wavelength  $k$  the energy density is given by

$$\begin{aligned} S_w(k) &= (16/3)[2\pi(1.339)]^{-5/3} \cdot (\sigma_w/L^{1/3})^2 \cdot k^{-5/3} \\ &= 0.1532 (\sigma_w/L^{1/3})^2 k^{-5/3} \end{aligned} \quad (2.7)$$

so that  $(\sigma_w/L^{1/3})^2$  is a measure of the intensity of the energy at high inverse wavelengths.

The measurements were taken at many different places and at different times and it would be dangerous to use them to predict variation of intensity with height. The scale of turbulence  $L$  increases with height and the magnitude does not differ much from the height\* except for the two runs at 2000 ft.

### 2.5.2. Turbulence Measured Directly on Aircraft

According to G. I. Taylor's (1938) hypothesis the same turbulence energy will be measured whether it is done at a fixed point or at a point moving in the direction of the stream containing the turbulence. As a corollary to this the same turbulence will also be measured on an aircraft flying in a straight line in a stream moving in a straight line but not necessarily in the same direction as the aircraft.

Crane and Chilton (1956) describe a flight at 290 ft/sec at 1700 ft pressure altitude (the height above the ground is not stated) by a jet fighter fitted with an angle of attack vane to measure the vertical component of the turbulence velocity. The flight was over 170 miles (i.e. 900,000 ft) and wavelengths from 10 ft to 60,000 ft were measured on three types of instrument; for the long waves the aircraft was tracked by a sun camera but for the medium and short waves none of the instruments used any external datum. The distribution of energy at different wavelengths is given in Fig. 2.7 and is compared with the theoretical distribution of equation (2.6). The r.m.s. vertical velocity  $\sigma_w$  used in the equation is the measured value and the scale of turbulence  $L$  is chosen to correspond to  $kS_w(k)$  being a maximum at a wavelength of 6000 ft. This is the same method as that used for the fixed point measurements and was possible because accurate measurements were made of the energy at long wavelengths by instruments which included a sun camera. It can be seen in Fig. 2.7 that the measurements from the instruments used for the medium range of wavelengths did not show the same flattening out of the curves at the longest wavelengths as did those for the long waves. It seems probable that the corrections for aircraft motion are not so accurate in this case where none of the instruments used any external datum. A similar experiment was made by Zbrozek and Ridland (1960a) at 534 ft/sec at a pressure altitude of about 2500 ft (height above ground about 2000 ft) for a distance of 53,400 ft. The distribution of energy at different wavelengths is shown in Fig. 2.8 and, as in Fig. 2.7, it is compared with the theoretical distribution of equation (2.6). The measured value of r.m.s. vertical velocity  $\sigma_w$  is used but the measured distribution of energy density  $S_w(k)$  cannot be used to determine  $L$  with sufficient accuracy, as it is

\* Panofsky and McCormick's (1959) suggestion of the peak being at 4 times the height is equivalent to  $L$  being 85 per cent of the height.

probable that the measured values of  $S_w(k)$  at the longest wavelengths will be high due to insufficient correction for the aircraft motion (as was noticed in Fig. 2.7 for the measurements made by instruments without any external datum). In the theoretical analysis described in Chapter 9,  $L$  is defined as

$$L = 2 \int_0^{\infty} f_w(r) dr \quad (2.8)$$

where

$$f_w(r) = (1/\sigma_w^2) \int_0^{\infty} S_w(k) \cos(kr/2\pi) dk$$

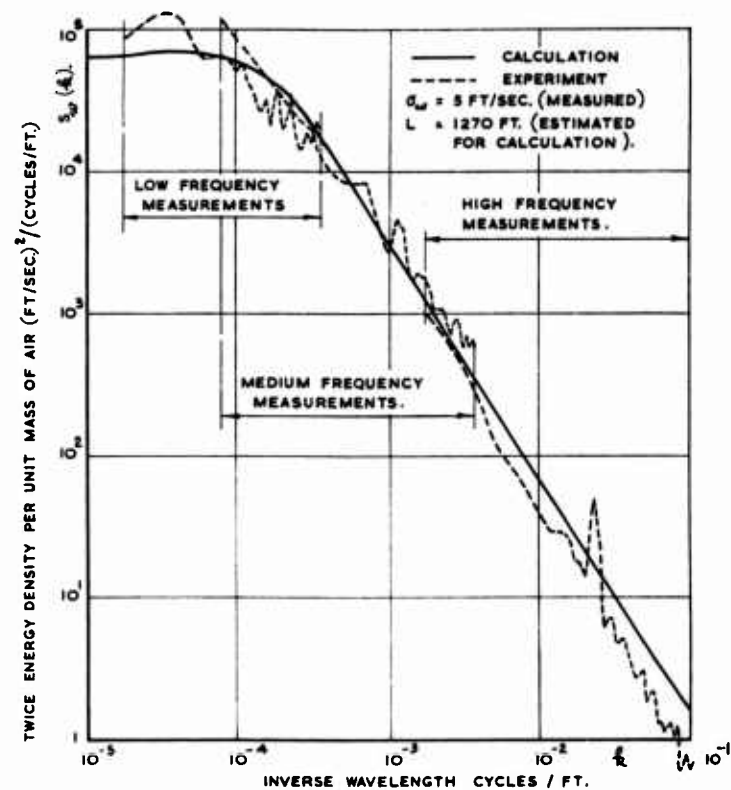


Fig. 2.7. Distribution of energy of turbulence per unit mass of air  $\{ \frac{1}{2} S_w(k) \}$  at different wavelengths.

Measurements (Crane and Chilton, 1956) made on aircraft at 290 ft/sec at a pressure altitude of 1700 ft and compared with

$$S_w(k) = 2L\sigma_w^2 [1 + (8/3)(L_1 k)^2] / [1 + (L_1 k)^2]^{11/6}$$

where  $\sigma_w$  = r.m.s. velocity;  $L_1 = 1.339(2\pi L)$ .



# ATMOSPHERIC ENVIRONMENT

and is called the lateral auto-correlation function. Zbrozek and Ridland (1960a) quote the auto-correlation function as well as the distribution of energy density. An estimate of the scale of turbulence  $L$  can be obtained by comparing this experimental function with the theoretical auto-correlation function  $f_w(r)$  calculated for  $S_w(k)$  as given by equation (2.6). Making the comparison by the method described in Chapter 9 gives a scale of turbulence  $L$  of 296 ft. This value of  $L$  is used in the theoretical distribution of  $S_w(k)$  in

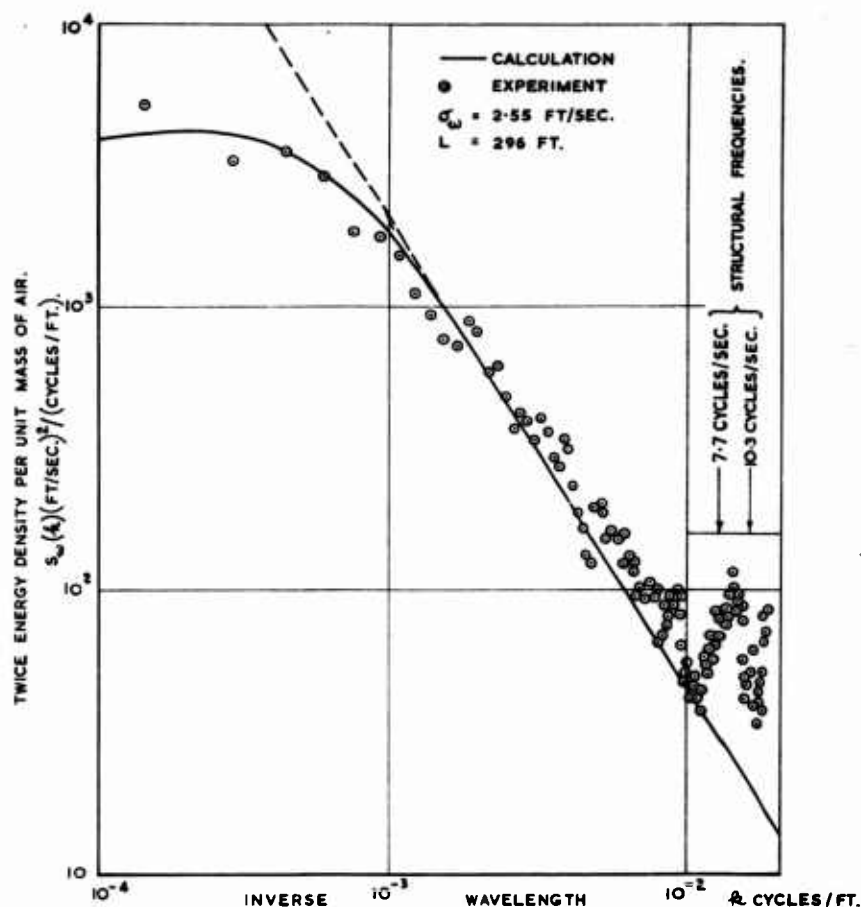


Fig. 2.8. Distribution of energy of turbulence per unit mass of air  $\{S_w(k)\}$  at different wavelengths.

Measurements (Zbrozek and Ridland, 1960) made on aircraft at 534 ft/sec at a pressure altitude of 2500 ft and compared with

$$S_w(k) = 2L\sigma_w^2 [1 + (8/3)(L_1 k)^2] / [1 + (L_1 k)^2]^{11/6}$$

where  $\sigma_w$  = r.m.s. vertical velocity;  $L_1 = 1.339(2\pi L)$ .

Fig. 2.8. The agreement between the experimental and theoretical distributions is good except at the very high wavelengths where the measured energy is too high, and at wavelengths between 50 and 100 ft where the measured energy is also too high.

In Figs. 2.7 and 2.8 the measurements show peaks of energy at wavelengths below 100 ft. These are at resonance frequencies of the structure as shown in Fig. 2.8. This will be a source of inaccuracy in measurements on any aircraft, especially at frequencies of the fundamental resonances of wings and fuselage. There is a tendency for the measured energies to be too high at the long wavelengths presumably due to inadequate compensation for deliberate movements by the pilot.

An extensive series of flight measurements on B-66B aircraft at altitudes of less than 1000 ft above the terrain is described by K. D. Saunders (1961). The gust data that are reported are 391 four-minute runs covering approximately 11,000 miles of flight. The turbulence was measured in all three planes but not on every flight. There were, however, 42 flights in which it was measured in all three planes and from which a comparison can be made. The lapse rate was measured on most of the runs and on more than 80 per cent of the runs the air was unstable or neutrally stable.

The r.m.s. of the vertical velocity was measured on 384 runs and had a mean of 3.17 ft/sec and a standard deviation of 1.28 ft/sec; out of these 384 runs 224 were over flat terrain and had a mean and standard deviation of (2.73 ft/sec, 1.09 ft/sec), the other 160 runs over hills had a mean and standard deviation of (3.79 ft/sec, 1.26 ft/sec). A large number of runs were made in groups of 3 at different heights within an hour. These offer a good opportunity of examining the variation in the intensity of turbulence with height. Table 2.5 compares the mean r.m.s. vertical velocity at different heights. The scatter at the individual heights is a standard deviation of about 1 ft/sec over flat terrain and about 1.2 ft/sec over hilly terrain.

Table 2.5. Variation of R.M.S. Vertical Velocity of Turbulence with Height

	No. of runs at each height	Height			
		200 ft	400 ft	600 ft	1000 ft
Over flat terrain	32	ft/sec 2.21	ft/sec 2.32	ft/sec 2.50	ft/sec 2.50
	14	3.37		3.95	3.87
Over hilly terrain	21	3.59	3.72	3.78	
	9	3.46		3.45	3.29

The values for the 42 runs in which lateral and forward velocity were measured at the same time were (3.36 ft/sec, 1.20 ft/sec), (3.67 ft/sec, 1.27 ft/sec) and (3.78 ft/sec, 1.30 ft/sec) respectively for the vertical, lateral and forward components of the turbulence. In the 42 runs there are 25 that

#### ATMOSPHERIC ENVIRONMENT

are over flat terrain and if these are taken separately the mean and standard deviations of the r.m.s. velocity become (3.06 ft/sec, 1.04 ft/sec), (3.30 ft/sec, 1.02 ft/sec) and (3.62 ft/sec, 1.22 ft/sec) respectively. Under these conditions it would be expected that the energy of the turbulence at long wavelengths would be less and also that there would be less influence from the aircraft's motion relative to the direction of the stream of the turbulence so that the actual recordings are a little lower and probably have less scatter due to experimental error.

The proportion of the energy at different wavelengths was determined for most of the runs. K. D. Saunders (1961) has given these mainly as overlapping curves but separate curves have been given for 4 curves for the vertical component of energy. These are reproduced in Fig. 2.9 and compared with the theoretical distribution of  $S_w(k)$  given in equation (2.6). Wavelengths less than 100 ft are omitted as the measurements would be subject to error due to structural resonances. Agreement between theory and experiment is good except that there is the same tendency as in Figs. 2.7 and 2.8 for the measurements to be too high at long wavelengths. This tendency is apparent also in most of the other 380 runs in which the vertical component was measured.

The scale of turbulence was estimated for the vertical component for the 42 runs in which the components in all three planes was measured. It is found by comparing the experimental auto-correlation function with the theoretical one given by equation (9.44). Saunders used the theoretical auto-correlation function given by equation (9.37) but recalculation using equation (9.44) does not show any significant differences. The scale of turbulence, as quoted by Saunders, is given in Table 2.6 for the 42 runs. The runs have been separated into the 17 over hilly terrain and 25 over flat terrain and grouped according to height above the terrain. Over the flat terrain the scale of turbulence does not differ much from the height, although there seems to be a tendency for some of the runs at 200 ft to have a larger scale of turbulence. This may be due in part to the ground contours affecting the direction of the stream velocity of the turbulence. In flights over hilly terrain there is no doubt that the contours affect the scale of the turbulence. The larger scatter may be due to low and high mountains being grouped together; if the runs over low mountains 2, 5, 11, 16, 23, 28, 37 are taken separately the average scale is 750 ft, the standard deviation reduced to that for the runs over flat terrain, and the difference between height bands negligible.

The check on the distribution of velocities has to be made from the distribution of peak velocities as the distribution of crossings was not measured. However, Rice (1944) has shown that for a Normal distribution the number of peaks will be negligibly more than the number of crossings at large departures. For the system being examined the difference can be ignored for peak velocities greater than about a r.m.s. value. The 25 runs over flat terrain are split into 6 groups according to the r.m.s. velocity and the numbers of peaks compared with the expected number of crossings in Fig. 2.10. The measured and the calculated curves are made to coincide at a velocity equal to the r.m.s. velocity of the group of runs. In all cases the numbers measured are greater than the calculated curves at velocities in

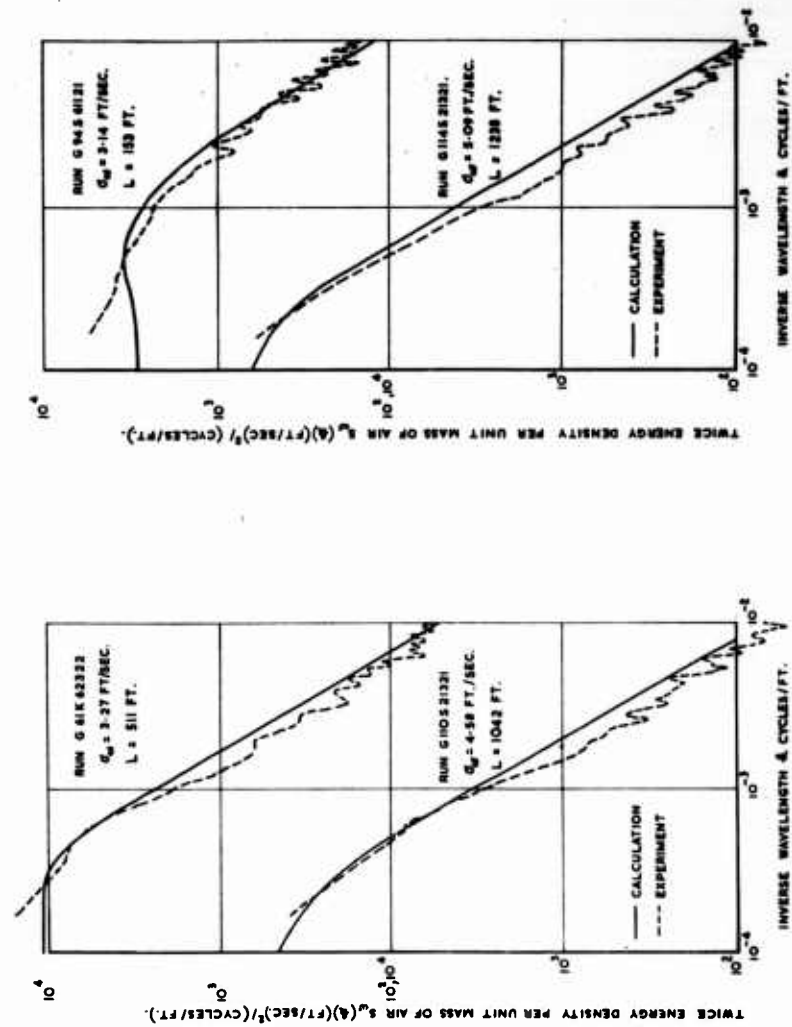


Fig. 2.9. Distribution of energy of turbulence per unit mass of air  $\{S_w(k)\}$  at different wavelengths  $(1/k)$ .

Measurements (K. D. Saunders, 1961) made on B-66B and compared with

$$S_w(k) = 2L\sigma_w^2[1 + (8/3)(L_1/k)^2][1 + (L_1/k)^2]^{1/2}$$

where  $\sigma_w = r.m.s.$  vertical velocity;  $L_1 = 1.339(2\pi L)$ .

# ATMOSPHERIC ENVIRONMENT

**Table 2.6. Scale of Turbulence as Measured on Aircraft Flying at Different Heights. Run Numbers are the same as those given by K. D. Saunders (1961) in his Table 7**

	Height above terrain					
	200 ft		600 ft		1000 ft	
	Run no.	L ft	Run no.	L ft	Run no.	L ft
Over flat terrain	1	277	4	359	18	402
	6	220	7	834	22	739
	9	414	12	675	36	1327
	13	480	14	511		
	17	374	24	570		
	19	223	26	413		
	25	410	27	510		
	31	153	30	383		
	32	167	34	649		
	35	346				
	40	252				
	42	499				
	Mean	318		545		823
	Std. dev.	130		160		
Over hilly terrain	11	803	2	624	16	727
	23	608	3	383	21	823
	29	923	5	804		
	33	1258	8	747		
	37	924	15	618		
	39	1016	20	1270		
			28	687		
			38	1042		
			41	1238		
	Mean	922		824		775
	Std. dev.	200		290		

Run No. 10 was over flat terrain at height 400 ft and L was 640 ft.

excess of about twice the r.m.s. velocity. A better fit could be obtained if it were assumed that the turbulence was intermittent along the runs, but even then the high velocities would occur more often than expected. The only way a satisfactory fit could be made would be by assuming that the intensity varied along the runs.

## 2.5.3. Comparison of Measurements at Fixed Points and on Aircraft

The estimates of turbulence at fixed points and on aircraft have many common features. Measurements were made on 24th April, 1956, and

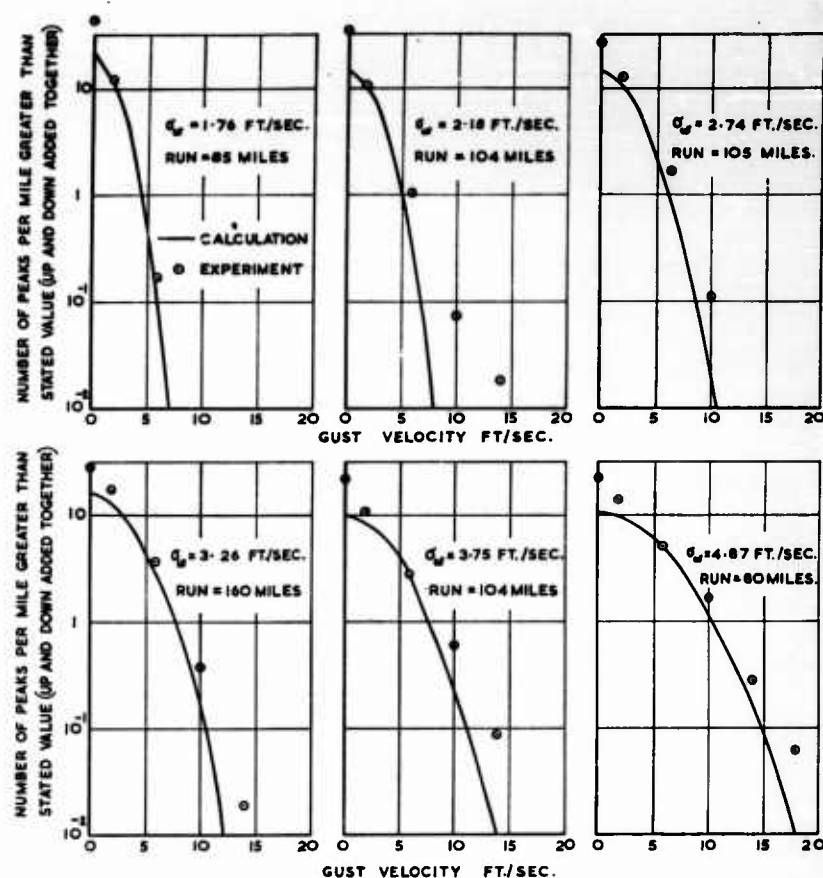


Fig. 2.10. Comparison of distribution of number of peak velocities (gusts) at different r.m.s. vertical velocity of turbulence  $\sigma_w$ .

Measurement on B-66B deduced from K. D. Saunders (1961) and compared with normal distribution, with standard deviations  $\sigma_w$  and same number of peaks at a velocity equal to the r.m.s. value.

30th April, 1956, on towers and on an aircraft at the same time and are described in Anon ASTIA (1959a). By taking advantage of the general information given in paragraphs 2.5.1 and 2.5.2, it is possible to compare the data from the two sources. In all the measurements, both on aircraft and at fixed points, the distribution of the energy density of the turbulence agrees well with the distribution given in equation (2.6). This theoretical distribution has two parameters  $L$  and  $\sigma_w$ . By choosing the experimental value of the r.m.s. vertical component of velocity as the value of  $\sigma_w$  there remains only the one parameter  $L$  on which the comparison between theory

## ATMOSPHERIC ENVIRONMENT

and experiment has to be made. This can be done either by making the two distributions have the same energy density at one point or by making them have the same rate of change of energy density at one point. Making the comparison on rate of change of energy density at high inverse wavelengths ( $k$ ) has the advantage that the energy density should be proportional to  $k^{-5/3}$  and a plot of  $\log$  (energy density) against  $\log$  (inverse wavelength) should have a slope of  $-5/3$  and the estimate of the experimental value at one point is made from a best straight line drawn through a number of experimental points. Figure 2.11 shows the comparison between measurements and theoretical distributions; in each case the value of  $L$ , the scale of turbulence, is chosen in this way. In both experiments the energy density of the vertical component of turbulence is the same for the flights at 400 ft and the tower measurements at 300 ft. The scale of turbulence of 300 ft on the tower measurements agrees well with the prediction from Table 2.4. The scale of turbulence in flight inevitably depends more on the ground contours and Table 2.5 indicates that any departure from completely flat terrain would increase the scale of turbulence. A scale of turbulence of 500 ft for flights at 400 ft over fairly flat terrain agrees well with Table 2.5.

### 2.6 GENERAL CONCLUSIONS ON THE STRUCTURE OF ATMOSPHERIC TURBULENCE

Sufficient measurements have been made of the turbulence in the atmosphere at fixed points and on aircraft, under conditions of moderate to good visibility and conditions with little or no precipitation, to demonstrate that the same results will be obtained by both methods.

The measurements which are mainly at less than 1000 ft are all consistent with the contention that the atmosphere is made up of patches of turbulence that are homogeneous and isotropic. The distribution of energy density  $S_w(k)$  at different wavelengths ( $1/k$ ) of the vertical component of the turbulence may be given by

$$S_w(k) = 2L\sigma_w^2[1 + (8/3)(L_1k)^2]/[1 + (L_1k)^2]^{11/6} \quad (2.6)$$

where  $\sigma_w$  = r.m.s. vertical velocity

(repeat)

$L$  = scale of turbulence

$$L_1 = 1.339 (2\pi L)$$

for each patch of turbulence. The scale of turbulence increases with height and over flat terrain is approximately equal to the height. Figure 2.12 shows this relationship for the 23 fixed point measurements of Table 2.4 and 27 flight measurements (25 of Table 2.5, 1 of Fig. 2.7 and 1 of Fig. 2.8). The fixed point measurements give better agreement than those on aircraft as many of the aircraft measurements, particularly at low altitudes, have a scale length rather more than the height. The flights over hilly terrain show a more marked increase at low altitudes. It would seem, therefore, that if flights were made over absolutely flat terrain that the scale of turbulence would be equal to the height. The evidence above 1000 ft is small and extrapolation is inadvisable. All the measurements were in neutral or

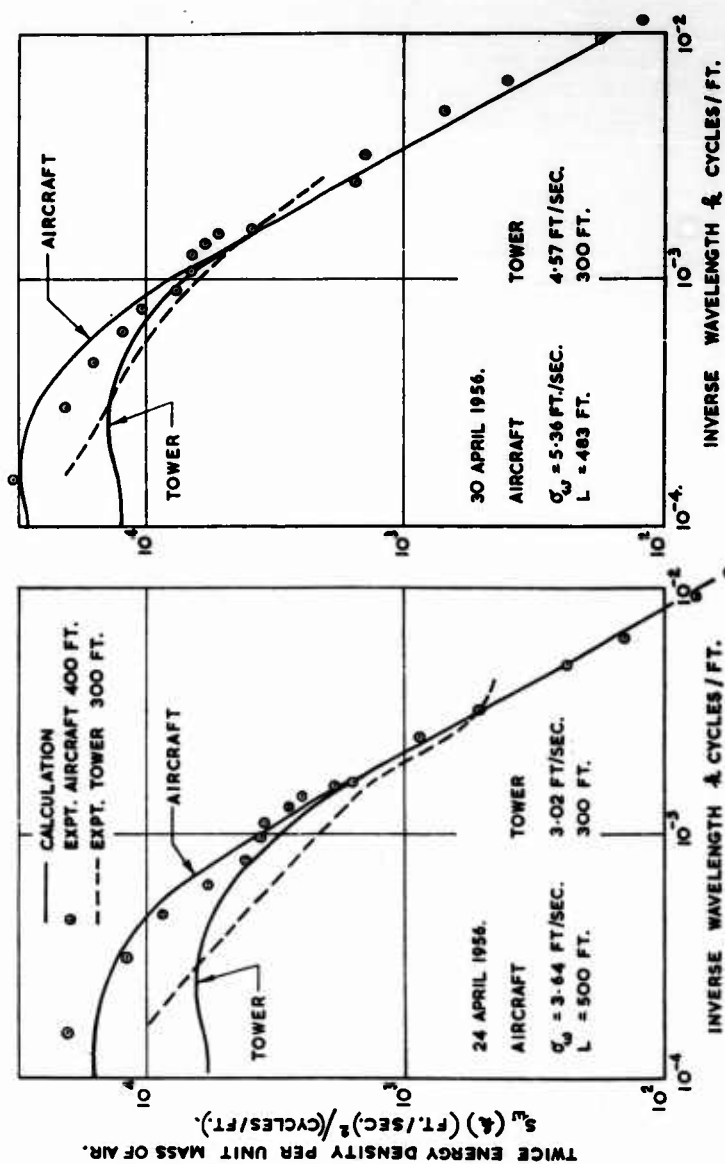


Fig. 2.11. Comparison of turbulence measurements (Anon ASTIA 1959a) on an aircraft and on a tower.  $\sigma_w$  measured and  $L$  estimated to fit distribution

$$S_w(k) = 2L\sigma_w^2[1 + (8/3)(L_k k)^2]/[1 + (L_k k)^2]^{11/6}$$

where  $\sigma_w$  = r.m.s. vertical velocity;  $L_k = 1.339/(2\pi L)$ .



# ATMOSPHERIC ENVIRONMENT

unstable air conditions and the earth's boundary layer would be of the order of 1000 ft. This is an added reason for not extrapolating above 1000 ft. It is worthy of note that Panofsky and McCormick (1959) noticed that in stable conditions (when the boundary layer should be about 100 ft) one run at 300 ft gave a scale of turbulence much less than 300 ft. The information is far from conclusive but until further data become available it is suggested that Fig. 2.12 be used within the earth's boundary layer; as unstable conditions are the only significant ones for aircraft loads this means up to a height of about 1000 ft and therefore up to a scale of turbulence of 1000 ft.

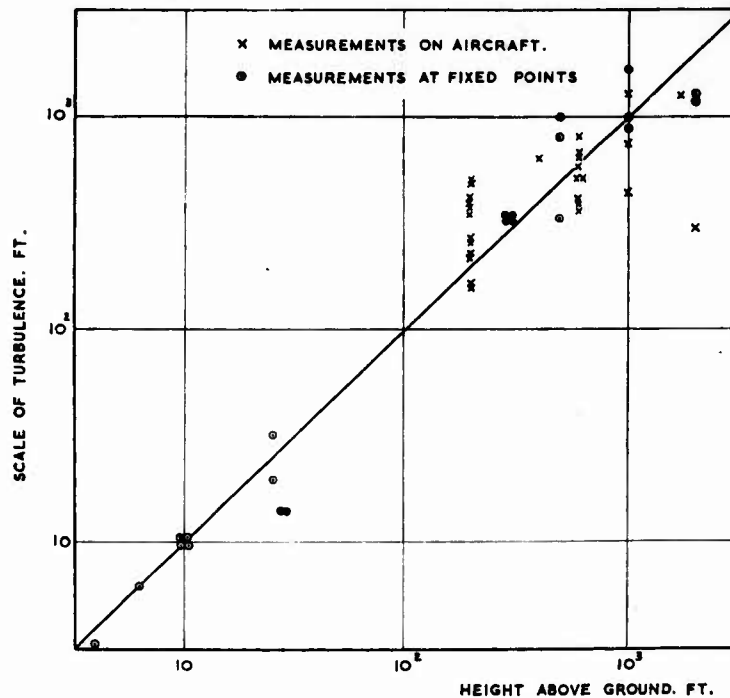


Fig. 2.12. Scale of turbulence at different heights.

Fortunately the dimensions of past aircraft are such that the contribution to their response at wavelengths above 3000 ft would be negligible. This means that the distribution of energy density at wavelengths above 3000 ft does not matter. For a scale of turbulence of 1000 ft or more the simplified formula (2.7) for high inverse wavelengths is not significantly different from equation (2.6) for wavelengths up to 3000 ft. Thus if it is assumed that the scale of turbulence is not less than 1000 ft at heights above 1000 ft it is sufficient to use equation (2.7) for which the two parameters  $L$  and  $\sigma_w$  combine into the single parameter  $(\sigma_w/L^{1/3})$ . Equation (2.7) is more severe than equation (2.6) and it would be advisable to use it for some current and

# MANUAL ON AIRCRAFT LOADS

future designs, which may respond to higher wavelengths, until reliable estimates of the scale of turbulence at heights above 1000 ft become available.

Whilst the measurements are sufficient to estimate accurately enough the shape of the energy density distribution, more extensive testing would be required to estimate the actual value of the intensity of turbulence. The measurements on the B-66B aircraft were made in America over 11,000 miles, which is rather small for this purpose, and the r.m.s. vertical velocity had a mean of 3.17 ft/sec and a standard deviation about the mean of 1.28 ft/sec. About 60 per cent of the flights were over flat terrain and the best estimate of the r.m.s. vertical velocity was a mean and standard deviation of (2.73 ft/sec, 1.1 ft/sec). The estimates from about 500 miles of wind run past a balloon cable in England at 500 to 2000 ft in unstable air conditions were (3 ft/sec, 0.9 ft/sec) and the estimates for about 1000 miles of wind in stable air conditions were (1.7 ft/sec, 0.93 ft/sec). If these are combined as 80 per cent unstable, 20 per cent stable, which is roughly the condition for the aircraft runs, the estimates would be (2.77 ft/sec, 1 ft/sec), and is in good agreement with the much more extensive aircraft measurements in America.

The energy density at high inverse wavelengths is proportional to  $(\sigma_w/L^{1/3})$  as shown in equation (2.7). A comparison of  $(\sigma_w/L^{1/3})$  shows much less variation with terrain than does a comparison of  $\sigma_w$ . In the 42 measurements on the B-66B in winter by K. D. Saunders (1961) in which the scale of turbulence was measured, the values at each height above the ground are the same over flat and over hilly terrain. By adding 39 measurements in summer by Gerlach (1963) to these and assuming the same scale of turbulence to hold, an estimate can be made of average values of  $\sigma_w/L^{1/3}$  as follows:

<i>No. of measurements</i>	<i>Height above ground ft</i>	$(\sigma_w/L^{1/3})$
38	200	0.413
20	600	0.381
22	1000	0.324

It is most probable that over flat and over hilly terrain up to 1000 ft there is turbulence with a scale equal to the height that is approximately homogeneous and isotropic and in addition turbulence at longer wavelengths that depends on the terrain. The energy at longer wavelengths is more apparent in the aircraft measurements, but it is noticeable in one or two of the measurements on balloon cables by F. B. Smith (1961).

Measurements at heights appreciably above the earth's boundary layer of the turbulence energy densities at different wavelengths are very scarce, but Houbolt, Steiner and Pratt (1962) quote a typical value for a flight in cumulus cloud at 15,000 ft and one in a thunderstorm at 40,000 ft. The values of  $(\sigma_w/L^{1/3})$  are 0.840 in the cumulus and 1.825 in the thunderstorm. The

## ATMOSPHERIC ENVIRONMENT

scale of turbulence was estimated for the particular traverse through the thunderstorm to be 5600 ft. There were four other traverses through the same thunderstorm, two of which were rather more intense and two less.

The distribution of velocities associated with the various r.m.s. velocities has been quoted for some of the fixed point records, Fig. 2.6, and for some of the aircraft records, Fig. 2.10. It has also been measured for the flight given in Fig. 2.7 and for the thunderstorm traverse. In all cases the distribution is either Normal or has more high velocities than would be expected on a Normal distribution.

It has been possible to describe the distribution of the density of the turbulence energy at different wavelengths by the same simple formula for the three following forms of turbulence:

- (i) clear air turbulence near the ground,
- (ii) turbulence near and in cumulus clouds,
- (iii) thunderstorms.

Clear air turbulence at high altitudes occurs infrequently and no direct measurements are available to confirm that it is of the same character.

The intensity of the turbulence is known fairly well for that in clear air near the ground and predictions of aircraft loads are compared with measured values in Chapter 10. The extent of this turbulence depends on a variety of meteorological conditions but when it is of moderate or severe intensity it does not seem to begin to fall off until after 1000 ft. In this zone, which is roughly the earth's boundary layer, the major portion of the turbulence has a scale roughly equal to the height and an intensity at low wavelengths (i.e. less than about 3 times the height) that is nearly independent of the contours of the terrain and drops only slowly with height until it reaches the surface of the zone. There is, however, some turbulence at higher wavelengths that depends on the terrain and is apparent in both fixed point measurements and on aircraft. Presumably this breaks down into turbulence of lower wavelengths but on present data the difference in its contribution between hilly and flat terrain is not detectable.

Turbulence is present much of the time in this zone near the ground. Above this zone turbulence is absent most of the time but when it is present it may be much more violent. The data on direct measurements of the air velocities are scarce and the intensity has to be deduced from aircraft load measurements. This is done in Chapter 10 where it is assumed that the distribution of energy at different wavelengths is the same as has been described in this chapter.

## REFERENCES

- |                                     |                               |
|-------------------------------------|-------------------------------|
| Anon ASTIA (1959a)                  | Idrac (1923)                  |
| Anon Institute of Navigation (1960) | Lin (1953)                    |
| Anon Institute of Navigation (1961) | Ludlam (1963)                 |
| Bannon (1963)                       | Ludlam and Scorer (1953)      |
| Byers and Braham (1949)             | McNaughtan (1958)             |
| Crane and Chilton (1956)            | Morgans (1931)                |
| Gerlach (1963)                      | Panofsky and McCormick (1959) |
| Houbolt, Steiner and Pratt (1962)   | Pockels (1901)                |

**MANUAL ON AIRCRAFT LOADS**

Rice (1944)  
Saunders, K. D. (1961)  
Saunders, P. M. (1961)  
Scorer (1957)  
Scorer (1963)  
Sheppard (1963)

Smith, F. B. (1961)  
Taylor, G. I. (1938)  
Wilkinson (1951)  
Wilkinson (1953)  
Zbrozek and Ridland (1960a)

**CHAPTER 3**  
**GROUND ENVIRONMENT**

**CONTENTS**

<b>3.1 Introduction</b>	<b>45</b>
<b>3.2 Physical representation of runways</b>	<b>45</b>
<b>3.3 Measurements of runway elevations along the length</b>	<b>48</b>
<b>References</b>	<b>56</b>

## CHAPTER 3

### GROUND ENVIRONMENT

#### 3.1 INTRODUCTION

At first sight ground loads appear to be more confined than atmospheric turbulence loads, as the routine ground loads all come from the runways and taxi tracks of the aerodromes of the world which are an infinitesimal fraction of the earth's surface; in addition the ground environment is two-dimensional, whereas the atmosphere is three-dimensional. The difficulty with ground loads is to know what are the significant dimensions of the surfaces of runways and taxi tracks, and what are the checks that should be made on changes that might take place with use.

If elevations taken at different positions on the surface are grouped together in some way, such as by wavelengths, care must be taken to ensure that the contributions along the whole length are reasonably uniform and can be added together or that account is taken of this non-linearity in the method of grouping. Non-linearity of an aircraft landing gear is great and effects of non-linearity of the ground input may well accentuate the loading.

#### 3.2 PHYSICAL REPRESENTATION OF RUNWAYS

A physical picture of the characteristics of a runway as it affects loads can be built up by looking at vertical sections at different distances from the centre-line of the runway; aircraft motion in a direction which is not quite along the length of the runway is of negligible importance. Barring local discontinuities the elevation may be regarded as made up of a design profile with superposed roughness along the length at different wavelengths. At the time a runway is built the amplitudes at small wavelengths will probably be reasonably homogeneous along the length of the runway as they are determined primarily by the method of construction. As the runway is used these amplitudes will change, due to construction flaws, severe atmospheric environment and the loads of the aircraft, and may not change uniformly along the length of the runway. With increasingly longer wavelengths there is a contribution to the amplitude from the design profile and the homogeneity reduces. At wavelengths approaching that of the length of the runway the design profile is the only significant parameter. Also a full representation of a runway must include an estimate of the effect of steps, particularly those between adjacent slabs of concrete and of the undesirable features wherever the runway has been repaired or where it crosses another runway or taxi track.

There is a strong indication that steps and other local deformations are more important than the average roughness, along the whole length of the

runway, in producing high loads of interest to the static design. Steps may be important in producing loads of interest in fatigue as they may excite oscillations in the undercarriage; the rate at which these die down will be strongly influenced by the roughness at wavelengths near the natural frequency of the undercarriage. Furthermore all aircraft start their take-off run at about the same place and each aircraft of a particular type will tend to encounter the same loads at the same positions on the runway, e.g. it will have attained approximately the same speed where the runway crosses another runway and the subsequent bouncing will occur at approximately the same positions. There will thus be a tendency for the runway to be worn at or near the steps and at preferential wavelengths. Therefore after a runway has been in use the homogeneity even of the short wavelengths may be suspect and the steps might have become more pronounced.

There is considerable interaction between the effects of the parameter that can be regarded as homogeneous roughness at different wavelengths and the effects of the parameters that are essentially discontinuities of elevation or slope. Thus although the direct effect of a change in one of these parameters may be known, the indirect effect may be such that it is not known whether the total effect would be an improvement or a worsening. Until more is known about the correlation between the elevations of a runway along its length and the loads that are produced in the aircraft it may be necessary to retain measurements that are known to have little direct effect. To assist in the correlation between runway elevations and aircraft loads it is an advantage to attempt to relate the parameters used in the description of the runway elevation measurements to the civil engineering practice used in the runway construction. In this way it might be possible to estimate changes in the aircraft loads that would occur from a knowledge of the changes in the civil engineering practice.

Basic background information can be obtained from an examination of the practice that has been used on the railways and on the roads. Each have developed a measuring cart that is towed along the track that is to be assessed. In each case roughness at wavelengths between about 4 ft and 30 ft is detected from which a numerical value of the roughness is determined. The absolute value depends on the design of the cart and also it increases rapidly with increase in the range of the wavelengths that are measured: however the relative values for any particular design of measuring cart give a good indication of the relative roughness in terms of the loads that will be experienced by the operational vehicles. The main differences to be taken into account in comparing runways and roads are that aircraft speeds and the general dimensions of both aircraft and runway are greater than those for roads and road vehicles. This means that an upper limit of wavelength of 30 ft for roughness measurements of runways is wholly inadequate, that the overall changes in slope should be more gradual and that local pot holes and bumps should be considered on a different scale. The speeds and overall lengths of train coaches are below but nearer to those of aircraft but on current requirements there is a major difference in tolerable slopes. On the French railways the slope must be less than 0.1 per cent, whereas on N.A.T.O. runways the slope need only be less than 1 per cent.

The design criteria for both roads and railways are in two parts; the

## GROUND ENVIRONMENT

first is the design profile, which is defined by changes of direction and by slopes, and the second is the roughness which is defined implicitly by the methods of construction and verified by an empirical number calculated from measurements on an appropriate cart. The design criteria for runways can also be defined by a design profile and a roughness. The design profile does not need to include changes of direction, as runways are always straight and at present the roughness criterion can only be defined by the method of construction. Extensive measurements have been made on the roughness, both by using a cart and by direct measurement of the elevation, but there has not yet been sufficient practical correlation of loads and roughness measurements for an empirical acceptability to be enumerated. The criteria for the profile and construction of N.A.T.O. runways is as follows:

### Profile

- (i) The longitudinal slope of the centre one-third of the runway length must not be more than 1 per cent.
- (ii) The longitudinal slope of the end thirds of the runway length must not be more than  $\frac{1}{2}$  per cent up or 1 per cent down in a direction from the centre outwards to the end of the runway.
- (iii) Changes of longitudinal grade must be at least 1000 ft apart, measured between intersections of tangents.
- (iv) The rate of change of longitudinal slope, at change of grade points must not exceed 0.167 per cent per 100 ft.
- (v) There is also a requirement for a line of sight, 6000 ft long, to be available at 10 ft above the runway surface and for a line of sight, 3000 ft long, at 5 ft above the runway surface.

### Construction

- (i) The level at any point, when checked by engineer's level and staff, must lie within  $\pm \frac{1}{4}$  in. of the designed level.
- (ii) The surface of the runway, when checked with a 10 ft long straight edge, must nowhere show a gap under the straight edge exceeding  $\frac{1}{16}$  in. The straight edge will be laid freely on the runway surface, parallel to the centre-line of the runway for this test. (A similar test is made transversely, but that does not affect the issue under discussion.)

At the speeds at which aircraft operate on runways the criteria for the construction methods have an important influence on the general level of the fluctuating loads that are imposed on the aircraft. They also have an important influence on the general level of the amplitudes of the components of the elevation along the length of the runways at wavelengths up to about 100 ft. This general level may be regarded as a level of runway roughness whether it is considered in relation to measurements of aircraft loads or to measurements of runway elevation. Superimposed on this general level of roughness there are small patches of roughness much rougher than the average and also there are isolated discontinuities in elevation.



The special significance of local troughs can be deduced from a statement by G. J. Morris and Stickle (1960) with regard to a grass runway, "... a noticeably rough place ... is a shallow wash where a road previously crossed. At this location the airplane pitched and bounced significantly more than elsewhere on the runway" and a statement by Hitch (unpublished 1960), "This trough at 1700 ft also produces the largest excursions in vertical accelerations which are substantially in excess of the general level."

The design profile has an important influence, especially at high speed, on changing the mean normal acceleration on which the fluctuations due to general roughness are superimposed. At 75 knots a change in gradient from a plane 1 per cent down to a plane 1 per cent up could produce in the limiting case of an instantaneous change from one to the other an increment of C.G. acceleration of  $\frac{1}{2}g$  on a particular transport aircraft (Vickers). This indicates the order of magnitude of the problem of change of slope; in practical cases the speed could be higher, there would be dynamic overshoot of the loads due to aircraft flexibility and runway roughness, but the change of gradient would not be instantaneous.

### 3.3 MEASUREMENTS OF RUNWAY ELEVATIONS ALONG THE LENGTH

Measurements made of the elevations of about 60 runways in various N.A.T.O. countries are given in A.G.A.R.D. Research Memoranda and a summary of 36 of them is given by W. E. Thompson (1958). With the physical concept of runways, as given in paragraph 3.2, in mind these profiles have been examined further. In making this analysis it should be emphasized that no information is available from the measurements on the small-scale steps in the runways at joints in the concrete slabs.\* Nor is any information available directly on places of crossings of runways or of special roughness. There is the indirect evidence of the former road across a grass runway quoted from G. J. Morris and Stickle, the trough in the runway quoted from Hitch, and a statement by Potter (1957) that a particular portion was an intersection of runways and had just been resurfaced.

The elevations of the runways are measured in feet, every 2 ft along the length at selected distances from the centre-line. These are analysed into waves, which are identified by their reduced frequency, i.e.  $2\pi/\text{wavelength}$  in radians per foot and grouped into frequency bands. The contribution to the roughness at any single frequency could be defined in many ways, but a way must be chosen so that contributions at different frequencies may be added together. By choosing the mean square of the component at each frequency band, addition is possible and the resultant for a combined band is independent of the size or number of the individual bands that make it up. It is appropriate to regard roughness as having the dimensions of length so that the mean square of the elevation component in any frequency band is the component of the (roughness)<sup>2</sup> for that band. The density of the (roughness)<sup>2</sup> will be the average value over the band, i.e. the (roughness)<sup>2</sup>

\* The significant size to the step is that whilst the concrete slabs are subjected to a moving load; this is analogous to the discontinuities at joints in railway lines.

# GROUND ENVIRONMENT

divided by the width of the band. Thus, using feet as the dimension of the length and rad/ft as the dimensions of the reduced frequency, (roughness)<sup>2</sup> will be measured in ft<sup>2</sup> and density of (roughness)<sup>2</sup> in ft<sup>2</sup>/(rad/ft). W. E. Thompson gives for each runway the density of the (roughness)<sup>2</sup> at the following reduced frequencies

$$\pi/80, 2\pi/80, 3\pi/80, \dots, 40\pi/80 \text{ rad/ft.}$$

He determines the (roughness)<sup>2</sup> over the whole frequency band investigated by assuming that the densities are a reasonable average for a frequency bandwidth of  $\pm\pi/160$  about each point. The absolute value of the roughness depends markedly on the value of the density at the lowest frequency and this is influenced appreciably by the "smoothing" process used. However, as the same method is used throughout the values are convenient for comparison amongst themselves but not with other estimates. Coleman and A. W. Hall (1963) point out that the method of computation may produce errors in the estimate of the density at the lowest reduced frequency, i.e.  $\pi/80$  rad/ft, but that the error is confined to this one estimate. In many cases this will give calculated values much greater than they should be. The

Table 3.1. Means and Standard Deviations of Roughness Properties of 36 Runways in N.A.T.O. Countries.

Values are Deduced from W. E. Thompson (1958)

Variable	Arithmetic		Geometric	
	Mean	Standard deviation factor	Mean	Standard deviation factor
Density of (roughness) <sup>2</sup> (ft <sup>2</sup> /rad/ft)				
at reduced frequency $\pi/80$			$7.6 \times 10^{-3}$	3.63
at reduced frequency 0.1			$1.82 \times 10^{-3}$	2.00
at reduced frequency 1			$8.1 \times 10^{-6}$	2.35
Total roughness measured (ft)			0.0550	1.82
Component of roughness at reduced frequency greater than 0.1			0.0118	1.35
For relationship that density of (roughness) <sup>2</sup> is proportional to (reduced frequency) <sup>-n</sup>				
n for reduced frequency between 0.1 and 1	2.38	0.21		
n for reduced frequency between $\pi/80$ and 0.1	3.8	1.3		

# MANUAL ON AIRCRAFT LOADS

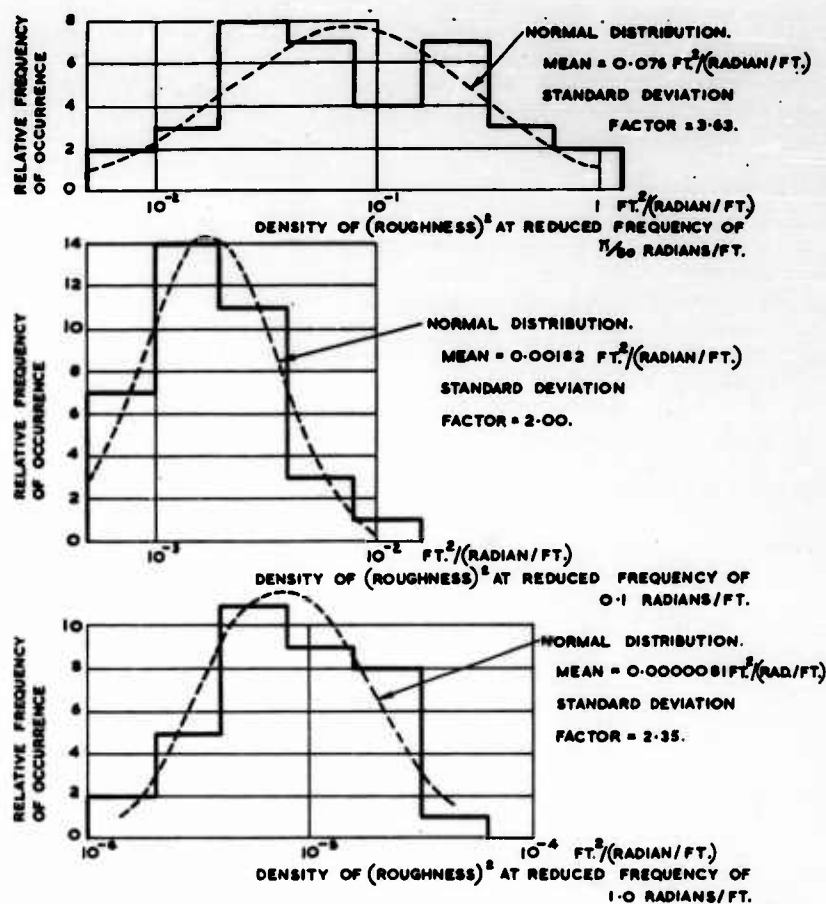


Fig. 3.1. Variation in density of roughness at various frequencies for 36 runway elevations in N.A.T.O. countries.

measurements by Dunn (1962) on 18 runways in U.S.A. do not suffer from this defect at a frequency of  $\pi/80$  rad/ft as the estimates are made to lower frequencies.

W. E. Thompson's data\* have been taken and grouped so that the properties of all the runways can be compared. The curves of the density of roughness have been split up into the frequencies above and below a reduced frequency of 0.1 rad/ft (i.e. wavelength  $20\pi$  ft). Best straight lines were drawn by eye on the log [density of (roughness)<sup>2</sup>] against log (reduced frequency) curves through the actual value at a reduced frequency of 0.1 rad/ft. The slope of the line was noted and an estimate made of the

\* The name used by W. E. Thompson for density of the (roughness)<sup>2</sup> is power spectral density; the numerical values are identical as the same units,  $\text{ft}^2/(\text{rad}/\text{ft})$  are used.

# GROUND ENVIRONMENT

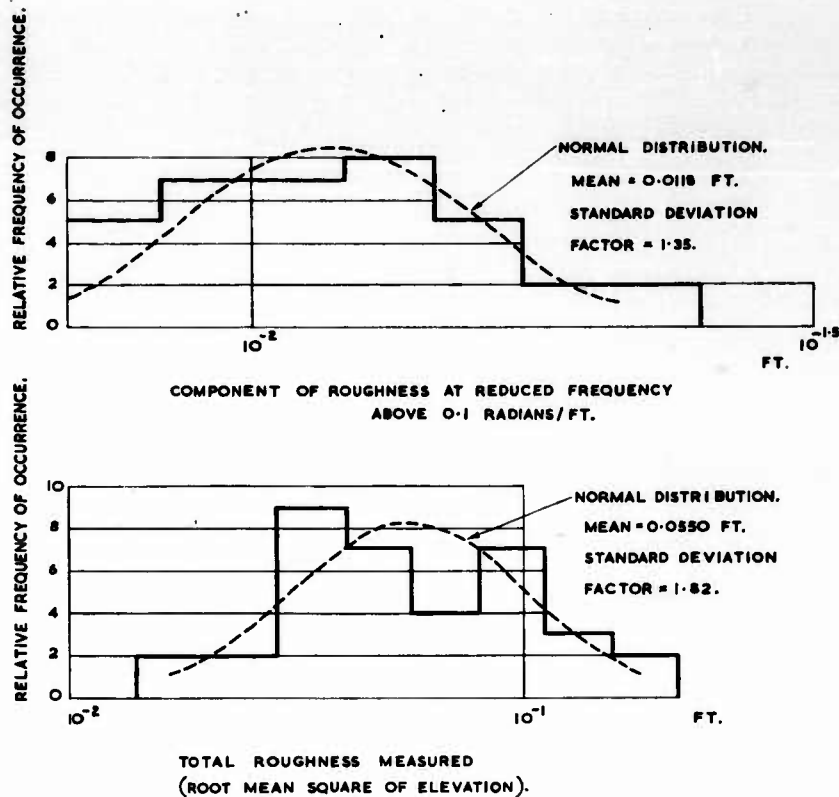


Fig. 3.2. Variation in roughness for 36 runway elevations in N.A.T.O. countries.

component of roughness at reduced frequencies above 0.1 rad/ft. The mean values and the standard deviation are given in Table 3.1 of the following:

- (i) The density of  $(\text{roughness})^2$  at reduced frequencies of  $\pi/80$ , 0.1 and 1 rad/ft.
- (ii) The total roughness measured and the component of roughness above 0.1 rad/ft.
- (iii) The slopes  $n$  above and below 0.1 rad/ft of the curves of  $\log [\text{density of } (\text{roughness})^2]$  against  $\log (\text{reduced frequency})$ , i.e.  $[\text{density of } (\text{roughness})^2]$  proportional to  $(\text{reduced frequency})^{-n}$ .

The geometric mean values of the densities of  $(\text{roughness})^2$  can be used to give a check on the values of mean slopes  $n$  already calculated. The mean slope obtained in this way is 2.36 for reduced frequencies between 0.1 and 1 compared with the mean of 2.38 which was obtained directly. For reduced frequencies between  $\pi/80$  and 0.1 rad/ft it is 4.06 compared with 3.8 but in this range the scatter on slope is very large.

The information given in Table 3.1 is displayed in Figs. 3.1 to 3.4. Figure

# MANUAL ON AIRCRAFT LOADS

3.1 shows the variation in density of roughness at reduced frequencies of  $\pi/80$ , 0.1 and 1 rad/ft (i.e. wavelengths 160,  $20\pi$  and  $2\pi$  ft). Figure 3.2 shows the variation in the total roughness measured and in the component of roughness above a reduced frequency of 0.1 rad/ft. Figure 3.3 shows the variation in slope of the curves of  $\log [\text{density of (roughness)}^2]$  against  $\log$

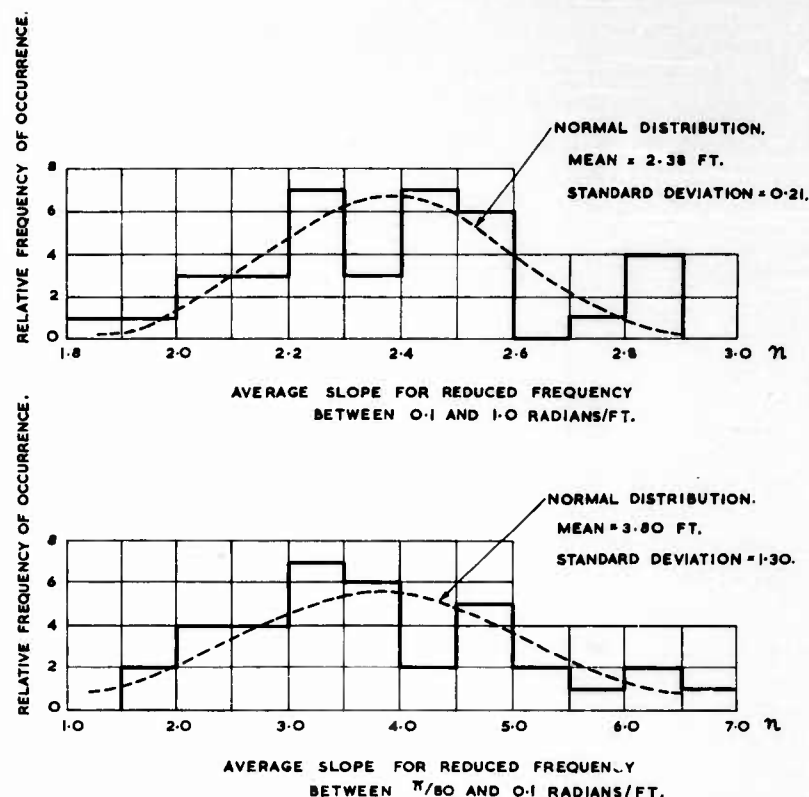


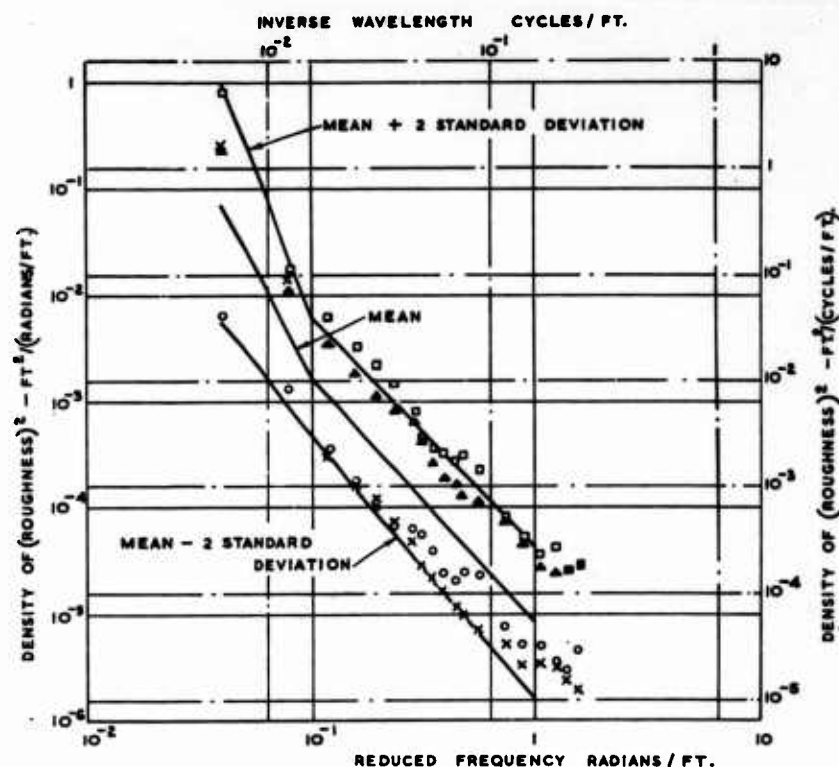
Fig. 3.3. Variation in slope of curves of  $\log \text{density of (roughness)}^2$  against  $\log$  (reduced frequency) for 36 runway elevations in N.A.T.O. countries.

(reduced frequency) for a reduced frequency between  $\pi/80$  and 0.1 rad/ft and for a reduced frequency between 0.1 and 1 rad/ft. Figure 3.4 is a composite picture showing the variation of roughness with reduced frequency. Lines approximately at two standard deviations from the mean are shown, and for comparison those of the two runways with the highest and the two with the lowest roughness at a reduced frequency of 0.1 rad/ft.

It is fortuitous that the runway with the lowest roughness in the range of reduced frequency between 0.1 and 1 had a value amongst the highest at a reduced frequency of  $\pi/80$  rad/ft. However, it serves to illustrate the large

# GROUND ENVIRONMENT

scatter in both shape and magnitude for wavelengths greater than about 60 ft (i.e. reduced frequency of 0.1 rad/ft). At shorter wavelengths there seems to be much more consistency. This is presumably because the roughness at the shorter wavelengths is much more directly connected with the



EXPERIMENTAL POINTS № 4 RUNWAY	○	FOR VALUES ABOVE A
EXPERIMENTAL POINTS № 5 RUNWAY	△	REDUCED FREQUENCY
EXPERIMENTAL POINTS № 11 RUNWAY	□	OF 0.63 EVERY FOURTH
EXPERIMENTAL POINTS № 13 RUNWAY	×	EXPERIMENTAL POINT
		IS SHOWN.

Fig. 3.4. Variation of roughness with reduced frequency for 36 runway elevations in N.A.T.O. countries.

Experimental estimates of density at reduced frequencies less than  $10^{-1}$  rad/ft are all likely to be too high.

methods of laying the runways and the inspections made with a 10 ft straight edge, whereas at longer wavelengths the design profile begins to have an influence. It is not really feasible to do much in respect of the design profile. The analysis has been limited to noting the maximum change of

slope for each runway and the distribution is given in Fig. 3.5; the gradient had to persist for at least 500 ft each side of the intersection of the tangents. All the changes of slope of more than 1 per cent were well faired in but below that value the changes were usually much more rapid than the 0.167 per cent rate of change per 100 ft specified by N.A.T.O. Figure 3.6 gives the profiles of five representative runways (Nos. 3, 15, 23, 26 and 32 of W. E. Thompson (1958)).

The basic measurements that have been used in the analysis of roughness are all of elevations at discrete points by rod and level. Grimes (1957) and

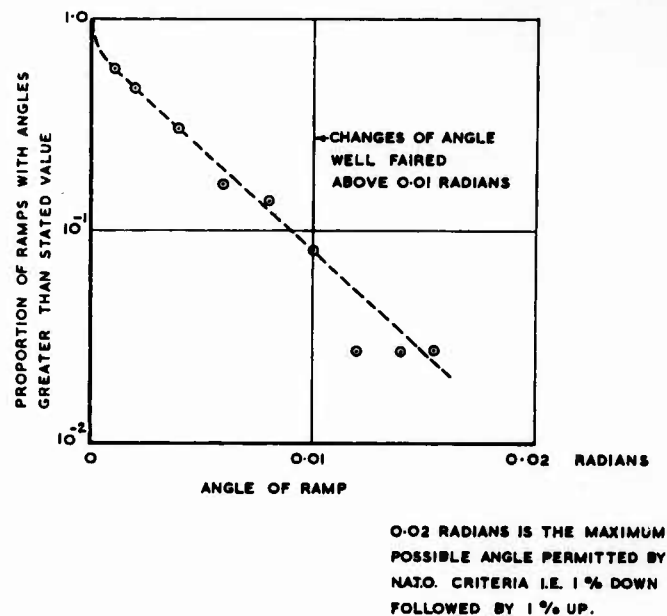


Fig. 3.5. Distribution of changes of gradient in 36 runways in N.A.T.O. countries. The maximum change to increase normal acceleration is taken for each runway.

Plantema and Buhram (1960) describe designs of measuring carts that are automatic means of recording elevations in such a way that substantially the same numerical procedure can be used in the determination of roughness. The time of surveying a runway is greatly reduced and routine checks may become practicable, but the analysis time remains extensive. Dunn (1962) gives a survey by the U.S. Air Force of 18 runways using the cart described by Grimes. The roughness of the runways at different frequencies is similar to that of the 36 N.A.T.O. runways using rod and level measurements. The density of the (roughness)<sup>2</sup> at different frequencies are given in Table 3.2 in the same form as that used in Table 3.1. The values at reduced frequencies of 0.1 and 1 ft<sup>2</sup>/(rad/ft) do not differ significantly from those

# GROUND ENVIRONMENT

of Table 3.1 in mean or standard deviation. Dunn's (1962) curves extend to frequencies appreciably below  $\pi/80 \text{ ft}^2/(\text{rad}/\text{ft})$  and are more reliable than W. E. Thompson's (1958) at  $\pi/80 \text{ ft}^2/(\text{rad}/\text{ft})$ . They are lower, as Coleman and A. W. Hall (1963) suggest they should be, and the mean is close to the

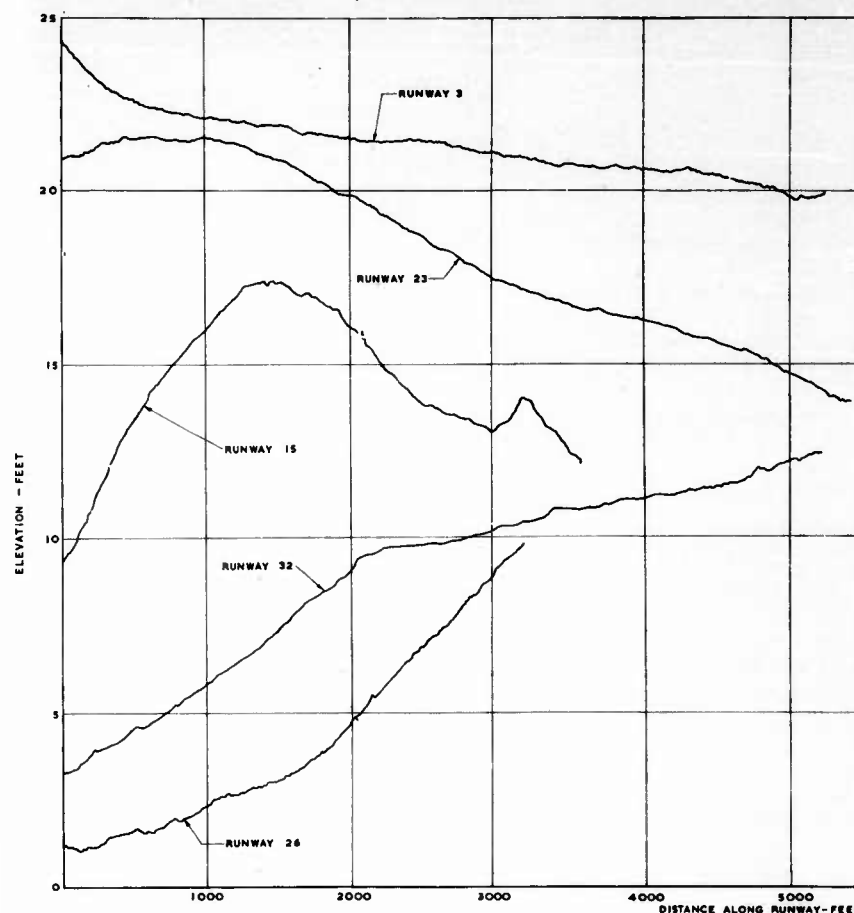


Fig. 3.6. Profiles of 5 typical runways.

Runway numbers are those used by W. E. Thompson (1958): elevation is from arbitrary datum.

extrapolated value from frequencies of 1 and 0.1  $\text{ft}^2/(\text{rad}/\text{ft})$ , but the scatter is much greater.

The description that has been given of runways is of the basic runway. During the course of the year the surface may be polluted by the aircraft



# MANUAL ON AIRCRAFT LOADS

**Table 3.2. Means and Standard Deviations of Roughness Properties of 18 Runways in U.S.A.**

*Values are Deduced from Dunn (1962)*

Variable	Arithmetic		Geometric	
	Mean	Standard deviation	Mean	Standard deviation factor
Density of (roughness) <sup>a</sup> (ft <sup>2</sup> /rad/ft)				
at reduced frequency $\pi/80$			$8.95 \times 10^{-3}$	3.26
at reduced frequency 0.1			$1.08 \times 10^{-3}$	2.00
at reduced frequency 1			$5.95 \times 10^{-6}$	2.30
For relationship that density of (roughness) <sup>a</sup> is proportional to (reduced frequency) <sup>-n</sup>				
<i>n</i> for reduced frequency between 0.1 and 1	2.22	0.2215		
<i>n</i> for reduced frequency between $\pi/80$ and 0.1	2.27	0.715		

*Note to Table 3.2.* Using the logarithms of the geometric means, given in column 3, as a check on the mean values for *n*, shown in column 1, gives 2.257 compared with 2.22 and 2.24 compared with 2.27.

using the runways, by precipitation of rain, snow or hail or by the means used to clear the runways. Also there are additions such as runway lights that may have to be accounted for in particular cases.

## REFERENCES

- |                                |                                   |
|--------------------------------|-----------------------------------|
| Coleman and Hall, A. W. (1963) | Morris, G. J., and Stickle (1960) |
| Dunn (1962)                    | Plantema and Buhram (1960)        |
| Grimes (1957)                  | Potter, D. M. (1957)              |
| Hitch (unpublished 1960)       | Thompson, W. E. (1958)            |

**CHAPTER 4**  
**MANOEUVRES—THEORETICAL ANALYSIS**  
**OF MOTION IN STILL AIR**

**CONTENTS**

4.1 Introduction	59
4.2 Equations of motion	59
4.3 Qualitative description of the manoeuvres of an aircraft	61
4.4 Analytical form of the aerodynamic loads	64
4.5 Analytical form of gravity loads	66
4.6 Symmetrical manoeuvres—linearized equations of motion	66
4.6.1 C.G. normal acceleration in pitching manoeuvres	69
4.6.2 Tail loads in pitching manoeuvres	70
4.7 Asymmetrical manoeuvres—linearized equations of motion	78
4.7.1 Asymmetrical manoeuvres—steady state conditions	80
4.7.2 Asymmetrical manoeuvres—non-steady conditions	83
References	83

## CHAPTER 4

### MANOEUVRES—THEORETICAL ANALYSIS OF MOTION IN STILL AIR

#### 4.1 INTRODUCTION

The atmosphere through which an aircraft travels is, for most of the time, stable and free from turbulence. For the purpose of determining manoeuvre loads it may be regarded that the aircraft is flying through still air as the absolute motion of the air relative to the earth does not influence the loads on the aircraft. There will be times at which an aircraft must manoeuvre in atmospheric turbulence, but for most purposes the theoretical analysis can be made of manoeuvre loads in still air and of atmospheric turbulence loads in the absence of deliberate manoeuvres and the two solutions added together in appropriate proportions. This is done in the present analysis, but care should be taken for any particular aircraft to check whether there may be a serious interaction if manoeuvres are made in atmospheric turbulence.

The properties of the still air environment that need to be known for a theoretical analysis of an aircraft manoeuvre are its density pressure temperature and viscosity. For most manoeuvres these may be taken as constant but in some exceptional cases, such as a long steep dive, the analysis may have to be done in several parts for each one of which the properties are taken to be constant.

#### 4.2 EQUATIONS OF MOTION

The total forces applied to the aircraft are the aerodynamic forces on the external surfaces, the gravitational forces and the forces from the propulsion unit. These forces taken in their entirety are related to the motion of the complete aircraft system in accordance with Newton's Law of Motion. Thus the motion of the centre of gravity of the system and the motion about the centre of gravity are given by

$$\bar{P} = \frac{d}{dt} \text{ (the vector of the momentum)} \quad (4.1)$$

$$\bar{M} = \frac{d}{dt} \text{ (the vector of the moment of momentum)} \quad (4.2)$$

where  $\bar{P}$  and  $\bar{M}$  are the vectors of the applied force and the couple about the centre of gravity and  $t$  is time.

In using these equations care must be taken to include all the elements of the whole momentum, e.g. the momentum of exhaust gases. In the present study of manoeuvres it will be assumed that the mass of the aircraft is a constant at the instantaneous value at which the manoeuvre takes place.

One complication arises immediately as the shape of the aircraft is not constant. The distribution of the forces is deliberately changed by movement of controls and the forces themselves distort the structure which distortion in turn alters the forces. The introduction of these influences immediately into the equations would make them non-linear and extremely complex and *ad hoc* solutions would be all that could be achieved. If the aircraft is represented in a manner that keeps the equations linear, solutions can be made for a range of aircraft and a physical understanding of the loads achieved.

Manoeuvre loads are on the whole applied relatively slowly compared with the frequencies of the natural modes of vibration of the structure, so that the total structural loads consist of slowly varying manoeuvre loads with superimposed vibrations. The effect of the vibrations on the magnitude of the slowly varying manoeuvre loads can usually be neglected and the two effects can be calculated separately without regard to any interaction, thus maintaining a linear system. Even excluding the superimposed vibrations the deflections of the structure under load have an influence on the loads themselves but this is usually sufficiently small for it to be possible to use a single effective deflection for any one manoeuvre. Normally the deflection chosen would be appropriate to the instantaneous value near to the maximum load. In extreme cases the analysis may have to be separated into several periods of time. The rate of change of the manoeuvre loads even on the control surfaces themselves is usually sufficiently slow for the aerodynamic forces to be taken at the steady values that would eventually be attained after a long time at the instantaneous configuration of the aircraft; in special cases it may be necessary to choose an equivalent linear system for the aerodynamic characteristics, in the same way that an equivalent system is chosen for the structural characteristics, by splitting up the analysis into several periods of time.

These simplifications result in a quasi-rigid-body system. The vectorial presentation of equations (4.1) and (4.2) is convenient for visualizing the equations of motion, but if solutions are to be obtained they must be written and analysed in three-dimensional coordinate axes. Each vectorial equation is replaced by three equations, the equations from (4.1) giving linear motions and the equations from (4.2) giving angular motions. In every case the left-hand side of the equation is the sum of the applied forces and the right-hand side the aircraft motion. The coordinate axes must be chosen relative to the configuration of the aircraft and will be taken as axes moving with the aircraft. Simplicity of the right-hand side can be achieved if the principal axes of inertia are chosen, whereas simplicity of the left-hand side can be achieved if axes normally used for aerodynamic measurements are chosen. It should be emphasized that the equations can be transformed from one to the other.

The equations of motion in a form suitable for examining the motion of

## MANOEUVRES

the aircraft are taken relative to the principal axes of inertia ( $Oxyz$ ) and are as follows

$$X = m(\dot{U} - rV + qW) \quad (4.3)$$

$$Y = m(\dot{V} - pW + rU) \quad (4.4)$$

$$Z = m(\dot{W} - qU + pV) \quad (4.5)$$

$$L = A\dot{p} + (C - B)qr \quad (4.6)$$

$$M = B\dot{q} + (A - C)rp \quad (4.7)$$

$$N = C\dot{r} + (B - A)pq \quad (4.8)$$

where  $XYZ$  are the forces in directions  $xyz$

$m$  is the mass of the aircraft

$LMN$  are the moments clockwise about directions  $xyz$

$ABC$  are the moments of inertia of the aircraft about axes  $xyz$

$UVW$  are the velocities in directions  $xyz$

$pqr$  are the angular velocities clockwise about directions  $xyz$ .

The principal axes are taken as follows:

$Ox$  is forward and is the principal axis most nearly along the centre-line of the fuselage

$Oy$  is to the right of a person facing forward in the fuselage

$Oz$  is at right angles to the other two in a direction which gives a right-handed system of axes, i.e. approximately downwards when the aircraft is in straight and level flight.

### 4.3 QUALITATIVE DESCRIPTION OF THE MANOEUVRES OF AN AIRCRAFT

There are wide variations in the aerodynamic shape of aircraft but they all have certain features in common. The crew are invariably housed in a fuselage that approximates to a body of revolution. The other components are aerofoil sections which are attached to this fuselage for the purpose of applying loads to it. Usually they consist of wings and a tail unit: the wings will have control surfaces in the form of ailerons and flaps and the tail unit will consist of a tailplane with elevator and a fin with rudder. In most designs the control surfaces will in addition have tabs. The actual proportions of the various components vary considerably between different designs and there can be a limiting case in which there is no tailplane and the fuselage is virtually buried in the wings. Also it is possible for the tailplane to be replaced by a unit forward of the wings and in addition either of these units may combine the functions of tailplane and elevator by having an all-moving unit.

Before discussing the methods of control employed in aircraft the kinematics of the three-dimensional motion of an aircraft will be examined. The axes have been chosen such that the direction of flight is predominantly along  $Ox$ . The complete motion of such a vehicle can be represented by a

displacement along the moving axis  $Ox$  and rotations about the three moving axes. Changes in forward velocity  $U$  are made by changing  $X$ : the direct way of doing this is by changing the thrust but it can also be done by changing the direction of  $Ox$  relative to the horizontal, so that the gravity forces change. Changes in the direction of flight are made by rotating the principal axes of inertia, but if more than one is rotated at the same time, there will be gyroscopic effects. There is a small consequential change of direction due to change in forward velocity or acceleration in the direction  $Oz$  which, for aerodynamic reasons, changes the incidence of the principal axis  $Ox$  to the direction of flight. If these small changes are neglected the principle adopted in ideal practical manoeuvres, that may be regarded as essentially a flight along a specified path, is one that keeps the rotation about axis  $Oz$  zero. The resultant motion is a velocity  $U$  along  $Ox$  with an acceleration  $\dot{U}$  along  $Oz$ . Such a motion requires forces in directions  $Ox$  and  $Oz$  and couples in all three directions, that in direction  $Oz$ , where there is no rotation, being due to inertia-cross-coupling. A pilot may deliberately or inadvertently depart from this ideal manoeuvre, but the total loads in direction  $Oy$  will never be large. The two main forces on the aircraft are (i) the forward force made up of the algebraic sum of the components of the engine thrust, the aerodynamic drag forces and the weight, and (ii) the normal force made up of the algebraic sum of the components of the aerodynamic lift forces and the weight: the main contribution to the normal aerodynamic forces is from the wings, but there is only a small increase in computing time if the other contributions are included. The controlling couples are supplied mainly by the three main control surfaces; the roll  $L$  is provided by the ailerons, the pitch  $M$  by the elevator and tailplane and the yaw  $N$  by the fin and rudder. In the resulting motion the aircraft will be inclined at an angle to its direction of motion and the main aerodynamic forces will change accordingly. The system is non-linear and a rigorous treatment could only be made for specific numerical values. However, it is possible to make simplifying assumptions that maintain an equivalent linear system and allow a study to be made of the physical aspects of the motion.

The main simplification arises from the fact that the controls are not capable of producing large angular velocities in pitch or yaw, nor is there any advantage to be gained by having such a capability. Thus it is possible to assume  $q$  and  $r$  are small and to ignore completely  $q^2$ ,  $r^2$  and  $qr$ . The next simplification is that  $U$  may be assumed to be constant during any manoeuvre from straight flight. For many manoeuvres changes in the gravity component may be ignored: this linearizes the equations but Thomas and Price (1960) have shown that it is not necessary to ignore the gravity terms completely to linearize the equations. With these simplifications equation (4.3) disappears,  $U$  becomes a constant in equations (4.4) and (4.5) and equation (4.6) becomes

$$L = A\dot{p} \quad (4.9)$$

A general manoeuvre of an aircraft will involve the solution of all five equations but it can often be regarded as made up of simpler manoeuvres involving the equations singly or in pairs. In such cases that the system may be assumed to be linear the solution for the general manoeuvre is the

## MANOEUVRES

sum of a number of simple manoeuvres. The following are all the possible manoeuvres that can be made:

1. Forward acceleration
2. Roll
3. Pitch
4. Yaw
5. Pitch and Yaw
6. Roll and Pitch
7. Roll and Yaw
8. Roll, Pitch and Yaw

The first three manoeuvres will have the angle of yaw zero and no yawing couple, and are normally regarded as symmetrical manoeuvres. In all the others the angle of yaw and the yawing couple will not both be zero and these manoeuvres are termed asymmetrical manoeuvres.

The simplest of all manoeuvres is change in forward speed alone and is given by the simplified form of equation (4.3) as

$$X = m\dot{U} \quad (4.10)$$

It has already been stated that this is omitted from studies of all other manoeuvres. Pure roll is given by equation (4.9) (the simplified form of equation (4.6))

$$L = A\dot{p} \quad (4.11)$$

For this to be possible  $p$  must not induce changes in the terms on either side of equations (4.4) and (4.5), which means that even apart from gravity forces the  $x$  axis must remain in the line of flight; this is hardly a practical case. Pure pitch is given by the simplified form of equations (4.5) and (4.7) as

$$\left. \begin{aligned} Z &= m(\dot{W} - qU) \\ M &= B\dot{q} \end{aligned} \right\} \quad (4.12)$$

Pure yaw is given by the simplified form of equations (4.4) and (4.8) as

$$\left. \begin{aligned} Y &= m(\dot{V} + rU) \\ N &= C\dot{r} \end{aligned} \right\} \quad (4.13)$$

Pitch and yaw would be given by the simplified equations (4.4), (4.5), (4.7), (4.8) (equation (4.6) vanishing because  $qr$  is small) as

$$\left. \begin{aligned} Y &= n(\dot{V} + rU) \\ Z &= m(\dot{W} - qU) \\ M &= B\dot{q} \\ N &= C\dot{r} \end{aligned} \right\} \quad (4.14)$$

For the other manoeuvres all five equations are involved and the simplification by omitting a few terms is not great.

For any of these manoeuvres to be attainable it must be possible to apply the three control couples separately and for the trim of the aircraft in other directions to be unaltered. The tailplane plus elevator is probably the purest



control and induces almost entirely a pitching couple and normal force in the complete aircraft. The control action involving fin and rudder will influence the normal forces on the wings, as well as the yawing couples and side forces, due to the change in forward velocity over the two wings. Also the aileron control will influence the normal forces over the two wings as the forces on the ailerons can only approximate to an equal up and down force each side. However a good understanding of the loads on an aircraft can be achieved by considering many of the manoeuvres as being reasonably pure.

For the manoeuvres to be practicable it must be possible for a human pilot or an automatic pilot to apply the controls, which in turn means that it must be possible to detect changes in magnitude and direction of the motion. In the case of roll, pitch or yaw applied separately, the human senses are adequate, but if there is a combination of roll and either pitch or yaw such that there is inertia cross-coupling, Meyer (1957) and Nethaway and Clark (1960a) have found that a pilot is less able to detect changes in normal acceleration. Thus in simple manoeuvres the pilot can readily increase or decrease the severity, but in manoeuvres involving inertia cross-coupling, whilst the corrective controls are known theoretically the pilot is not able to sense fully the necessity for making the correction.

#### 4.4 ANALYTICAL FORM OF THE AERODYNAMIC LOADS

In all forms of the equations of motion (4.1) to (4.14) the left-hand side is the applied force at or the applied couple about the centre of gravity, and the right hand side is the corresponding rate of change of momentum or moment of momentum. The aerodynamic component of the applied force or couple will depend on the distortion and displacement of the whole aircraft relative to the direction of flight under the action of the controls. The aerodynamic derivatives relating the force to the displacement will depend on the time taken for the displacement to be achieved (derivatives for unsteady motion), the magnitude of the displacement and other aerodynamic conditions such as Mach number; it will depend also on the elastic distortion. The equations are linearized by neglecting coefficients for unsteady motion and taking constant values for the derivatives for any one manoeuvre. In some of the manoeuvres that are considered the manoeuvre is split up into several time periods with derivatives that are constant for each period but differing from one period to the next.

If the aircraft is made to rotate about its principal axes of inertia the subsequent motion for a roll will be different in character from the motion initiated by rotation about either of the other two axes. In the hypothetical case of a pure roll the motion is entirely an angular velocity with no linear velocity of the centre of gravity other than in a forward direction. The total aerodynamic couple will be

$$L_a = l_p p + l_z \xi \quad (4.15)$$

where  $l_p$  is the coefficient of the angular velocity (derivative)  
 $l_z$  is the coefficient of the aileron angle (derivative)  
 $\xi$  is the aileron angle.



# MANOEUVRES

In both pitch and yaw the control forces are in a single direction at a distance from the aircraft centre of gravity and consequently produce a force at and a couple about the centre of gravity. In pitch the resultant control force on the elevators alters the incidence of the wings to the direction of flight, which in turn alters the normal force on the whole aircraft; contributions from the body and change in elevator incidence can usually be neglected. In yaw the resultant control force on the rudder alters the incidence of the fuselage to the direction of flight, which in turn alters the side force on the whole aircraft; in this case contributions from the wings and change in rudder incidence can usually be neglected. In equations (4.12) the total aerodynamic force and couple will be

$$\left. \begin{aligned} Z_a &= z_W(W - W_0) - mg \\ M_a &= m_q q + m_\eta \eta + m_{\dot{W}} \dot{W} + m_W(W - W_0) \end{aligned} \right\} \quad (4.16)$$

where  $m_q$ ,  $m_\eta$ ,  $m_{\dot{W}}$ ,  $m_W$ ,  $z_W$  are the derivatives respectively for  $q$ ,  $\eta$ ,  $\dot{W}$  and  $(W - W_0)$

$W_0$  is the value of  $W$  for straight and level flight

$\eta$  is the angular deflection of the elevator from the position for straight and level flight.

Similarly in equations (4.13) the total aerodynamic force and couple will be

$$\left. \begin{aligned} Y_a &= y_V V \\ N_a &= n_r r + n_\zeta \zeta + n_{\dot{V}} \dot{V} + n_V V \end{aligned} \right\} \quad (4.17)$$

where  $y_V$ ,  $n_r$ ,  $n_\zeta$ ,  $n_{\dot{V}}$ ,  $n_V$  are the derivatives respectively for  $V$ ,  $r$ ,  $\zeta$ ,  $\dot{V}$  and  $V$ .  $\zeta$  is the rudder angle.

For this to be possible the yawing must not induce rolling, but in practice this could only be done by the application of aileron, which in turn would produce a further yawing couple.

For the case of pitch and yaw combined there is no coupling between the equations and the separate solutions of equations (4.12) and (4.13) may be added together in any proportions.

The determination of any manoeuvre consisting of a combination of roll and any other rotation necessitates the solution of all five equations (4.4) to (4.8) (with equation (4.6) simplified to the form of equation (4.9)). In this general case the left-hand side of the equations cannot be given by equations (4.15) and (4.17) as they stand, in equation (4.15) there must be two additional terms due to yaw and in equation (4.17) two additional terms due to roll; equation (4.16), however, remains unaltered. These aerodynamic forces and couples for this general case are

$$\left. \begin{aligned} Y_a &= y_V V \\ Z_a &= z_W(W - W_0) \\ L_a &= l_p p + l_\zeta \zeta + l_V V + l_r r \\ M_a &= m_q q + m_\eta \eta + m_{\dot{W}} \dot{W} + m_W(W - W_0) \\ N_a &= n_r r + n_\zeta \zeta + n_{\dot{V}} \dot{V} + n_V V + n_p p + n_\zeta \zeta \end{aligned} \right\} \quad (4.18)$$

When these values are substituted into equations (4.4) to (4.8) the equations become non-linear due to the inertia coupling terms  $pW$ ,  $pV$ ,  $(A - C)rp$  and

## MANUAL ON AIRCRAFT LOADS

$(B - A)pq$  respectively in equations (4.4), (4.5), (4.7) and (4.8). Thomas and Price (1960) have shown that the equations can be linearized if  $p$  is replaced by

$$p = p_0 + p^* \quad (4.19)$$

where  $p_0$  is constant

$p^*$  is small in the same way that  $q$  and  $r$  are small

so that  $pW$ ,  $pV$ ,  $(A - C)rp$  and  $(B - A)pq$  are replaced by  $p_0W$ ,  $p_0V$ ,  $(A - C)p_0r$  and  $(B - A)p_0q$  respectively.

### 4.5 ANALYTICAL FORM OF GRAVITY LOADS

The weight of the aircraft acts vertically so that if the  $x$  axis makes an angle  $\theta$  with the horizontal and the  $y$  axis rolls through an angle  $\phi$  from the horizontal then the gravity loads in equation (4.4) and in equation (4.5) are respectively

$$\begin{aligned} Y_g &= mg \cos \theta \sin \phi \\ Z_g &= mg \cos \theta \cos \phi \end{aligned} \quad (4.20)$$

The rate of change of  $\phi$  is equal to  $p$ , the angular velocity of roll, i.e.  $\dot{\phi} = p \times \phi_0$ .

If  $\cos \theta$  may be regarded as approximately unity and  $p = p_0 + p^*$ , as in equation (4.19), these gravity loads reduce to

$$Y_g = mg (\sin \phi_0 \cos p_0 t + \cos \phi_0 \sin p_0 t) \quad (4.21)$$

$$Z_g = mg (\cos \phi_0 \cos p_0 t - \sin \phi_0 \sin p_0 t) \quad (4.22)$$

These components may be inserted in equations (4.4) and (4.5) without making them non-linear.

In solving these linearized equations of motion it is convenient to split up the manoeuvres into symmetrical and asymmetrical ones.

### 4.6 SYMMETRICAL MANOEUVRES—LINEARIZED EQUATIONS OF MOTION

The only three possible symmetrical manoeuvres are forward acceleration, pure roll and pure pitch. The forward acceleration alone is the trivial case of  $X = m\dot{U}$  where  $X$  is the net thrust and  $U$  the forward velocity. The pure roll is only a little more complex and is given by combining equations (4.11) and (4.15) as

$$Ap - I_p \dot{p} = I_z \dot{\xi} \quad (4.23)$$

This is soluble in closed form for all functions of  $\xi$  as

$$p = \exp(I_p t/A) / (I_z \dot{\xi}/A) \exp(-I_p t/A) dt \quad (4.24)$$

The pure pitch condition is solved for the case in which the forward velocity and gravity terms remain unaltered throughout the manoeuvre by combining equations (4.12), (4.16) and (4.20) with  $\phi = 0$  to give

$$\begin{aligned} m\dot{W} - z_W(W - W_0) - mqU + mg(1 - \cos \theta) &= 0 \\ B\dot{q} - m_q q - m_W \dot{W} - m_W(W - W_0) &= m_n \eta \end{aligned} \quad (4.25)$$

# MANOEUVRES

These equations are put into non-dimensional form using the notation adopted by Czaykowski (1955) and Neumark (1958) with minor changes, and the solution follows the same general lines. The gravity term is removed by replacing  $W$  by its incremental value  $w$ . For this to be permissible the change in the gravity term in direction  $Oz$  must be negligible. The equations become

$$D\bar{w} + \frac{1}{2}a\bar{w} - \bar{q} = 0 \quad (4.26)$$

$$\chi D\bar{w} + \omega\bar{w} + D\bar{q} + \nu\bar{q} = -\delta\eta \quad (4.27)$$

where  $D = \frac{d}{d\tau}$

$S$  = wing area

$\rho$  = true air density

$\bar{t} = m/(\rho SU)$

$\bar{w} = w/U$

$\bar{q} = \bar{t}q$

$\tau = t/\bar{t}$

$C_L$  = lift coefficient of aeroplane

$\alpha$  = wing incidence incremental value

$a = \partial C_L / \partial \alpha$

$\chi, \omega, \nu, \delta$  are derivatives in non-dimensional form

A number of assumptions have been stated as they have been introduced in forming the equations. The following is a list of these assumptions.

- (1) The forward speed and corresponding Mach number are constant.
- (2) The component of the aircraft weight in the direction of the principal axis  $Oz$  remains the same.
- (3) The elastic distortion of the structure is neglected.
- (4) The contribution of lift due to elevator deflection is neglected in equation (4.26).
- (5) The contribution of tailplane pitching moment due to elevator deflection is neglected in equation (4.27).
- (6) The aerodynamic derivatives are constant throughout the manoeuvre and independent of the time of application, i.e. unsteady lift coefficients neglected.

Assumptions (4) and (5) are normally adopted, but Czaykowski (1955) shows how these effects can easily be taken into account if required. In cases where use of assumptions (3) and (6) produce serious errors a correction can be made by splitting up the analysis into several periods of time during each of which the assumptions are made to hold.

The operational solutions to equations (4.26) and (4.27) are

$$\bar{w} = -\delta\eta/(D^2 + 2RD + R^2 + J^2) \quad (4.28)$$

$$\bar{q} = -\delta(D + \frac{1}{2}a)\eta/(D^2 + 2RD + R^2 + J^2) \quad (4.29)$$

where  $R = \frac{1}{2}(\frac{1}{2}a + \nu + \chi)$  = the dimensionless damping factor

$J = \sqrt{(w + \frac{1}{2}\nu a - R^2)}$  = the dimensionless frequency of the short-period oscillation.

A pitch manoeuvre is performed by moving the elevator without altering any of the other controls. This is identical to putting  $\eta$  as a function of non-dimensional time  $\tau$  in these equations. Finally the loads on the aeroplane are obtained as functions of  $\bar{w}$  and  $\bar{q}$ . The total loads are the sum of the inertia and aerodynamic loads added to the gravity loads which are taken to remain unaltered. The total loads are the sum of the inertia and aerodynamic loads added to the gravity loads which are taken to remain unaltered. The total system is essentially a tail load and wing load with a resultant load on the fuselage. For most purposes it is sufficient to know the maximum loads; within the accuracy of the basic assumptions the inertia and aerodynamic loads on the wings are both a maximum when the normal acceleration is a maximum, but the maxima inertia and aerodynamic loads on the tail may not coincide and in that case time is a more important parameter.

The total incremental load on the wing is proportional to the incremental incidence  $\bar{w}$ . This can be retained in non-dimensional form as the incremental normal acceleration  $n_g$  and is given by

$$n = a\bar{w}/C_{LE} \quad (4.30)$$

where  $C_{LE}$  = the datum value of  $C_L$ .

The total load on the tailplane is a combination of the inertia loads and the aerodynamic loads. The inertia loads may be given as normal acceleration as before, but this time there is a second component due to the angular acceleration in pitch about the aircraft centre of gravity. Thus the incremental normal acceleration  $n_T g$  at the tail is given by

$$\begin{aligned} n_T &= n - (l/g)Dq \\ &= a\bar{w}/C_{LE} - (2/\mu C_{LE})D\bar{q} \end{aligned} \quad (4.31)$$

where  $l$  = distance of the reference point of the tail from the centre of gravity of the aircraft

$$\mu = m/(\rho S l)$$

The aerodynamic load on the tail unit is in two parts, one on the whole tailplane and the other on the elevator alone. The total incremental aerodynamic load  $P_a$  is given by

$$\begin{aligned} P_a &= \frac{1}{2}\rho U^2 S' (a_1 \alpha'_{eff} + a_2 \eta) \\ \alpha'_{eff} &= (1 - d\varepsilon/d\alpha)\bar{w} + \bar{q}/\mu + (d\varepsilon/d\alpha)D\bar{w}/\mu \end{aligned} \quad (4.32)$$

where  $\alpha'_{eff}$  = effective tail incidence, incremental value

$S'$  = tailplane area

$C'_L$  = lift coefficient of tailplane

$$a_1 = \partial C'_L / \partial \alpha'_{eff}$$

$$a_2 = \partial C'_L / \partial \eta$$

$\varepsilon$  = downwash angle at the tail.

In the limiting case of an all-moving tailplane  $a_2 = a_1$  and  $\eta$  is the control movement of the whole tailplane.

Summarizing, the loads on the wings are given by equation (4.30) and the loads on the tailplane by equations (4.31) and (4.32) where  $\bar{w}$  and  $q$  are

## MANOEUVRES

given by equations (4.28) and (4.29). The loads on the fuselage are the resultant of the loads on the wings and tailplane together with an appropriate normal acceleration varying linearly along its length to balance those on the wings and on the tailplane.

### 4.6.1. C.G. Normal Acceleration in Pitching Manoeuvres

The total incremental load on the wings is directly proportional to the incremental normal acceleration of the centre of gravity of the aircraft, and for this purpose it is sufficient to solve equation (4.28) for  $\ddot{w}$  using the relationship (4.30) to give the normal acceleration. If the elevator is applied in a variety of ways up to a prescribed angle  $\eta_\infty$  and then held there indefinitely, the aircraft will finally attain a steady circling condition with a constant incremental normal acceleration  $n_\infty g$ . The acceleration can be described most generally by giving it in terms of  $n_\infty$ , in this way the maximum acceleration is identified by the percentage that it exceeds  $n_\infty$ .

The value of  $n_\infty$  is obtained by putting  $\eta = \eta_\infty$  in equation (4.28) and ignoring the operator  $D$ . Thus

$$n_\infty = -a\sigma\eta_\infty/C_{LE}(R^2 + J^2) \quad (4.33)$$

The variation of  $n$  with time before it settles down to its limiting value depends on the variation of  $\eta$  with time. A family of distributions can be achieved by considering a ramp shape for  $\eta$  in which  $\eta$  increases linearly for time  $\tau_1$  to a value  $\eta_\infty$  and thereafter remains constant. This is algebraically equivalent to a linear input starting at time  $\tau = 0$  and another of the same slope but opposite sign starting at time  $\tau = \tau_1$ . Neumark (1958) gives the solution as

$$\text{for } 0 < \tau < \tau_1 \quad n/n_\infty = F(\tau)/\tau_1 \quad (4.34)$$

$$\text{for } \tau_1 \leq \tau \quad n/n_\infty = \{F(\tau) - F(\tau - \tau_1)\}/\tau_1 \quad (4.35)$$

$$\text{where } F(\tau) = [\tau - 2R/(R^2 + J^2) + \{2R/(R^2 + J^2)\} \cos J\tau \exp(-R\tau) + \{- (J^2 - R^2)/J(R^2 + J^2)\} \sin J\tau \exp(-R\tau)]$$

In the limiting case of  $\tau_1$  becoming zero the ramp has become a step and equation (4.35) reduces to

$$\begin{aligned} n/n_\infty &= \frac{d}{d\tau} F(\tau) \\ &= 1 - \{\cos J\tau + (R/J) \sin J\tau \exp(-R\tau)\} \end{aligned} \quad (4.36)$$

The maximum value of  $n$  for the ramp shape occurs after  $\tau = \tau_1$  and is given by

$$\begin{aligned} n_{\max}/n_\infty &= 1 + E = 1 + \{\exp(-R\tau_m + R\tau_1)/\tau_1\} \cdot \sqrt{[1 + \exp(-2R\tau_1) - 2 \cos J\tau_1 \exp(-R\tau_1)]/J^2 + R^2} \end{aligned} \quad (4.37)$$

where  $\tau_m$  the time at which the maximum occurs is given by

$$\begin{aligned} \tan(J\tau_m - J\tau_1) &= [J\{\exp(R\tau_1) - \cos J\tau_1\} - R \sin J\tau_1] / \\ &\quad [R\{\cos J\tau_1 - \exp(R\tau_1)\} - J \sin J\tau_1] \end{aligned} \quad (4.38)$$

The normal acceleration is a decaying oscillation and a typical curve of normal acceleration against time for  $R/J = 0.4$ ,  $J\tau_1 = \pi/2$ , is shown in

Fig. 4.1. The acceleration reaches its greatest value after the elevator has reached its full angle and thereafter the maxima and minima occur at non-dimensional time intervals of  $\pi$ . For other rates of application of elevator the shape of the acceleration-time curve will be similar but the first and greatest overshoot and the time at which it occurs will be different. The

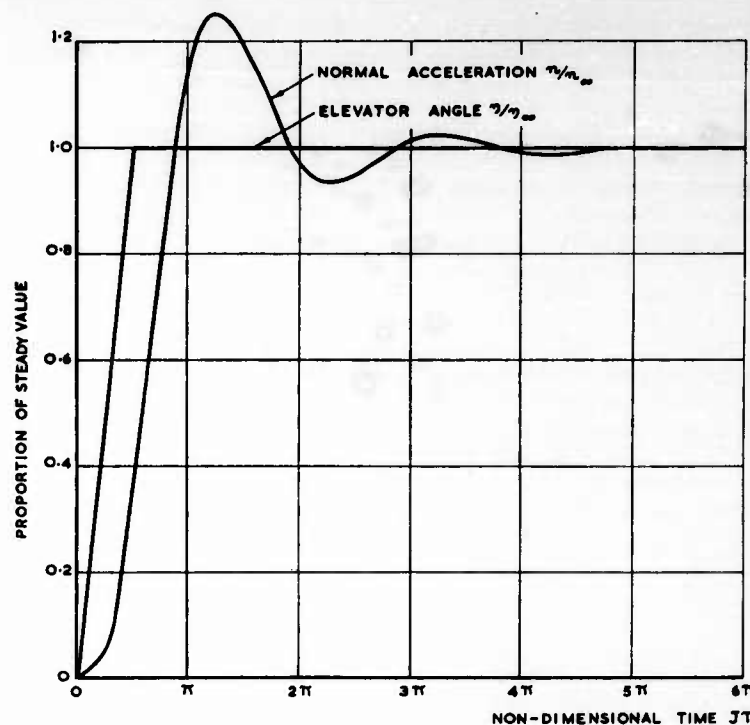


Fig. 4.1. Variation in normal acceleration at aircraft C.G. for a ramp shaped elevator movement.

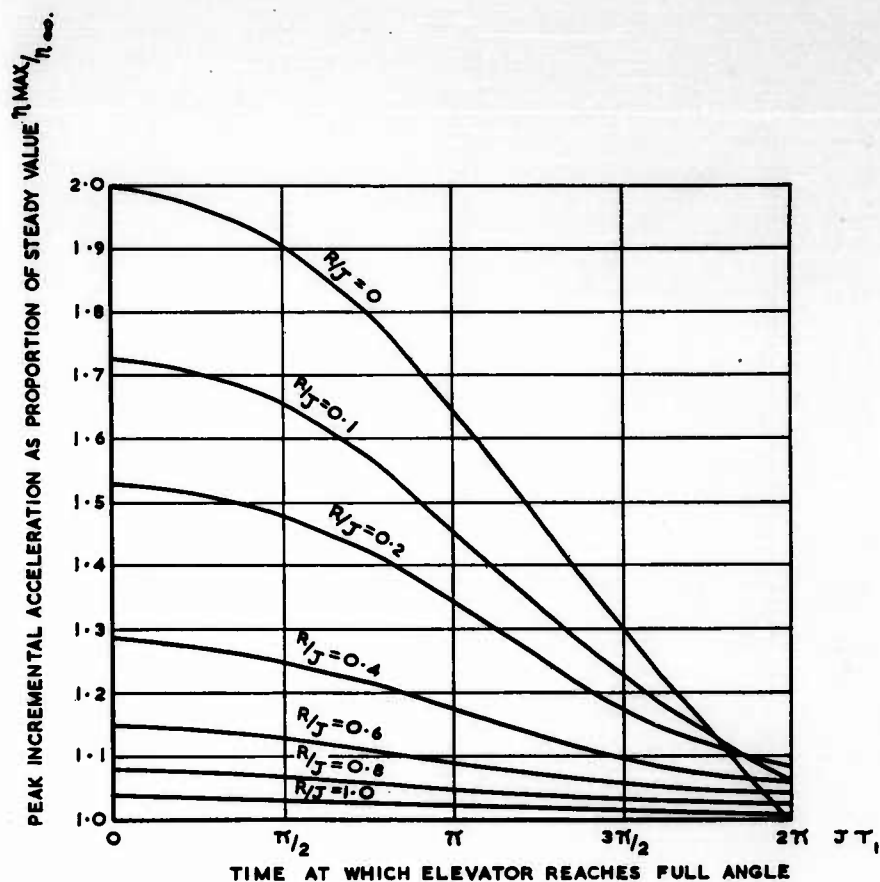
Ratio of damping factor to natural frequency of pitching oscillation, in non-dimensional terms of  $R/J$ , equals 0.4.

magnitude of the greatest normal accelerations and the time at which they occur are shown in Fig. 4.2 for a range of  $R/J$  up to 1.0 and a range of  $J\tau_1$  up to  $2\pi$ .

#### 4.6.2. Tail Loads in Pitching Manoeuvres

Unlike the wings, the inertia and aerodynamic loads on the tail (even apart from the elastic distortion of the structure which is neglected in accordance with assumption 3) do not occur completely in phase. The inertia loads will be directly proportional to the normal acceleration as given by equation (4.31), and the aerodynamic loads will be given by equation (4.32).

The steady state condition is determined by substituting  $\eta = \eta_\infty$  and



#### A - MAXIMUM ACCELERATIONS.

Fig. 4.2. The maximum normal accelerations at aircraft C.G. and time at which it occurs for a range of ramp shaped elevator movements and a range of natural frequencies of pitching oscillations.

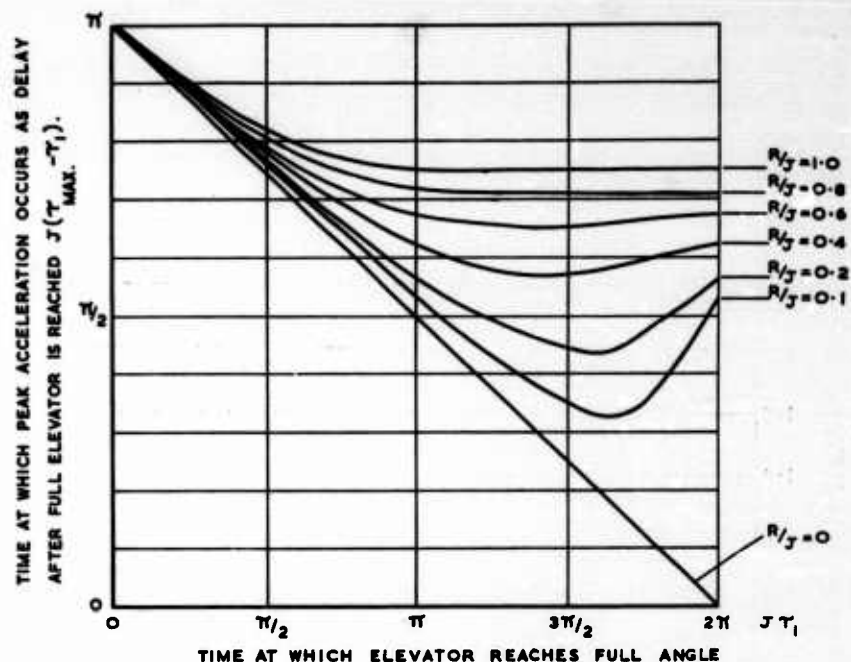
$R/J$  is the ratio of the damping factor to the natural frequency of the pitching oscillation;  
 $J\tau_1$  is time in non-dimensional units.

ignoring the operator  $D$  in equations (4.28), (4.29), (4.31) and (4.32). Thus

$$n_{T\infty} = n_{\infty} = -a\sigma\eta_{\infty}/C_{LE}(R^2 + J^2) \quad (4.39)$$

$$P_a = -\frac{1}{2}\rho U^2 S'(a_1\alpha'_{eff\infty} + a_2\eta_{\infty}) \quad (4.40)$$

where  $\alpha'_{eff\infty} = -\{\delta\eta_{\infty}/R^2 + J^2\}\{1 - d\epsilon/d\alpha + \frac{1}{2}a/\mu\}$



#### B-TIME AT WHICH PEAK ACCELERATION OCCURS.

Fig. 4.2. (continued)

Neumark (1958) shows for the same ramp shape that was used for wings that

$$\text{for } 0 < \tau < \tau_1 \quad n_T/n_{\infty} = \left[ F(\tau) - (1/\mu) \frac{d}{d\tau} F(\tau) - (2/\mu a) \frac{d^2}{d\tau^2} F(\tau) \right] / \tau_1 \quad (4.41)$$

$$\text{for } \tau_1 \leq \tau \quad n_T/n_{\infty} = \left[ F(\tau) - (1/\mu) \frac{d}{d\tau} F(\tau) - (2/\mu a) \frac{d^2}{d\tau^2} F(\tau) \right] / \tau_1 - \left[ F(\tau - \tau_1) - (1/\mu) \frac{d}{d\tau} F(\tau - \tau_1) - (2/\mu a) \frac{d^2}{d\tau^2} F(\tau - \tau_1) \right] / \tau_1 \quad (4.42)$$



# MANOEUVRES

$$\text{for } 0 < \tau < \tau_1 \quad \alpha'_{\text{eff}}/\alpha'_{\text{eff}\infty} = \left[ F(\tau) + \lambda \frac{d}{d\tau} F(\tau) \right] / \tau_1 \quad (4.43)$$

$$\text{for } \tau_1 \leq \tau \quad \alpha'_{\text{eff}}/\alpha'_{\text{eff}\infty} = \left[ F(\tau) - \lambda \frac{d}{d\tau} F(\tau) \right] / \tau_1 - \left[ F(\tau - \tau_1) + \lambda \frac{d}{d\tau} F(\tau - \tau_1) \right] / \lambda_1 \quad (4.44)$$

where  $F(\tau)$  = the same function as given for equations (4.34) and (4.35)

$$\lambda = (1 + d\varepsilon/d\alpha)/\mu(1 - d\varepsilon/d\alpha + a/2\mu)$$

The maxima are given by

$$n_{T \text{ max}}/n_{\infty} = 1 + EE_1 \quad (4.45)$$

which occurs at  $\tau = \tau''_n$ , and

$$\alpha'_{\text{eff max}}/\alpha'_{\text{eff}\infty} = 1 + EE' \quad (4.46)$$

which occurs at  $\tau = \tau''_m$ ,

$$\text{where } \tau''_n = \tau_m - \sigma_n$$

$$\tau''_m = \tau_m - \sigma_m$$

$$\tan(J\sigma_n) = J(4R - a)/\{\mu a + 2(R^2 + J^2) - R(4R - a)\}$$

$$\tan(J\sigma_m) = J\lambda/(1 - R\lambda)$$

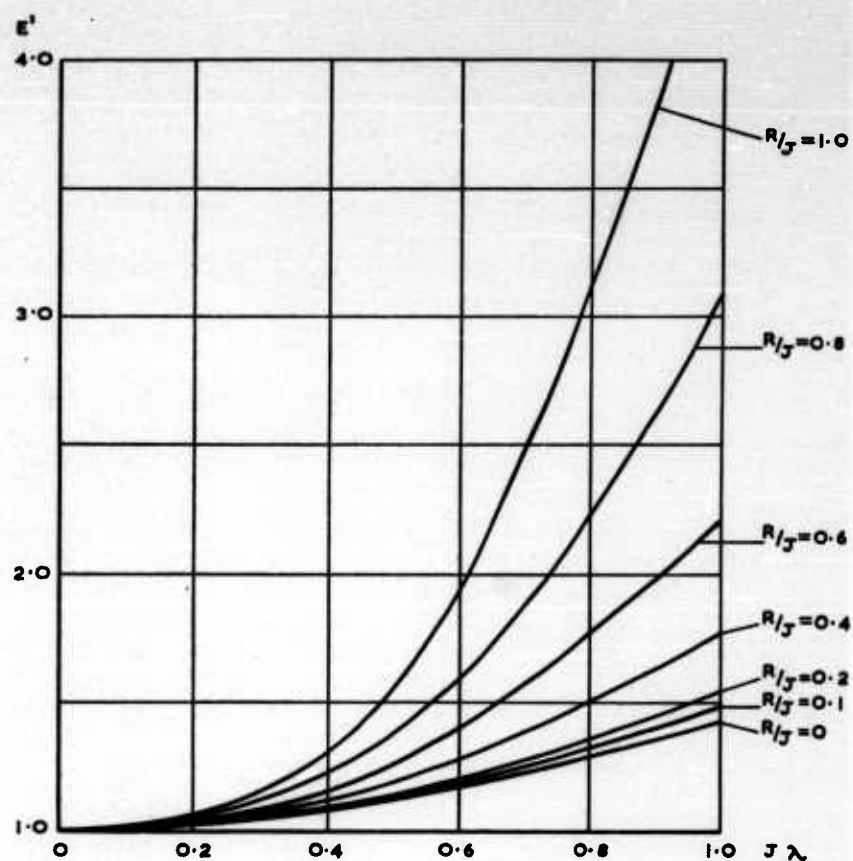
$$E_1 = \exp(R\sigma_n) \sqrt{[(1 + 2(R^2 + J^2)/\mu a)^2 - \{2R/\mu + (R^2 + J^2)/\mu^2\}(4R/a - 1)]}$$

$$E' = \exp(R\sigma_m) \sqrt{[1 - 2R\lambda + \lambda^2(J^2 + R^2)]}$$

$\tau_m$ ,  $E$  are the same functions as those given in equation (4.37).

The maxima of the normal acceleration  $n_{T \text{ max}}$  and the effective incidence  $\alpha'_{\text{eff max}}$  do not occur at the same time but for all practical conditions both occur after the elevator has reached its full angle and before the peak C.G. normal acceleration occurs. The normal acceleration of the tail depends on so many aircraft properties that it is hardly feasible to give general curves. However, the inertia loads will usually be much less than the aerodynamic loads and little error will be introduced by assuming the tail has the same normal acceleration as the C.G. of the aircraft: the maximum normal acceleration at the tail will usually be a little greater than the maximum C.G. normal acceleration but not quite in phase with it. The effective incidence of the tail can be dealt with generally as it can be related to the C.G. normal acceleration in terms of only one further parameter  $\lambda$  as shown in equations (4.43) and (4.44). The magnitude of the greatest effective incidence of the tail and the time at which it occurs are given in Fig. 4.3 in terms of the maximum C.G. accelerations shown in Fig. 4.2.

The total aerodynamic load on the tail is the algebraic sum of the elevator load and the tail load due to its effective incidence. For the case of a positive increment of C.G. normal acceleration there will invariably be an algebraic

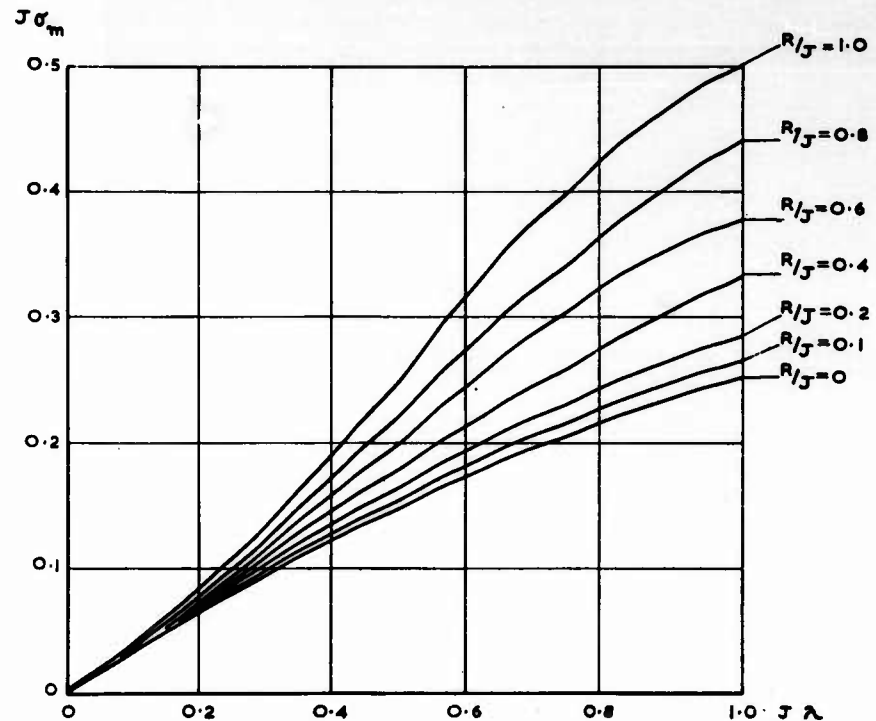


**A - MAXIMUM EFFECTIVE INCIDENCE.**

GIVEN AS THE RATIO OF OVERSHOOT OF TAIL  
INCIDENCE TO OVERSHOOT OF C.G. NORMAL  
ACCELERATION ( $E'$  OF EQUATION 4.46).

Fig. 4.3. Maximum effective incidence of the tail and the time at which it occurs.  
 $R/J$  is the ratio of the damping factor to the natural frequency of the pitching oscillation;  
 $\lambda$  is defined in equation (4.44) and  $\sigma_m$  in equation (4.46).

minimum due to the negative elevator angle before the tail's effective incidence attains its first maximum. This down load on the tail may be a much more serious case in design than the maxima that have already been considered. Also it is much more seriously influenced by the rate and manner in which the elevator is applied. This download is so important that the



B - TIME BY WHICH PEAK TAIL INCIDENCE PRECEDES  
PEAK C.G. NORMAL ACCELERATION ( $J\sigma_m$ ).

Fig. 4.3. (continued)

study of it has been isolated from that of the other loads, although the same formulae are used as those for upload. In the upload case the maximum always occurred after the elevator had reached its final value. For the download the situation is quite different. The maximum incremental download that can possibly occur is that for the elevator fully deflected as a step thus preventing any relieving upload on the tailplane from being developed whilst the elevator is being applied; the magnitude is obtained by putting  $\alpha'_{eH}$  zero in equation (4.32). If the elevator deflection curve is a

ramp, the contribution from the first term in equation (4.32) relieves the total load on the tailplane. For rapid rates of application of elevator the load on the elevator increases faster than the relieving load on the tailplane, and the total download increases until the elevator deflection is a maximum, i.e. at  $\tau = \tau_1$ . At lower rates of application of elevator the load on the elevator is at first increasing faster than the load on the tailplane, but a stage is reached in which the net download on the tail is greatest before the elevator has reached its maximum deflection.

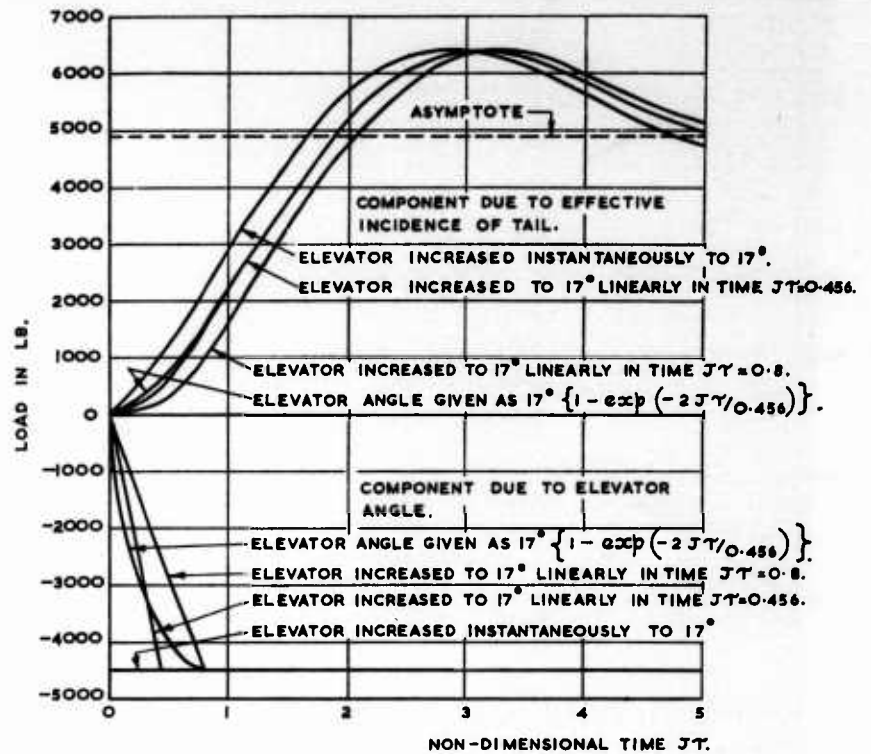


Fig. 4.4. The components of the aerodynamic load on the tail of a particular aircraft for elevator movements.

As maximum elevator is always present when the maximum uploads occur, the peak loads may be considered as those due to the effective incidence plus the constant elevator load. In downloads both elevator and tail components are varying, and the ratio of  $a_1$  to  $a_2$  becomes an important parameter. This extra parameter makes it impracticable to study downloads for a full range of parameters. In any particular case the separate components are readily calculable; it is necessary to know the constant of multiplication of the elevator angle and also the constant for the effective

# MANOEUVRES

incidence of the tail. As an example of a typical aeroplane, the numerical characteristics of the one used by Czaykowski (1955) are taken and the resultant loads shown for an elevator angle increased linearly to its final value of  $17^\circ$  in times  $J\tau_1 = 0, 0.456$  and  $0.8$  and also according to the formula that elevator angle equals to  $17^\circ \{1 - \exp(-2J\tau/0.456)\}$ . The total aerodynamic tail load is given by Czaykowski (1955) for the exponential movement and by Neumark (1958) for the linear movements. The individual components due to the elevator angle and due to the effective incidence of the tail have been deduced from these totals and are presented in Fig. 4.4. The asymptotic value of both components is identical in all cases and the differences in

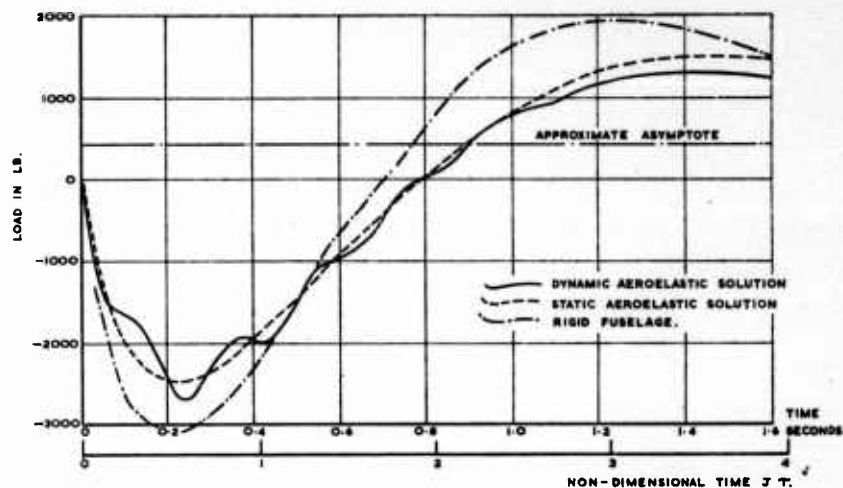


Fig. 4.5. Effect of fuselage flexibility on calculated aerodynamic tail load of a particular aircraft for elevator angle  $17^\circ \{1 - \exp(-t/0.093)\}$ .

The rigid fuselage case is identical to one used in Fig. 4.4. All curves are copied from Czaykowski (1962).

the magnitude of the maximum upload are small but the differences in downloads, which are so dependent on the elevator angle are great. In the case of the exponential movement the smoothing of the action just before maximum elevator is reached allows more upload due to effective incidence of the tail to develop with consequential reduction of total download. The total aerodynamic tail load for this case is shown in Fig. 4.5 and compared with further solutions by Czaykowski (1962) taking account of the stiffness of the fuselage in a quasi-static manner (static aerolastic solution) and also including the structural dynamic response (dynamic aeroelastic solution). When the flexible deformation is included the natural frequency of the pitching oscillations decreases slightly, but for comparison with Fig. 4.4 the non-dimensional time appropriate to the rigid-body solution is shown as well as the time in seconds. This figure indicates the effects of flexibility for one particular elevator movement on one particular aircraft, but in view of

the large variation in fuselage flexibility of different aircraft generalization is not possible.

Czaykowski (1962) points out that close approximations to a given curve of normal accelerations can be attained by a wide range of elevator movements with consequential large variations in total download on the tail. There are two broad classes of heavy manoeuvre:

- (1) The unchecked one in which the elevator is deflected rapidly to an angle and kept there until the limiting acceleration is practically reached.
- (2) The checked one in which the elevator is deflected rapidly beyond the angle of the unchecked manoeuvre and immediately reversed to an angle that will give the same limiting acceleration.

If all changes of elevator angle in both types of manoeuvre are done at the same rate in degrees of angle per second, the checked manoeuvre will produce the higher tail loads. For both ramp examples of Fig. 4.4 the downloads will be increased in the checked manoeuvre very nearly in proportion to the maximum elevator angles, i.e. the effective elevator movement is nearly a step. The maximum acceleration will be achieved a little sooner with the checked manoeuvre, but even if the checked manoeuvre was done a little slower the effective elevator movement would remain a step so that the maximum acceleration occurred at the same time, it would still produce nearly the same maximum download on the tail.

#### 4.7 ASYMMETRICAL MANOEUVRES—LINEARIZED EQUATIONS OF MOTION

All manoeuvres involving yawing displacements or forces are asymmetrical. The simplest is that of pure yaw. This can only be achieved in practice by applying additionally to the yawing couple of the tail controls just sufficient aileron to compensate for the difference in forward speed of the two wings. If it were done and the yawing couple due to the ailerons could be neglected, the equations to be solved would be equations (4.13), which are of identical form, to equations (4.12) for pure pitch and whose solutions are given in paragraph 4.6. The main difference between the two motions is that in pitch the angle of incidence of the wings to the direction of motion is changed, whereas in yaw it is the fuselage that changes its incidence and the forces developed are correspondingly much smaller. It is rare for this manoeuvre to be a serious loading condition, but if it were, the solutions for pitch are directly applicable. In a combination of pitch and yaw only, the inertia cross coupling terms are negligible and the equations (4.14), that are to be solved, are identical to the sum of the solutions for pitch and for yaw each taken separately.

The remaining manoeuvres all involve roll and the complete set of equations (4.4) to (4.8) (with (4.6) simplified to the form of (4.9)) have to be solved; these equations are linearized by representing the angle of roll ( $p$ ) by equation (4.19). If pitch were completely eliminated  $q$  and  $\dot{q}$  could be made zero and if yaw were completely eliminated  $r$  and  $\dot{r}$  could be made

zero but neither of these simplifications is likely to reduce much the computational time. The forces and couples that have to be substituted in these equations are given by equations (4.18), (4.21) and (4.22). The resulting equations of motion become

$$\left. \begin{aligned} m(\dot{V} - p_0 W + rU) &= \gamma_V V + mg (\sin \phi_0 \cos p_0 t + \cos \phi_0 \sin p_0 t) \\ m(W - qU + p_0 V) &= z_W(W - W_0) \\ &\quad + mg (\cos \phi_0 \cos p_0 t - \sin \phi_0 \sin p_0 t) \\ A\dot{p} &= l_p p + l_z \xi + l_V V + l_r r \\ B\dot{q} + (A - C)p_0 r &= m_q q + m_n \eta + m_{\dot{W}} \dot{W} + m_W(W - W_0) \\ C\dot{r} + (B - A)p_0 q &= n_r r + n_z \zeta + n_{\dot{V}} \dot{V} + n_V V + n_p p + n_z \xi \end{aligned} \right\} \quad (4.47)$$

These equations are put into non-dimensional form, in the same way as for equation (4.25) and  $W$  replaced by its incremental value  $w$ , and become

$$D\bar{v} + \bar{y}_v \bar{v} - \bar{p}_0 \bar{w} - \bar{W}_1 \bar{p} + \bar{r} = \frac{1}{2} C_{LE} (\sin \phi_0 \cos \bar{p}_0 \tau + \cos \phi_0 \sin \bar{p}_0 \tau) \quad (4.48)$$

$$D\bar{w} - \bar{z}_w \bar{w} - \bar{q} + \bar{p}_0 \bar{v} = \frac{1}{2} C_{LE} (\cos \phi_0 \cos \bar{p}_0 \tau \sin \phi_0 \sin \bar{p}_0 \tau - 1) \quad (4.49)$$

$$D\bar{p} + \nu_p \bar{p} - \nu_r \bar{r} + \omega_v \bar{v} = -\delta_{\ell z} \xi \quad (4.50)$$

$$D\bar{q} + \nu_q \bar{q} + \delta_v \bar{p}_0 \bar{r} + \chi D\bar{w} + \omega \bar{w} = -\delta \eta \quad (4.51)$$

$$\nu_{np} \bar{p} + \sigma_z \bar{p}_0 \dot{\bar{q}} + D\bar{r} + \nu_n \bar{r} - \omega_n \bar{v} + \chi_n D\bar{v} = -\delta_{nz} \xi - \delta_{nz} \zeta \quad (4.52)$$

where  $\bar{r} = \bar{l}r$

$$\bar{p} = \bar{l}p$$

$$\bar{p}_0 = \bar{l}p_0$$

$$\bar{v} = V/U \text{ (the increment of } V \text{ is taken to be the same as } V)$$

$$\bar{W}_1 = \text{datum value of } W/U$$

$$C_{LE} = \text{datum value of } C_L$$

$$\delta_v, \delta_z \text{ are the non-dimensional form of } A-C \text{ and } B-A$$

$$\bar{y}_v, \bar{z}_w, \nu_p, \nu_r, \omega_v, \delta_{\ell z}, \nu_{np}, \nu_n, \omega_n, \delta_{nz}, \delta_{nz}, \chi_n \text{ are derivatives in non-dimensional form}$$

The term  $\chi_n D\bar{v}$  is included in equation (4.52) to maintain symmetry with equation (4.51), but it may in fact be ignored in all solutions appertaining to aircraft. W. H. Phillips (1948) solved the simple case of constant roll with fixed elevator and rudder, neglecting gravity and all damping derivatives. Thomas and Price (1960) solved the full equations (4.48) to (4.52) for a constant roll with fixed elevator and rudder and showed that provided the rate of roll is sufficiently large for the inertia cross-coupling effects to be appreciable the effect of gravity may be neglected. As it is only justified to solve all five equations simultaneously if inertia cross-coupling is appreciable, then it is equally justified to neglect the effect of gravity. In fact



gravity will be neglected for the general case also which is equivalent to making the right-hand-side of equations (4.48) and (4.49) zero.

Before looking at the general case it is worthwhile to look at the special cases in which an aircraft is flying with  $\bar{v} = \bar{w} = \bar{p} = \bar{q} = \bar{r} = 0$  (i.e. straight with no yaw, pitch or roll) and one only of the controls is applied as a step to a fixed value.

If the elevator is applied,  $\eta = \eta_0$  and for all equations to hold at zero time  $(D\bar{q})_0 = -\delta\eta_0$  (equation (4.51)); subsequently as  $\bar{q}$  changes  $\bar{w}$  must change (equation (4.49)) but because all parameters were zero at zero time there is no interaction from  $\bar{q}$  and  $\bar{w}$  and the full solution is obtained from equations (4.49) and (4.51). This is the case of pure pitch and was examined in detail in paragraph 4.6.

If the rudder is applied,  $\zeta = \zeta_0$  and for all the equations to hold at zero time  $(D\bar{r})_0 = -\delta\zeta_0$  (equation (4.52)); subsequently as  $\bar{r}$  changes  $\bar{v}$  must change (equation (4.48)) and  $\bar{p}$  must change (equation (4.50)); in the next phase when  $\bar{p}$  has become so large that  $\bar{p}_0$  may no longer be taken as zero  $\bar{q}$  and  $\bar{w}$  are involved and a completely general motion ensues. As  $v_{ir}$  cannot be zero the only way that the equations can degenerate into equations (4.48) and (4.52) is by the aileron being moved in such a way that  $-\delta_{ir}\xi$  is kept identical to  $(\omega_r\bar{v} - v_{ir}\bar{r})$  throughout the manoeuvre.

If the ailerons are applied,  $\xi = \xi_0$  and for all equations to hold at zero time  $(D\bar{p})_0 = -\delta_{ir}\xi_0$  (equation (4.50)); subsequently as  $\bar{p}$  changes  $\bar{v}$  must change (equation (4.48)) and  $\bar{r}$  must change (equation (4.52)); in the next phase as with rudder application  $\bar{q}$  and  $\bar{w}$  become involved and a completely general motion ensues. Degeneration from the full equations is only possible if all the coefficients of  $\bar{p}$  and  $\bar{p}_0$  are zero; in this case only equation (4.50) remains but the rudder has to be moved so that  $-\delta_{ir}\xi$  is kept identical to  $(v_{nr}\bar{p} + \delta_{nr}\xi_0)$  and in addition  $\bar{W}_1$  must be zero. This latter condition of  $\bar{W}_1$  zero means that in the initial condition the forward principal inertia axis is in the line of flight, which can only occur in the singular condition of having the appropriate forward speed. So it may be assumed that in all rolling conditions inertia cross-coupling will take place.

#### 4.7.1. Asymmetrical Manoeuvres—Steady State Conditions

In the case of pure pitching manoeuvres there are no cross-coupling forces and the steady state conditions are a single function of the applied elevator deflection as given in equation (4.33). In asymmetrical manoeuvres there are cross-coupling forces and the 5 governing conditions, as given by equations (4.48) to (4.52) with the gravity terms zero, produce 5 steady state conditions (there would be 8 steady state conditions if the terms in  $qr$  were not neglected). In the symmetrical case a negligible elevator deflection produces a steady state with a negligible amount of pitch. In the asymmetrical case with negligible deflection of any of the three controls, one of the steady states has a negligible departure from flight with no yaw, pitch or roll, but the other four steady states have not; they are in fact rotations about fixed axes that are at an angle to all three principal axes.

The steady state conditions are obtained by making zero all the terms containing the operator  $D$  and the gravity terms and putting  $\bar{p} = \bar{p}_0$ . Equations (4.48)–(4.52) reduce to



$$\left. \begin{aligned} \dot{p}_v \bar{v} - \bar{p}(\bar{w} + W_1) + \bar{r} &= 0 \\ -\bar{z}_w \bar{w} - \bar{q} + \bar{p} \bar{v} &= 0 \\ v_r \bar{p} - v_r \bar{r} + \omega_r \bar{v} &= -\delta_{rz} \xi \\ v_q + \delta_v \bar{p} \bar{r} + \omega \bar{w} &= -\delta \eta \\ v_{n\bar{p}} \bar{p} + \delta_z \bar{p} \bar{q} + v_n \bar{r} - \omega_n \bar{v} &= -\delta_{nz} \xi - \delta_{nr} \zeta \end{aligned} \right\} \quad (4.53)$$

The solution of these equations results in a quintic for each of the variables. The quintic for roll is of the form

$$a_0(\xi, \zeta) + [a_1(\eta) + b_1] \bar{p} + a_2(\xi, \zeta) \bar{p}^2 + [a_3(\eta) + b_3] \bar{p}^3 + a_4(\xi) \bar{p}^4 + b_4 \bar{p}^5 = 0 \quad (4.54)$$

where  $a$ 's and  $b$ 's are functions of the coefficients in equation (4.53). When the control positions are neutral  $\xi = \zeta = \eta = 0$  all the  $a$ -functions disappear and the values of  $\bar{p}$  are  $0, \pm p_1, \pm p_2$ . If there is only elevator displacement the values of  $\bar{p}$  retain the same form. If there is no elevator displacement ( $\eta = 0$ ) and the even  $a$ -functions are small as well, the solutions will be of the form  $\bar{p}_{00}, \pm \bar{p}_1 + p_{11}, \pm \bar{p}_2 + p_{22}$ . Thomas and Price (1960) give the algebraic values for the  $b$ -functions for the case of all controls neutral and also examine the stability. The perturbations about the steady state are given by a quintic

$$G_0 + G_1 D + G_2 D^2 + G_3 D^3 + G_4 D^4 + G_5 D^5 = 0 \quad (4.55)$$

and instability ensues whenever one of the real parts of the roots is positive. A great simplification can be made to the algebra if it is postulated that the ailerons and rudder controls are varied continuously to ensure that the aircraft rolls with constant velocity and further that the combined yawing moment is zero, i.e.  $\delta_{nz} \xi + \delta_{nr} \zeta = 0$ , and the elevator is in a neutral position. The equation giving the aileron angle for small perturbations may then be ignored as the change in aileron angle is not of interest: all terms containing perturbations in  $\bar{p}$  are neglected because it is postulated that the aircraft is compelled to roll at constant speed. With only a slight further simplification of  $\bar{y}_v = \bar{z}_w = 0$  the stability equation becomes a quartic

$$\begin{aligned} D^4 + (\chi + v + v_n) D^3 + [\omega + \omega_n + v v_n + \chi v_n + p^2(1 - \delta_v \delta_z)] D^2 \\ + [v_n \omega + v \omega_n + \chi \omega_n + p^2(v + v_n - \delta_z \chi)] D \\ + [\omega_n \omega - \delta_v \delta_z p^4 + p^2(\delta_v \omega_n - \delta_z \omega + v_n v)] = 0 \end{aligned} \quad (4.56)$$

This equation simplifies still further if  $\chi = v = v_n = 0$  and becomes the stability equation postulated by W. H. Phillips (1948). In this limiting case the motion is stable if

$$(\omega_n - \delta_z p^2)(\omega + \delta_v p^2) > 0 \quad (4.57)$$

Thus it is only when the rolling velocity lies between the two values  $\sqrt{(-\omega/\delta_v)}$  and  $\sqrt{(\omega_n/\delta_z)}$  that the motion will be unstable; the motion will be a divergence which is predominantly in pitch when  $\sqrt{(-\omega/\delta_v)}$  is the lower and predominantly in yaw when it is the higher. In the special case of the two frequencies being equal there is no rolling velocity for which the

motion is unstable. Pinsker (1955) points out that if damping terms are included, there is a range of frequencies for which there is no instability.

It must be remembered that the analysis of W. H. Phillips (1948) and Pinsker (1955) that has just been described is for the restrictive case of constant rate of rolling. This means that the degree of freedom in roll has been removed and instability is only allowed to develop in pitch or yaw. The significance of this restriction can only be assessed for particular numerical values for the aircraft characteristics. As an example the values used by Pinsker (1955) are taken and are given in Table 4.1. Thomas and Price

Table 4.1. *Geometric, Inertia and Aerodynamic Derivatives (with Respect to Principal Inertia Axes) Assumed for the Aircraft used as Example*

Weight 25,000 lb		
Span 35 ft		
Wing area 400 ft <sup>2</sup>		
$\alpha$ = angle of incidence		
$A$ = 900,000 lb ft <sup>2</sup>		
$B$ = 4,100,000 lb ft <sup>2</sup>		
$C$ = 5,000,000 lb ft <sup>2</sup>		
Mach No. 0.8		
Height 40,000 ft		
$t$ = 4.2318 sec		
$y_v = -0.32$		$m_w = -0.083$
$l_{\xi} = -0.25$		$m_{\dot{w}} = -0.218$
$l_p = -0.25$		$m_{\dot{r}} = -0.376$
$l_v = -0.10$		$z_w = -2.175$
$n_{\xi} = -0.07\alpha$		$l_r = 0$
$n_p = 0.05 - 0.3\alpha$		$y_p = 0$
$n_v = 0.20$		$m_{\eta} = 0$
$n_r = -0.46$		$n_{\xi} = 0$
		$n_{\dot{r}} = 0$

(1960) use the same values and determine the steady state conditions for all controls neutral, which are also given in the same table; they find that both conditions are unstable, the slower roll having a divergent mode and the faster one an unstable oscillatory mode. In this example the equilibrium frequencies in non-dimensional time are (6.8, 9.4), (6.9, 9.3), (4.9, 10.2) respectively for the conditions of

- (i) no freedom in roll without damping,
- (ii) no freedom in roll with damping,
- (iii) freedom in roll with damping.

In the first two conditions the motion is unstable between the two frequencies and stable outside them. In the third condition the condition is stable below 4.9, it has a divergent mode between 4.9 and 10.2 and an unstable oscillation above 10.2. In this particular example the simplification of neglecting the degree of freedom in roll is serious. It increases the apparent rate of roll at which a divergent mode is introduced by 40 per cent, which is serious enough in itself, but it also replaces an unstable mode by an apparently stable one. Meyer (1957) and Nethaway and Clark (1960) have

## MANOEUVRES

noticed in flight tests that when inertia cross coupling is present that pilots are unable to control the motion of their own accord and should release the controls. Thus in practical conditions it is imperative to include the rolling degree of freedom.

### 4.7.2. *Asymmetrical Manoeuvres—Non-steady Conditions*

The steady state conditions in which roll is present are liable to be conditions of unstable characteristics and there is no simple method of correlating peak accelerations and loads as in the case of symmetrical manoeuvres. Consequently correlation between different rolling manoeuvres on one aircraft is difficult and correlation between aircraft almost impossible. In addition in the unstable region the non-linearities will be most important and there is no alternative for any particular manoeuvre but to make full calculations of the non-linear equations of motion.

## REFERENCES

- |                            |                         |
|----------------------------|-------------------------|
| Czaykowski (1955)          | Neumark (1958)          |
| Czaykowski (1962)          | Phillips, W. H. (1948)  |
| Meyer (1957)               | Pinsker (1955)          |
| Nethaway and Clark (1960a) | Thomas and Price (1960) |

## CHAPTER 5

### MEASURED SYMMETRICAL MANOEUVRES

#### CONTENTS

5.1 Introduction	87
5.2 Frequency of occurrence of normal accelerations	88
5.3 Frequency of occurrence of high velocities	112
5.4 Distribution of the forward velocities, at which the peak normal accelerations occur	118
5.5 Frequency of combined occurrence of normal accelerations and forward velocities	122
References	130

## CHAPTER 5

### MEASURED SYMMETRICAL MANOEUVRES

#### 5.1 INTRODUCTION

Symmetrical manoeuvres have been regarded as those in which yaw is absent. The three possibilities are forward acceleration, roll and pitch. Forward acceleration alone other than as a means of producing high speeds is of almost trivial importance and no measurements for general use have been made. Pure roll is not important of itself but is most important in conjunction with other manoeuvres especially asymmetrical ones. The measured values of roll are given in Chapter 6 on asymmetrical manoeuvres. The most important symmetrical manoeuvre is pure pitch.

The overall pitching manoeuvres have been measured on a large number of types of aircraft flying a variety of different operational roles. It is considered that the overall manoeuvre is defined with sufficient accuracy if the maximum normal acceleration is known together with the aircraft speed and height at which it occurs. For most designs of aircraft the acceleration is the most significant parameter, the speed and height mainly influencing the distribution of the loads over the different parts of the aircraft. Sometimes it is necessary to measure roughly the duration of the acceleration so that atmospheric turbulence accelerations can be separated from the manoeuvres. Fortunately the duration of a gust acceleration is almost invariably less than 1 sec and the duration of a manoeuvre greater than 3 sec and little ambiguity occurs if 2 sec is used as the dividing line; all accelerations of less duration than 2 sec are assumed to be gusts and all those above to be manoeuvres plus whatever gusts happen to be superimposed. As the gusts cannot be avoided in the manoeuvres, any frequency of occurrence of manoeuvres that is deduced from actual measurements must include gusts in typical proportions. The total number of occurrences of any given acceleration are the sum of the manoeuvres with the associated gusts and the gusts unaccompanied by manoeuvres.

As the normal accelerations must be measured over very long periods of time, it is essential that automatic recording be employed. A  $V$ - $g$  recorder was introduced by Rhode (1937). This instrument records on a slide the variables  $V$  and  $g$  approximately at right angles to each other. All the variations of acceleration and velocity are superimposed on each other, so that after a period of time in service the frequently occurring records appear as a continuous pattern with no individual line discernible. The rarely occurring values retain their identity and appear as individual peaks of acceleration. It is possible generally to distinguish those accelerations that are purely gusts as the forward velocity will not have changed appreciably whilst they are being applied. Little has been done with  $V$ - $g$  recorders to separate the accelerations occurring at different height bands. The other

limitation is that a certain number of accelerations are omitted whatever method of analysis is used, and it is almost impossible to estimate in what proportions. Much later a counting accelerometer was introduced (J. Taylor, 1950). This instrument counts all accelerations that cross given thresholds; a threshold has a finite width so that one count at an increment of acceleration  $ng$  from level flight is made only when the increment reduces to  $(n - n_T)g$  thus ignoring fluctuations between  $(n - n_T)g$  and  $ng$ . The number of counts recorded is not sensitive to the width of the threshold  $n_T$  so that large changes in the value of  $n_T$  do not significantly affect the number of counts. The limitations of this instrument are that it is impossible to separate the accelerations that are purely due to gusts from the remainder, and no record is made of the velocities at which the peak accelerations occur. Recently instruments have been used for moderate periods of time on selected aircraft to record continuously the normal acceleration, forward velocity and height.

These three groups of instruments are complementary in determining the magnitude of pitching manoeuvres. The counting accelerometer requires the minimum of analysis and can be used for the greatest numbers of hours for a given effort. It should give the most reliable estimate of the frequency of occurrence of levels of normal acceleration but gives no information on the forward velocities at which the normal accelerations were experienced. The  $V$ - $g$  recorder is used for the second longest period and gives a good estimate of the frequency of occurrence of the high forward velocities and of the distribution of the forward velocities at which the higher normal accelerations occur. The continuous recording instruments give the complete relationship of normal acceleration, forward velocity and height. If the same effort is used as on the other two instruments they can only be employed for relatively few hours and consequently they will not give as good an estimate of total frequencies of occurrence of either forward velocity or normal acceleration.

The data are presented under the three separate groups of (1) frequency of occurrence of normal accelerations, (2) frequency of occurrence of high velocities and (3) distribution of the forward velocities at which the normal accelerations occur. Further the aircraft are separated into (1) trainers, (2) fighters, including fighter bombers, and (3) transports and bombers.

## 5.2 FREQUENCY OF OCCURRENCE OF NORMAL ACCELERATIONS

The frequency at which manoeuvres have normal accelerations exceeding given values depends very markedly on the type of aircraft, the operational duties on which it is employed, and to a lesser extent on the actual design of the aircraft. The normal accelerations experienced by fighters and trainers are predominantly due to manoeuvres so that those due to gusts, in the absence of manoeuvres, may be neglected. Thus all the normal accelerations that occur may be counted as manoeuvres and no correction made for those that are purely gusts, except possibly at acceleration increments much less than  $1g$ . The simplest way to do this is to use a counting accelerometer, which gives totals without discrimination. Data are available from counting

accelerometers for a few types of aircraft and extend over a large number of flying hours. It is important to include a variety of types of aircraft, and this is done by taking data from *V-g* recorders and from continuous recordings; these data, particularly the continuous recordings, are normally from relatively few flying hours per type of aircraft. The normal accelerations experienced by transports and bombers on the other hand are for the most part due to gusts and data for manoeuvres can only be obtained by excluding those accelerations that are purely gusts; this can be done from continuous records and to some extent from *V-g* recorders, but not from counting accelerometer readings.

Tables 5.1, 5.2, 5.3 and 5.4 give the normal accelerations that have been measured in manoeuvres for land-based fighters, Naval fighters, trainers and transports respectively. The accelerations are given as the level that will be achieved on average in different numbers of hours. The majority of values quoted have been deduced by W. A. P. Fisher (1964) from the original data, references to which are shown in the tables. The numbers of flying hours and the design ultimate normal acceleration, whenever available, are shown for each type of aircraft. Data which were obtained from *V-g* records are restricted to the higher numbers of flying hours, as the records of frequently occurring accelerations are superimposed on each other and cannot be read. Data from counting accelerometers and continuous trace recordings are limited merely by the value the authors of the original data considered the minimum of significance as a fatigue load.

In fighters the physiology of the pilots (blacking-out, etc.) has always been an influence on the maximum accelerations, but the introduction of anti-*g* suits did not have as great an influence on the higher accelerations of the Hunter (Table 5.1) as might have been expected. The effect of introducing visual accelerometers for the pilot has not been studied as none of the reports state whether or not they are present; it is probable that visual accelerometers are standard equipment for the majority of the fighters examined. The accelerations that occur between once per 100 hr and once per 1000 hr are probably of about the magnitude that pilots will apply willingly if required to do so, and are much the same for all fighters regardless of the service limit. However there is a strong indication that the distribution at very low frequencies of occurrence are of a different family from those occurring often. Several authors have commented on occasional very high accelerations and suggested reasons for their occurrence. With visual accelerometers and anti-*g* suits as standard equipment the difference in control characteristics of the different types of aircraft probably has much less influence on the frequency of occurrence of the very high accelerations.

A comparison of land-based and naval fighters does not show any significant difference in the frequency of occurrence of normal accelerations. Nor is there any evidence to suggest that the size of the aircraft or the service limit on acceleration influence the accelerations that are actually applied. Thus it is possible to combine the results from all the fighters and estimate average distributions of frequency of occurrence of different levels of acceleration. As only a small proportion of the results were on obsolete aircraft it was decided to omit them in the analysis, but none of the available results on



Table 5.1. Normal Accelerations in Flight of Land-based Fighters and Fighter-Bombers  
A. Types of Aircraft and Duties

Reference	Type of recorder	Aircraft	$\frac{2}{3}$ Ultimate design acceleration $g$	Duties	No. of flying hours
Owen, E. M. (1954)	$V-g$	Meteor 8	6.7	(i) All including ground attack	280
Owen, E. M. (1955a)				(ii) All including ground attack, but speed limit in dives above $10^\circ$	360
Owen, E. M. (1955)	$V-g$	Vampire 5	6.7	(i) All except ground attack	952
				(ii) All except ground attack	246
				(iii) Ground attack	80
				(iv) Anti-g suit trials	180
R.A.E., unpublished	$V-g$	Spitfire		(i) Interception	350
				(ii) Ground attack and armed reconnaissance	560
Owen, E. M. and Sellers (1956)	$V-g$	Venom FB 1		(i) Combined duties	495
Owen, E. M. and Sellers (1958)	$V-g$	Hunter 4	7.5	(ii) Ground attack	238
				(a) (i) Combined duties—with anti-g suit	203
				(ii) Combined duties—without anti-g suit	231
				(b) (i) and (ii) combined + 50 hr unidentified duties	484
Owen, E. M. (1958b)	$V-g$	Javelin Mk 1	6.6	Combined duties	256
Owen, E. M. (1955b)	$V-g$	Meteor NF 11	6.7	Combined duties	549
R.A.E., unpublished	Counting accelerometer	U		Combined duties	4315



MEASURED SYMMETRICAL MANOEUVRES

A. Types of Aircraft and Duties (continued)

Reference	Type of recorder	Aircraft	$\frac{2}{3}$ Ultimate design acceleration $g$	Duties	No. of flying hours
R.A.E., unpublished	Counting accelerometer	Javelin		Combined duties	2779
R.A.E., unpublished	Counting accelerometer	Hunter		Ground attack	4320
Gray (1955)	Continuous chart	F-86		Air-to-air enemy engagements Korea	231
Gray (1955)	Continuous chart	E and F F-86F		All air-to-air missions Korea	
				(a) (i) 0-5000 ft	61
				(ii) 5-15,000 ft	52
				(iii) 15-25,000 ft	77
				(iv) 25-30,000 ft	54
				(v) 30-35,000 ft	57
				(i), (ii), (iii), (iv) and (v) combined + 281 unidentified by height	582
				(b) Ground attack Korea	55
				Ground attack Korea	349
				Ground attack—gunnery meet	38
Gray (1955)	Continuous chart	F-84G		(a) (i) Transition	328
Titus (1961)	Continuous chart	F-100A		(ii) Air-to-air gunnery	159
Titus (1961)	Continuous chart	F-100D		(iii) Air tactics	420
				(iv) High angle bombing	11.4

## A. Types of Aircraft and Duties (continued)

Reference	Type of recorder	Aircraft	§ Ultimate design acceleration $g$	Duties	No. of flying hours
Titus (1961)	Continuous chart	F-100D (Continued)		(a) (v) Low angle bombing (i), (ii), (iii), (iv) and (v) combined + 1-6 hr other duties	51
Titus (1961)	Continuous chart	F-100C		(a) (i) Transition George A.F.B. (ii) Air-to-air gunnery George A.F.B. (iii) Air tactics George A.F.B. (iv) High angle bombing George A.F.B. (v) Low angle bombing George A.F.B. (i), (ii), (iii), (iv) and (v) combined	971 121 57 160 6-7 12-9
Titus (1961)	Continuous chart	F-100 class		(b) Combined duties George A.F.B. Combined duties including all in F-100 A, C and D above	358 45-5
Vahldick (1961)	Continuous chart	F-102A		(i) Combined duties	6050
Mullins (1961)	Continuous chart	F-104A		(ii) Combined duties	478
	Continuous chart			(i) Combined duties	1608
	Continuous chart			(ii) Combined duties, mainly high altitude	634
Vahldick (1961a)	Continuous chart	F-105B	5-85	Combined duties	220
Ward (1963a)	Continuous chart	RF-101C		Combined duties	381
Mullins (1962)	Continuous chart	F-104C		Combined duties	2025
Clay and Berens (1963)	Continuous chart	F-106A		Combined duties	1106
				Combined duties	3773

MEASURED SYMMETRICAL MANOEUVRES

B. Measured Normal Accelerations. (Figures in brackets are subject to appreciable extrapolation errors)

Aircraft and duties	Upward acceleration reached per					Downward acceleration reached per				
	30 hr	100 hr	300 hr	1000 hr	g	30 hr	100 hr	300 hr	1000 hr	g
	g	g	g	g	g	g	g	g	g	g
Meteor 8										
(i)	6.5	7.75	8.4	(8.8)	(8.8)	-1.45	-1.9	-2.3	(-2.6)	
(ii)	6.15	6.8	7.05	(7.1)	(7.1)	-1.67	-1.98	-2.25	(-2.5)	
Vampire 5										
(i)	6.35	6.85	7.15	(7.5)	(7.5)	-2.5	-3.4	-4.1	-4.5	
(ii)	6.35	6.85	7.30	(7.7)	(7.7)	-2.4	-3.05	-3.55	(-4.0)	
(iii)	8.1	8.55	(8.85)	(9.2)	(9.2)	-3.4	-3.75	-4.1	(-4.5)	
(iv)	7.0	7.4	7.65	(8.1)	(8.1)	-2.65	-3.0	-3.2	(-3.5)	
Spitfire										
(i)		7.25	8.05	8.85	8.85					
(ii)		6.65	7.7	8.9	8.9					
Venom FB 1										
(i)	6.25	6.9	7.3	(7.55)	(7.55)	-0.55	-0.8	-1.05	(-1.75)	
(ii)	7.4	7.95	8.45	(8.85)	(8.85)	-1.7	-2.1	-2.4	(-2.7)	
Hunter										
(a)(i)	5.55	6.05	6.6	(7.1)	(7.1)		-1.7	-2.1	(-2.65)	
(ii)	5.7	6.25	6.8	(7.4)	(7.4)		-1.3	-1.6	(-1.9)	
(b)	5.7	6.4	7.0	(7.65)	(7.65)		-1.32	-1.75	(-2.25)	
Javelin Mk 1	4.7	5.0	5.27	(5.55)	(5.55)	-1.75	-1.88	-1.97	(-2.06)	
Meteor NF 11	5.3	5.75	6.1	6.4	6.4	-0.9	-1.55	-2.05	(-2.75)	
U	5.5	6.2	6.9	(7.5)	(7.5)	-1.1	-1.8	(-2.6)	(-3.3)	



### MEASURED SYMMETRICAL MANOEUVRES

**B. Measured Normal Accelerations (continued).** (Figures in brackets are subject to appreciable extrapolation errors)

<i>Aircraft and duties</i>	<i>Upward acceleration reached per</i>					<i>Downward acceleration reached per</i>				
	30 hr	100 hr	300 hr	1000 hr		30 hr	100 hr	300 hr	1000 hr	
	<i>g</i>	<i>g</i>	<i>g</i>	<i>g</i>		<i>g</i>	<i>g</i>	<i>g</i>	<i>g</i>	
F-100C (a)	5·5	5·8	6·1	6·4			Rarely negative			
(b)	5·6	5·9	(6·1)				Rarely negative			
F-100 Class	6·0	6·7	7·8	8·9						
F-102A (i)	4·6	5·1	5·5	5·95						
(ii)	4·36	5·0	5·55	6·2						
F-104A (i)	4·45	5·1	5·6	6·3						
(ii)	3·7	4·1	4·55	4·95						
F-105B	5·4	5·9	6·3	6·8						
RF-101C	4·6	5·2	5·9	6·6		-0·1				
F-104C	6·1	6·4	(6·8)	(7·2)						
F-106A	4·5	5·0	5·6	6·3			-0·7	-0·7	-1·1	

Table 5.2. Normal Accelerations in Flight of Naval Fighters and Fighter-Bombers  
A. Types of Aircraft and Duties

Reference	Type of recorder	Aircraft	$\frac{1}{2}$ Ultimate design acceleration g	Duties	No. of flying hours
Lewis (1956)	V-g	Sea Hawk	7.0	(i) Combined duties	245
Lewis (1956a)	V-g	Sea Fury	7.0	(ii) Ground attack	67
Owen, E. M. and Malcom (1959)	V-g	Gannet A/S Mk. 1		(i) Combined duties	126
Owen, E. M. (1957)	V-g	Wyvern S 4	7.33	(ii) Ground attack	84
				(i) Operational training	179
				(ii) Other duties	171
				(a) Gun and rocket attack	178
				(ii) Dive bombing	50
				(iii) Low level bombing	22
				(i), (ii) and (iii) combined. All ground attack	
				(b) (i) Air tactics	250
				(ii) Cross country	178
				(i) and (ii) combined. All except (a)	127
				Combined duties	305
					19,400
R.A.E., unpublished	Counting accelerometer	L		Combined duties	3049
R.A.E., unpublished	Counting accelerometer	Sea Vixen		Combined duties	5444
Mayer, J. P. and Harris (1955)	134 V-g slides	F2H-2	6.4	Combined duties	1370
Mayer, J. P. and Harris (1955)	30 V-g slides	F9F-2B	7.5	Combined duties	
Mayer, J. P. and Harris (1955)	41 V-g slides	F8F-2	6.3	Combined duties, propeller aircraft	1092
Mayer, J. P. and Harris (1955)	61 V-g slides	AD-4	7.0	(i) Bomber training	1552
	51 V-g slides			(ii) Bomber combat	2936

MEASURED SYMMETRICAL MANOEUVRES

Aircraft and duties	Upward acceleration reached per				Downward acceleration reached per			
	30 hr	100 hr	300 hr	1000 hr	30 hr	100 hr	300 hr	1000 hr
	g	g	g	g	h	g	g	g
Sea Hawk (i) (ii)	5.5 7.8	6.1 (9.0)	6.7	(7.4)	-0.65 -0.82	-1.05 -0.9	-1.45	(-1.9)
Sea Fury (i) (ii)	5.9 7.8	6.55 8.7	(7.15) (9.6)	(7.8) (10.5)	-1.4 -1.25	-1.8 -1.6	-2.2 -1.95	(-2.6) (-2.35)
Gannet A/S Mk 1 (i) (ii)	3.7 2.95	4.8 3.35	5.0 3.7	(5.17) (4.1)				
Wyvern (a) (i) (ii) (iii)	5.9 6.5 4.85	6.28 6.63 5.0	6.55 6.74 (5.14)	(6.8) (6.9) (5.28)				
(b) (i) (ii)	6.13 5.33 4.4 5.1 7.3	6.40 6.0 4.65 5.75 7.9	6.62 6.62 4.85 6.27 8.7	(6.8) (7.25) (5.05) (6.9) 9.5		-1.2	-1.5	(-1.82)
L Sea Vixen F2H-2 F9F-2B F8F-2 AD-4 (i) (ii)	6.2	7.0 5.95 6.6 6.5	(7.67) 6.7 7.3 7.45	(8.35) 7.5 7.85 8.55		-0.7	-0.85	(-1.05)
						Rarely negative Rarely negative Rarely negative		
						Rarely negative Rarely negative		

Table 5.3. Normal Accelerations in Flight of Trainers  
A. Types of Aircraft and Duties

Reference	Type of recorder	Aircraft	$\frac{1}{2}$ Ultimate design acceleration g	Duties	No. of flying hours
Owen, E. M. (1957a)	V-g slides	Jet Provost	6.7	(a) (i) Aerobatics (ii) Circuits and landings (iii) Other duties	219 75 201
Lewis (1957)	V-g slides	Provost T 1	6.7	(i), (ii) and (iii) combined (a) (i) Combined duties, propeller aircraft (ii) Aerobatics (i) and (ii) combined Combined duties	495 615 652 1267 1229
R.A.E., unpublished	Counting accelerometer 174 V-g slides	Vampire TV-1	7.33	Naval jet-trainer	5660
Mayer, J. P., and Harris (1955) Titus (1959)	Continuous chart	T-34		Primary trainer, combined duties	426
Titus (1959)	Continuous chart	T-33		Advanced trainer, combined duties	479
Titus (1960)	Continuous chart	T-37	5.85	Advanced trainer, combined duties	1356



MEASURED SYMMETRICAL MANOEUVRES

B. Measured Normal Accelerations. (Figures in brackets are subject to appreciable extrapolation errors)

Aircraft and duties	Upward acceleration reached per					Downward acceleration reached per				
	30 hr	100 hr	300 hr	1000 hr	30 hr	100 hr	300 hr	1000 hr	30 hr	1000 hr
	g	g	g	g	g	g	g	g	g	g
Jet Provost (a) (i) (ii) (iii)		6.15 3.9 4.8 5.75	6.7 4.3 5.0 6.3	7.28 4.7 5.12 6.9		-2.45 -0.55 -1.3	-2.75 -0.75 -1.45	-3.0		
Provost T 1 (a) (i) (ii)		4.85 6.1 5.75	5.2 6.7 6.4	5.6 7.25 7.0		-1.95 -2.4 -2.3		-2.5 -2.75 -2.85 (-2.6)		
Vampire TV.1 T-34 T-33 T-37	6.2 4.1 5.75 5.3	6.6 6.5 4.5 6.25 5.7	(6.9) 7.4 4.85 6.7 5.95	(7.3) 8.35 5.2 7.2 6.25	-1.7		-2.55 (-2.3) Rarely negative			

Table 5.4. Normal Accelerations in Flight of Transports and Bombers.  
The Accelerations are due to Gusts and Manoeuvres Combined except where Otherwise Stated

## A. Types of Aircraft and Duties

Reference	Type of recorder	Aircraft	§ Ultimate design acceleration $g$	Duties	No. of flying hours
Usher (1953)	V-g slides	Canberra B 2	5.0	(i) Operational squadron	1799
Owen, E. M. (1958a)	V-g slides	Canberra B 6	5.0	(ii) Conversion unit	1246
				(i) Cross country	889
				(ii) Ground attack	117
				(iii) Continuation training	96
				(iv) Formation	64
R.A.E., unpublished	Counting accelerometers	Various bombers		(i) Operational squadrons	14,969
Mayer, J. P. and Harris (1955)	28 V-g slides	P4M-1	2.8	(ii) Conversion units	5114
Mayer, J. P. and Harris (1955)	24 V-g slides	PBM-5S	2.6	Naval patrol bomber	916
Phillips, L. (1961)	Continuous chart	C-130		Flying boat	1072
Perry and Rievley (1961)	Continuous chart	KC-135A		Transport manoeuvres only	1077
Durkee (1961)	Continuous chart	B-47E		Transport	1167
Wallace (1961)	Continuous chart	B-52		Bomber	610
				(i) Bomber	534
				(ii) Bomber	486
				Castle A.F.B. Walker A.F.B.	

MEASURED SYMMETRICAL MANOEUVRES

A. Types of Aircraft and Duties (continued)

Reference	Type of recorder	Aircraft	$\frac{1}{2}$ Ultimate design acceleration g	Duties	No. of flying hours
Kelly, L. G. and Brown (1962) Walker, W. G. and Copp (1959)	Continuous chart Continuous chart	B-52G 6 Civil		(i) Bomber, non-heavy	558
				(ii) Bomber, heavy	624
				(i) Operational manoeuvres only— 4-engined propeller	12,063
				(ii) Check-flight manoeuvres only— 4-engined propeller	132

B. Measured Normal Accelerations. (Figures in brackets are subject to appreciable extrapolation errors)

Aircraft and duties	Upward acceleration reached per				Downward acceleration reached per			
	30 hr	100 hr	300 hr	1000 hr	30 hr	100 hr	300 hr	1000 hr
	g	g	g	g	g	g	g	g
Canberra B 2								
(i)	1.83	3.55	4.15	4.75		-0.4	-0.6	-0.82
(ii)	2.13	4.55	5.6	6.7		-0.72	-1.0	-1.28
Canberra B 6								
(i)		3.75	4.25	4.65		Rarely negative	Rarely negative	
(ii)		4.8	5.0	(5.2)		Rarely negative	Rarely negative	
(iii)		4.2	4.4	(4.5)		Rarely negative	Rarely negative	
(iv)		3.2	3.35			Rarely negative		
Various Bombers								
(i)	1.83	2.00	2.15	2.32	0.46	0.33	0.21	0.07
(ii)	2.13	2.34	(2.52)	(3.22)	0.30	0.16	0.02	-0.13
P4M-1		5.55	6.0	6.5		Rarely negative	Rarely negative	
PRM-5S		4.75	5.0	5.22		Rarely negative	Rarely negative	
C-130A	1.85	2.1	2.32	(2.55)	0.53	Rarely negative	Rarely negative	0.30
KC-135A	1.72	1.84	1.92	2.00		0.44	0.36	
B-47E	1.67	1.77	1.85	(1.94)				
B-52 (i)	1.75	1.87	2.0	2.3				
(ii)	1.8	1.95	2.07	2.2				
B-52G (i)	1.66	1.76	1.85	1.94	0.48	0.40	0.24	0.06
(ii)	1.52	1.58	1.65	1.72	0.56	0.50	0.44	0.38
6 Civil (i)	1.38	1.47	1.55	1.63	0.68	0.62	0.53	0.43
(ii)	2.08	2.27			0.25	0.10		

# MEASURED SYMMETRICAL MANOEUVRES

current aircraft has been omitted. The frequency of occurrence of normal accelerations of all fighters except Delta aircraft on combined duties is given in Figs. 5.1 and 5.2; that for Delta aircraft is given in Fig. 5.3. The frequency for fighters on combined duties is compared in Fig. 5.4 with that that occurs for fighters engaged primarily on specific duties.

In Fig. 5.1 the upward accelerations of ten types of aircraft are given

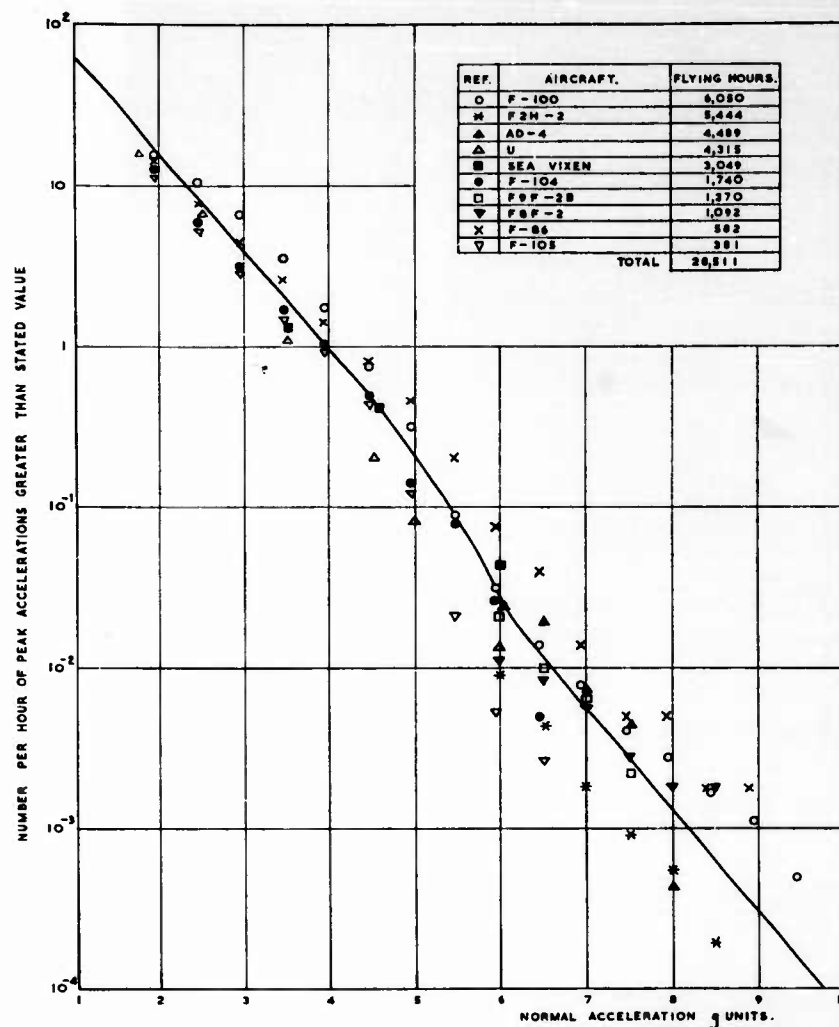


Fig. 5.1. Upward normal accelerations in flight of fighters on combined duties. Delta aircraft are excluded.

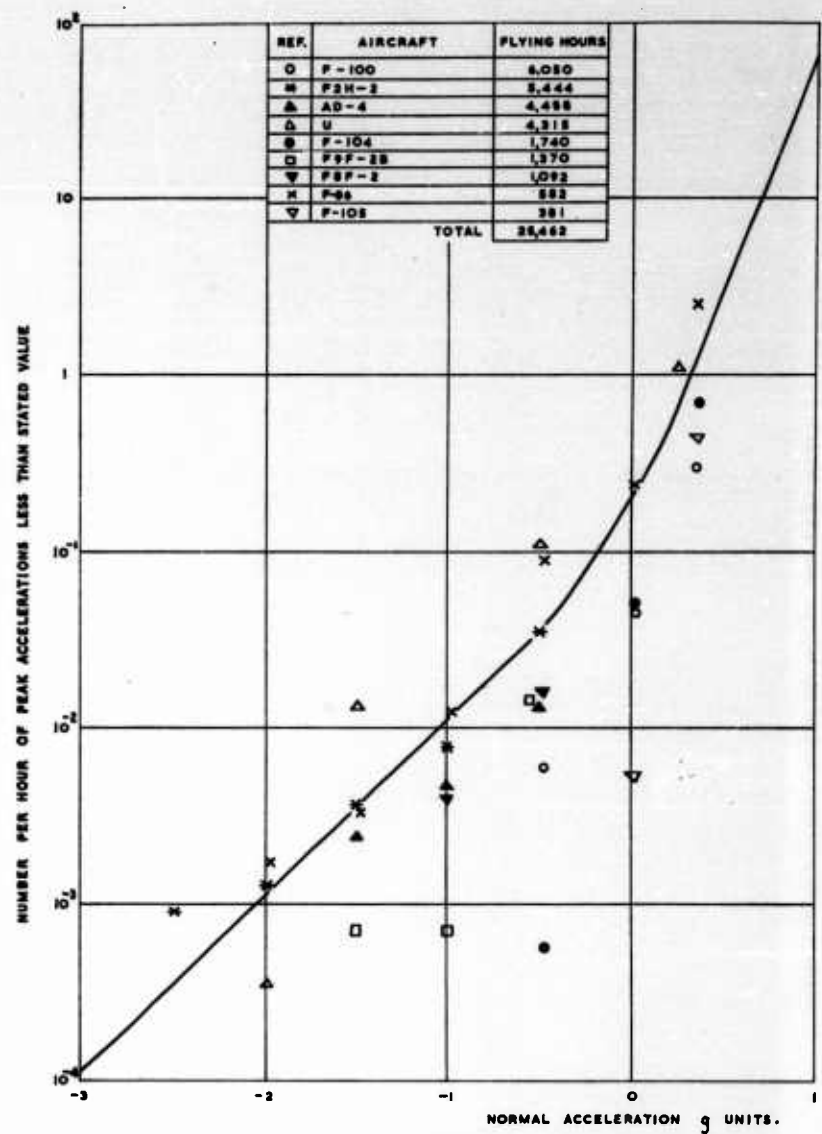


Fig. 5.2. Downward normal accelerations in flight of fighters on combined duties. Delta aircraft are excluded.

# MEASURED SYMMETRICAL MANOEUVRES

together with the averages for the results of all ten combined. There are 28,511 hr of records but they do not all cover the whole range of accelerations: the results from continuous trace records cover the whole range but the results from the other two instruments do not, the *V-g* records are not used for accelerations below 6*g* and the counting accelerometers omit counts above 6*g* in all except 1966 hr from aircraft *U*. This means that above 6*g*

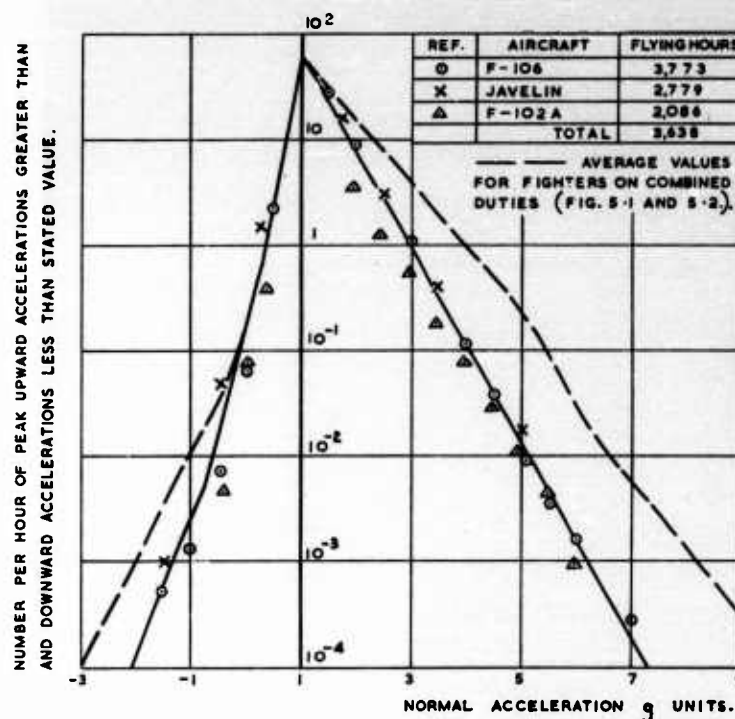


Fig. 5.3. Comparison of normal accelerations in flight of Delta with other fighter aircraft on combined duties.

the average results were based on 23,113 hr, which included 3 occurrences above 9.5*g* and 26 above 8*g*. The variation between the different aircraft is small, at accelerations above 6*g* few of the experimental measurements have an increment of acceleration more than 10 per cent from the average, at lower accelerations the variation is greater but rarely more than 15 per cent. In Fig. 5.2 the downward accelerations are shown for the same aircraft, except that no results were available for the Sea Vixen. The variation is much greater and the average value cannot be used for individual aircraft with the same confidence.

The combined results of Figs. 5.1 and 5.2 show the following characteristics

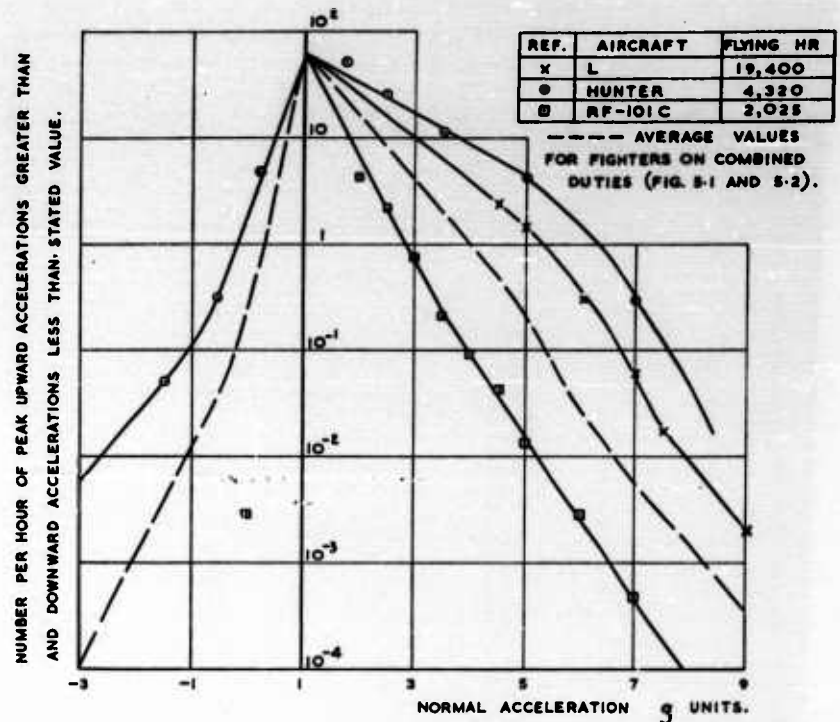


Fig. 5.4. Comparison of normal acceleration in flight of fighters on specific duties with those on combined duties.

*Hunter*—ground attack.

*Type L*—large proportion of ground attack.

*RF-101C*—95 per cent photographic reconnaissance.

that are of interest when examining fighter aircraft engaged primarily on specific duties, trainers and even bombers and transports

- (i) The extrapolated value of frequency of occurrence of a negligible increment of normal acceleration (i.e. total number of accelerations) is 60 per hour for both upward and downward accelerations.
- (ii) The upward increment of acceleration that occurs once per 1000 hr is approximately 30 per cent greater than that that occurs once per 100 hr.
- (iii) The downward increment of acceleration that occurs once per 1000 hr is approximately 50 per cent greater than that that occurs once per 100 hr.

As the extrapolation to a negligible increment of normal acceleration is based on accelerations below 0.3g and above 2g it refers primarily to accelerations due to manoeuvres. At smaller increments gusts may become



significant and the total frequency of occurrence of gusts and manoeuvres combined may be greater than shown.

Results are available for 8638 flying hours on 3 Delta aircraft. These are shown in Fig. 5.3 and compared with the average values for other fighters on combined duties. The variation between the three aircraft is very small particularly at the high increments. The total number of normal accelerations remains about 60 per hour up and 60 per hour down as for the other fighters, but the size of the increments of acceleration that occur once per 100 hr and once per 1000 hr are approximately 27 per cent less than those for the other fighters for both upward and downward accelerations.

When fighters are engaged primarily on specific duties the frequency of occurrence of normal accelerations may be appreciably different from the average for combined duties. Results are available for three aircraft so engaged and are shown in Fig. 5.4. The results on the RF-101C were from 2025 flying hours, of which 93 per cent were on photographic reconnaissance and similar missions. The results on the Hunter were from 4320 flying hours on ground attack missions. The results on aircraft L were from 19,400 flying hours which included a large proportion of time on ground attack missions but the actual percentage is not known. In all cases the total number of manoeuvres appears to remain at about 60 per hour up and 60 down; as the number of gusts is likely to be high on ground attack missions it is probable that this is the cause of the higher number of accelerations met by the Hunter at 1.75g.

The upward accelerations applied to RF-101C once per 100 hr and once per 1000 hr are about 22 per cent less than those on combined duties. Although it has a high gross weight of 37,000 lb there is no evidence to suggest that the accelerations would be different from other fighters if it were engaged on the same duties. In fact during the 7 per cent of the time not on reconnaissance type of missions the RF-101C experienced upward accelerations that were very close to those of other aircraft on combined duties. The downward accelerations were small and no conclusions can be formed on their relative frequency at different levels.

Both aircraft L and the Hunter experienced much higher normal accelerations than fighters on combined duties. Records are not available for the downward accelerations experienced by aircraft L but the Hunter experienced greater increments than average for combined duties. Great confidence can be placed in the results at the high upward accelerations for aircraft L which included 39 recorded occurrences greater than 9g and 349 greater than 7½g. On the Hunter 7g is the highest acceleration at which records were taken, but the curve on the diagram has been extrapolated on the assumption that it will be of similar shape to that of fighters on combined duties and to that of aircraft L. A little information is available on an early mark of Hunter (the fifth aircraft in Table 5.1) on combined duties; the results of 484 flying hours gave accelerations a little lower, but not significantly so, than the average values quoted for combined duties. As with RF-101C it may be presumed that it is the duties rather than the aircraft that determine the accelerations that are experienced. The results from aircraft L and the Hunter indicate that for an aircraft engaged entirely on ground attack, accelerations exceeding 8.8g will be encountered once per

significant and the total frequency of occurrence of gusts and manoeuvres combined may be greater than shown.

Results are available for 8638 flying hours on 3 Delta aircraft. These are shown in Fig. 5.3 and compared with the average values for other fighters on combined duties. The variation between the three aircraft is very small particularly at the high increments. The total number of normal accelerations remains about 60 per hour up and 60 per hour down as for the other fighters, but the size of the increments of acceleration that occur once per 100 hr and once per 1000 hr are approximately 27 per cent less than those for the other fighters for both upward and downward accelerations.

When fighters are engaged primarily on specific duties the frequency of occurrence of normal accelerations may be appreciably different from the average for combined duties. Results are available for three aircraft so engaged and are shown in Fig. 5.4. The results on the RF-101C were from 2025 flying hours, of which 93 per cent were on photographic reconnaissance and similar missions. The results on the Hunter were from 4320 flying hours on ground attack missions. The results on aircraft L were from 19,400 flying hours which included a large proportion of time on ground attack missions but the actual percentage is not known. In all cases the total number of manoeuvres appears to remain at about 60 per hour up and 60 down; as the number of gusts is likely to be high on ground attack missions it is probable that this is the cause of the higher number of accelerations met by the Hunter at 1.75g.

The upward accelerations applied to RF-101C once per 100 hr and once per 1000 hr are about 22 per cent less than those on combined duties. Although it has a high gross weight of 37,000 lb there is no evidence to suggest that the accelerations would be different from other fighters if it were engaged on the same duties. In fact during the 7 per cent of the time not on reconnaissance type of missions the RF-101C experienced upward accelerations that were very close to those of other aircraft on combined duties. The downward accelerations were small and no conclusions can be formed on their relative frequency at different levels.

Both aircraft L and the Hunter experienced much higher normal accelerations than fighters on combined duties. Records are not available for the downward accelerations experienced by aircraft L but the Hunter experienced greater increments than average for combined duties. Great confidence can be placed in the results at the high upward accelerations for aircraft L which included 39 recorded occurrences greater than 9g and 349 greater than 7½g. On the Hunter 7g is the highest acceleration at which records were taken, but the curve on the diagram has been extrapolated on the assumption that it will be of similar shape to that of fighters on combined duties and to that of aircraft L. A little information is available on an early mark of Hunter (the fifth aircraft in Table 5.1) on combined duties; the results of 484 flying hours gave accelerations a little lower, but not significantly so, than the average values quoted for combined duties. As with RF-101C it may be presumed that it is the duties rather than the aircraft that determine the accelerations that are experienced. The results from aircraft L and the Hunter indicate that for an aircraft engaged entirely on ground attack, accelerations exceeding 8.8g will be encountered once per

hour. The data that are available on other aircraft is generally rather less than 100 hr per aircraft on ground attack, but this limited data on the Vampire 5, F-86F, Sea Fury and F-100A give estimated values respectively of 8.55g, 8.95g, 8.7g and 9.2g being exceeded once per 100 hr. It is more difficult to estimate the accelerations that will be experienced once per 1000 hr but the extensive data from aircraft L gave 1.6g greater increment

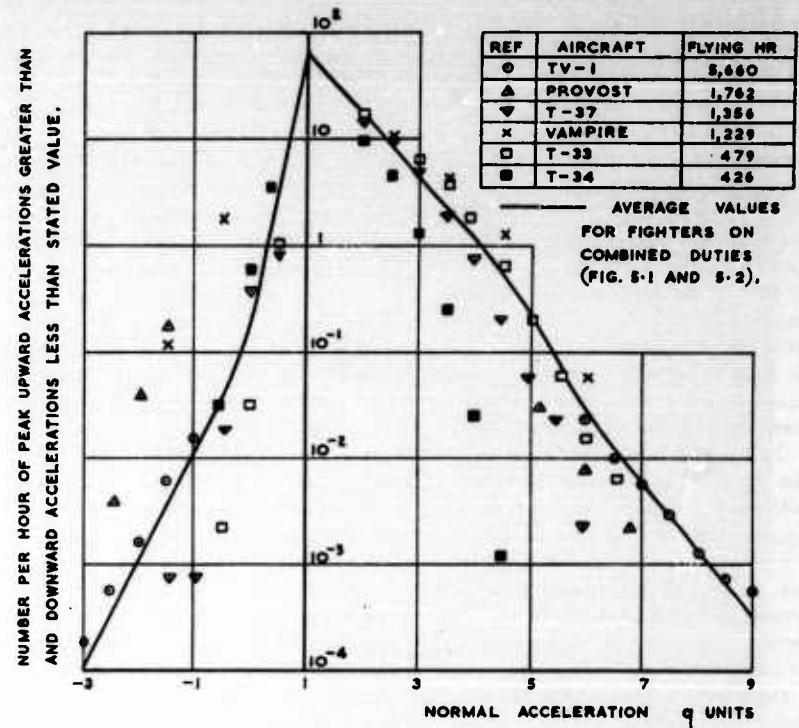


Fig. 5.5. Comparison of normal accelerations in flight of trainers with fighters on combined duties.

*T-34 is a primary trainer, all others are advanced.*

at once per 500 hr than that at once per 50 hr. This is the same change as the average for fighters on combined duties in spite of the higher value at once per 50 hr. Thus it may be expected that normal accelerations of the order of  $10\frac{1}{2}g$  will be exceeded once per 1000 hours on ground attack missions.

The results from 5 trainers are shown in Fig. 5.5 and compared with the average values for fighter aircraft on combined duties. Apart from T-34 which is a primary trainer and subject to relatively low accelerations, the average values for fighters on combined duties may be assumed to be representative for trainers also. There is a little more variation between the

# MEASURED SYMMETRICAL MANOEUVRES

trainers but there are a sufficient number of occurrences of downward accelerations below  $-2.5g$  to give increased confidence in the predicted frequencies of occurrence of downward accelerations in fighters as well as trainers.

The normal accelerations in manoeuvres of transports and bombers are much less than those of trainers and fighters. In consequence it is not permissible to assume that the normal accelerations are predominantly due to manoeuvres. An estimate is made in Fig. 5.6 of the normal accelerations

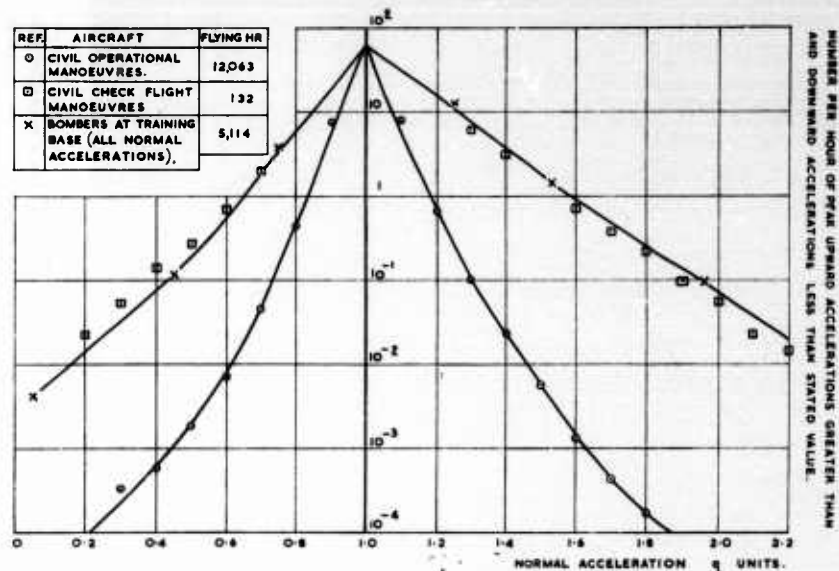


Fig. 5.6. Normal accelerations in flight manoeuvres of transports and bombers.

The results for the civil aircraft were obtained from 6 types of 4-engined aircraft: the 132 flying hours of check manoeuvres accompanied 15,580 hr of operational flying: the results for the bombers were obtained from various types and include gusts as well as manoeuvres but the proportion of gusts is likely to be small at all levels.

that would be experienced by transports and bombers in manoeuvres and then this estimate is combined with the predicted accelerations due to gusts, as given in Chapter 10, in Fig. 5.7 to compare total frequencies of occurrence of normal accelerations of 4 types of military aircraft. Walker, W. G. and Copp (1959) made an extensive survey of the normal accelerations experienced by civil airlines using piston-engine aircraft and separated the occurrences into gusts and manoeuvres and sub-divided the manoeuvres into those occurring on operational duties and those on check-flights. The manoeuvre results for the five 4-engined aircraft are taken together. Those for a 4-engined turbo-prop civil transport examined by Copp and Fetter (1959) are added to them and the combined results shown in Fig. 5.6. These combined results are from 12,063 flying hours on operational duties

and from 132 flying hours on check-flights, which accompanied 15,580 operational flying hours. In the same figure the total normal accelerations, due to gusts and manoeuvres combined, for 5114 flying hours of various bombers at a training base are also shown. The duties undertaken by the bombers are conversion training for crews flying that type of aircraft for the first time. By comparing the frequencies of occurrence of these accelerations with those that would be expected due to gusts it is evident that the records

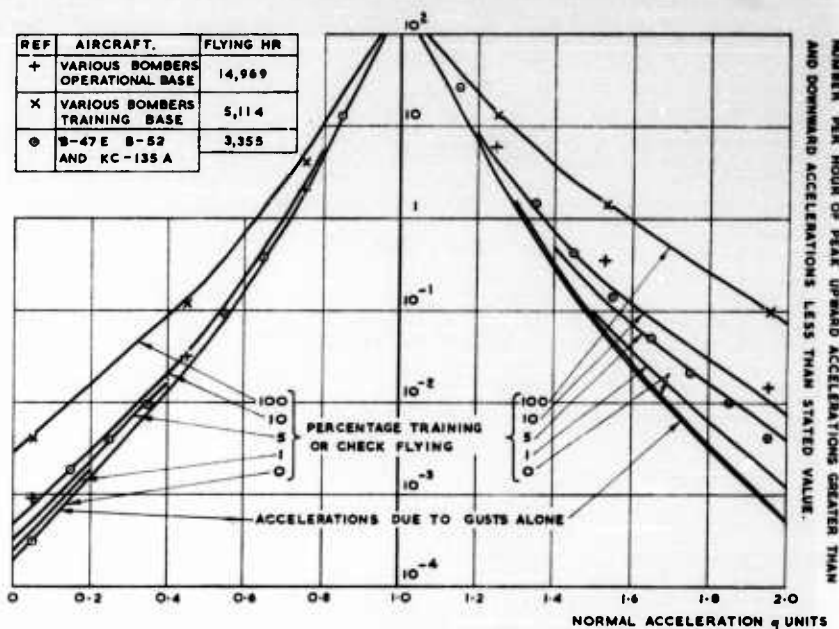


Fig. 5.7. Total normal accelerations in flight of gusts and manoeuvres of military transports and bombers.

Manoeuvres accelerations based on Fig. 5.6: gust accelerations based on Fig. 10.9 and on a 1g increment being produced by a 46 ft/sec gust (the average value for the B-47E, B-52 and KC-135A for the results quoted).

at increments of  $\frac{1}{2}g$  and more contain a negligible proportion of gusts. This fortuitous condition allows a comparison to be made between check-flights on a variety of civil transports with the flights on the bombers at the training base. Figure 5.6 shows that there is little difference between them, so that until more extensive data becomes available it may be assumed that roughly the same manoeuvres are used in check-flights and in training. Curves are drawn to represent manoeuvres on operational duties and manoeuvres on training or check-flights. In both cases the extrapolated values indicate 60 manoeuvres per hour up and 60 down, as was experienced by fighters and trainers; the frequency of occurrence of increments of  $\pm \frac{1}{2}g$  for the bombers is a little more than indicated by the curves as at this



level there will be a significant proportion of gusts. In the operational manoeuvres the upward increment that occurs once per 1000 hr is approximately 30 per cent greater than that that occurs once per 100 hr and the corresponding value for downward increments 50 per cent as in fighters. In the training and check-flight manoeuvres the highest recorded accelerations are those occurring about once per 100 hr but extrapolation suggests an increase of about 30 per cent for once per 1000 hr for both up and down accelerations. It has been necessary to rely entirely on civil airline practice for the operational manoeuvres, as none of the other data for military aircraft, not at training bases, is separated into training and non-training missions.

An indirect check on the accuracy of assuming that military transports and bombers have a similar intensity of operational manoeuvres is obtained by estimating the total frequency of occurrence of normal accelerations due to gusts and manoeuvres combined for a range of times spent on training or check-flights and then noting whether the apparent proportions on specific aircraft seem reasonable. This is done in Fig. 5.7 and compared with 14,969 flying hours of various bombers at operational bases and 3355 flying hours of B-47E, B-52 and KC-135A aircraft at operational bases. This comparison can only be done by using a conversion factor from gust velocities to normal accelerations. In most of the records on the B-47E, B-52 and KC-135A the manoeuvres and the gusts were given separately in terms of derived gust velocity and in terms of normal acceleration. For each of the three aircraft the conversion factor was close to 46 ft/sec gust velocity\* per 1g normal acceleration and was used for the predictions. The corresponding factor for the "various bombers" is not known but is probably not much different. The total of 3355 flying hours was made up of 1578 on B-52's, 1167 on KC-135A's and 610 on B-47E's. The individual relative frequencies at different acceleration levels on the B-52's and the KC-135A's were very close to each other and those for the much smaller sample on B-47E's were a little less at the higher increments; however it is considered that better accuracy is achieved by combining the results.

In the original analysis by Wallace (1961) on the B-52, by Perry and Rievley (1961) on the KC-135A and by Durkee (1961) on the B-47E secondary manoeuvres in which peaks which extended 0.1g beyond the preceding and following troughs were also counted and have not been included in the present analysis. L. G. Kelly and Broom (1962) do not include secondary manoeuvres in their measurements on the B-52. With the secondary manoeuvres omitted these measurements on the B-52, B-47E and KC-135A, those on the civil aircraft and those on the "various bombers" are all substantially the same and all are a good estimate of the increments of acceleration from a 1g datum. In order to retain a comparison with the civil transports no use has been made of the separation into gusts and manoeuvres of the B-47E, B-52 and KC-135A as many accelerations were counted as manoeuvres that would have been regarded as gusts in the civil aircraft. This procedure also maintains consistency in the examination of

\* The gust alleviation factors used in the original reports are approximately 7½ per cent lower than are used in Chapter 10 and the conversion factor on the gusts velocities quoted in the reports would be 50 ft/sec per g.

frequency of occurrence of gusts in Chapter 10. The number of gusts that have been assumed are those quoted in Chapter 10 and are the average obtained in 19,000 hr civil flying, which included 10 per cent of the time below 5000 ft where most of the gusts are encountered. Although the military aircraft being examined fly higher than the older civil types they nevertheless spend about 10 per cent below 5000 ft and would not be expected to meet an appreciably different number of gusts.

An examination of Fig. 5.7 shows that various bombers at training bases experience loads that would be expected if roughly 100 per cent of the time was used on training or check-flights; this, of course, was also demonstrated in Fig. 5.6 where the frequency of manoeuvre loads was examined. The various bombers at operational bases experienced upward and downward normal accelerations that were both consistent with about 12 per cent training flights and the B-47E, B-52, KC-135A group were consistent with about 5 per cent training flights. In addition to the results shown, there were 624 flying hours on a B-52G in a heavy gross weight condition but only 3 per cent of the flying was below 10,000 ft and relatively few gusts would be expected and a direct comparison is not possible. However the distribution between up and down accelerations is almost exactly that of gusts alone which is compatible with no training flights. Also 1077 flying hours have been quoted for manoeuvres only by L. Phillips (1961) on the C-130. The downward acceleration quoted did not differ much from civil aircraft on operational duties but the upward accelerations between 1.65g and 2.25g were approximately those that would be expected with 10 per cent training flights; the significant feature of these results is that they are in agreement with prediction up to 2.25g.

This indirect check of operational and training manoeuvres of Fig. 5.7 suggests that it may be assumed that all transports and bombers will experience manoeuvres as given in Fig. 5.6. In the case of civil transports the check-flights are approximately 0.8 per cent of the total flying time and the total manoeuvres will not add much to the accelerations due to gusts alone. In military transports the check-flying and training flights are liable to be an appreciably greater proportion and the manoeuvres will be significant. All the records that have been examined are under peace-time conditions and it is a matter of conjecture to estimate by how much the increments of acceleration would be increased in war-time.

### 5.3 FREQUENCY OF OCCURRENCE OF HIGH VELOCITIES

Aircraft make excursions to high forward velocities as well as to high normal accelerations but frequency of occurrence of forward velocities is a much more difficult concept to define than frequency of occurrence of normal accelerations. In the case of acceleration there is a natural datum at level flight, i.e. 1g, and any manoeuvre is an excursion from about 1g and back to 1g. As was stated in paragraph 5.2 it is convenient to make counts on the return after the peak has been reached, and the only decision to be made is the width of the threshold of acceleration before the count is made; furthermore the numerical value of the counts obtained is not critically affected by the width of the threshold. In the case of forward velocities the duration

# MEASURED SYMMETRICAL MANOEUVRES

at the maximum velocity is to some extent at the pilot's discretion and there is not the strong returning force that there is for normal accelerations. Somehow time must be introduced immediately either as flying hours or number of flights. In selecting the number of hours or flights that will be regarded as the scale of time, it should not be so short that one excursion is counted several times, likewise it should not be so long that only one count is made and a number of others of about the same magnitude omitted.

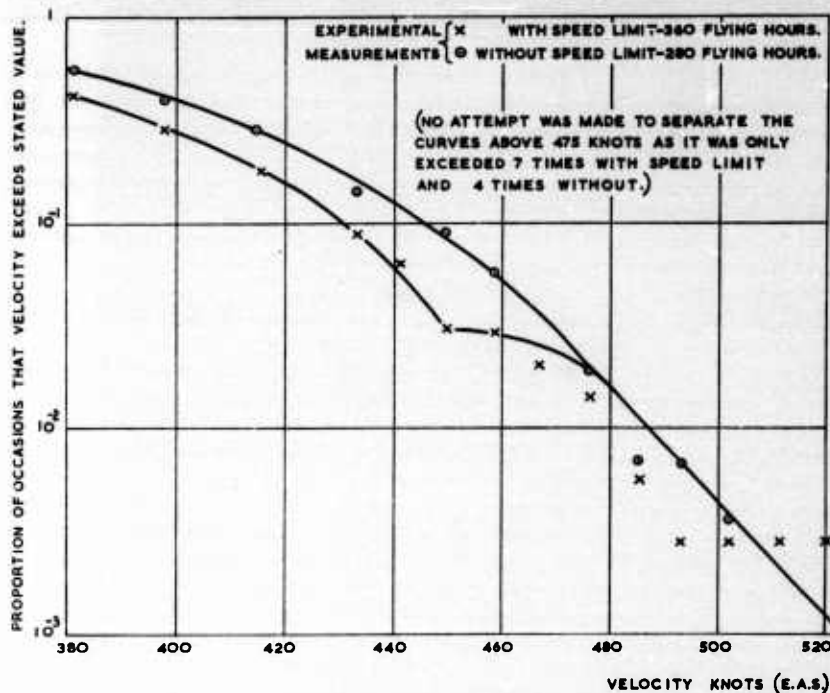


Fig. 5.8. Evidence to support the presumption that the highest velocities occur predominantly in straight and level flight.

Effect of speed limitation on a 10° dive on peak velocities of a Meteor fighter.

Before deciding empirically on the time-scale some concept must be acquired of the general character of the excursions to high velocities. An indication of this character can be deduced from some flying on the Meteor 8 fighter which was flown for about half the recording time with a speed limitation in dives of 10° and above. Figure 5.8 shows evidence to support the contention that the highest velocities occur predominantly in flight that is close to being straight and level. The distribution\* of peak velocities is

\* This is deduced from the highest velocity recorded on each V-g slide, which have an average duration of about one flying hour, and is in accordance with the proposals given later in this paragraph 5.3.



shown for the Meteor 8 with and without the speed limitation in a dive. With the limitation there is a sharp drop in frequency a little above the speed limit indicating that many excursions to high speed in a dive have been avoided. But the curve of log (frequency of occurrence) against forward velocity shows a well-defined cusp at a higher velocity and the curve at the highest velocities is the same for both conditions. Thus it may be concluded that the speed limitations in the dive did not influence the frequency of occurrence of the highest velocities and that the highest velocities rarely occurred in a dive whether or not there was a speed limitation in the dive.

The distribution of forward velocities may be considered as made up of three main families. The commonly used cruising velocities form the first group and in these conditions the aircraft will often be flown at a reasonably steady velocity for long periods; the main interest is the length of time spent at different speeds and this is discussed in Chapter 8. The other two groups are associated with manoeuvres starting from a condition of the first group. The highest velocities are predominantly in straight and level flight and are therefore a simple forward acceleration from the reasonably steady velocity to a peak velocity and back again, i.e. a symmetrical manoeuvre in the line of flight. The intermediate velocities are associated with symmetrical manoeuvres in pitch and are discussed in paragraph 5.4.

The order of the time-scale of the excursions from the cruising condition can be estimated both for the case of change of forward velocities due to forward acceleration alone and for the case of change of forward velocity due to the application of normal acceleration with steady engine thrust. The second case is amenable to direct estimation. The manoeuvre is essentially one of change of direction by pitching motion. Whatever plane this is in, from horizontal to vertical, the maximum change that need be made is  $180^\circ$ . The minimum time in which this can be done with a forward speed of  $V$  and a maximum increment of normal acceleration of  $ng$  is  $\pi V/ng$  (i.e. motion in a circle). Taking  $V = 800$  ft/sec  $n = 5$  as typical this gives a minimum time for the extreme manoeuvre as approximately 16 sec. To this must be added the time taken in accelerating up to the forward speed at which the manoeuvre is done and also any extra time due to part of the turn being at a normal acceleration below the peak value. This gives the maximum time that can be spent in the manoeuvre; also the average time will reduce because only a fraction of  $180^\circ$  change of direction will usually be used. Table 5.5 gives an analysis of the air to ground missions performed by F-84E, F-84G and F-86F aircraft in the war in Korea. The average time accelerating in the dive was about 20 sec for each of the missions. The average time in the pull-out depends on the change of angle and if it is assumed that the climb angle is roughly the same as the dive angle, the total change will be  $20^\circ$  to  $118^\circ$ , i.e. twice the dive angle. The time will also depend on the radius of the pull-out which is nearly proportional to the average normal acceleration rather than the peak normal acceleration. On average the manoeuvres quoted had a radius of the pull-out about  $1\frac{1}{2}$  times the minimum that would have been achieved had the peak acceleration been maintained for the whole pull-out. Thus for the typical case already mentioned of  $V = 800$  ft/sec  $n = 5$  the time in a  $118^\circ$  change of angle

would be 10 sec ( $= 16 \times 1.5 \times 118/180$ ). Thus the total time of the manoeuvre with regard to forward velocity changes is about 50 sec (assuming the time in the climb is roughly equal to that in the dive). The time scale for change in forward velocity due to forward acceleration alone can only be estimated indirectly from a knowledge of the total time spent at different speeds. The F-100 is the only aircraft with sufficient measurements for this to be done and it is estimated in Chapter 8 that the average time of excursions occurring once per 30 hr, or less frequently, is about 0.05 hr (i.e. 3 min) at speeds near the maximum velocity; the accuracy of the estimate does not justify attempting to make a correction for the time to reach the maximum.

It is convenient for analysis to count the frequency of occurrence of high velocities as the highest occurring in each flight or the highest recorded on each *V-g* slide which is an average of about 1 hour's flying for most of the *V-g* records examined. This is, in fact, the method that has been used and a check on the accuracy can be made by working backwards from the deduction in Chapter 8 that has just been stated, that the average time of excursions once per 30 hr is 0.05 hr. This means that unless there is a large scatter between the times of individual excursions the maximum velocity for every 0.5 hr, i.e.  $10 \times 0.05$  hr, flying could be read with a negligible risk of counting any one excursion twice. The only advantage in choosing such a short time would be that it would avoid missing excursions if there was a clustering of excursions to high velocities, i.e. there was a tendency for a pilot to repeat immediately an excursion to high velocity. Such a clustering does occur with gust loads (Chapter 10) but there seems to be little likelihood of it occurring for high forward velocities whether they are produced by forward acceleration or by normal acceleration. Thus there is considerable tolerance on the counting procedure and counts of the highest velocity either per flight or per hour should be a completely satisfactory basis from which to deduce the frequency of occurrence of velocities occurring not more frequently than once per 30 hr.

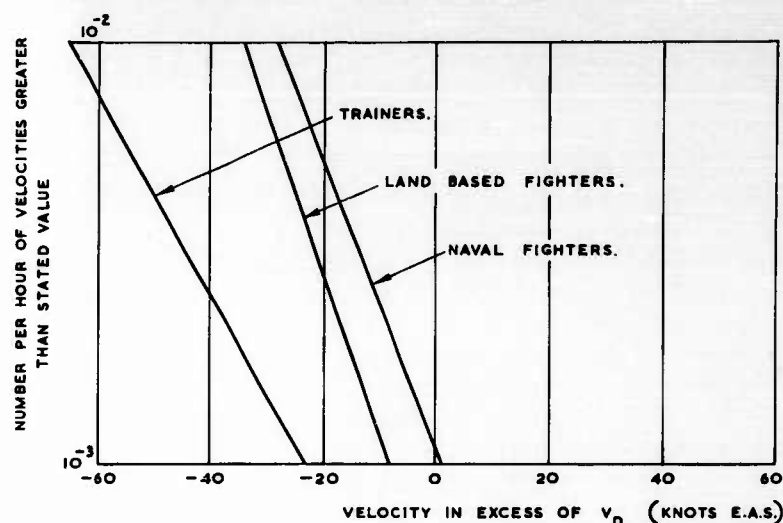
Strictly this analysis does not separate high velocities due to forward acceleration alone from those coupled with normal accelerations. It has been shown earlier in this paragraph 5.3 that the highest forward velocities are predominantly from the family of manoeuvres consisting only of forward acceleration. For lower values of the peak velocity there will be more likelihood of overlap with the high velocities coupled with normal acceleration but generally the forward velocity that is exceeded once per 30 hr will be sufficiently high for it not to be accompanied by an appreciable normal acceleration.

The frequencies of occurrence of high forward velocities are given in Tables 5.6, 5.7, 5.8, 5.9 for land-based fighters, naval fighters, trainers and one light-bomber respectively. In each case the design diving speed is shown. Although the data are for fewer aircraft than the data on frequency of occurrence of normal accelerations they are sufficient to give a reasonable impression for all the types except transports and bombers. The information is shown graphically in Fig. 5.9; the frequency of occurrence of the high forward velocities seems to be influenced greatly by the design diving speed and the curves in the figure are given in terms of it.



# MEASURED SYMMETRICAL MANOEUVRES

There is a slight difference in the way the military pilots are informed of the speed limits in U.S.A. and U.K. In U.S.A. the Design diving velocity is quoted to the pilots as the Service limit but in U.K. the pilots are given a Service limit that is approximately 90 per cent of the Design diving velocity.



THE ABOVE CURVES ARE AVERAGE VALUES FROM THE FOLLOWING:-			
TYPE	FLYING HOURS	TYPE	FLYING HOURS
LAND BASED FIGHTERS		NAVAL FIGHTERS	
VAMPIRE	1,032	F 2 H - 2	5,444
METEOR	640	F 9 F - 2 B	1,370
HUNTER	484	WYVERN	555
		SEA HAWK	312
TRAINERS		SEA FURY	210
TV - I	5660		
JET PROVOST	495		

Fig. 5.9. Frequency of occurrence of peak forward velocities.

On the limited data examined no significant difference was found between U.S. and U.K. aircraft. The frequency with which 90 per cent of the design diving speed is exceeded depends more on the aircraft duties than on the aircraft design. For a given group of aircraft, e.g. land-based fighters, there is less variation in the relative frequency between the velocities occurring once per 100 hr and once per 1000 hr than there is variation in the absolute value of the frequency at once per 100 hr. The average frequencies

for the land-based fighters, naval fighters and trainers are given in Table 5.10.

For all except transports and bombers the design diving speed exceeds the average cruising speed by so much that the cruising speed has little influence. For the transports and bombers the design diving speed is much more nearly a limiting cruising speed and it should be to some extent related

Table 5.6. Frequency of Occurrence of Peak Forward Velocities of Land-based Fighters

(Figures in brackets are subject to appreciable extrapolation error)

Aircraft and duties details in Table 5.1	Design diving velocity $V_D$ knots	Velocity exceeded once per			
		30 hr knots	100 hr knots	300 hr knots	1000 hr knots
Meteor 8					
(i)	522	461	482	502	(523)
(ii)		450	482	502	(523)
Vampire 5					
(i)	478	428	440	450	458
(ii)		435	447	459	(469)
(iii)		441	460	(468)	
(iv)		430	443	(452)	
Venom FB 1					
(i)		445	481	498	542
(ii)		467	490	510	(537)
Hunter 4					
(a) (i)	620	547	566	581	(594)
(ii)		580	590	601	(612)
		570	595	607	(617)
Meteor NF 11	550	445	464	480	494

to the design cruising speed. Unfortunately no data are available for this group of aircraft (the light bomber of Table 5.9 is not really representative as it has a small gross weight and a Service limit of 5g normal acceleration) and extrapolation from fighters or trainers would not be possible.

#### 5.4 DISTRIBUTION OF THE FORWARD VELOCITIES, AT WHICH THE PEAK NORMAL ACCELERATIONS OCCUR

In paragraphs 5.2 and 5.3 the frequency of occurrence of all the high normal accelerations and all the high forward velocities are given. The combined occurrence of normal acceleration and forward velocities can not be deduced from this information as it was noticed that normal accelerations are avoided as far as possible when the highest forward velocities are being attained.

# MEASURED SYMMETRICAL MANOEUVRES

**Table 5.7. Frequency of Occurrence of Peak Forward Velocities of Naval Fighters**

(Figures in brackets are subject to appreciable extrapolation error)

Aircraft and duties details in Table 5.2	Design diving velocity $V_D$ knots	Velocity exceeded once per			
		30 hr knots	100 hr knots	300 hr knots	1000 hr knots
Sea Hawk					
(i)	565	471	494	510	(525)
(ii)		500	517	(534)	(551)
Sea Fury					
(i)	456	409	439	(450)	
(ii)		449	462	(475)	
Wyvern S4					
(a) (i)	479	412	440	465	491
(ii)		426	439	(450)	(461)
(iii)		412	455		
		407	437	452	(466)
(b) (i)		435	442	452	(458)
(ii)		396	432	(465)	(502)
		417	440	454	(465)
F2H-2	510		480	500	515
F9F-2B	505		490	515	522

**Table 5.8. Frequency of Occurrence of Peak Forward Velocities of Trainers**

(Figures in brackets are subject to appreciable extrapolation error)

Aircraft and duties details in Table 5.3	Design diving velocity $V_D$ knots	Velocity exceeded once per			
		30 hr knots	100 hr knots	300 hr knots	1000 hr knots
Jet Provost					
(a) (i)	380		345	357	(367)
(ii)			337	(350)	(364)
(iii)			292	305	(317)
			315	334	355
TV-1	510		444	466	490

# MANUAL ON AIRCRAFT LOADS

**Table 5.9. Frequency of Occurrence of Peak Forward Velocities of a Light Bomber**

(Figures in brackets are subject to appreciable extrapolation error)

Aircraft and duties details in Table 5.4	Design diving velocity $V_D$ knots	Velocity exceeded once per			
		30 hr knots	100 hr knots	300 hr knots	1000 hr knots
Canberra B6	500				
(i)			435	460	480
(ii)			465	485	(505)
(iii)			452	474	(490)
(iv)				low speeds	

**Table 5.10. Average Frequency of Occurrence of High Forward Velocities**

No. of times per hour that the velocity is exceeded	Velocity in excess of design diving speed		
	Land-based fighters knots (EAS)	Naval fighters knots (EAS)	Trainers knots (EAS)
$10^{-2}$	-34	-28	-65
$10^{-3}$	-8	+1	-23

However, for a full knowledge of the aircraft loads in pitching manoeuvres it is necessary to know not only the normal accelerations but the relative frequency of occurrence of different forward velocities at the time the peak normal accelerations occur. Fisher (1964) has examined the moderate to high normal accelerations of a number of aircraft and he has shown that the distribution of forward velocities for each aircraft remains substantially the same for each level of normal acceleration. He has shown further that provided the aircraft is engaged primarily on one type of operation the distribution is fairly symmetrical and not significantly different from a Normal distribution. When a number of types of operation are combined the distribution appears to be made up of a number of symmetrical distributions. The relative frequency of occurrence of different forward velocities of an F-100D is shown in Fig. 5.10; the records of 420 pitching manoeuvres all exceeding 4.5g are used to prepare this diagram. The histogram, in 25 knot bandwidths, of the measured data is shown, the calculated



# MEASURED SYMMETRICAL MANOEUVRES

curve is the relative frequency that would occur with 120 manoeuvres at a mean forward velocity of 330 knots and standard deviation of 25 knots and 300 manoeuvres at a mean of 404 knots and standard deviation of 38 knots. The mean forward velocity of 330 knots of the smaller group of manoeuvres is about 40 knots above the usual cruising velocity (see Chapter 8) and this group seems to be predominantly of manoeuvres initiated from

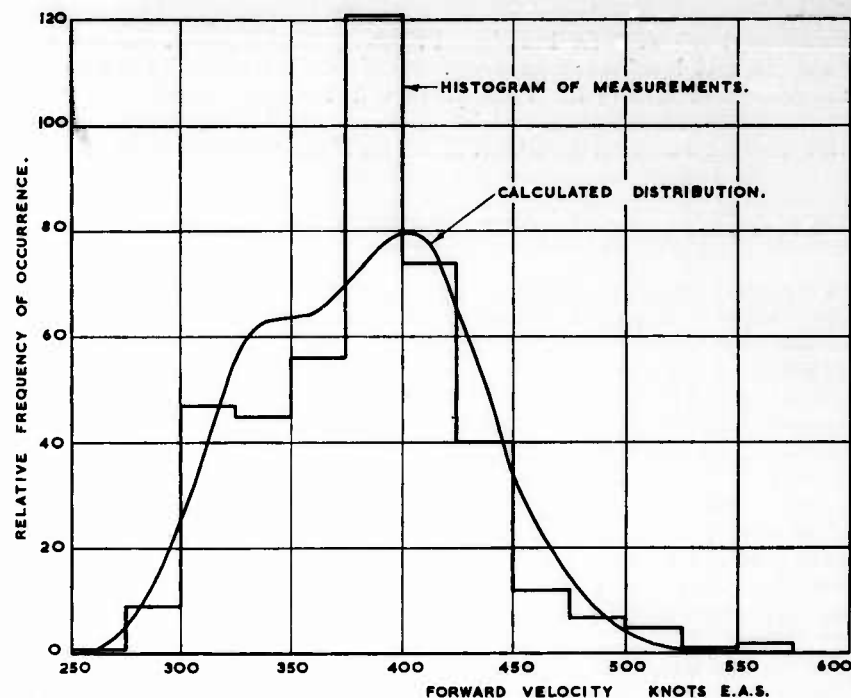


Fig. 5.10. Relative frequency of occurrence of forward velocities at the time peak normal accelerations occur on an F-100D in manoeuvres.

The measurements are for 420 manoeuvres above 4.5g. The calculated distribution is the sum of two normal distributions, one for 120 manoeuvres with mean 330 knots E.A.S. and standard deviation 25 knots E.A.S. and one for 300 manoeuvres with mean 404 knots E.A.S. and standard deviation 38 knots E.A.S.

the cruising condition, the group of manoeuvres with mean velocity of 404 knots are probably mainly in ground attack with the peak normal acceleration being applied a short time after the peak forward velocity is attained.

The combined distribution of peak normal accelerations and the forward velocity at which they occur can be given in a simple form by making the assumption, found by Fisher to be valid for a number of aircraft, that the distribution of forward velocity is independent of the magnitude of the peak normal acceleration. The distribution is given as two independent formulae,



one for normal acceleration and one for forward velocity. In determining the distribution of forward velocities the normal accelerations greater than those that occur once in 3 hr are all grouped together and the average distribution of forward velocities taken. If higher accelerations had been taken there would have been rather few records and if much lower ones had been included the distributions would have become less accurate for the more interesting high normal accelerations. Tables 5.11, 5.12, 5.13, 5.14 give the mean  $V_m$ , standard deviation  $\sigma_v$  and skewness  $\zeta$  (third moment) of the forward velocities for land-based fighters, naval fighters, trainers and transports and bombers respectively. Within the accuracy of the data the distributions of most of them may be regarded as being Normal and those few cases where there is appreciable skewness may be regarded as Normal with different standard deviations above and below the mean.

### 5.5 FREQUENCY OF COMBINED OCCURRENCE OF NORMAL ACCELERATIONS AND FORWARD VELOCITIES

So far the normal accelerations and forward velocities have been kept substantially separate. In paragraph 5.2 the frequency of occurrence of normal acceleration was examined without any consideration of forward velocity, then in paragraph 5.3 the frequency of occurrence of forward velocity was taken without regard to normal acceleration. In paragraph 5.4 the distribution of the forward velocities at which the peak normal accelerations occurred was examined. These three functional relationships can be combined to give the frequency of the combined occurrence of prescribed normal accelerations and prescribed forward velocities. If the distribution of forward velocities at which the peak normal accelerations occur were to be maintained for all normal accelerations only two of the relationships instead of three would be necessary. In practice the average distribution has been determined for accelerations exceeded once per 3 hr. If all normal accelerations are grouped together instead of merely those exceeded once per 3 hr, the separately obtained distribution of forward velocities will give a better estimate; also it is possible to check whether the distributions of forward velocities at the peak normal accelerations of the manoeuvres is similar to the distribution of forward velocities unrelated to the manoeuvres. The comparison gives an indication when there are two families of distributions of forward velocity.

The basic principles involved in determining frequencies of combined occurrence can be illustrated by taking simple formulae for the various relationships and illustrating them diagrammatically. For high normal accelerations the frequency of occurrence,  $N_n$  per hour, of normal accelerations exceeding  $ng$  is given by

$$N_n = N'_0 \exp (-n/n_1) \quad (5.1)$$

The parameters  $N'_0$  and  $n_1$  are chosen to give the best estimate for frequencies of occurrence less than once per 100 hr. In many cases, particularly fighters on combined duties (Figs. 5.1 and 5.2) this distribution does not differ much from the measured values at frequencies of occurrence of once per hour.

# MEASURED SYMMETRICAL MANOEUVRES

Table 5.11. Distribution of Forward Velocities at which Peak Normal Accelerations occur in Land-based Fighters for all Normal Accelerations Greater than the Value Indicated

Aircraft and duties for details see Table 5.1	Min. peak normal acceleration (g)	Upward			Downward below 0g		
		$V_m$ knots	$\sigma_V$ knots	$\zeta$	$V_m$ knots	$\sigma_V$ knots	$\zeta$
Meteor 8							
(i)		338	44.7	-0.06	320	58.8	
(ii)	4.95	348	39	+0.085	306	52.2	
Vampire 5							
(i)	5.15	330	45	-0.48	282	61.5	+0.36
(ii)		315	36.5	+0.145	292	45.6	-0.38
(iii)		325	27.5		307	38.2	+0.205
(iv)		325	36		303	38.2	-0.34
Venom FB 1							
(i)		296	57	+0.58	290	49.5	
(ii)	5.65	313	26.5	+0.85	282	81	
Hunter 4							
(i)	4.35	370	46	+0.183	328	72.5	+0.55
(ii)	4.35	391	57	+0.33	321.5	84.5	+0.43
(iii)	4.35	371.5	53.5	small	327	78	+0.425
Javelin Mk 1	3.75	342.5	60	+0.61	309	51.4	+0.2
Gannet A/S Mk 1							
(i)	2.75	264.5	62.5	+0.078			
(ii)	1.95	232	62.5	+0.123			
Meteor NF 11	3.55	320	38.5	+1.32	304	57.0	+0.8
F86							
E and F	5.45	380	41	-0.1	315	78	+1.17
F86F							
(a) (i)	5.0	450	82.5	-1.07			
(ii)	5.5	400	51.5	+0.58			
(iii)	5.5	372	46	-0.05			
(iv)	4.0	332	37.4	+0.54			
(v)	3.5	312	34.3	+0.267			
		383	74	-0.23	352	86	+0.25
F86F	6.0	440	42	-0.51	Only 3 recorded		
F84G	4.5	382	36.2	-0.276			
F-100D							
(a) (i)	3.5	350	59	+0.07			
(ii)	5.0	386.3	40	-0.30			
(iii)	4.5	387					
(iv)	4.5	412	56.5	-0.44			
(v)	4.0	381	32.3	+1.03			
		383	48	-0.08			

Table 5.11 (continued)

Aircraft and duties for details see Table 5.1	Min. peak normal acceleration (g)	Upward			Downward below 0g		
		$V_m$ knots	$\sigma_V$ knots	$\zeta$	$V_m$ knots	$\sigma_V$ knots	$\zeta$
F-100C							
(a) (i)	4.5	351.5	51.5	+0.82			
(ii)	4.5	380	41	-0.175			
(iii)	4.5	351.5	51.5	+0.82			
(iv)	4.5	387	23	+0.5			
(v)	4.5	381	37.5	-0.153			
		368	48	small			
(b)	4.5	466	70	+0.34			
F-102A	3.5	380	75	+0.44			
F-104A	3.0	405	82.7				
	3.0	403.7	71.3	+0.1			
F-105B	4.5	509	58	0			
RF-101C	3.0	391	55	+0.16			
F-104C	4.45	459	38	-0.55			

Table 5.12. Distribution of Forward Velocities at which Peak Normal Accelerations occur in Naval Fighters for all Normal Accelerations Greater than the Value Indicated

Aircraft and duties for details see Table 5.2	Min. peak normal acceleration (g)	Upward			Downward below 0g		
		$V_m$ knots	$\sigma_V$ knots	$\zeta$	$V_m$ knots	$\sigma_V$ knots	$\zeta$
Sea Hawk							
(i)	4.45	352	45	+0.43	312	61	
(ii)		379	57	-0.40	324	68	
Sea Fury							
(i)	4.35	288	48	+0.31	257	43.5	
(ii)	5.15	380	29.7	-0.38	287	65	
Wyvern S 4							
(a)	4.95	350	34.3	+0.374	274	51.7	+0.13
(b)	3.95	307	54.5	+0.455	282	59.5	+0.178
F2H-2	6.0	381	45.5	+0.36			
F9F-2B	5.5	392	49	+0.44			
F8F-2	4.5	383	48.5	+0.19			
AD-4							
(i)	5.0	329	52	+0.26			
(ii)	5.5	302	39	-0.24			

# MEASURED SYMMETRICAL MANOEUVRES

Table 5.13. Distribution of Forward Velocities at which Peak Normal Accelerations occur in Trainer Aircraft for all Normal Accelerations Greater than the Value Indicated

Aircraft and duties for details see Table 5.3	Min. peak normal acceleration (g)	Upward			Downward below 0g		
		$V_m$ knots	$\sigma_v$ knots	$\zeta$	$V_m$ knots	$\sigma_v$ knots	$\zeta$
Jet Provost							
(a) (i)	4.35	234	53	0			
(ii)	2.15	183	53.5	+0.3			
(iii)	3.35	205	49	+0.47	169	43	+1.04
	3.95	213	49.5	+0.3			
T-34	3.0	138	19	-0.25			
T-33	5.0	336	38	+1.61			
T-37	4.5	240	32.5	+0.07			
TV-1	6.0	316	39	-0.10			

Table 5.14. Distribution of Forward Velocities at which Peak Normal Accelerations occur in Transports and Bomber Aircraft for all Normal Accelerations Greater than the Value Indicated

Aircraft and duties for details see Table 5.4	Min. peak normal acceleration (g)	Upward			Downward below 0g		
		$V_m$ knots	$\sigma_v$ knots	$\sigma$	$V_m$ knots	$\sigma_v$ knots	$\zeta$
Canberra							
B2							
(i)	2.95	286	53.5	+0.85	286	78	-0.34
(ii)	2.75	282	52	0	246	78	+0.31
Canberra							
B 6							
(i)	2.15	278	55.3	+0.17			
(ii)	3.55	290	44	+0.19			
(iii)	2.35	320	65	+0.5			
C-130A	1.35	190	32	+0.3			
KC-135A	1.40	270	26	-0.63			
B-47E	1.35	243	50.5	-0.26			
B-52G (i)	1.45	257	31	-0.03			
(ii)	1.35	258	27	-1.44			
P4M-1	1.75	209	45.5	+0.74			
PBM-55	1.25	158	20.6	+0.56			

For high forward velocities  $V$  it was suggested, in paragraph 5.3, that

$$N_V = N'_0 \exp(-V/V_1) \quad (5.2)$$

The parameters  $N'_0$ ,  $V_1$  are chosen similarly to give the best estimate for frequencies of occurrence less than once per 100 hr. For high velocities extrapolation to more frequent occurrences than once per 100 hr is not advisable.

In paragraph 5.4 it was suggested that for all normal accelerations that occurred less frequently than  $\frac{1}{3}$  per hour the forward velocities at which the peaks occurred were distributed normally. Thus

$$N_{Vn}/N_n = (1/\sigma_V \sqrt{2\pi}) \cdot \int_V^\infty \exp\{-(V - V_m)^2/2\sigma_V^2\} dV \quad (5.3)$$

where  $N_{Vn}$  = number per hour with forward velocity exceeding  $V$  and normal acceleration exceeding  $ng$

$V_m$  = the mean velocity

$\sigma_V$  = the standard deviation about the mean velocity

Combining (5.1) and (5.3)

$$N_{Vn} = N'_0 \exp(-n/n_1) \cdot (1/\sigma_V \sqrt{2\pi}) \cdot \int_V^\infty \exp\{-(V - V_m)^2/2\sigma_V^2\} dV \quad (5.4)$$

The reliability of using equation (5.3) depends on the accuracy of the distributions from which Tables 5.11 to 5.14 were produced. These distributions are based on relatively few events and the extreme values will in consequence be of limited accuracy. Whilst the normal distribution is probably quite adequate at forward speeds within 2 standard deviations of the mean, it would cease to be applicable at the extreme values, i.e. equation (5.3) holds for  $N_{Vn}/N_n$  greater than about 0.01. Thus  $N_n$  must be less than  $100N_{Vn}$  so that for a given value of  $N_{Vn}$   $n$  has a minimum value. The frequency of occurrence of high forward velocities without any restriction on normal accelerations, i.e.  $n = 1$ , is given by equation (5.2). These values can be used as extrapolated values for  $N_{Vn}$  bearing in mind that many of the highest forward velocities will be unaccompanied by appreciable normal accelerations.

The frequency of the combined occurrence of normal acceleration greater than  $ng$  and forward velocity greater than  $V$  is shown in non-dimensional form in Fig. 5.11. The normal acceleration scale is chosen such that a unit equals the change in acceleration for a ten-fold change in frequency of occurrence. The forward velocity scale is chosen such that a unit equals the standard deviation of velocity of equation (5.3); there is a second unit of velocity corresponding to a ten-fold change in frequency of occurrence in equation (5.2) and this is taken arbitrarily as 0.6 standard deviations. In this general diagram the zero normal acceleration is at an unknown number of units from the acceleration that occurs once per 100 hr. Also the forward velocity that occurs once per 100 hr is an unknown number of units from the mean velocity  $V_m$  at which the high peak normal accelerations occur. Thus

# MEASURED SYMMETRICAL MANOEUVRES

the position of the lowest line showing the velocity distribution of equation (5.2) is not known either horizontally or vertically but merely in direction. In practical examples the position will be known and the smoothness of the extrapolations from the upper diagram to the lower line can be seen.

The method of presenting the data of equations (5.1), (5.2) and (5.3) in the form of Fig. 5.11 has the limitation that the information is cramped

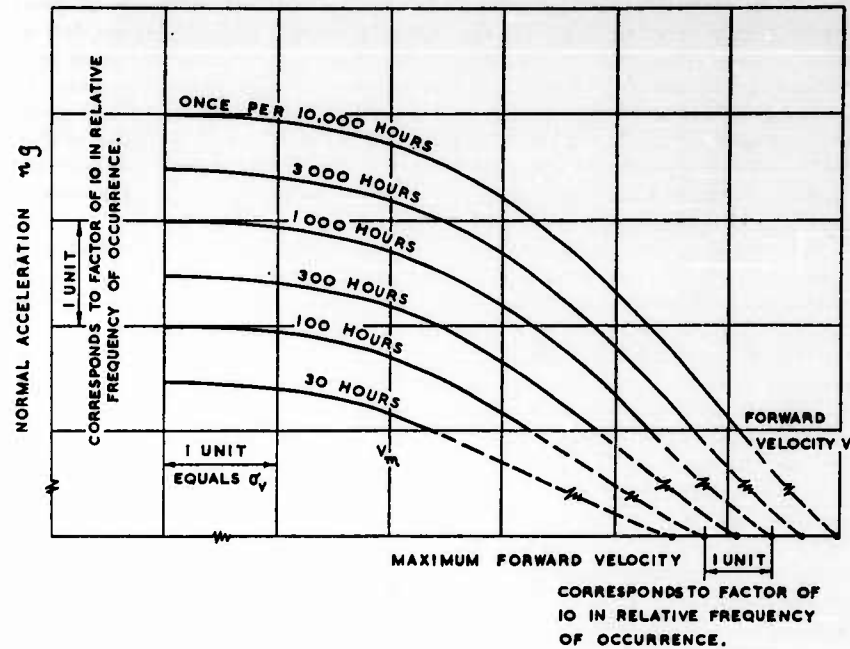


Fig. 5.11. Frequency of combined occurrence of forward velocity greater than  $V$  and normal acceleration greater than  $ng$ .

Peak normal accelerations  $ng$  occur at forward velocity  $V$  which has a mean of  $V_m$  and a standard deviation of  $\sigma_v$  about the mean.

The position of the axis for maximum forward velocity is not correct either relative to normal acceleration or to forward velocity.

below and extended above the average velocity  $V_m$  at which peak accelerations occur. If on the other hand the frequency of occurrence of forward velocities less than the stated value were plotted the opposite situation would arise and the information would be cramped above  $V_m$ . Usually however the presentation as given in Fig. 5.11 is of more practical interest. The practical significance of  $N_{Vn}$  is fairly straight forward for the limiting cases of  $V = 0$  and  $n = 1$ . When  $V = 0$ ,  $N_n$  is the frequency of occurrence of a normal acceleration greater than  $ng$  and its value corresponding to a given strength (in terms of  $ng$ ) is a reasonable representation of reliability of those parts primarily affected by normal acceleration rather than forward velocity.

When  $n = 1$ ,  $N_V$  is the frequency of occurrence of a forward velocity greater than  $V$ . Again the numerical value of  $N_V$  is a reasonable representation of the reliability of those parts affected primarily by forward velocity. In these two extreme cases there is one feature in common, an increase in the parameter concerned ( $ng$  or  $V$ ) produces an increase in load. For the intermediate points on the diagram the curves are only of significance if a small increase in  $ng$  or  $V$  produces an increase in load. It is probably almost invariable that an increase in  $ng$  will produce an increase in load. An increase in speed is not nearly so automatic. At the higher speeds it is probably so, but at lower speeds there may be conditions in which a reduction in speed may change the distribution of load and increase it in certain structural parts. In such special cases the curves in which forward velocity is less than a given value should be used, i.e. the complementary set of curves to those of Fig. 5.11; for cases where  $V$  is greater than  $V_m$  the curves of Fig. 5.11 are not severe enough and for  $V$  less than  $V_m$ , which is probably the more common, they will be too severe.

An aircraft will in general have a strength that can be identified as a composite  $V$ - $g$  diagram and every point on the diagram will be cut by the curves of the form shown in Fig. 5.11. The lowest value of  $N_{V_n}$  of all these curves is a measure of the reliability of the aircraft of the strength given in the  $V$ - $g$  diagram, for all those parts in which an increase in the critical forward velocity or normal acceleration produces an increase in load. Finally it is necessary to check on any parts in which a decrease in the critical value produces an increase in load and if necessary to use curves complementary to those of Fig. 5.11.

As has already been stated the full significance of the curves at forward velocities below the mean at which the peak normal accelerations occur depends on the characteristics of the aircraft to which they are to be applied. One feature common to all is that at some forward velocity for each normal acceleration the aircraft will stall and the curves should not be extended to lower forward velocities. Another feature that at first sight seems anomalous is a curve of  $N_{V_n}$  which starts at a maximum at the lowest forward speed at which the aircraft can fly without stalling. This maximum normal acceleration is exceeded once at some velocity above the stall, it does not mean that the velocity will be at the stall, nor does it mean that this highest acceleration produces necessarily the highest load. If on moving along the curve the drop in normal acceleration with increase in forward velocity produces a load decrease smaller than the increase produced by the forward velocity, then the maximum load will occur at a normal acceleration less than its maximum but accompanied by a forward velocity greater than its minimum. Thus whilst it remains true that a specific normal acceleration has a certain frequency of occurrence the equivalent load for that frequency of occurrence corresponds to a lower normal acceleration.

Numerical values are taken for an F2H-2 and an F-100 and are inserted in equations (5.1), (5.2) and (5.3) and combined in the manner used in Fig. 5.9, the resulting graphs are shown in Figs. 5.12 and 5.13 respectively. This form of presentation allows a comparison to be made of the distributions of forward velocities for the high normal accelerations and the total distribution of forward velocities for all normal accelerations, but care must be taken in



# MEASURED SYMMETRICAL MANOEUVRES

extrapolating the information, especially as the highest forward velocities are predominantly achieved in straight and level flight. In the case of the F2H-2 all the values of the parameters in equations (5.1), (5.2) and (5.3) were deduced from the experimental measurements but for the F-100 the

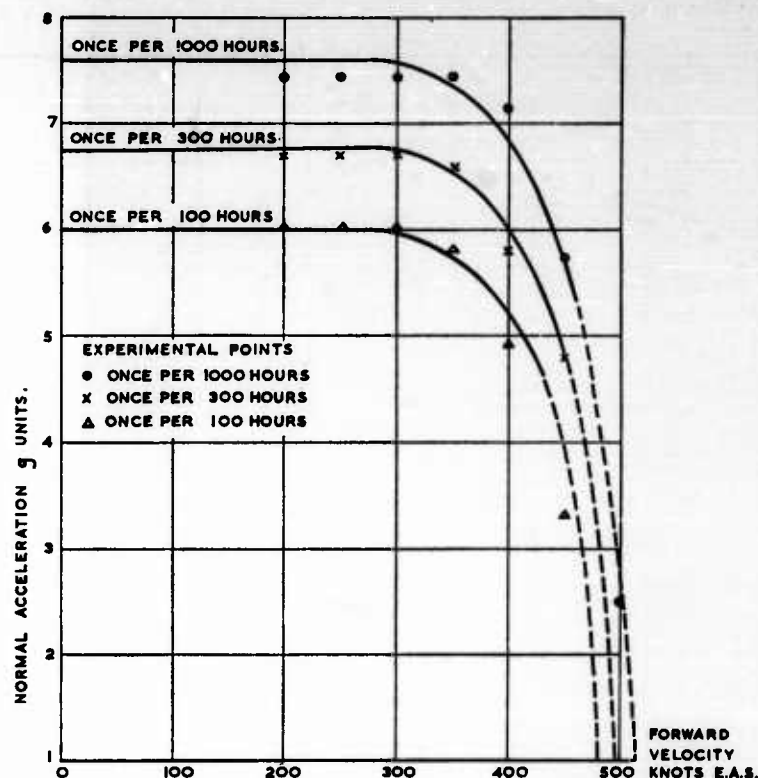


Fig. 5.12. Frequency of combined occurrence of forward velocity greater than stated value and normal acceleration greater than stated value for F2H-2 in 5444 flying hours. Calculated curve given by equations (5.1), (5.2) and (5.3). Parameters of (5.1) based on 6g and 7.6g being exceeded once per 100 hr and once per 1000 hr. Parameters of (5.2) based on 480 knots E.A.S. and 515 knots E.A.S. being exceeded once per 100 hr and once per 1000 hr. Parameters of (5.3) based on peak normal accelerations occurring at a forward velocity with a mean of 381 knots E.A.S. and a standard deviation of 45 knots E.A.S.

frequency of occurrence of the high velocities for equation (5.2) was not measured and the average values of Fig. 5.9 for fighters were used. The values of the forward velocity from equation (5.2) are shown in the curves at a normal acceleration of 1g, i.e. on the abscissa. The curves from equation (5.3) hold at low velocities and are plotted as full lines up to velocities of 90



per cent of the corresponding velocities on the abscissa. The curves are completed by dotted lines drawn by eye.

It can be that the calculated curves agree well with the experimental points for both fighters which have approximately the same average forward velocity at which peak normal accelerations occur but greatly different design diving speeds.

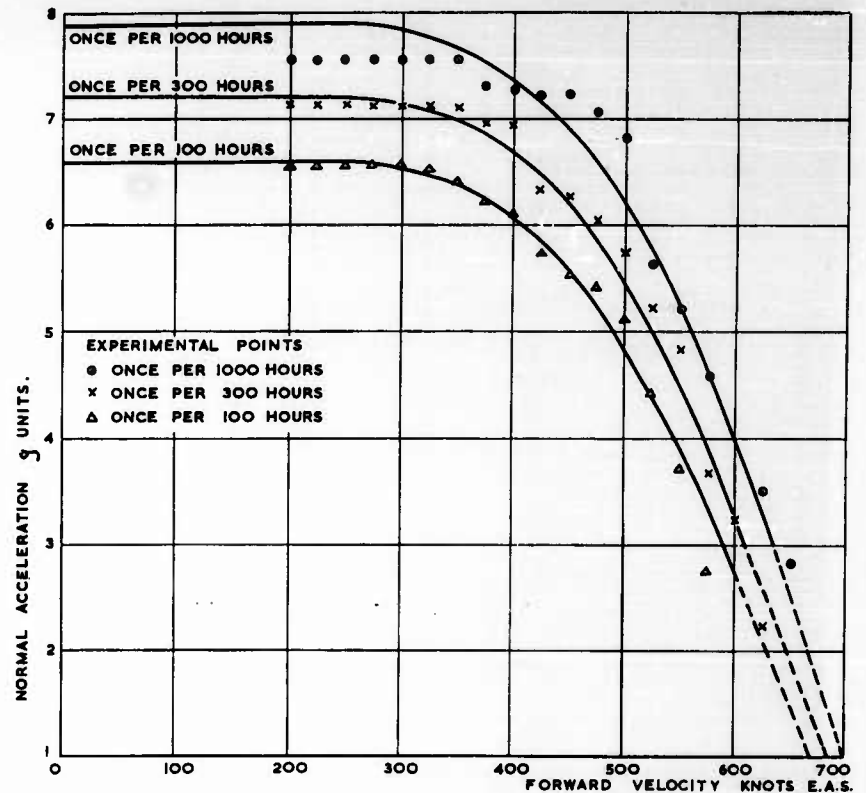


Fig. 5.13. Frequency of combined occurrence of forward velocity greater than stated value and normal acceleration greater than stated value F-100 in 3405 flying hours. Calculated curve given by equations (5.1), (5.2) and (5.3). Parameters of (5.1) based on 6.6g and 7.9g being exceeded once per 100 hr and once per 1000 hr. Parameters of (5.2) based on 670 knots E.A.S. and 700 knots E.A.S. being exceeded once per 100 hr and once per 1000 hr. Parameters of (5.3) based on peak normal accelerations occurring at a forward velocity with a mean of 385 knots E.A.S. and a standard deviation of 70 knots E.A.S.

#### REFERENCES

- |                        |                         |
|------------------------|-------------------------|
| Clay and Berens (1963) | Durkee (1961)           |
| Copp and Fetner (1959) | Fisher, W. A. P. (1964) |

# MEASURED SYMMETRICAL MANOEUVRES

Gray (1955)	Owen, E. M. (1958a)
Kelly, L. G., and Broom (1962)	Owen, E. M. (1958b)
Lewis (1956)	Owen, E. M., and Malcom (1959)
Lewis (1956a)	Perry and Rievley (1961)
Lewis (1957)	Phillips, L. (1961)
Mayer, J. P., and Harris (1955)	Rhode (1937)
Mayer, J. P., and Hamer (1955b)	Taylor, J. (1950)
Mullins (1961)	Titus (1959)
Mullins (1962)	Titus (1960)
Owen, E. M. (1954)	Titus (1961)
Owen, E. M. (1955)	Usher (1953)
Owen, E. M. (1955a)	Vahldiek (1961)
Owen, E. M. (1955b)	Vahldiek (1961a)
Owen, E. M., and Sellers (1956)	Walker, W. G., and Copp (1959)
Owen, E. M. (1957)	Wallace (1961)
Owen, E. M. (1957a)	Ward (1963a)
Owen, E. M., and Sellers (1958)	

**CHAPTER 6**  
**MEASURED ASYMMETRICAL MANOEUVRES**  
**AND MOVEMENTS OF THE CONTROL**  
**SURFACES**

**CONTENTS**

6.1 Introduction	135
6.2 Movement of control surfaces	136
6.3 Manoeuvres initiated by the ailerons	142
6.4 Transverse accelerations and sideslip	145
References	147

## CHAPTER 6

# MEASURED ASYMMETRICAL MANOEUVRES AND MOVEMENTS OF THE CONTROL SURFACES

### 6.1 INTRODUCTION

Asymmetrical manoeuvres are so closely connected with the movement of the controls that it is an advantage to examine them together. The application of the elevators, or all-moving tailplanes in certain designs, alone produces the purely symmetrical manoeuvre of pitching. The resulting maxima normal accelerations of the centre of gravity were studied in Chapter 5. The data available on the tail loads were so few that no attempt was made to form general opinions from them. It was decided therefore that it would be more appropriate to group the elevator movements with those of the aileron and rudder movements, both of which produce asymmetrical manoeuvres.

All the data that are available are for Fighters and Fighter-bombers. These types of aircraft are the ones in which asymmetrical manoeuvres are most frequently executed deliberately and therefore the more important. In view of the different nature of the manoeuvres in other types of aircraft, extrapolation from the Fighter and Fighter-bomber data is not advisable.

Although the details of the motion of any manoeuvre will depend markedly on the aerodynamic characteristics of the actual aircraft type that is doing it, there are a number of general features that can be isolated in a manner that gives basic data for all Fighter types. An added reason for not giving data on tail loads is that isolation of the general features from the particular design of aircraft has not been found possible. It was shown in paragraph 4.6 that the tail load depends on the normal acceleration and on the pitching acceleration. As the maxima values of these two accelerations occur at different times neither maxima can be used to predict tail loads and an empirical approach would be very involved as the time difference between the maxima depends so much on the design of aircraft.

There are two main types of asymmetrical manoeuvre, one in which rolling is the predominant motion and the other in which sideslip predominates. The rolling manoeuvre is at its most severe when gyroscopic forces are initiated and this happens when the rolling is combined with another rotation about an axis at right angles to the rolling axis. This secondary rotation will be a combination of pitching and yawing but at the initiation of the gyroscopic forces it will usually be predominantly pitching. A manoeuvre involving sideslip alone is strictly a symmetrical manoeuvre, but this will rarely be attempted in practice and it is more realistic to regard the sideslip as only part of the motion and therefore an

asymmetrical manoeuvre. However, in giving experimental results the sideslip is quoted, without reference to the other movements, and agreement is achieved with prediction of fin loads on the assumption that sideslip is in fact independent of the other movements.

The data were collected from service operational flying but the recording times were selected for those occasions when the proportion of time in manoeuvres was expected to be high. Thus the information is of more value in giving the relative frequencies of occurrence than the absolute values. Mayer, Hamer and Huss (1954) quote measurements on the F-86A, F2H-2, F-84G and F-94B, Hamer and Mayer (1960a) on the F-84G and F-84F, and Pembo and Matranga (1958) and Matranga (1959) on the F-100A. The total number of flying hours recorded is 125 and it is thought that it represents about 400 hr of normal service flying of which about 40 hr are actually spent in manoeuvres.

## 6.2 MOVEMENT OF CONTROL SURFACES

The movement of the control surfaces produces directly loads on the control surfaces and indirectly loads on the whole aircraft. In every case the load on a control surface depends on the deflection of the control surface and on the movement of the whole aircraft. In the case of the ailerons and rudder the neutral position is one of approximately zero deflection at all speeds, but elevators and all moving tailplanes will have a neutral deflection that varies with speed. This makes it much more difficult to describe tailplane movements.

A little speculation is necessary to combine the data from the various sources. The data from the F-84F include the frequency of occurrence of peak aileron and rudder deflections greater than stated values and also the distribution of the higher deflections with airspeed, but no statement is made of the proportion of the time actually spent in manoeuvres. The data from the F-86A, F2H-2, F-84G, F-94B include the distribution of the higher aileron and rudder deflections with airspeed and also the actual time spent in manoeuvres, but do not include the frequency of occurrence of peak deflections greater than stated values. In order to combine the data it is assumed that the 45 hr flying on the F-84F included the same proportion in manoeuvres as did the 60 hr on the F-86A, F2H-2, F-84G and F-94B combined, i.e. 30 per cent. It is assumed further that the data represent 3 times as much flying on ordinary service operations; this is a little more conservative than the estimate given by Hamer and Mayer (1960a) for the F-84F which is three to four times. An estimate is made of the frequency of occurrence of the higher peak values for the aircraft other than the F-84F by counting the experimental points on the distributions with airspeed. On these speculative assumptions the total data are representative of 315 flying hours of ordinary service of which 31.5 hr are in manoeuvres.

The frequency of occurrence of peak aileron deflections greater than stated values is given in Fig. 6.1 and that for peak rudder deflections in Fig. 6.2. The data are for fighters on combined duties and do not include stalls, spins, take-offs and landings. In these figures the experimental readings from the F-84F are given and also the combined totals from the F-86A,

# CONTROL SURFACES

F2H-2, F-84G and F-94B, the readings for the individual aircraft being rather too few to be shown separately. The distributions of the higher peak values with airspeed all show a drop in the value of the highest peaks recorded at the higher speeds. This is due in part to the smaller proportion of time spent at the higher speeds. An estimate is made of the values to be expected by using the data of the proportion of time spent at different airspeeds. The same method, as that used in Figs. 5.11-5.13 to obtain a frequency of

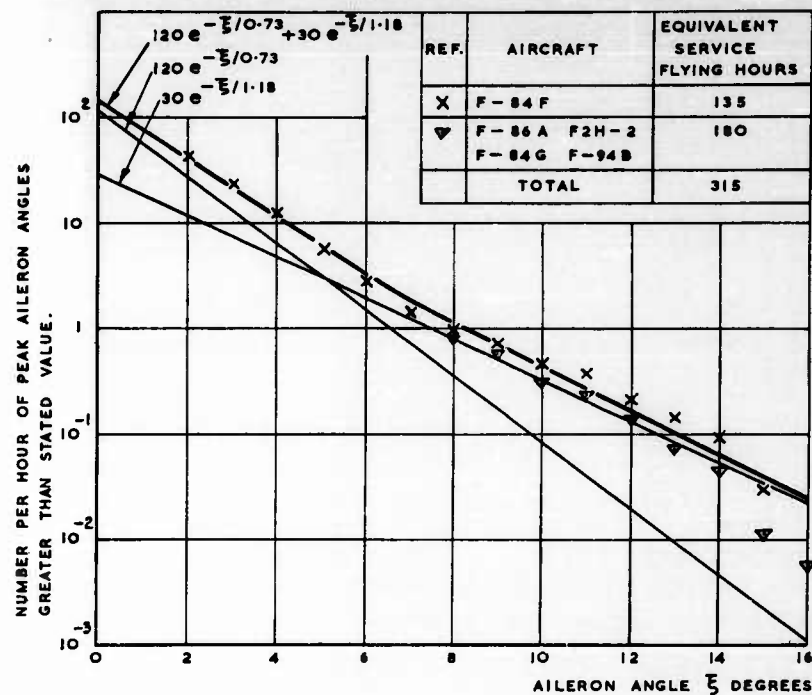


Fig. 6.1. Aileron deflections in flight of fighters on combined duties.  
Stalls, spins, take-offs and landings are excluded.

combined occurrence of a forward velocity greater than a stated value and a normal acceleration greater than a stated value, is used to obtain a frequency of combined occurrence of a control surface deflection and an airspeed. It is within the accuracy of the basic data to assume that the proportion of time at different airspeeds has a Normal distribution. The mean values and standard deviations for the different aircraft are given in Table 6.1.

The data of Figs. 6.1 and 6.2 and Table 6.1 are combined to give the combined frequency of occurrence of control surface deflection and airspeed above stated values; Fig. 6.3 is for ailerons and Fig. 6.4 for rudders. In each case the abscissa is given in units of standard deviation of airspeed in

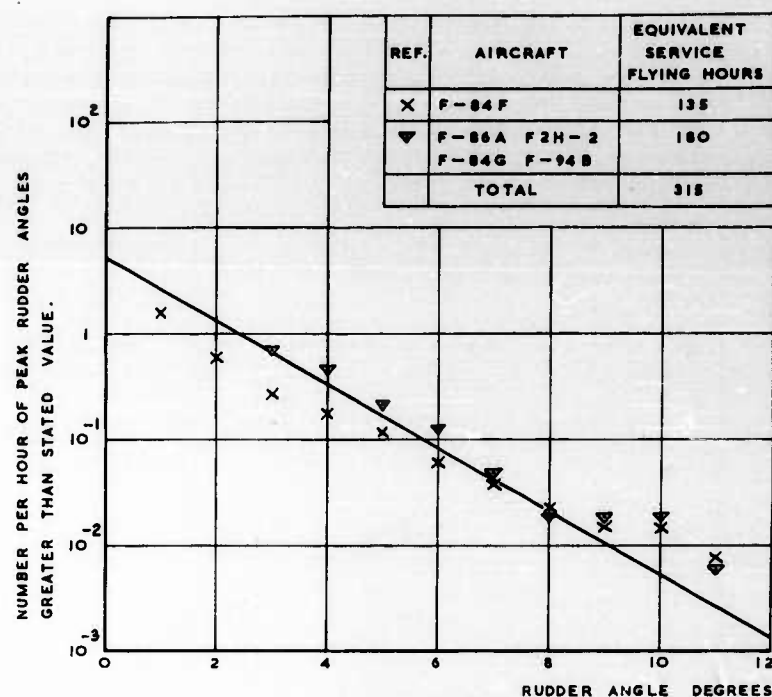


Fig. 6.2. Rudder deflections in flight of fighters on combined duties.  
Stalls, spins, take-offs and landings are excluded.

excess of the mean value so that the results from the different aircraft can be added together. The experimental curve, for all the aircraft flying combined, that is drawn on each figure is for a frequency of occurrence during ordinary service of once per 40 hr; the experimental points for each aircraft are also

Table 6.1. Proportion of Time at Different Airspeeds during the Experiments and Total Time in Manoeuvres

Aircraft	Time in manoeuvres hr	Mean airspeed knots E.A.S.	Standard deviation knots E.A.S.
F-86A	3.6	294	90
F2H-2	2.5	287	71
F-84G	8.0	273	75
F-94B	3.9	267	80
F-84F	13.5 (estimated)	360	84

# CONTROL SURFACES

for once per 40 hr. It will be seen that for both aileron and rudder deflections the frequency of occurrence at high airspeeds of once per 40 hr corresponds fairly closely to the calculated value for once per 10 hr. This is because the high deflections are more likely to be imposed at low airspeeds;

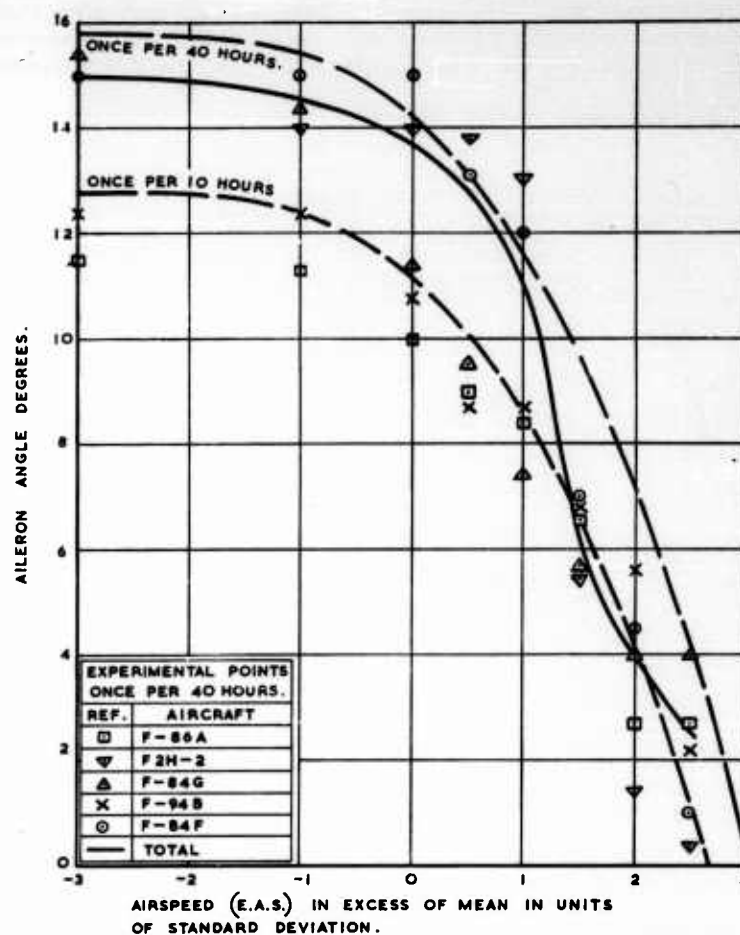


Fig. 6.3. Frequency of combined occurrence of airspeed greater than stated value and peak aileron angle greater than stated value for fighters on combined duties.

Calculated curves are deduced from Fig. 6.1 and Table 6.1.

all the aircraft show this tendency with respect to rudder motion but only the F2H-2 and F-84F do so with respect to aileron motion. Until further data are available it is suggested that Figs. 6.1 and 6.2 be used for control surface deflections at airspeeds up to the mean plus one standard deviation



and that at higher airspeeds the frequency of occurrence is one quarter of the values shown for each deflection. More accurate estimates of time spent at different airspeeds are given in Chapter 8 for aircraft generally.

The peak rudder deflections that have been given are for ordinary operational air manoeuvres and do not include take-offs and landings, nor do they include stalls or spins. In stalls or spins very high rudder deflections may be imposed; the data from the F-84G included two manoeuvres with practically full rudder angle of  $23.5^\circ$  and the F-86A had three

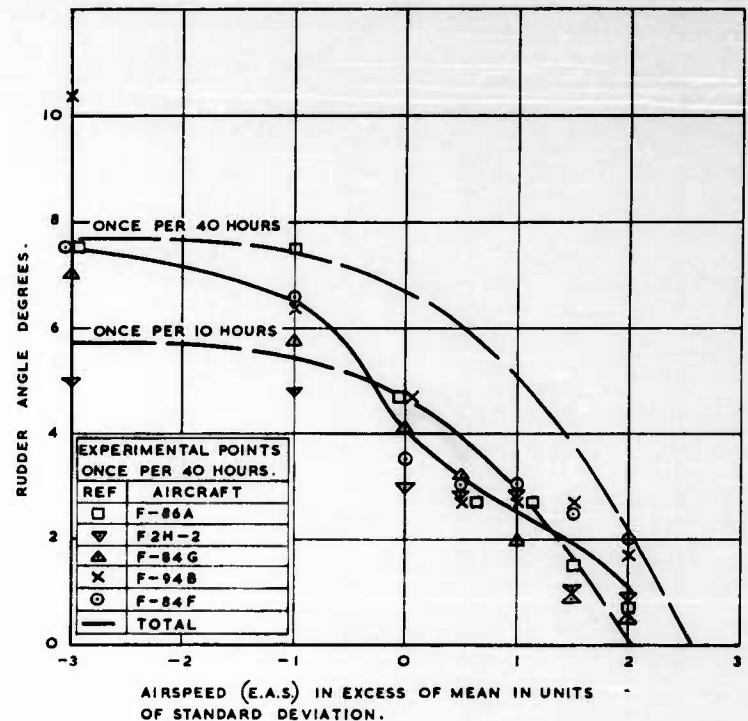


Fig. 6.4. Frequency of combined occurrence of airspeed greater than stated value and peak rudder angle greater than stated value for fighters on combined duties.

Calculated curves are deduced from Fig. 6.2 and Table 6.1.

manoeuvres with more than 75 per cent of full rudder angle of  $27.5^\circ$ . In take-off and landing the rudder angles may be appreciably higher than in ordinary operational air manoeuvres. For most fighters it is probably not unduly conservative to assume that in stalls and spins and in take-offs and landings that full rudder might be applied.

The aileron deflections do not include stalls, spins, take-offs and landings either, but the effect is not so marked as with rudder deflections. The effect of take-offs and landings would not be noticeable in Fig. 6.1. The effect of

stalls and spins was significant only\* in the F-84G data which included full aileron on three occasions.

The data from the F-100A cannot readily be added to that already quoted. On the same assumptions as those used for the F-84F the data would be for 60 hr ordinary service flying of which 6 hr were spent in manoeuvres. The distribution of airspeeds is not given and only the peak control surface deflections at each speed are given. On the assumption that the distribution of airspeeds in knots E.A.S. is roughly the same as that for the F-84F the distribution of peak aileron deflections at each speed is approximately that that would be predicted from Fig. 6.1; full aileron deflection of  $15^\circ$  was experienced up to just above the mean airspeed plus one standard deviation. The distribution of peak rudder deflections is also as would be expected at all speeds above the mean. No statement is given of whether stalls or spins occurred; as nothing is mentioned to the contrary it may be presumed that take-offs and landings have been included. Up to speeds of 250 knots full rudder deflections of  $20^\circ$  were experienced. Pembo and Matranga (1958) suggest that "the reason for the extensive use of the rudder on the F-100A airplane was that the pilots were made aware of adverse yaw particularly below 250 knots and were instructed in the flight training manual to use the rudder in turning flight to counteract this effect". Whilst the deflections do seem rather high compared with those of the other aircraft they are not so high as to suggest that the aircraft is particularly unusual in this respect.

Because of the change in datum position of the elevators, or all-moving tailplane, with airspeed, diagrams on the same lines as those for ailerons and rudders would have a somewhat different meaning and are not presented. The total deflection of these tailplane control surfaces is the sum of the deflections for trim and for manoeuvres. There is rather more variation between aircraft than for the other two control movements. The proportion of full travel that is used is of the same order as for ailerons. Roughly half the movement is for trim and this is particularly apparent for the all-moving tailplane of the F-84F. In the case of the F-100A full deflection, with the tailplane leading edge down, of  $25^\circ$  was experienced up to speeds of 340 knots E.A.S. This is rather more severe than for the other aircraft, with either elevators or all-moving tailplanes, but in the absence of other data it should be assumed that full deflections can be experienced on any fighter up to speeds approaching the average flight speed of the aircraft.

The rates at which the control deflections are changed are given for all the aircraft except the F-100A. It is difficult to assess the full significance in terms of aircraft loads as so much depends on the deflections when the highest rates are imposed and also the length of time for which the rates are maintained. The aileron rates that are applied once per 40 hr are such that, if they were maintained, full aileron would be achieved from the neutral position in 0.28 sec for the F-86A, F2H-2, F-84G and the F-84F whilst the F-84F's ailerons are applied a little more rapidly in 0.21 sec. The rate of

\* In the F-84F data stalls and spins are not specifically isolated from the other data, but as the data were prepared by two authors, who were authors of the earlier paper on the other aircraft, it may safely be presumed that the effect of stalls and spins was not significant in this respect.

moving the other two control surfaces is very variable but it seems that they would take about 2 or 3 times as long to reach full deflections, except for the F-84F rudder which would take 0.29 sec, in ordinary operations. However, in stalls or spins, when presumably the pilot is more in need of rapid movements, the elevators and rudders are also applied at rates corresponding to full deflection in 0.28 sec. The extrapolated values for once in 400 hr from those of once in 40 hr are approximately 0.2 sec. The expected time to apply full control must be more than the values quoted for all except the ideal case of the peak rate being maintained throughout. The allowance to be made in prediction cannot be assessed from the data available.

### 6.3 MANOEUVRES INITIATED BY THE AILERONS

The ailerons may be applied either to bank the aircraft for a turn or to roll the aircraft. Figure 6.1 gives the number per hour of peak aileron angles greater than a stated value  $\xi$  as the sum of two distributions,  $120 \exp(-\xi/0.73)$  and  $30 \exp(-\xi/1.18)$ . A comparison of the first distribution with Figs. 5.1 and 5.2 and the second with Fig. 6.5 suggests that the first is produced mainly from turns and the second from rolls. In Fig. 6.5 the extrapolated value of the total number of rolls, in the experiments being described, is 30 per hour which is the same number as those of peak aileron deflections of the second distribution. In Figs. 5.1 and 5.2 the extrapolated values of the total number of normal accelerations is 60 per hour up and 60 per hour down, making 120 per hour in all, which is the same number as those of the peak aileron deflections of the first distribution. This distribution of aileron deflections is obtained from one aircraft only, the F-84F, but the agreement suggests that the distribution is mainly associated with the production of normal accelerations and it also gives a little support to the contention that the experimental flying was, in fact, representative of three times as much ordinary service flying.

The majority of the high aileron angles will be from the second distribution and therefore it may be expected that a roll will be produced. When the roll is superimposed on a pitching movement this produces the important asymmetrical manoeuvre in which gyroscopic forces are produced. It was noted in Chapter 4 that pilots seem unable to sense inertia coupling in such a way that they can take corrective action and would normally release the controls. Thus this asymmetrical manoeuvre may be described by the conditions appertaining at its initiation. The subsequent movement will be directly connected with the particular design of aircraft, but the initial conditions may be described fairly well for all Fighters.

The motion of the aircraft as a whole, as a result of application of ailerons, will depend on the time history of the aileron deflection. The F-100A data show rolling velocities for each aileron deflection. Some are as high as would occur if the ailerons were held indefinitely at the deflection and others, particularly very low rolling velocities, correspond to an impulsive application of ailerons. The bank angles vary over a wide range from 90° or less to well over 760° for all except the small rolling velocities. These data suggest that the assumption that steady rolling may be set up with any aileron deflection should not be very conservative. It also greatly simplifies the

# CONTROL SURFACES

presentation of the data as the time associated with a rolling condition need not be given.

Better agreement is reached between the different aircraft if the wing-tip helix angles produced by the roll are compared rather than the rolling velocity. Figure 6.5 shows the frequency of occurrence of peak helix angles greater than stated values for the F-84F. The values for the combined totals from the F-86A, F2H-2, F-84G and F-94B, which are available only above

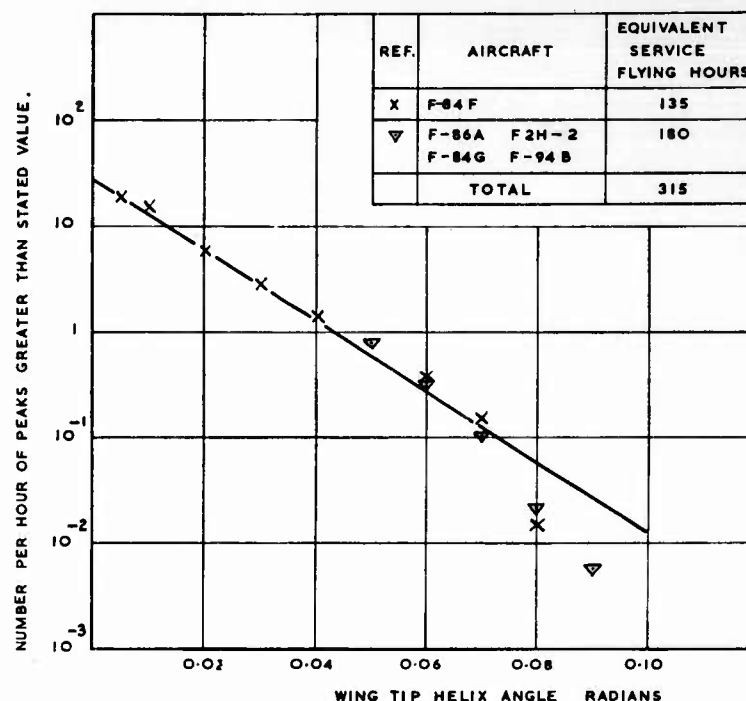


Fig. 6.5. Wing-tip helix angles in flight of fighters on combined duties.  
Stalls, spins and snap rolls are excluded.

0.05 rad, are shown for comparison. The data do not include stalls, spins or snap-rolls. There will be a maximum possible wing-tip helix angle for each aircraft, but this is not achieved in the conditions relating to Fig. 6.5. Stalls or spins produced a wing-tip helix angle of 0.12 rad for one manoeuvre for the F-86A and one for the F2H-2; they also produced for the F-84G seven greater than 0.1 rad of which two were greater than 0.14 rad. In addition the F-84G performed two snap rolls with helix angles greater than 0.1 rad. The data of Fig. 6.5 and Table 6.1 are combined to give in Fig. 6.6 the combined frequency of occurrence of wing-tip helix angle and airspeed above stated values. As with Fig. 6.1 for aileron deflections the experimental points for a frequency of occurrence of once per 40 hr are shown for each aircraft. In the case of helix angle the experimental points agree with the

calculated curve for once per 40 hr at speeds below the mean airspeed, but above that they tend to be less severe than the calculated curve for once per 10 hr. It was shown in Fig. 6.1 that there is an attenuation of aileron deflection at higher speeds and this greater attenuation of helix angle is probably due to the aileron deflections being maintained for shorter times at the higher speeds.

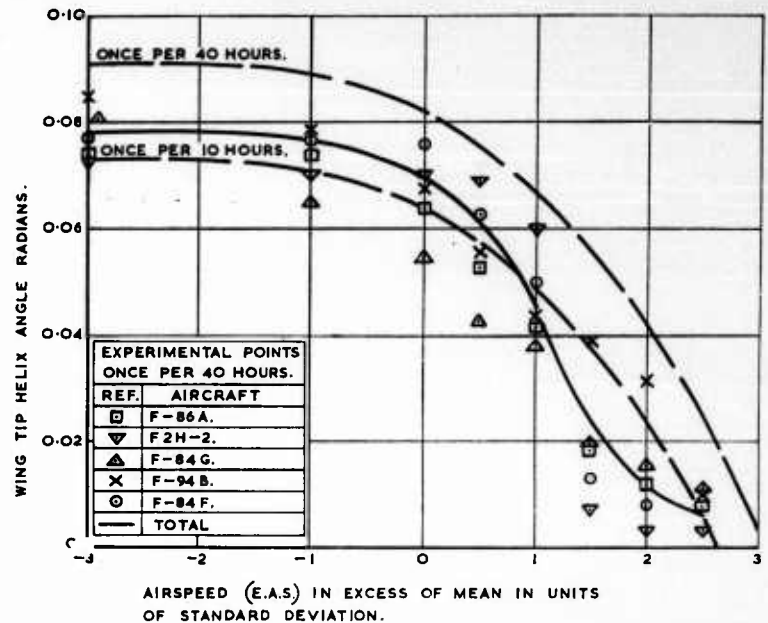


Fig. 6.6. Frequency of combined occurrence of airspeed greater than stated value and wing-tip helix angle greater than stated value for fighters on combined duties.

Calculated curves are deduced from Fig. 6.5 and Table 6.1.

The rolling velocities are compared in the original papers with normal acceleration for each of the aircraft. Matranga (1959) is the only author to quote specifically that the normal accelerations are at the start of the roll. His data are for the F-100A and they show that roughly the same rolling velocities are initiated at normal accelerations between 1g and 4g. There is a falling off in the magnitude of rolling velocities initiated outside this range with negligible rolling velocities associated with negative normal accelerations. The other aircraft show similar characteristics, the rolling velocities associated with negative normal accelerations are small but not negligible. However, it is not known whether these values were at the beginning of, or during, the asymmetrical manoeuvre and if they were during it the information would be too specific to the particular aircraft to be used generally.

Whatever the rolling velocity utilized, time will be required to build up

to it. Measurements of time taken to roll  $90^\circ$  were made for all the aircraft. The minimum time in excess of the theoretical limit for the once in 40 hr manoeuvre is approximately  $\frac{1}{4}$  sec for all rates of roll. This time delay cannot be compared directly with the time taken to apply the ailerons because the whole aerodynamic and structural characteristics are involved. However, it is, as would be expected, of the same order of time.

#### 6.4 TRANSVERSE ACCELERATIONS AND SIDESLIP

The transverse acceleration and sideslip angles were measured for the F-86A, F2H-2, F-84G, F-94B and the F-84F and both parameters were quoted for the airspeed at which the peak values occurred. For each of the aircraft a comparison was made by the authors of the two papers between  $n_T$  and  $\beta q_D$ , the fin load parameter,

where  $n_T$  = transverse acceleration in  $g$ -units

$\beta$  = sideslip angle

$q_D$  = dynamic pressure,  $\frac{1}{2}\rho V_T^2$ , lb/ft<sup>2</sup>

$\rho$  = air density slugs/ft<sup>3</sup>

$V_T$  = true airspeed ft/sec

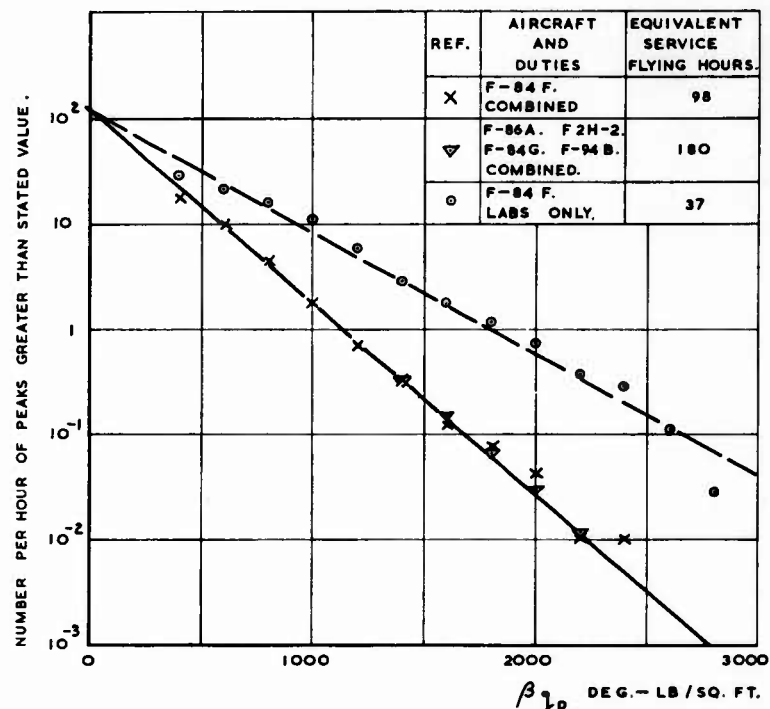


Fig. 6.7. Values of fin load parameter ( $\beta q_D$ ) in flight of fighters on combined duties. Stalls, spins, lateral oscillations at high speed, take-offs and landings are excluded.

It was found that there was not much scatter on a linear relationship between  $n_T$  and  $\beta q_D$ .

A further examination of the basic data shows that better agreement is achieved between the different aircraft if comparisons are made in terms of  $\beta q_D$  rather than in terms of  $n_T$ . Although  $\beta q_D$  is the more basic parameter the data that are deduced will not be applicable to other aircraft of greatly different design as both parameters are influenced by the design of the tail-plane.

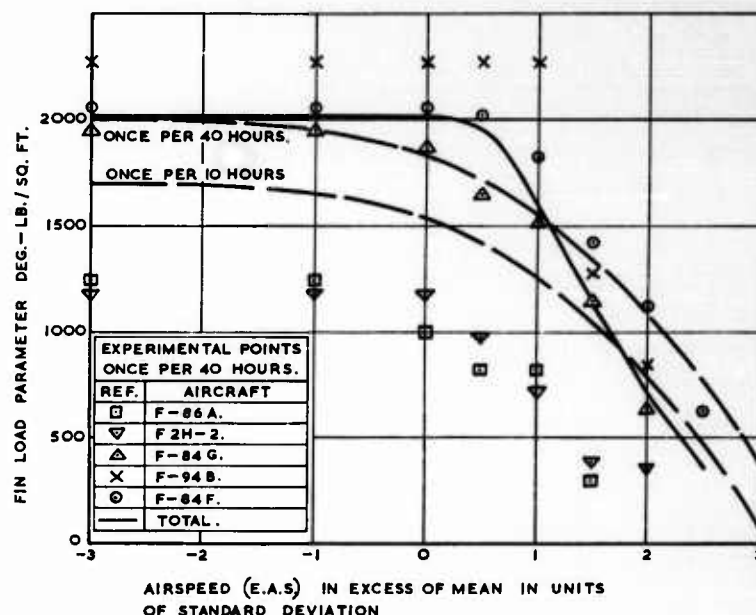


Fig. 6.8. Frequency of combined occurrence of airspeed greater than stated value and peak value of fin load parameter greater than stated value for fighters on combined duties.

Calculated curves are deduced from Fig. 6.7 and Table 6.1.

The frequency of occurrence of peak values of the fin load parameter greater than stated values is given in Fig. 6.7, but the data do not include stalls, spins, lateral oscillations at high speed, take-offs and landings. The LABS manoeuvres of the F-84F are shown separately from all other manoeuvres. The manoeuvres of all the aircraft, excluding LABS manoeuvres, agree well with each other and the curve shown is the average one. The extrapolated value of total number of manoeuvres in which there is a fin load is practically the same as the total number in which the ailerons are applied. The LABS manoeuvres of the F-84F introduce peak values of the fin load parameter about 1.5 times the average values of the other manoeuvres. The data of Fig. 6.7 and Table 6.1 are combined to give in Fig. 6.8 the combined frequency of occurrence of the fin load parameter and airspeed above



## CONTROL SURFACES

stated values. As in the earlier comparisons of control deflections and wing-tip helix angle the experimental points for a frequency of occurrence of once per 40 hr are shown for each aircraft. There is much more scatter than with any of the other parameters. Any conclusions that are drawn will be less reliable than with the other parameters but there is one feature that seems to be fairly well defined. The experimental points for once per 40 hr at high airspeeds are much the same as those for the other parameters in that they agree with those deduced from Fig. 6.7 and Table 6.1 for once per 10 hr. However, over much of the lower speed range the experimental points for once per 40 hr are for higher fin loads than the calculated ones for once per 40 hr. The reason for this is that there is a tendency for fin loads to increase with airspeed, in terms of frequency of occurrence per hour spent at that speed, up to a speed of mean plus one standard deviation.

In the case of the F-84F data, that are almost exclusively for LABS manoeuvres, this tendency is even more marked and, apart from airspeeds near the stall, the sideslip angle itself occurs practically with the same frequency at all airspeeds, in terms of time spent at the speed concerned.

## REFERENCES

Hamer and Mayer (1960a)  
Matranga (1959)

Mayer, Hamer and Huss (1954)  
Pembo and Matranga (1958)



## CHAPTER 7

### GROUND LOADS

#### CONTENTS

7.1 Introduction	151
7.2 Taxiing loads	152
7.2.1 Effects of aircraft flexibility	154
7.3 Normal accelerations at take-off	156
7.4 Normal accelerations on landing	157
7.4.1 Vertical velocity at touchdown	158
7.4.2 Horizontal velocity at touchdown	161
7.4.3 Bank angle and rolling velocity at touchdown	163
7.4.4 Comparison of impact of first and second wheels	167
7.4.5 Direct measurement of normal acceleration	168
7.5 Fore and aft and lateral accelerations	169
References	169

## CHAPTER 7

### GROUND LOADS

#### 7.1 INTRODUCTION

Loads on aircraft from runways have increased in importance markedly in recent years, and in aircraft of very low aspect ratio it is the design case for practically the whole structure. Thus information on the magnitude of these loads is of the utmost importance. There are three distinct types of load: (i) taxiing, (ii) take-off, (iii) landing.

It is immediately apparent that the ground environment, as described in Chapter 3, is an important feature in the determination of ground loads. However, the flight techniques adopted by pilots and the atmospheric conditions, especially visibility and precipitation of rain and snow, are also important. This means that runways with identical profiles could produce very different loads in different parts of the world, due to differences in atmospheric conditions and to differences in the ground navigational aids that are available. Changes in the ground aids and in the equipment carried in the aeroplane can appreciably alter the techniques of landing and take-off adopted by pilots and also the regulations defining when landings or take-offs shall be forbidden. There is no technical reason why the regulations forbidding a take-off need ever be waived, but some tolerance is needed for the regulations for landings, as there can always be emergency landings due to a defect developing in some part of the aircraft or due to such rapid and widespread changes in the atmospheric conditions that a diversion to another airport would involve more rather than less risk. One of the incidental limitations to the data that have been collected on landing loads is that they had to be obtained at a small number of airports for short periods of time in good visibility, and this could not be representative of all airports throughout the world and of all landings throughout the year.

The simplest way of defining ground loads would be to state that they were all the loads that occurred between the first touch of the landing gear on landing to the last touch in the take-off of the next flight, but this has the disadvantage of grouping the three phases of (i) deceleration from a condition with roughly  $1g$  lift, (ii) a fairly steady velocity with negligible lift and (iii) an acceleration up to  $1g$  lift. Any other definition will introduce some sort of overlap of these three conditions. Fortunately the significance of the three conditions to the aircraft is quite pronounced, being primarily fatigue loadings except for a single landing and a single take-off load. The take-off load is more difficult to separate from the adjacent taxiing loads and might best be regarded as a continuation of them. The landing loads are readily identifiable and can be related statistically to the attitude of the aircraft at touchdown; when the landing loads are very small they can easily be missed in experimental readings of normal acceleration as the subsequent

taxying normal accelerations will be greater, but this has little practical significance other than in the purely research considerations of correlation between velocity of descent and normal acceleration.

## 7.2 TAXYING LOADS

In order to determine the taxying loads that an aircraft will encounter it is necessary to know the runway profile and the time spent taxying at different speeds. Westfall *et al.* (1957) found that the time spent taxying was remarkably constant for three transport types averaging within a few seconds of 5 min. The accelerations that will be encountered will depend on the

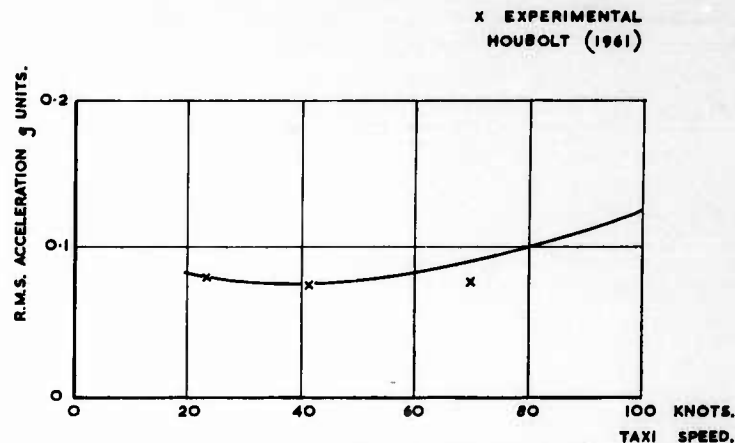


Fig. 7.1. Comparison of measured taxi C.G. acceleration on F-100 with calculation.

transfer function of the aircraft. Houbolt (1961) compares the calculated with the measured average acceleration for an F-100 on a particular runway and the comparison is shown in Fig. 7.1. It is probably reasonable to assume that the calculated average acceleration on any runway will be reasonably close to the measured values, but the calculations of the distribution of the number of occurrences at different levels will not be so accurate. Houbolt does not give such a comparison but does emphasize that "The roughness treated [by him] is that of a continuous type. Taxying over discrete bumps such as chuck holes or running off the edge of the pavement are conditions distinct and separate enough to require a different treatment from that given." Hitch, as quoted in Chapter 3, mentions that a trough produces vertical accelerations substantially in excess of the general level.

From a study of VGH records Houbolt (1961) notices that the average acceleration peak on airline operations is 0.12g. Westfall *et al.* (1957) notice in several hundred taxying runs that the maximum taxying loads occurred at speeds usually below 20 m.p.h.; they also notice that there is little variation from a frequency of 1.75 cycles per second of C.G. accelerations for 5 aircraft ranging from the B-36 to a small jet fighter. The

## GROUND LOADS

distribution of occurrences of acceleration quoted by Westfall is given in Fig. 7.2 (this is identical to that quoted by Houbolt for which he quotes an average peak of 0.12g) and compared with the distribution given by J. Taylor (1956) and with unpublished data by J. Taylor (1951).

There are insufficient data available for a comparison to be made of the runway profiles and measured accelerations. The results of Westfall suggest

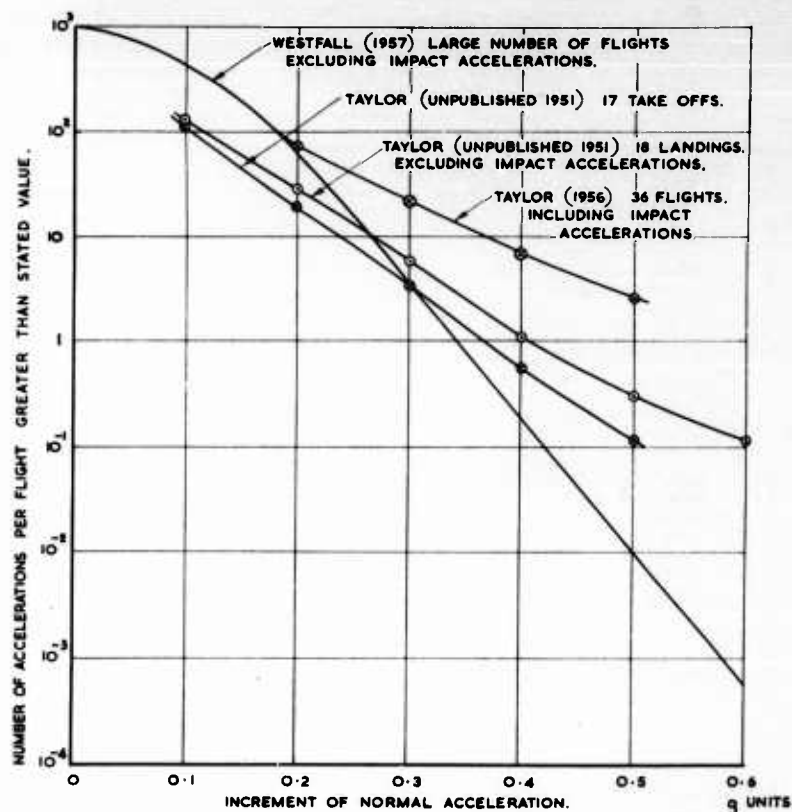


Fig. 7.2. Distribution of taxiing loads per flight.

that wavelengths corresponding to speeds up to 20 m.p.h. and frequencies of 1.75 c.p.s. are the important ones. These wavelengths are 17 ft. It is probably reasonable to use these values in assessing the frequently occurring accelerations. Little can be done to differentiate between different aircraft and Fig. 7.2 is probably all that can be used until more information is available on the correlation of actual accelerations with those predicted from the runway profiles given in Chapter 3.

Although Westfall noticed that the maximum taxiing loads occurred at speeds usually below 20 m.p.h., it cannot be assumed that the very infrequent

high loads also occurred below 20 m.p.h. Thus the longer wavelengths and abrupt changes of slope or elevation may play an important part in generating the high loads and must be considered if an attempt is made to replace the predictions of Fig. 7.2 by predictions direct from the runway profiles.

### 7.2.1. Effects of Aircraft Flexibility

B. R. Morris (unpublished, 1962) investigated the behaviour of a fighter aircraft taxiing over a rough runway at different speeds and tyre pressures, taking account of aircraft flexibility. Special attention was paid to the normal accelerations at the wing tips and at the cockpit which was almost

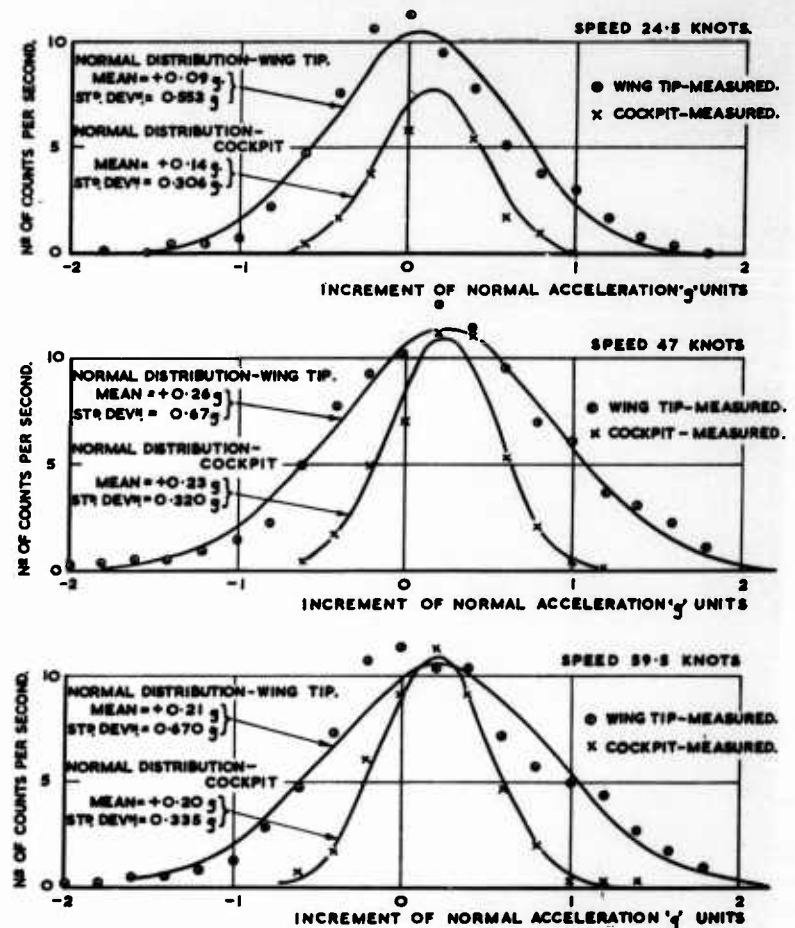


Fig. 7.3. Distribution of threshold crossing of normal acceleration of aircraft L taxiing at different speeds with tyre pressure 80 lb/in<sup>2</sup> (a count is made for each crossing in one direction only).

# GROUND LOADS

immediately above the nose wheel. The natural frequencies of the fundamental modes of symmetrical wing bending, antisymmetrical wing bending and fuselage bending were 10, 13 and 14 c.p.s. respectively: it was found that these were predominant frequencies in the aircraft response. At such high frequencies there are a large number of crossings of the acceleration

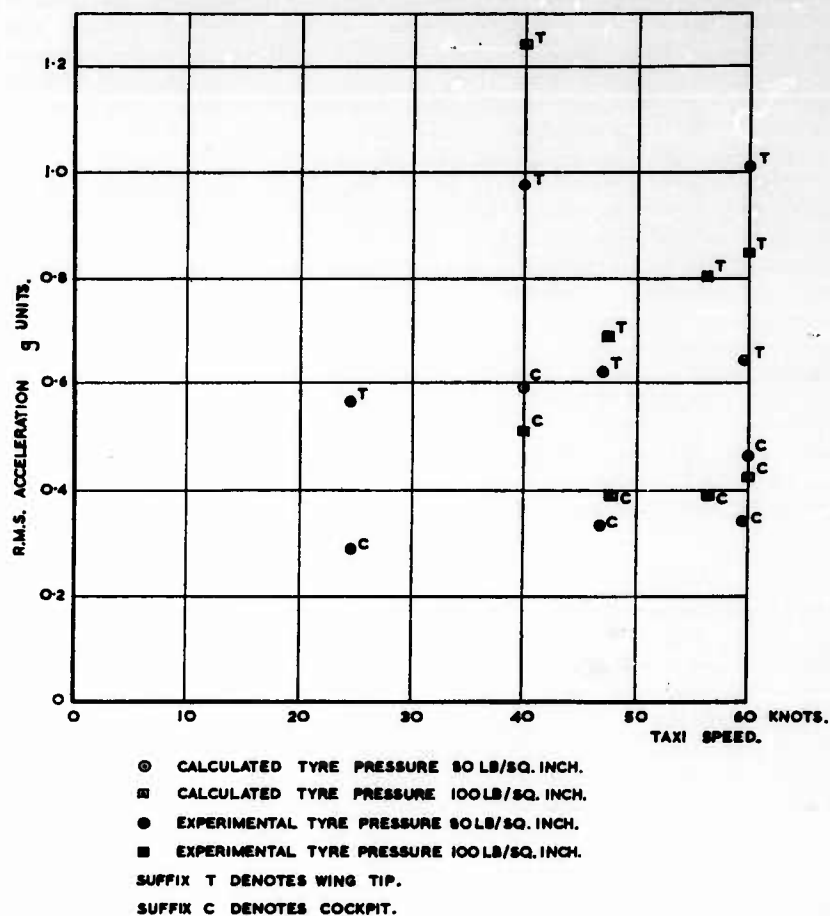


Fig. 7.4. Comparison of measured taxi acceleration with calculation for cockpit and wing tip.

with zero increment and a check can be made for each run of the distribution of crossings of other accelerations up to two or three times the root mean square of the acceleration (r.m.s.). The distributions are compared with Normal distributions in Fig. 7.3 for 3 speeds and a tyre pressure of 80 lb/in<sup>2</sup>. The r.m.s. values are shown in Fig. 7.4 for these runs and also for some others with a tyre pressure of 100 lb/in<sup>2</sup>. An inspection of the measurements

at the aircraft C.G. indicates that they resemble closely those at the cockpit but with about half the amplitude.

Analogue computations were made involving 10 degrees of freedom for the aircraft structure with its landing gear. The actual inputs of runway spectra could not be controlled very closely especially for the important frequencies of the order of 10-15 c.p.s. If rough account is taken of these discrepancies it is considered that the experimental readings agree reasonably with prediction. It seems probable, though, that the differences in the measured values of normal acceleration of the aircraft with tyre pressures of 80 lb/in<sup>2</sup> and with tyre pressures of 100 lb/in<sup>2</sup> are merely experimental variation between runs; the analogue studies also suggest that for the particular runway the variation with speed is negligible.

The restrictions that have to be imposed in the representation of the actual runway roughness and the aircraft characteristics when using Spectral methods do not seem to alter seriously the prediction of the frequently occurring loads. In particular the non-linear characteristics of the landing gear do not seem to influence seriously the accelerations. It should be emphasized, however, that in a sinusoidal motion at 10 c.p.s. an amplitude of  $\pm 1g$  corresponds to an amplitude of  $\pm 0.1$  in. and at 14 c.p.s. to  $\pm 0.05$  in. so that many of the acceleration fluctuations are not associated with great non-linear changes in the landing gear oleos.

For the rare large accelerations, particularly those at about 2 c.p.s., associated with the landing gear natural frequencies, or slower, the same care will have to be exercised in studying flexibility that has to be exercised when studying C.G. motion.

### 7.3 NORMAL ACCELERATIONS AT TAKE-OFF

For many of the frequently occurring loads the take-off may be considered an extension of the taxiing condition. In fact for runways such as the ones for which accelerations are quoted in Figs. 7.1 and 7.4 the r.m.s. accelerations do not seem to vary much up to take-off speeds.

In theory high loads may occur occasionally due to the random association of different components of ground roughness and different attitudes of the aircraft and its landing gear. In practice it is much more likely that the highest loads will be mainly influenced by the specific design profile of the runway, especially in the region where the aircraft will normally be near to its take-off speeds. In this connection the runway is regarded as having a design profile on which roughness is superposed; the N.A.T.O. criteria given in Chapter 3 state that changes in longitudinal gradients of the profile shall be at least 1000 ft apart and the roughness of the runways is measured only up to wavelengths of 150 ft. In view of the paucity of the data it is not possible to do a full probability study of a combined profile and roughness. Some empiricism must be introduced and perhaps the simplest way is to select somewhat arbitrarily a few profiles, determine the maximum normal acceleration that ensues and then add the accelerations due to roughness. For such an approach it may be assumed that rare events due to profiles and due to roughness will not occur at the same time. Thus either the profiles must be those that occur fairly frequently or the accelerations



due to roughness have to be those occurring frequently. In Chapter 3, Fig. 3.5 shows the cumulative frequency of occurrence of ramps of different angles. The maximum ramp angle permitted by the N.A.T.O. criteria is 0.02 rad, but a ramp angle of 0.01 rad is present in about 10 per cent of the runways. The N.A.T.O. criteria include a limitation on rate of change of longitudinal slope of 0.167 per cent per 100 ft, but many of the changes of angle are not nearly so well faired. It is probably not being unduly conservative in aircraft design to assume that the ramp angle of 0.01 rad is achieved at a rate of change of longitudinal slope of 1.67 per cent per 100 ft (i.e. 10 times the criterion).

The single load that is produced by the change of slope of 0.01 rad and occurs in 10 per cent of take-offs only lasts for part of the take-off. The accuracy of the data does not warrant an elaborate procedure and it is suggested that the portion of the runway in which this change of slope influences the taxiing loads is taken arbitrarily to be 10 per cent and that the aircraft speed at the time is take-off speed. Thus a mean acceleration corresponding to a traverse of the ramp at take-off speed must be added to about 1 per cent (i.e. roughly equivalent to 10 per cent of the taxiing time of 10 per cent of the take-offs) of the fluctuating taxiing loads.

The change of slope may not be the only condition that introduces higher loads than would be expected from considerations of average roughness. Other conditions are patches of unusually high roughness or possibly local steps. The runway roughness measurements on the 36 N.A.T.O. runways give no indication of the magnitude to be assumed and until more data are collected it will have to be dealt with on an *ad hoc* basis of reports on conditions on individual runways.

#### 7.4 NORMAL ACCELERATIONS ON LANDING

The landing loads are much more easily separable from the taxiing loads than are the take-off loads. Also the conditions governing the landing loads are much more easily definable. For all practicable purposes they may be defined by the attitude of the aircraft at touchdown relative to the tangential plane of the runway at the point of touchdown together with the vectorial velocity of the centre of gravity of the aircraft and the vectorial angular velocity about its centre of gravity. This greatly simplifies the problem of obtaining statistics of landing loads as the actual flight path and relevant velocities at the instant of touchdown can be measured on a relatively large number of aircraft with only a limited number of check measurements on selected aircraft.

The attitude of the aircraft at touchdown is fully defined if the following parameters are known:

- (i) Vertical velocity
- (ii) Horizontal velocity
- (iii) Bank angle
- (iv) Rolling angular velocity
- (v) Yaw angle
- (vi) Yawing angular velocity
- (vii) Pitch angle
- (viii) Pitching angular velocities



Westfall *et al.* (1957) have examined statistical data from a number of experiments of Dreher (1956), Harrin (1956), Kolnick and Morris (1955), Silsby (1955, 1956) and Silsby and Harrin (1955a, 1955b) on vertical velocity, horizontal velocity, bank angle and rolling angular velocity and did not find any correlation between any two of the parameters; they do not state explicitly that they checked the correlation between horizontal and vertical velocity, but they do state that the statistical analysis indicated no significant correlations between wing lift and vertical velocity. The normal accelerations of an aircraft on landing are given mainly by these four parameters, vertical velocity, horizontal velocity, bank angle, rolling angular velocity, and a good estimate of their contribution can be obtained by treating them as independent parameters. There is, however, in addition a significant effect on the normal acceleration due to pitch and an indirect effect due to yaw. The angle and angular velocity of yaw of the aircraft at touchdown induce fore and aft and lateral loads on the landing gear, thus influencing the motion of the oleo. The nature of the experiments is such that pitch and yaw cannot be measured so that if information is required theoretical predictions must be used.

#### 7.4.1. Vertical Velocity at Touchdown

The most important parameter influencing the normal acceleration is the vertical velocity. In the bibliography quoted by Westfall *et al.* (1957) and mentioned earlier, the vertical velocity is measured photographically in the majority of the landings. There are 268 landings by a trainer that are not measured in this way and should be treated separately. There are 1361 landings of military aircraft for which the experimental readings are available and are presumably the same 1361 landings quoted by Westfall (this omits 215 landings of a B-47 measured at Boeings and 59 landings of a KC-97, all of which are in substantial agreement with the 222 landings of a B-47 measured by N.A.S.A.); also there are 478 landings of civil aircraft (Westfall quotes 2385 civil landings but gives no indication of the source from which the additional measurements were taken). In the present analysis the following more recent measurements of civil landings are included: 340 records by Silsby and Livingston (1959) and 495 records by Stickle and Silsby (1960) and Stickle (1961). The analysis now being made is on 2674 landings: the recordings of one aircraft (302 landings) are regarded as unrepresentative, for reasons to be stated later, but the remainder are used to compare military landings (1059) and civil (1313), large aircraft landings (760) and small (1612), turbojet aircraft landings (1085) and propeller aircraft (1287).

In making a comparison of types of aircraft it is convenient to reduce the data for each aircraft to one parameter. It was decided that the landing that was exceeded in severity about once per 25 landings would be suitable for this purpose. The mean vertical velocity ( $V_V$ ) and the standard deviation ( $\sigma$ ) about the mean are given in Table 7.1 for all the aircraft for which there were sufficient landings for the standard deviation to be estimated with reasonable confidence: the velocity corresponding to ( $V_V + 2\sigma$ ) is exceeded roughly once per 25 landings and is used to compare the different aircraft.

## GROUND LOADS

Table 7.1. Vertical Velocity of Descent of Different Aircraft

Reference	Aircraft	No. of landings	All-up-weight lb	Vertical velocity ft/sec		
				Average $V_v$	Standard deviation $\sigma$	$V_v + 2\sigma$
Silsby (1955)	B (Civ. Prop.)	67	27,000	1.00	0.48	1.96
Silsby (1955)	E (Civ. Prop.)	91	42,750	1.65	0.82	3.29
Silsby (1955)	F (Civ. Prop.)	75	73,000	1.34	0.63	2.60
Silsby (1955)	G (Civ. Prop.)	100	41,790	1.39	0.66	2.71
Silsby (1955)	H (Civ. Prop.)	36	107,000	1.58	0.85	3.28
Silsby (1955)	J (Civ. Prop.)	71	88,000	1.47	0.64	2.75
			or 103,000			
Stickle (1961)	A (Civ. Jet)	282	245,000	1.52	0.90	3.32
Stickle (1961)	B (Civ. Jet)	112	265,000	1.45	0.94	3.33
Stickle (1961)	Civ. Turbo-prop	101	113,000	1.06	0.71	2.48
Silsby and Harrin (1955a)	B-36 (Mil. prop)	144	357,000 to 410,000	2.29	1.08	4.45
Kolnick (1955)	B-47 (Mil. Jet)	222	185,000	1.97	0.81	3.59
Silsby (1956)	B-26 (Mil. Prop)	224	32,400	1.31	0.67	2.65
Silsby (1956)	T-33 (Mil. Jet)	166	15,000	1.03	0.68	2.39
Silsby (1956)	B-57 (Mil. Jet)	109	53,400	0.95	0.63	2.21
Silsby (1956)	F-94C (Mil. Jet)	194	19,200	1.01	0.67	2.35
Silsby (1956)	F-84F (Mil. Jet)	302	27,000	1.72	1.22	4.16

The only marked division that can be made between aircraft is on size, those below 150,000 lb all-up-weight experiencing rather lower vertical velocities than those aircraft above 150,000 lb all-up-weight: no tendency is apparent of variation with all-up-weight of the 12 aircraft below 150,000 lb and no separation can be made above 150,000 lb as there are only 4 aircraft. Apart from the recordings of the F-84F the variation from one aircraft to another of the group of smaller aircraft is small. The average velocity for ( $V_v + 2\sigma$ ) for the 11 aircraft is 2.60 ft/sec and the standard deviation about this average is 0.38 ft/sec. The averages of various groups of aircraft are:

7 civil aircraft	2.72 ft/sec
4 military aircraft	2.40 ft/sec
3 turbojets	2.32 ft/sec
8 propeller aircraft	2.72 ft/sec

All these groups are within a standard deviation from the mean and the greatest departure of any single aircraft is less than 2 standard deviations. Thus no significant variation exists between any of these groups. However,

the F-84F is about 4 standard deviations above the average of all the other aircraft with less than 150,000 lb all-up-weight. If the analysis is done with the F-84F records included the average of ( $V_V + 2\sigma$ ) and standard deviation are increased to 2.73 ft/sec and 0.60 ft/sec and the average of the groups for civil, military, turbojet and propeller are respectively 2.72, 2.75, 2.78 and 2.72 ft/sec. Thus the total separation of all the groups is even less than before, being only one-tenth of a standard deviation, but the F-84F records are  $2\frac{1}{2}$  standard deviations from the mean. Whether or not the F-84F records are included there is no significant difference between civil and military and

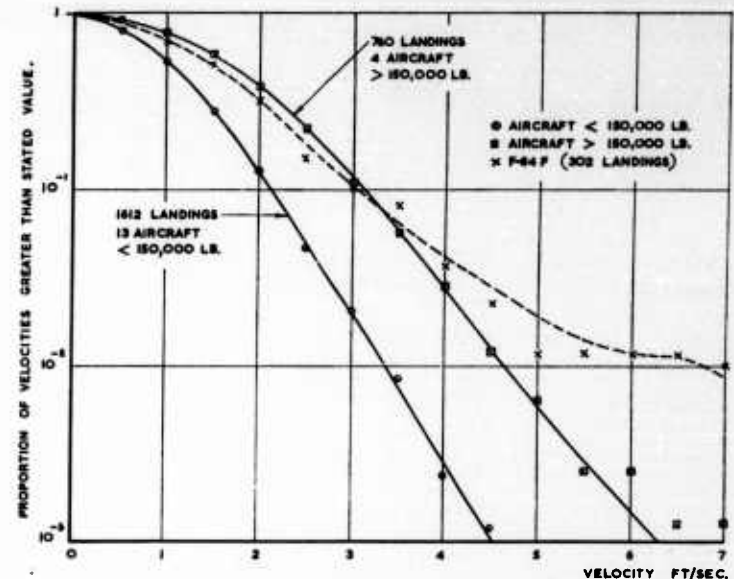


Fig. 7.5. Vertical velocity at touchdown.

between propeller and turbojets, but in view of the large difference from all the other aircraft of the F-84F records they are omitted in this analysis. There are only 4 aircraft larger than 150,000 lb and the average of ( $V_V + 2\sigma$ ) is 3.7 ft/sec compared with 2.6 ft/sec for the aircraft smaller than 150,000 lb. This difference is significant, but it would be dangerous to draw any further conclusions from the fact that the vertical velocity of the propeller aircraft was greater than that for the average for the 3 turbojets and the fact that the average for the 2 military aircraft was greater than that for the 2 civil aircraft.

The frequency of occurrence of different vertical velocities at touchdown is given in Fig. 7.5. The aircraft above and below 150,000 lb are shown separately; the 340 landings of Silsby and Livingston (1959) and 38 of Silsby (1955) that are for unidentified aircraft of less than 150,000 lb are included. In using this diagram it must be remembered that all the landings were photographed and thus night-landings and landings in bad visibility

# GROUND LOADS

are not included. Silsby and Harrin (1955b) expressly state that "the tests were conducted in clear weather conditions and . . . [do] not include . . . squall or other storm conditions".

## 7.4.2. Horizontal Velocity at Touchdown

The horizontal velocity at touchdown was measured on many of the landings on which vertical velocity of descent was measured. Although the F-84F appeared unrepresentative of all other aircraft with respect to vertical velocity, there was nothing unusual about its horizontal velocity. Thus these landings were included in the analysis. In the results given by Silsby (1955) for 478 landings of civil transport aircraft horizontal velocity was measured in all cases. Ten aircraft were examined but three of them each made only 3 landings. Of the other 7 aircraft the stalling speed ranged from 67 to 90 m.p.h. Silsby gives the average landing speed and the standard deviation as a percentage of the stalling speed. A re-examination of the original data suggests that there is much less variation between aircraft if they are compared on the basis of giving each landing in terms of miles per hour (or knots of course) in excess of the stall. Table 7.2 gives the comparative values for the two aircraft with the lowest stalling speed and for the two with the highest stalling speed.

Table 7.2. Landing Speeds of Selected Civil Aircraft (Silsby 1955)

Aircraft	No. of landings	Stalling speed	Landing speed minus stalling speed		Standard deviation	
		m.p.h.	m.p.h.	% stall	m.p.h.	% stall
A	19	67	27.4	40.9	8.2	12.2
B	67	67	21.4	32.1	8.2	12.2
H	36	85	20.6	24.3	6.9	8.1
I	10	90	22.5	25.0	7.3	8.2
Average for all aircraft A to K	478	81	23.2	28.7	7.8	9.6

If the results of all landings are examined in terms of speed in excess of the stall rather than percentage above the stall, there is nevertheless an appreciable difference between propeller and jet aircraft. The results are accordingly separated and in addition the military and civil aircraft are shown separated. Other landings of propeller aircraft than the 478 of Silsby (1955) that can be analysed in terms of knots above the stall include 101 landings of a civil turbo-propeller (Stickle, 1961), 144 landings of a B-36 heavy bomber (Silsby and Harrin, 1955a) and 224 landings of a B-26 twin-propeller bomber (Silsby, 1956). The civil turbo-propeller aircraft has a stalling speed 25 per

cent higher than the average of the other civil aircraft, but its average landing speed above the stall and its standard deviation are 20 knots and 6.6 knots compared with an average of 20.2 knots and 6.8 knots for the other civil aircraft. The B-26 and B-36 military aircraft have values of (20.8, 8.6) and (16.5, 7.6) knots respectively. Silsby and Livingston (1959) quote 340 landings of 7 different propeller aircraft in terms of percentage of stalling speed. As they have not been given for separate types a full analysis is not possible, but rough calculations indicate that the results do not differ much from the 947 landings that have been examined. The variation between different jet aircraft is much greater for both civil and military types, but for consistency of presentation they are analysed on the same basis. Table 7.3 gives a summary of the results.

Table 7.3. Landing Speeds of Jet Aircraft

Reference	Aircraft	No. of landings	Stalling speed	Landing speed minus stalling speed	Standard deviation
			knots	knots	knots
	<i>Civil</i>				
Stickle and Silsby (1960)	Turbojet A	103	100	32.5	7.86
Stickle and Silsby (1961)	Turbojet A	179	100	26.5	8.60
Stickle and Silsby (1961)	Turbojet B	110	97	21.5	7.48
	<i>Military</i>				
Silsby (1956)	T-33	166	90	23.8	6.25
Silsby (1956)	B-57	109	80	37.4	9.70
Silsby (1956)	F-94C	194	120	19.8	8.55
Silsby (1956)	F-84F	302	114	33	10.80

The horizontal velocities at touchdown are given in Fig. 7.6. The propeller aircraft are fairly consistent amongst themselves; military and civil types are hardly distinguishable for landing speeds up to 30 knots above the stall. There is an indication that a few per cent of landings form a small separate family of landings at much higher speeds than the rest and that the military aircraft are more likely to be flown in this way than are the civil. With the turbojet aircraft there is a greater speed margin between the average landings and the stall; this has probably been found necessary because of the relative inefficiency of turbojet engines at low speeds and correspondingly smaller power margins. It was shown in Table 7.3 that the variation between different aircraft was large, so that less confidence can be placed in the results for turbojets than for propeller aircraft. It seems

## GROUND LOADS

probable that some of the variation is due to the relative newness of turbojets with the consequential lack of standardization of methods of landing. In this respect it should be noticed that there is an appreciable difference in landing technique of the civil turbojet A in September 1959 (Stickle and Silsby, 1960) and in April-May 1960 (Stickle, 1961) at the same airport;

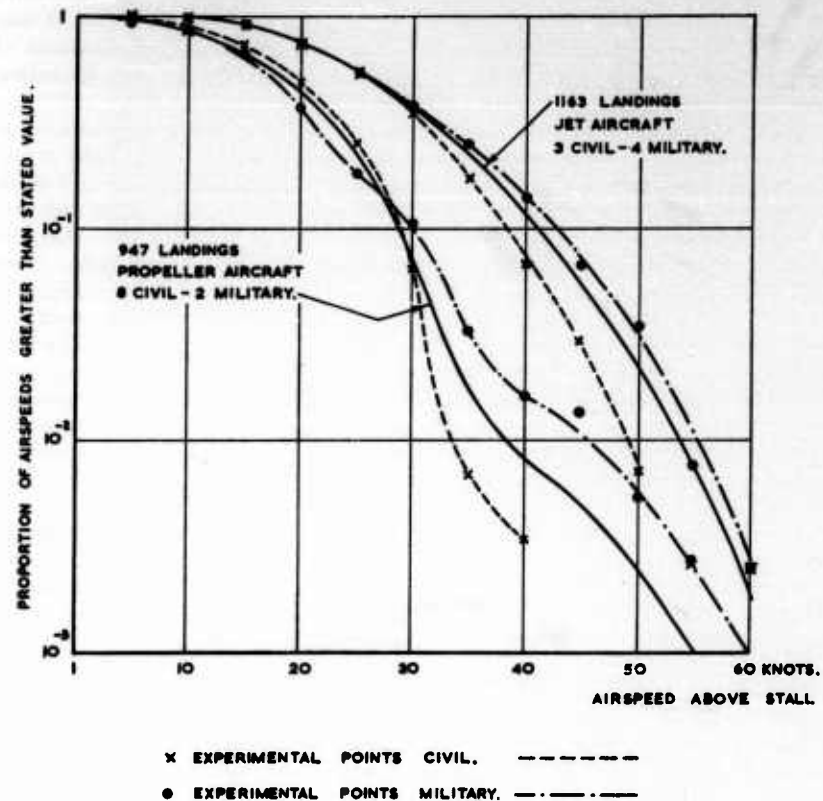


Fig. 7.6. Horizontal velocity at touchdown.

also two of the four military aircraft land much slower than the average of civil and military aircraft combined, whereas the other two land much faster.

### 7.4.3. Bank Angle and Rolling Velocity at Touchdown

To complete the information on landing attitude directly related to the normal acceleration on the aircraft it is necessary to know the angle of bank and the rolling velocity at the moment of touchdown. A comprehensive series of 478 landings of civil transports are given by Silsby (1955). In 413 of the landings the bank angle and rolling velocity were measured. In all cases they were obtained on a single runway on which all the landings were



in one direction and in only 6 landings was there a following wind. Silsby (1955a) also gives the details of 86 landings on a B-36. Silsby (1956) gives a summary of the bank angles and rolling velocities measured on 990 landings on 5 other military aircraft, B-57, B-26, T-33, F-94C, F-84F. The N.A.S.A. have kindly supplied the details of these landings.

All the landings have been grouped by aircraft (except for the civil ones which are combined), by the severity of the cross-wind and whether it was from the left or the right. The means, standard deviation and skewness of the distribution of bank angle are given in Table 7.4 and the corresponding data for rolling angular velocity in Table 7.5.

These are insufficient data to form other than qualitative conclusions as there are so many variations between the different aircraft. In light cross-winds the mean values of both bank angle and rolling velocity do not seem to depend on the role or size of the aircraft and the variation from one aircraft to another is not great. The mean bank angle is to the left, and less than  $1^\circ$ , for all the aircraft except the B-36 which is  $0.1^\circ$  to the right. The mean rolling velocity is towards the first wheel to touch, and less than  $1^\circ$  per second, for all the aircraft except the B-57 which is  $0.3^\circ$  away from the first wheel to touch. Cross-wind affects the mean bank angle of all the aircraft in much the same way, a cross-wind from the left tends to increase the mean bank angle to the left and a cross-wind from the right increases the mean bank angle to the right. The amount of the change depends on the severity of the cross-wind and is of the order of  $1^\circ$  per 20 m.p.h. wind speed. There is no consistency in the change in mean rolling velocity with cross-winds.

The scatter in both bank angle and rolling velocity between individual landings definitely depends on the size of the aircraft. On general reasoning it would be presumed that the moment of inertia about the longitudinal direction would be an important parameter. In left cross-winds the three small aircraft, T-33, F-94C, F-84F, have a standard deviation of bank angle of about  $1.4^\circ$  and of rolling velocity of  $2.8^\circ$  per second. The B-26, B-57, B-36 and the civil aircraft all have a standard deviation of bank angle of about  $1^\circ$  but the standard deviation of rolling velocity decreases with the moment of inertia about the longitudinal axis being about  $1.7^\circ$  per second for the B-57 and  $0.7^\circ$  per second for the B-36. As the cross-winds increase there is a tendency for the scatter to increase but this is not very definite up to 15 m.p.h.

The civil aircraft were the only ones that experienced cross-winds greater than 15 m.p.h. and 49 out of the 413 landings were in this category. It will be seen from Tables 7.4 and 7.5 that the standard deviations of the bank angle and rolling velocity are each about 50 per cent greater than those for landings in light cross-winds. Of these 49 landings, 28 were twin-engined aircraft of 25,000 to 40,000 lb landing weight and 21 four-engined aircraft of 60,000 to 100,000 lb landing weight. The smaller aircraft had a standard deviation of bank angle only 8 per cent above that for the larger aircraft but the standard deviation of rolling velocity was 50 per cent greater. The amount of data for cross-winds above 15 m.p.h. is rather small but it indicates that there may be serious loads in aircraft with low moments of inertia about the longitudinal axis.

## GROUND LOADS

Table 7.4. Bank Angle at Touchdown of Different Aircraft

Reference	Aircraft	No. of landings	Cross-wind m.p.h. R from right L from left	Bank angle degrees		
				Mean	Standard deviation	Skewness
Silsby (1956)	B-57	13	9-9R to 5R	-1.03	0.86	+0.51
		48	4-9R to 5L	-0.90	0.67	+1.00
		22	5-1L to 10L	-0.96	0.84	+0.12
		26	10-1L to 15L	-1.16	0.87	+0.12
		109	Total	-0.99	0.77	+0.34
Silsby (1956)	B-26	64	9-9R to 5R	-0.30	1.27	+0.41
		71	4-9R to 5L	-0.67	0.98	+0.31
		64	5-1L to 10L	-0.86	1.01	+0.27
		25	10-1L to 15L	-1.13	0.86	+0.67
		224	Total	-0.67	1.10	+0.67
Silsby (1956)	T-33	44	9-9R to 5R	-0.12	1.57	+0.35
		57	4-9R to 5L	-0.63	1.22	+0.33
		44	5-1L to 10L	-0.88	1.02	+0.19
		20	10-1L to 15L	-1.54	1.02	-0.65
		165	Total	-0.67	1.33	+0.52
Silsby (1956)	F-94C	28	9-9R to 5R	-0.31	1.52	+0.47
		99	4-9R to 5L	-0.82	1.45	+0.34
		27	5-1L to 10L	-1.22	1.68	-0.01
		40	10-1L to 15L	-2.56	1.75	+0.24
		194	Total	-1.16	1.69	+0.26
Silsby (1956)	F-84F	83	9-9R to 5R	-0.75	1.24	+0.35
		127	4-9R to 5L	-1.02	1.47	-0.28
		61	5-1L to 10L	-1.18	1.72	0.00
		27	10-1L to 15L	-1.44	1.57	-0.40
		298	Total	-1.02	1.48	-0.01
Silsby and Harrin (1955a)	B-36	18	9-9R to 5R	+0.44	0.96	+0.02
		19	4-9R to 5L	+0.19	0.83	+0.13
		19	5-1L to 10L	+0.04	1.14	-0.38
		30	10-1L to 15L	+0.30	1.24	+0.86
		86	Total	+0.25	1.07	+0.36
Silsby (1955)	Various Civil: 6 twin- engine 5 four- engine	144	9-9R to 5R	-0.36	1.01	0.00
		98	4-9R to 5L	-1.21	1.11	-0.51
		122	5-1L to 10L	-1.16	1.50	+0.09
		49	10-1L to 15L	-1.44	1.53	+0.10
		413	Total	-0.93	1.32	-0.23



Table 7.5. Rolling Velocity at Touchdown of Different Aircraft

Reference	Aircraft	No. of landings	Cross-wind m.p.h. R from right L from left	Rolling velocity degrees per second		
				Mean	Standard deviation	Skewness
Silsby (1956)	B-57	13	9.9R to 5R	-0.03	1.94	+0.48
		48	4.9R to 5L	-0.29	1.70	-0.09
		22	5.1L to 10L	-0.34	1.42	-0.83
		26	10.1L to 15L	-0.09	1.97	+0.64
		109	Total	-0.22	1.72	+0.20
Silsby (1956)	B-26	64	9.9R to 5R	0.00	1.73	+0.65
		71	4.9R to 5L	0.00	1.30	+0.90
		64	5.1L to 10L	+0.68	1.39	-0.63
		25	10.1L to 15L	+0.76	1.40	-0.24
		224	Total	+0.27	1.52	+0.27
Silsby (1956)	T-33	44	9.9R to 5R	+1.02	2.69	+0.28
		57	4.9R to 5L	+0.38	2.91	+0.47
		44	5.1L to 10L	-0.29	2.82	-0.57
		20	10.1L to 15L	-1.49	3.62	-0.22
		165	Total	+0.15	3.00	-0.10
Silsby (1956)	F-94C	28	9.9R to 5R	+0.64	2.84	+0.88
		99	4.9R to 5L	+0.90	2.28	+0.45
		27	5.1L to 10L	+0.80	2.47	-0.17
		40	10.1L to 15L	+0.90	3.12	+0.19
		194	Total	+0.76	3.07	+0.20
Silsby (1956)	F-84F	83	9.9R to 5R	+0.52	2.55	+0.22
		127	4.9R to 5L	+1.00	2.70	+1.08
		61	5.1L to 10L	+0.29	3.08	-0.26
		27	10.1L to 15L	+0.93	2.57	+0.34
		298	Total	+0.71	2.73	+0.42
Silsby and Harrin (1955a)	B-36	18	9.9R to 5R	+0.10	0.80	+1.05
		19	4.9R to 5L	+0.14	0.73	+0.25
		19	5.1L to 10L	+0.27	0.70	+0.93
		30	10.1L to 15L	-0.10	0.70	+0.12
		86	Total	+0.09	0.73	+0.06
Silsby (1955)	Various Civil: 6 twin- engine 5 four- engine	144	9.9R to 5R	+0.16	1.21	-0.01
		98	4.9R to 5L	+0.41	1.25	+0.09
		122	5.1L to 10L	+0.35	1.39	-0.10
		49	10.1L to 15L	+0.77	2.04	-0.30
		413	Total	+0.35	1.40	-0.02

The skewness of the distributions for the civil aircraft is very small and the distributions can be represented fairly well by a Normal distribution for the full range of the measurements, i.e. up to about 2 standard deviations from the mean. The distributions for the military aircraft are rather more skew, but even in these cases the error introduced by assuming a Normal distribution up to two standard deviations from the mean should not be great.

#### 7.4.4. Comparison of Impact of First and Second Wheels

As has already been mentioned the four parameters horizontal velocity, vertical velocity, bank angle and rolling velocity do not appear to be correlated. Thus it should be possible to deduce the vertical velocity of the

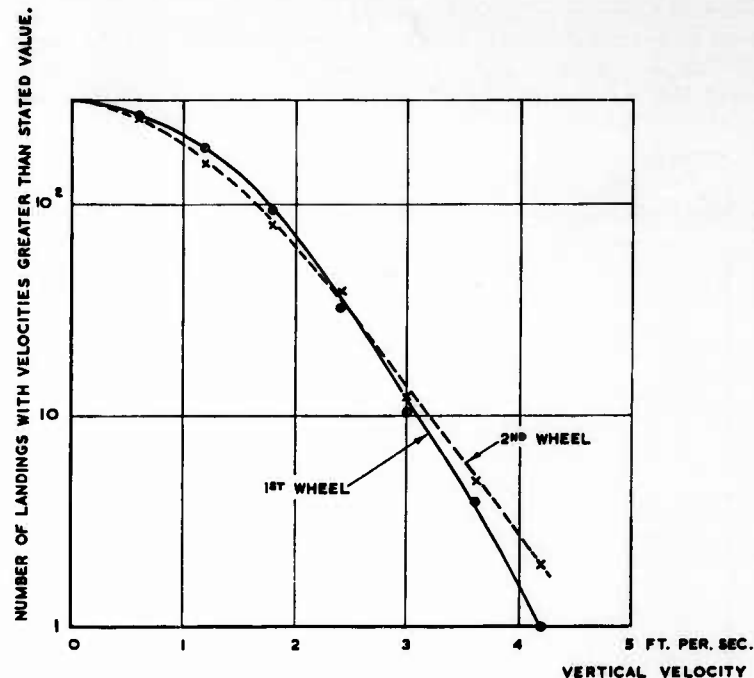


Fig. 7.7. Comparison of vertical velocity at touchdown of first and second wheels.

second wheel to touch from the distributions of the values of the four parameters with respect to the first wheel to touch. However, vertical velocity of descent is so important of itself that a direct correlation of its values for both wheels is worthwhile. In 312 landings of the 478 transport measurements by Silsby (1955) the vertical velocities of both wheels were measured and Harrin (1956) summarizes them in two groups according to the direction of the angular velocity at touchdown. He shows that the wheel towards which the aircraft is rolling at the first impact is more likely to have the higher velocity. Figure 7.7 is obtained of the relative total distributions for each

wheel by adding these two groups given by Harrin. This is a more appropriate comparison than one deduced from bank angles and rolling velocities and, until further information becomes available, can be used with reasonable confidence for all aircraft. It can be seen that the second wheel has slightly fewer low velocity landings and slightly more landings that have higher velocity.

#### 7.4.5. Direct Measurement of Normal Acceleration

The attitude of the aircraft on impact determines the loads that will be applied by the undercarriages to it. The undercarriage is a non-linear system and the influence of yaw will be great on the correlation between the peak normal acceleration at the centre of gravity. Dreher (1956) has examined 268 landings on a trainer and has shown that despite some scatter, as would be expected, there is a definite relationship between the maximum incremental acceleration and the vertical velocity measured at one wheel only and this relationship agrees well with Milwitzky's (1953) analytical

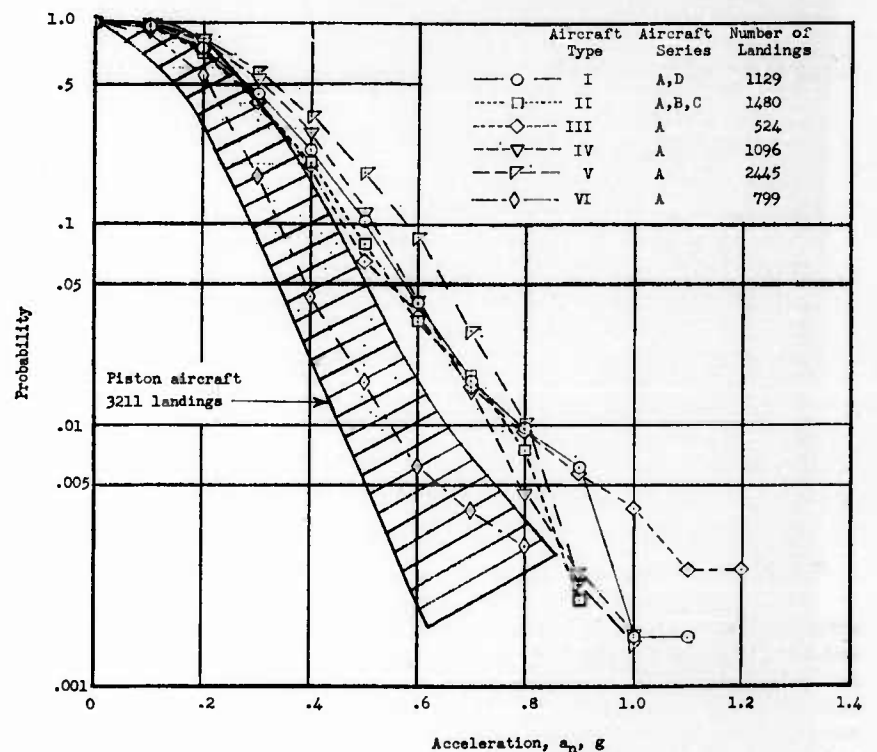


Fig. 7.8. Normal acceleration at touchdown.

Reproduced from Operational experiences of turbine-powered commercial transport airplanes, by staff of Langley Airworthiness Branch. N.A.S.A. TN. D-1392.

## GROUND LOADS

method. Using the maximum incremental normal acceleration to estimate vertical velocity has the advantage over the photographic method that it can be used for all landings especially those in bad visibility. Acceleration records have been made of about 3000 landings by piston-engined aircraft and about 7000 turbine-powered aircraft. Figure 7.8 reproduces the diagram given in the paper by the Staff of Langley Airworthiness Branch (1962). Data are not available for a comparison to be made with the vertical velocity at touchdown.

### 7.5 FORE AND AFT AND LATERAL ACCELERATIONS

The accelerations in the plane of the runway surface have important effects on the loads on the undercarriage and also on the take-off and landing aerodynamic performance of the aircraft. Joyner (1963) has summarized a great amount of work done at the Langley Research Center on wet runway braking and slush drag. Much of this data must relate to particular aircraft and tyres. It should be possible to make some conclusions that would be applicable to aircraft generally but no attempt has been made to analyse in this way this recent paper of Joyner's (1963) or the papers to which he refers.

### REFERENCES

- |                                  |                                       |
|----------------------------------|---------------------------------------|
| Dreher (1956)                    | Silsby and Harrin (1955b)             |
| Dreher and Batterson (1958)      | Silsby (1956)                         |
| Harrin (1956)                    | Silsby and Livingston (1959)          |
| Houbolt (1961)                   | Staff of Langley Airworthiness Branch |
| Joyner (1963)                    | (1962)                                |
| Kolnick and Morris (1955)        | Stickle and Silsby (1960)             |
| Milwitzky and Cook (1953)        | Stickle (1961)                        |
| Morris, B. R. (unpublished 1962) | Taylor, J. (1956)                     |
| Silsby (1955)                    | Westfall <i>et al.</i> (1957)         |
| Silsby and Harrin (1955a)        |                                       |

**CHAPTER 8**  
**TEMPERATURE AND AIRSPEED**  
**IN FLIGHT**

**CONTENTS**

8.1 Introduction	173
8.2 Time spent at different speeds (E.A.S.)	174
8.3 Variation with height of proportion of time spent at different airspeeds	181
8.4 Temperature perturbations from the average ambient con- ditions	187
References	188

## CHAPTER 8

# TEMPERATURE AND AIRSPEED IN FLIGHT

### 8.1 INTRODUCTION

There is a direct relationship between the temperature of the structure and the Mach No. in flight and also an indirect one due to the action of the pilot. The operation of turbo-jet engines is limited very much by temperature in much the same way that the structure is limited; each has a limiting Mach No. that depends on the ambient air temperature and the time spent at that temperature. The heating rates for engine and structure are different, but the instructions given to the pilot must be influenced by both engine and structural requirements. In addition to engine and structural considerations, there is also the relationship of Mach No. to true air speed. When the ambient temperature is higher the temperature rise for a given Mach No. is higher, but the true air speed is also higher although not by the same amount. Thus to maintain a constant true speed it is possible to reduce the Mach No. whenever the ambient temperature rises, but not by so much that the structural temperature does not rise.

The pilot has a considerable freedom of choice of Mach No. and he will be influenced by the knowledge that at a given Mach No. the engine and structural temperatures and the true air speed will all increase with ambient temperature. The simple approach of selecting the atmospheric temperatures from the information given in Chapter 2 but making no allowance for the pilot's discrimination of speed because of the ambient temperature would be of little value. Moreover, changes in atmospheric temperature that occur in relatively short distances, such that the aircraft velocity could not readily be changed by the pilot's action, must be tolerated.

The information available on the whole subject of airframe temperatures and Mach No. is so sparse that extensive empiricism and extrapolation must be employed to describe it in a form suitable for determining structural loadings. To assess the confidence that can be placed in the various parameters and also to facilitate the replacement of some data by data more suitable for a particular aircraft, the subject is divided into separate fields. The main breakdown is into

- (i) Total time spent at each equivalent air speed (E.A.S.).
- (ii) Numbers of occurrences of each speed.
- (iii) Time spent at different speeds at different height bands for selected aircraft.
- (iv) Temperature perturbations from the average ambient conditions.

These fields are essentially interrelated and an attempt is made to give a qualitative review of this.

## 8.2 TIME SPENT AT DIFFERENT SPEEDS (E.A.S.)

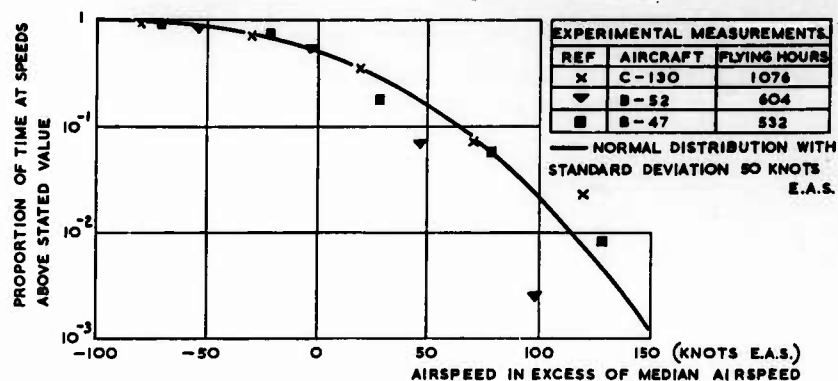
Most of the data available are for aircraft with maximum speeds less than Mach No. 1.5. A limited amount is available up to a Mach No. 2.8 but this is insufficient to predict with confidence distributions up to a Mach No. 2.5 and it has to be used in conjunction with extrapolations from the data up to a Mach No. 1.5. The associated temperatures vary roughly as the square of the speeds and above a Mach No. 2 will rapidly become important for aluminium aircraft. The method adopted in flying aluminium aircraft at such speeds may change greatly and introduce corresponding uncertainties in forming general conclusions from such data.

As the main interest is in the time spent at the higher speeds the data may be presented as the proportion of time that is spent above each speed. This gives a cramped scale at the lower speeds but it does not matter much as the interest in it is small.

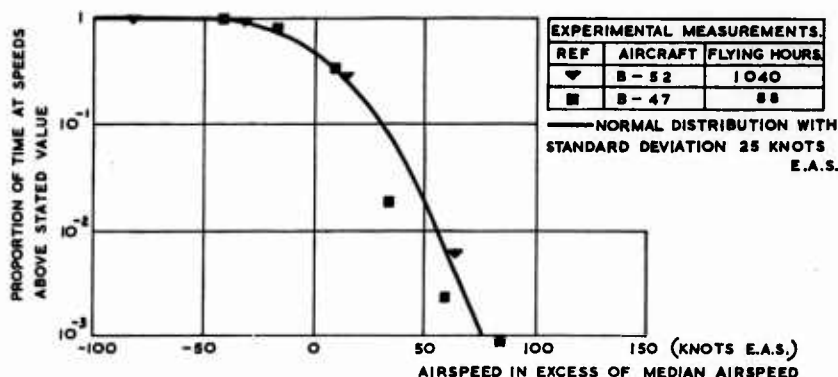
In performing manoeuvres the pilot will be attempting directly or indirectly to apply a particular acceleration normal to the line of flight at a particular forward speed, and departures from this will be more or less random. Thus provided there is no intrinsic limit to cut off the distribution, such as the stall in a pitching manoeuvre or the impossibility of an upward velocity at a landing touchdown, the departures are likely to be fairly equally distributed on both sides of the mean values. In Chapter 5 it was shown to be the case for the distribution of forward speeds at which pitching manoeuvres were performed. These were given as mean velocities with standard deviations about the mean. The skewness was also given but in most cases it was small, so that the median velocity was not appreciably different from the mean velocity. The distributions found for both forward velocity and normal acceleration in pitching manoeuvres are of interest in obtaining an understanding of time spent at different speeds. In this respect it would be convenient to maintain the same way of defining the distribution of speed. However, for many operational purposes an aircraft is flown for the majority of its time at or about a certain speed, but with two deliberate types of departure from this, one a high speed run and the other a reduction of speed to land. As these departures are quite different in character it would be fortuitous if the complete distribution were symmetrical. Where these deliberate departures occupy a very small proportion of the time the distributions will be fairly symmetrical and not markedly different from Normal distributions. Transports and heavy bombers will usually fall into this category. Fighters, fighter bombers and trainers will usually be called upon to make high speed runs that will make the distributions skew and it is often more convenient to consider these distributions relative to the median velocity rather than to the mean velocity.

The data on time spent at different speeds are mainly from aircraft with turbojet engines. This means that the distributions at high speeds should not be applied to propeller driven aircraft. The main differences arise because the design limit speed is more easily achievable. Thus random departures from the cruising speed are not seriously limited by the absolute top speed of the aircraft, and also the aircraft has to be kept below its limiting speed more by observation of the flying speed than by lack of engine power.

A speed limitation that has to be observed by reference to an indicator in the cockpit, will influence the distribution of time spent at speeds near to it. This effect should be least for the bombers and transport class of aircraft which are examined first. There are three aircraft in this group, the B-47 by Dunkee (1961), the C-130 by L. Phillips (1961) and the B-52 by Wallace (1961) and by L. G. Kelly and Broom (1962). All the distributions are



A. BELOW 30,000 FEET.



B. ABOVE 30,000 FEET.

Fig. 8.1. Proportion of time spent above different speeds by bombers and transport aircraft.

fairly symmetrical and, at flights below 30,000 ft, the means are 272, 230 and 253 knots (E.A.S.) respectively for the B-47, C-130 and B-52. At flights above 30,000 ft the means are 240 and 235 knots (E.A.S.) respectively for the B-47 and the B-52. The total time spent at different speeds is shown in Fig. 8.1; the speeds are given in knots E.A.S. exceeding the mean speed. A Normal distribution with a standard deviation of 50 knots is also shown for comparison with the distributions below 30,000 ft and it will be seen that none of the three distributions differs much from this Normal distribution.



At heights above 30,000 ft a Normal distribution with a standard deviation of 25 knots gives a good representation.

The distributions for the fighters and fighter bombers include a number of deliberate excursions to high speeds and an examination of the individual records suggests that the total time above any speed varies exponentially with speed up to about 80 per cent of the design diving speed. Above this speed the effect of the design diving speed has an important effect that must be examined independently.

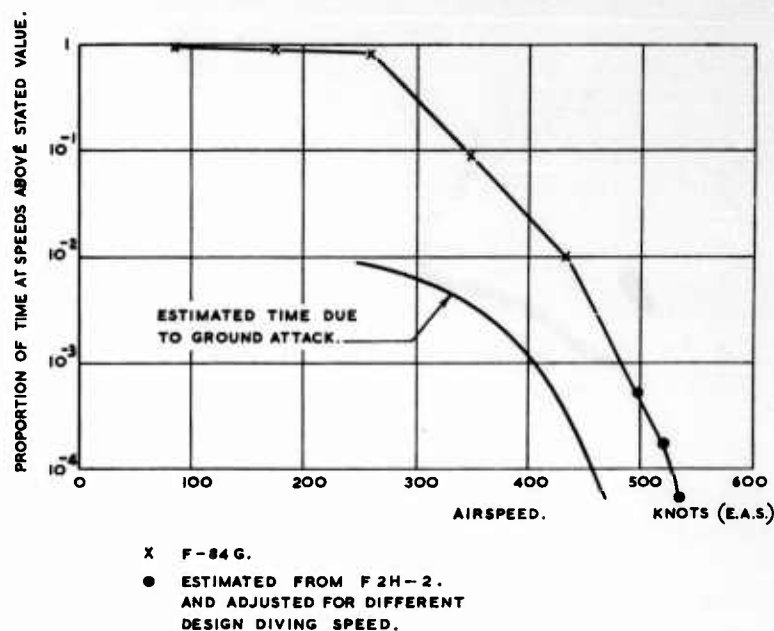


Fig. 8.2. Proportion of time spent above different speeds by an F-84G fighter in 349 flying hours air-to-ground combat in Korea.

Information is available for the F-84G in air to ground combat in Korea (Gray, 1955), and it is possible using a few simplifying assumptions to estimate the distribution to be expected at higher speeds. Figure 8.2 gives the total time spent by the F-84G above different speeds. A curve for speeds in excess of those at which readings were taken has been deduced from the data presented in Chapter 5 on the assumption that the excursions to speeds in the neighbourhood of limit load are all roughly of the same duration and of 0.05 hr. It will be appreciated that if these excursions are in fact all of the same duration the shape of the curve is fixed but the position on the time scale depends on the actual duration (in the absence of data of the F-84G the values for an F-2H2 Naval Jet Fighter by J. P. Mayer and Harris (1955) were used). One of the ways in which high speeds are achieved is in ground attack when the aircraft is accelerated in a dive and then pulled up with

high normal accelerations. This would be the main way of achieving high speeds with propeller driven aircraft but it need not be so with turbojet aircraft. In order to estimate the time spent at different speeds in ground attack a number of simplifying assumptions must be made. This has been done for the F-84G and the estimates are shown on the same diagram as those for total times at different speeds. The following are the simplifying assumptions. Gray (1955) finds that the most severe mission of the F-84G is the high angle bombing and it is assumed that all the missions are of this severity and occur once per hour. In high angle bombing the F-84G on average starts its dive at 245 knots at a dive angle of  $39^\circ$  from 9700 ft and pulls out at a radius of 4000 ft at 396 knots 5600 ft lower. Taking the scatter on speed to be 36 knots, as was shown in Chapter 5 to be the case for the speed at which the peak acceleration occurred, and arbitrarily doubling the time at any speed to allow for the reduction in speed in the subsequent climb, the values shown in the diagram are found. It is thought that these assumptions are conservative so that these times are probably rather higher than the actual totals, but nevertheless at no speed more than a few per cent of the total time. It seems reasonable to assume that for all fighters the times spent in manoeuvres at any speed is so small that any change in technique of making manoeuvres will have a negligible effect on the total time spent at any speed.

Extensive information is also available for fighters of the F-100 class on normal operational duties (Titus, 1961). The total time is 6050 flying hours and the higher velocities are probably achieved primarily in air-to-air manoeuvres at approximately constant heights well above the ground. Figure 8.3 gives the proportion of time at different speeds of the F-100. The records agree closely to an exponential decay from the median airspeed up to about 0.8 times the design diving speed, thereafter the proportion is less than would be expected from an exponential decay. The values at 600 knots (E.A.S.) and 650 knots (E.A.S.) can be compared with the frequency of occurrence of these high speeds and an estimate made of the average time spent for each occurrence. No information is available for the F-100 but by scaling the speeds for the Hunter in the ratio of the design diving speeds for the two aircraft an estimate can be made. The Hunter data (Owen, E. M. and Sellers, 1958) for frequency of occurrence of high speeds (i.e. those occurring once per 30 hr or less frequently) agree quite well with the time spent above 600 knots E.A.S. and above 650 knots E.A.S. for the F-100 if the average time for each occurrence were 0.05 hr. It was estimated that the F-84G even on ground attack duties spent rather more time at higher speeds than would have been expected from the excursions to high speed during the actual attack. The F-100, which makes its high speed runs mainly at higher altitudes spends an even greater proportion of time at higher speeds. The exponential decay for the air to ground missions of the F-84G was about 90 knots E.A.S. per decade and that for the predominantly air-to-air missions of the F-100 was about 150 knots E.A.S. per decade.

The proportion of time spent at different speeds by a number of fighters is shown in Fig. 8.4. The curves for the F-84G and the F-100 are reproduced as a basis of comparison. In order to compare fighters of widely different

speeds the proportion of time has been plotted in terms of airspeed in excess of the median airspeed for each type: median airspeed, rather than mean airspeed, has been chosen as it is probably more nearly equal to the commonly used cruising speed and therefore more easily estimated at the design stage of an aircraft. For any of the aircraft examined the abscissa can be changed to actual airspeed by adding the value of the median airspeed which is 275, 296, 320, 302, 339, 273 knots (E.A.S.) respectively for the F-106 (Clay and Berens, 1963), F-102 (Vahldiek, 1961), RF-101C (Ward, 1963a), F-104 (Mullins, 1961 and 1962), F-105 (Vahldiek, 1961a), F-86 (Gray, 1955)

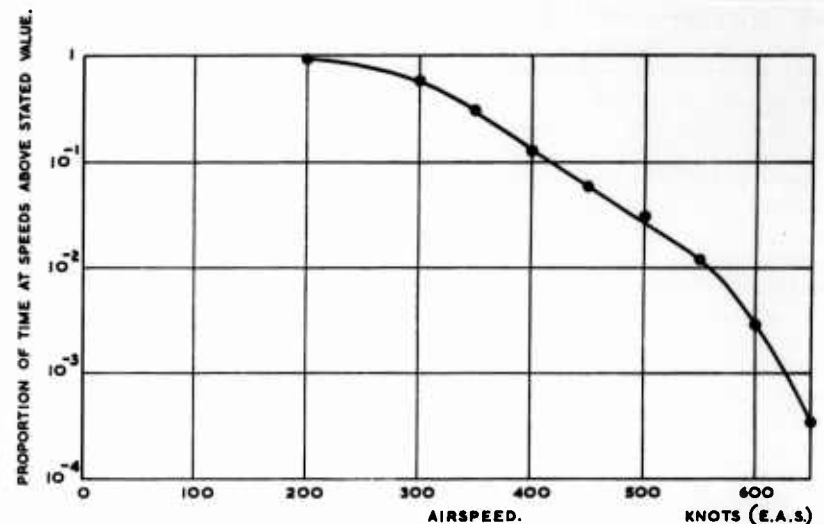
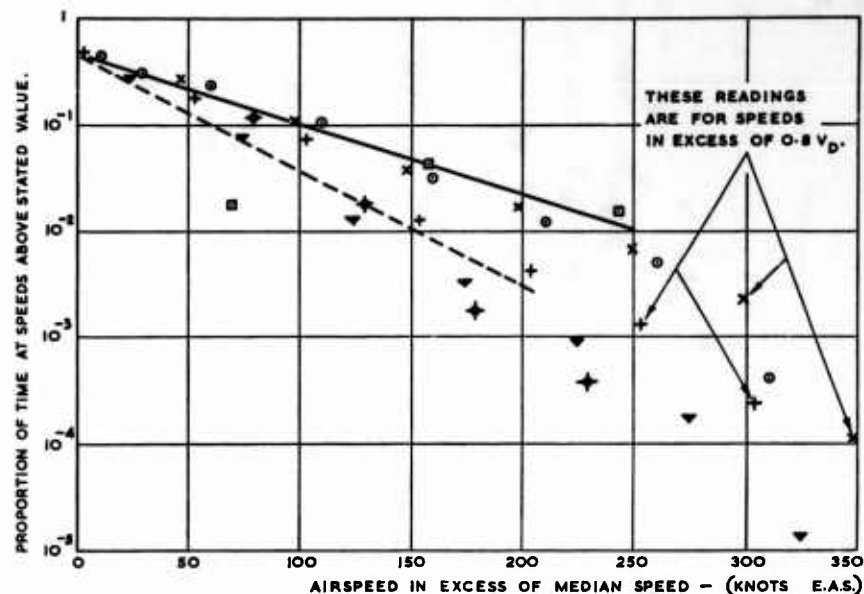


Fig. 8.3. Proportion of time spent above different speeds by F-100 class fighters in 6050 flying hours combined duties.

classes of aircraft. The F-106 and RF-101C have similar distributions to the F-84G; in the case of the RF-101C this is mainly due to a predominance of the high speeds being made below 5000 ft, but the similarity of the F-106 is somewhat fortuitous. The distributions at different heights are available for these two aircraft and they are discussed in more detail in paragraph 8.3. The other four aircraft appear to have similar distributions to that of the F-100 class and the average distribution of the four classes is almost indistinguishable from that of the F-100. It is, however, worth examining the F-102 results in a little more detail. The actual curve is far from an exponential decay, the proportion of time above 104 knots in excess of the median speed being appreciably above the line and that above 154 knots being appreciably below the line; the line joining these points is in fact a little steeper than the decay for the F-84G air-to-ground missions. A further breakdown of the original F-102 data shows that the median airspeed at a gunnery meet was about 30 knots higher than the overall median and also that the reduction of time at higher speeds was a little more rapid than

# TEMPERATURE AND AIRSPEED IN FLIGHT

that for the F-84G air-to-ground missions. The breakdown suggests also that the complete distribution is made up of two distributions, one similar to that for the F-100 and the other similar to that for the F-84G. The median airspeed for the air-to-ground missions is appreciably the greater and results in the kink in the curve. Whenever the air-to-ground missions



REF	AIRCRAFT	FLYING HOURS.
—	F-100 FROM FIG. 8.3	
- - -	F-84 G FROM FIG. 8.2	
▼	F-106	3,773
+	F-102	2,086
✦	RF-101 C	2,025
x	F-104	1,840
□	F-86	1,577
●	F-105	380

Fig. 8.4. Proportion of time spent above different speeds by fighter aircraft. Measurements are compared with F-84G air-to-ground combat and F-100 on combined duties. Both aircraft up to speeds of 0.8 times design diving speed.

are normally done at airspeeds not appreciably in excess of those of the air-to-air missions, their contribution to the time at higher speeds will be negligible, because of the more rapid decay with airspeed, and will hardly influence the shapes of the curves. This seems to be what may have happened in the cases of the F-104 and F-105. In using this figure for other designs, an estimate should be made of the contributions from air-to-air missions and also from air-to-ground missions.

The data available for trainer aircraft (Titus, 1959 and 1960) are not very extensive but are shown in Fig. 8.5. There are three trainers, one for primary training (T-34), one for advanced training (T-33), and one for instructor upgrading (T-37). Most of this flying will be done under supervision and this seems to produce, on the whole, a smaller variation of the proportion of time at different speeds than that of fighters. The comparison

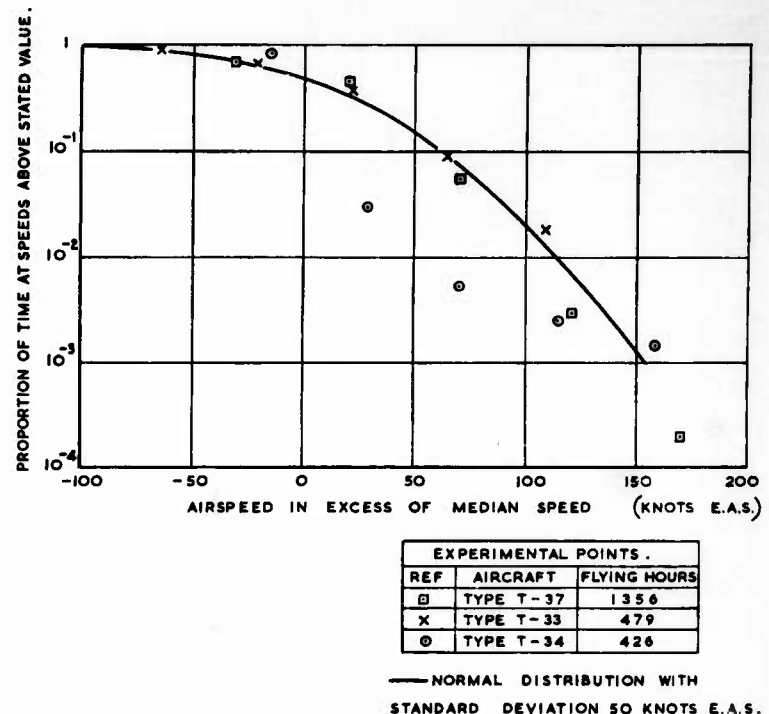


Fig. 8.5. Proportion of time spent above different speeds by trainer aircraft.

has therefore been made with that for bombers and transports; the mean speeds are 239, 103, 180 knots (E.A.S.) respectively for the T-33, T-34 and T-37. The agreement is very good for the two advanced trainers but the primary trainer shows a marked difference. The tolerance on speed for the primary trainer is usually very small indeed but the occasional excursions to high speed is much greater than those of the other trainers. It is appreciated that this primary trainer is very slow but the speed of 261 knots (i.e. 158 knots above the mean) which is exceeded 0.15 per cent of the time is 21 knots above the design diving speed. The readings must be regarded as exceptional, as the original report gives 0.05 per cent of the time 65 knots above the design diving speed.

## 8.3 VARIATION WITH HEIGHT OF PROPORTION OF TIME SPENT AT DIFFERENT AIRSPEEDS

The main value of the data on equivalent airspeed is the associated Mach No. At low altitudes the Mach Nos. are relatively low and do not produce very significant temperatures. They do, however, help appreciably in giving confidence to the extrapolations that are made to higher Mach No. of the data at high altitudes.

The data for total times at different speeds with only a coarse breakdown into heights indicates that there are basically four distributions of equivalent airspeeds as follows:

- A. A normal distribution with standard deviation 50 knots E.A.S. below 30,000 ft, measured on bombers, transports and trainers.
- B. A normal distribution with standard deviation 25 knots E.A.S. above 30,000 ft, measured on bombers.
- C. An exponential decay above the median airspeed of 150 knots E.A.S. per decade at heights well above the ground, measured on fighters.
- D. An exponential decay above the median airspeed of 90 knots E.A.S. per decade near the ground, measured on fighters.

Data from 3773 flying hours (226,402 min) on the F-106 are given in Table 8.1 of the time spent at different heights and speeds. The original data of equivalent airspeeds has been grouped into three height bands, up to 5000 ft, between 5000 and 30,000 ft, above 30,000 ft. The corresponding distributions of Mach No. have been deduced and are included in the table. Similar data for 2025 flying hours on the RF-101C are given in Table 8.2. An examination of these two tables shows that it is possible to obtain good agreement with the experimental data by assuming that it is made up of various proportions of the four distributions *A*, *B*, *C*, *D* given above, except that for distribution *B* a standard deviation of 30 knots E.A.S. seems to be more appropriate for fighters rather than the 25 knots E.A.S. measured on bombers. The more extensive breakdown into height bands that has been possible on the F-106 and the RF-101C indicates that the distribution *D* will mainly occur below a height of 5000 ft and that distribution *C* will mainly occur at the usual cruising height band.

Figure 8.6 shows the proportion of time spent above different speeds by an F-106, Fig. 8.6A is for heights below 5000 ft, Fig. 8.6B for heights between 5000 and 30,000 ft and Fig. 8.6C for heights above 30,000 ft. Good agreement is reached with experiment if it is assumed that distributions *A* and *D* are in equal proportions below 5000 ft, distribution *A* holds between 5000 and 30,000 ft and distribution *B* (with standard deviation 30 knots E.A.S.) and *C* have respectively 92 per cent and 8 per cent of the total above 30,000 ft. The worst agreement takes place in the height band 5000 to 30,000 ft which is presumably due to the presence of a distribution with an exponential decay similar to distributions *C* and *D*. These distributions may be regarded as typical for a fighter aircraft. Distributions for other fighters may be predicted by estimating the proportion of the time high speed runs are made and assuming that distributions *C* or *D* hold for them; the remainder of the

MANUAL ON AIRCRAFT LOADS

time may be regarded as cruising in which distributions *A* or *B* hold. The RF-101C is used mainly on photographic reconnaissance duties, it spends more than half its time below 5000 ft of which 30 per cent appear to be high speed runs. At altitudes above 30,000 it is not capable of such high

Table 8.1. Time in Minutes Spent at Different Heights and at Different Airspeeds by an F-106 on Combined Fighter Duties (Deduced from Clay and Berens, 1963)

Airspeed	Height in thousands of feet			Total
	0-4-99	5-29-99	30-69-99	
Equivalent airspeed knots				
150-199	2860	223	947	4030
200-249	7927	5649	39,003	52,579
250-299	9906	21,348	74,677	105,931
300-349	8128	25,961	12,048	46,137
350-399	2509	11,757	610	14,876
400-449	391	1507	240	2138
450-499	76	292	147	515
500-549	22	35	102	159
550-599	6	5	23	34
600-649	1	1	1	3
Total	31,826	66,778	127,798	226,402
Mach No.				
0.2-0.399	11,092	1754		12,846
0.4-0.599	18,934	23,316	131	42,381
0.6-0.799	1767	29,901	7093	38,761
0.8-0.999	33	11,252	60,020	71,305
1.0-1.199		542	54,847	55,389
1.2-1.399		11	3619	3630
1.4-1.599		2	1371	1373
1.6-1.799			356	356
1.8-1.999			195	195
2.0-2.199			113	113
2.2-2.399			37	37
2.4-2.599			11	11
2.6-2.799			5	5
Total	31,826	66,778	127,798	226,402

speeds as the F-106 and very little time appears to be spent in high speed runs; the best fit to the experimental data is 0.3 per cent of the time. Unpublished data from 7 other U.S. fighters with similar capabilities show similar distributions in all three height bands. The total flying time for

# TEMPERATURE AND AIRSPEED IN FLIGHT

each aircraft was about 300 flying hours. Above 30,000 ft 6 out of 7 of the aircraft could be represented by distribution *B* (with standard deviation 30 knots E.A.S.) each with less than 1 per cent of distribution *D*, the other aircraft had a standard deviation of about 50 knots (E.A.S.). The data below 30,000 ft were separated into 10,000 ft bands and separation for the lowest 5000 ft was not possible. However, by analysing the data above and

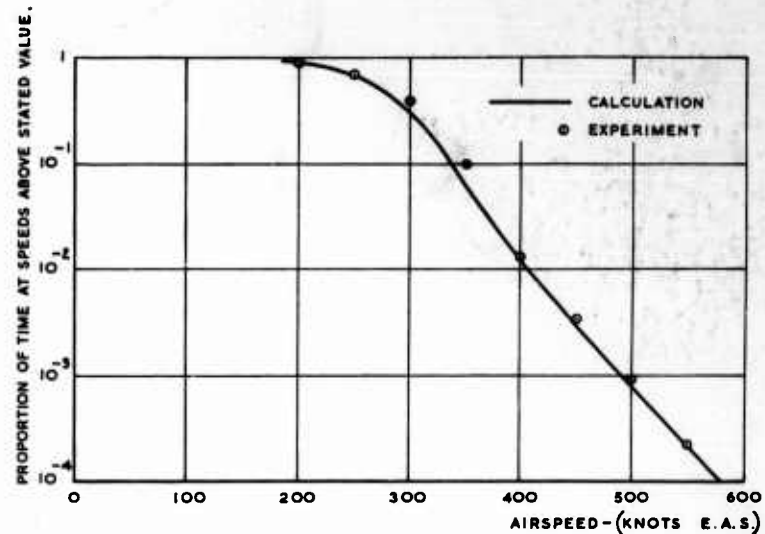
Table 8.2. Time in Hours Spent at Different Heights and at Different Airspeeds by an RF-101C on Combined Reconnaissance Duties (Deduced from Ward, 1963a)

Airspeed	Height in thousands of feet			Total
	0-4.99	5-29.99	30-59.99	
Equivalent airspeed knots				
150-199	29.42	4.21	6.27	39.90
200-249	60.00	39.95	36.21	136.16
250-299	143.11	204.71	218.18	566.00
300-349	278.31	311.78	54.20	644.29
350-399	319.59	82.21	0.35	402.15
400-449	188.56	12.55	0.04	201.15
450-499	30.07	2.09	0.02	32.18
500-549	2.37	0.32		2.69
550-599	0.76			0.76
Total	1052.19	657.82	315.27	2025.28
Mach No.				
0.2-0.399	112.16	5.86		118.02
0.4-0.599	635.08	158.34	7.25	800.67
0.6-0.799	302.52	355.27	101.35	759.14
0.8-0.999	2.43	136.57	188.45	327.45
1.0-1.199		1.76	17.93	19.69
1.2-1.399		0.02	0.24	0.26
1.4-1.599			0.05	0.05
Total	1052.19	657.82	315.27	2025.28

below 10,000 ft an estimate of the conditions near the ground and in the climb and descent can be made. In the climb all the aircraft have roughly distribution *A* and near the ground they have a combination of distributions *A* and *B* in various proportions. In the present analysis the actual proportions are not given as they are for the lowest 10,000 ft instead of the 5000 ft used for the other aircraft.

The numerical values of the times at different equivalent airspeeds that were used to obtain the curves for the B-47 and the B-52 above 30,000 ft in Fig. 8.1 are given in Table 8.3 together with the associated Mach No. These





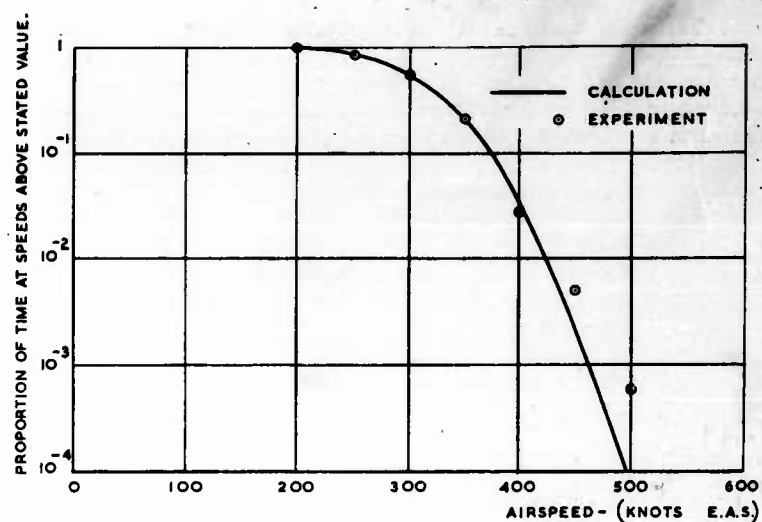
**A — BELOW 5,000 FT. — 530 FLYING HOURS.**

Fig. 8.6. Proportion of time spent above different speeds by an F-106.

Measurements deduced from Clay and Berens (1963) and compared with calculated curves as follows:

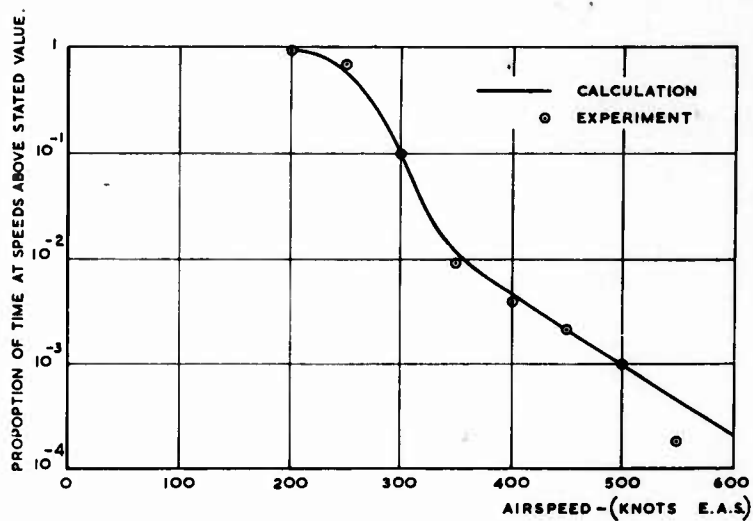
- A. Below 5000 ft normal distribution with experimental median value and standard deviation 50 knots E.A.S. but with 50 per cent of the calculated value above the median replaced by a logarithmic decay of 90 knots E.A.S. per decade.
- B. 5000 ft to 30,000 ft normal distribution with standard deviation 50 knots E.A.S.
- C. Above 30,000 ft normal distribution with standard deviation 30 knots E.A.S. but with 8 per cent of the calculated value above the median replaced by a logarithmic decay of 150 knots E.A.S. per decade.

# TEMPERATURE AND AIRSPEED IN FLIGHT



B - 5,000 FT. TO 30,000 FT. - 1113 FLYING HOURS.

Fig. 8.6. (continued)



C - ABOVE 30,000 FT. - 2,130 FLYING HOURS.

Fig. 8.6. (continued)

# MANUAL ON AIRCRAFT LOADS

values were the ones actually used to obtain distribution *B*. It has been noticed that apart from the high speed runs the fighters were flown at what appears to be a cruising condition which has a Normal distribution with a standard of about 30 knots. The bombers seem to avoid high speed runs and have a cruising condition with a standard deviation of 25 knots.

The data on times at different speeds are extensive and it can be used with confidence down to proportions of 0.1 per cent of the time. There are limitations at equivalent airspeeds greater than 0.8 times the design diving

*Table 8.3. Time in Minutes Spent at Different Airspeeds at Heights above 30,000 ft by a B-47E (Deduced from Durkee, 1961) and by a B-52 (Deduced from Wallace, 1961, and from the Non-heavy Condition of Kelly, L. G. and Broom, 1962)*

Airspeed	B-47E	B-52
Equivalent airspeed knots		
100-149	5	2
150-199	103	846
200-249	3372	42,349
250-299	1800	18,845
300-349	9	362
350-399	3	1
<i>Total</i>	5292	62,405
Mach No.		
0.4-0.599	93	244
0.6-0.799	3631	39,841
0.8-0.999	1560	20,913
1.0-1.199	8	1407
<i>Total</i>	5292	62,405

speed that were discussed in detail in Figs. 8.2 and 8.3 for the F-84G and the F-100. Similar limitations will presumably apply to Mach Numbers approaching the design diving speed, but insufficient data are available to make estimates. In the absence of such data it should not introduce much error to use the distributions established for equivalent airspeeds. This distribution is roughly 30 knots per decade passing through limit speed at about  $10^{-4}$  hr (the actual value for particular aircraft should be deduced from Chapter 5 with an empirical duration of 0.05 hr per excursion if service data is unavailable).

In the data used in the present analysis it is highly probable that little restraint was exercised by the pilots to maintain low structural temperatures. Thus when the data are used for aluminium aircraft at speeds above a

Mach No. 2, some allowance may have to be made on the same lines that the allowance is made for the restraint exercised at speeds approaching the design diving speed. This means that, whilst the above data may be used for average atmospheric temperatures, corrections will be needed for high atmospheric temperatures.

The structural effects will be influenced seriously by the way in which the total time at each speed is achieved. The loads due to differential heating will depend on the rate at which the speeds are changed. Usually the maximum loads will be achieved after the aircraft has reached its final velocity, but for any rate of change of speed the maximum load will have exceeded 90 per cent of its final value within a few minutes at heights below 100,000 ft (many references, including J. Taylor, 1958). It may be assumed, therefore, without much conservatism in design that the maximum calculated loads due to a change in speed will always occur. For the very high speeds the number of occurrences is known but the forward accelerations to achieve that speed, or the retardation from it are not known. At lower speeds the number of occurrences can only be guessed. The saturation temperature at any speed exceeding the cruising speed by even a few knots will rarely if ever be achieved. Thus it will be very conservative to assume that the saturation temperature is achieved for the total time at that speed. It will be conservative even for the outer surface, but in this case it will probably not involve a serious penalty.

#### 8.4 TEMPERATURE PERTURBATIONS FROM THE AVERAGE AMBIENT CONDITIONS

The ambient atmospheric conditions on a geographical scale are known very well as are the variations that occur daily and by seasons. These values are given in Chapter 2. As far as the airframe is concerned perturbations in the nature of temperature "gusts" are also of interest. The scale of the perturbations is that that may influence the temperature of the structure and is, of course, related to the heating time-constant of the structural surface in contact with the atmosphere through the aerodynamic boundary layer. No attempt has yet been made to measure these perturbations but an indirect assessment of the problem can be made from a study of free-flight models that have been used to measure kinetic heating rates.

Picken (1960), Picken and D. Walker (1961) and Rumsey, Piland and Hopko (1960) measure heat transfer in free-flight models and use the temperature rise of the surface of the model as a measure of the heat transfer; Picken isolates the part of the model where the thermometers are installed by deliberately inserting insulation material and Rumsey satisfies himself that he can neglect heat flow along the skin. In both cases both from the size of the models and also from the areas chosen for the measurements, the heating time-constant will be appreciably less than full scale and so any temperature perturbations will be less attenuated. However, neither author states that he has noticed such fluctuations, but there are several reasons for not accepting this with complacency. There were only 2 flights by Rumsey and 6 by Picken, so that there is no certainty that typical perturbations would be present: in fact if there is any relationship between "gusts" of

temperature and gusts of velocity there may not have been any temperature perturbations present at all. Also Rumsey did have scatter in his heat transfer for one model but is not too much concerned about it as he (1960, p. 9) says "[the heat transfer coefficients] are in fair agreement with Van Driest's (1952) theory for turbulent flow on a cone, except for the scatter in the data between 7.5 seconds and 9.5 seconds . . ."; Picken (1960, p. 6) states, ". . . The thermocouple signals were read every cycle of the commutator switch, that is about every  $\frac{1}{16}$ th second for each station and were smoothed and differentiated by means of cubic least square polynomials . . ." and in no example gives any experimental readings which were, of course, rather too numerous.

## REFERENCES

- |                                 |                                 |
|---------------------------------|---------------------------------|
| Clay and Berens (1963)          | Rumsey, Piland and Hopko (1960) |
| Durkee (1961)                   | Taylor, J. (1958)               |
| Gray (1955)                     | Titus (1959)                    |
| Kelly, L. G., and Broom (1962)  | Titus (1960)                    |
| Mayer, J. P., and Harris (1955) | Titus (1961)                    |
| Mullins (1961)                  | Vahldiek (1961)                 |
| Mullins (1962)                  | Vahldiek (1961a)                |
| Owen, E. M., and Sellars (1958) | Van Driest (1952)               |
| Phillips, L. (1961)             | Wallace (1961)                  |
| Picken (1960)                   | Ward (1963a)                    |
| Picken and Walker (1961)        |                                 |

CHAPTER 9  
THEORETICAL ANALYSIS OF  
TURBULENCE

CONTENTS

9.1 Introduction	191
9.2 Physical representation of turbulence	191
9.3 Analytical representation of turbulence	194
9.3.1 Correlation of energy distributions in time and space	195
9.3.2 Transformation from three-dimensional energy to the one-dimensional energy components	195
9.3.3 Algebraic functions for calculation purposes	196
9.3.4 Scale of turbulence	198
9.3.5 Distribution of velocities of turbulence	198
9.3.6 Two-dimensional lateral turbulence energy	199
9.4 Specific analytical distributions of turbulence energy	200
9.4.1 Dryden's model ( $n = \frac{1}{2}$ )	201
9.4.2 von Kármán's model ( $n = \frac{1}{3}$ )	201
References	202

## CHAPTER 9

# THEORETICAL ANALYSIS OF TURBULENCE

### 9.1 INTRODUCTION

A stream of air that is not subject to external forces will move with uniform velocity in a straight line, the whole stream has the same velocity and the flow is laminar. When the stream is subject to external forces there will be a transfer of energy to or from the stream. The air in the stream will cease to move in straight lines, there will be a commotion of many of the particles of air and, in this turbulent air, eddies will build up and die down. For relatively small transfers of energy the stream may continue at approximately the same mean velocity but with a turbulence of the air relative to the stream velocity. The size and velocity of the eddies in the turbulence will depend on the source of the external forces. The energy of the turbulence will be proportional to the mean square of the velocity of the eddies and the scale of the turbulence will depend on their size. The dimensions of the source of the external forces in contact with the stream will roughly determine the dimensions of the largest eddies that are produced.

The character of turbulence has many common features over a wide range of scale that can be described in terms of the scale. Atmospheric turbulence is the largest scale of turbulence experienced by aircraft. The scale is roughly proportional to the height up to 1000 ft and increases more slowly at greater heights. The character of this turbulence is the atmosphere itself and is independent of the aircraft. A second type of turbulence is initiated mainly by the shape of the aircraft and is called buffeting. This can occur in cavities, on control surfaces and on complete wings. The scale of the turbulence is of the same order as the dimensions of the part causing it. In a cavity the depth would probably be the most important dimension and in control surfaces or wings the chord. A third type is set up in the region of the jets from the engines and tends to be rather smaller than buffeting. The scale is of the same order as the thickness of the mixing region round the jets and is such that the turbulence always produces audible noise and is usually referred to as noise.

In considering turbulence due to the flow of air over the wings and fuselage there is a tendency to use the description buffeting only when it occurs in abnormal circumstances. The turbulence that is always present in the boundary layer and produces audible noise is usually referred to as noise even though it might be more properly described as buffeting.

### 9.2 PHYSICAL REPRESENTATION OF TURBULENCE

The two salient parameters of any form of turbulence are the scale and the intensity. Definitions of scale and intensity are required so that practical

turbulence can be given numerical values. The total intensity may be defined as the kinetic energy of the turbulence per unit mass of air. This of itself is too broad a description as the kinetic energy will have components at different wavelengths. This distribution at different wavelengths will be a characteristic of the turbulence. In an idealized model of turbulence this distribution will be given in two parts: (i) the value at one wavelength, and (ii) the relative values at all other wavelengths. The choice of wavelength to fix the distribution will be made with a view to identifying it as proportional to the scale of the turbulence. If this is done well the relative values at other wavelengths should be independent of scale for any particular type of turbulence. Thus practical examples of turbulence can be compared and if a good idealized model for all turbulences could be found, the practical measurements could be given in terms of it together with small perturbations.

The objective is to define the turbulence in such a way that loads on the aircraft can be determined. In all circumstances the loads on the aircraft will result from the effect of a combination of turbulence and the main air flow. This allows some latitude in the definition of turbulence and of the dividing line between what is regarded as turbulence and what is the main flow. Any turbulence is produced by some action on the main flow and during the process of its build up there is a rapidly varying interaction between the two flows; any valid solution would have to be of the whole system and is virtually intractable. Once the turbulence has been set up it is possible to neglect the interaction from the main flow but even then only the simplest of models are tractable. The properties of the turbulence are identified over volumes sufficiently small that they are reasonably uniform. In effect the properties are given as those at a point and variations from one point to another associated empirically with the main flow. This separation of turbulence from the stream flow should be possible provided the adjacent patches of turbulence do not influence each other appreciably. It should be so provided the distances required to produce an appreciable change in turbulence intensity or stream velocity are large compared with the scale of turbulence. With these simplifications the turbulence is then regarded as homogeneous and isotropic. Turbulence is considered to be homogeneous when its intensity is the same at all positions and isotropic when there are no preferential directions of motion. Thus all turbulence can be given as its intensity and scale at every point and a stream velocity at that point.

A typical distribution of the turbulence energy at different wavelengths is shown diagrammatically in Fig. 9.1. The turbulence energy may be in any direction and will vary at random along the length of the stream. The abscissa is  $\log$  (inverse wavelength) and the ordinate is  $\log$  (inverse wavelength times energy density with respect to inverse wavelength). The abscissa is in cycles per foot and so the maximum value of the ordinate has to be shown at a definite value of cycles per foot but this has not any particular significance. The distribution is made up of three distinct parts

- (i) at low inverse wavelengths the main characteristic is that it is the range in which most of the input of energy into the turbulence occurs,



# THEORETICAL ANALYSIS OF TURBULENCE

- (ii) at intermediate inverse wavelengths there is little input or loss of energy but there is a transfer of energy towards higher inverse wavelengths through break-down of the larger eddies into smaller ones,
- (iii) at high inverse wavelengths there is a conversion of turbulence energy into heat due to viscous motion.

These three ranges are called the energy input, the inertial subrange and the viscous subrange respectively. Zbrozek (1960) has estimated that the inertial subrange merges into the viscous subrange at a wavelength of the order of one centimetre.

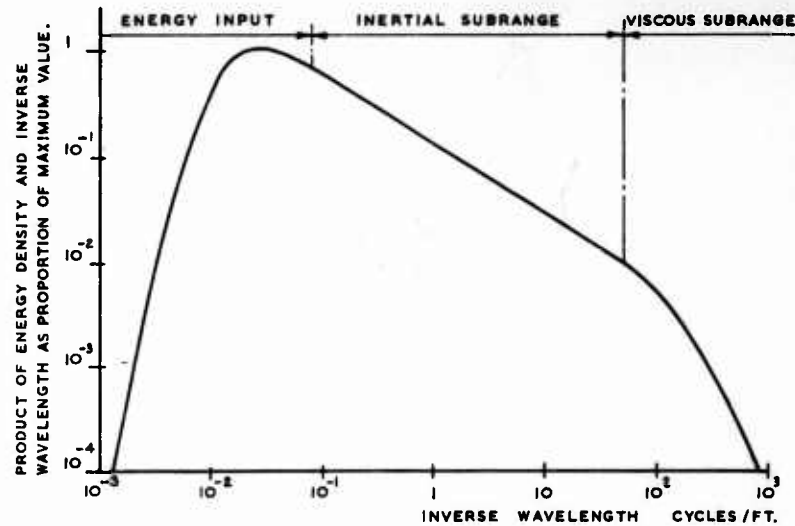


Fig. 9.1. A diagram of a typical distribution of turbulence energy at different wavelengths.

The proportion of turbulence energy in atmospheric turbulence, buffeting or even jet noise at wavelengths below 1 cm is so small that the viscous subrange can be neglected. Thus any turbulence on aircraft can be treated as consisting of a region of input energy and an inertial subrange. For most analytical purposes it may be assumed that the input energy starts at zero inverse wavelength and the inertial subrange continues to an infinite inverse wavelength, i.e. zero wavelength. Kolmogoroff (1941) has shown that for the inertial subrange the energy density is proportional to the inverse wavelength to the power  $-\frac{5}{3}$ . This can be demonstrated on dimensional equivalence. The density with respect to inverse wavelength of the energy per unit mass has the dimensions of  $[\text{Length}]^3 [\text{Time}]^{-2}$ . The cascade process, of breaking down larger eddies into smaller ones, is a function of inverse wavelength, which has dimensions  $[\text{Length}]^{-1}$ , and the rate at which

the energy per unit mass is transferred from one wavelength to another, which has dimensions  $[\text{Length}]^2 [\text{Time}]^{-2}$ . The energy density will have the same dimensions as the cascade process if  $[\text{Length}]^3 [\text{Time}]^{-2} = [\text{Length}]^{-a} \times [\text{Length}]^{2b} [\text{Time}]^{-2b}$  and this occurs when  $a = -\frac{5}{3}$ ,  $b = \frac{2}{3}$ . Thus the energy density is proportional to the inverse wavelength to the power  $-\frac{5}{3}$ .

In Fig. 9.1 the energy density is made to obey this relationship at high inverse wavelengths, i.e. energy density times inverse wavelength is proportional to inverse wavelength to the power  $-\frac{5}{3}$ . For the purpose of the illustration the energy density is assumed to vary as inverse wavelength to the power 4 at low inverse wavelengths. Lin (1947) gives a theoretical reason for this, under the restrictive conditions of Loitsiansky (1939), but only for very low inverse wavelengths. The power of 4 must therefore be regarded as merely an empirical value. There are a number of examples of measured atmospheric turbulence (Chapters 2 and 10), buffeting (Chapter 11) and noise (Chapter 12) in which the energy density varies approximately as the inverse wavelength to the power 4. Departures from this empirical rule tend to be towards a power less than 4. This is in agreement with the suggestion by Heisenberg (1948), Batchelor (1948) and Lin (1948) that even if a fourth power law exists it should rapidly be replaced by a power of unity as the inverse wavelength increases.

Turbulence is a three-dimensional phenomenon but any practical means of measuring it examines a component of the turbulence in one direction. Radar can be used to measure in the direction of the radar beam the velocity of particles, relative to their mean velocity, in a known volume. By assuming that particles of water in a cloud move with the same velocity as the air, the component of the turbulence energy per unit mass in the direction of the beam can be determined. Temperature measurements on a hot wire in a stream of turbulence will be a direct measure of the component of the turbulence energy at right angles to the length of the wire in the plane containing the wire and the direction of the stream. The wire may be orientated in any direction but it will usually be at right angles to the stream. In addition to these types of measurement that are directly related to the turbulence energy there is also the possibility of measuring the velocity of the air at a point, which has a velocity relative to the stream. In this case analytical methods must be used to transpose this velocity into turbulence energy.

### 9.3 ANALYTICAL REPRESENTATION OF TURBULENCE

The analytical representation of the turbulence energy must allow the function for three-dimensional turbulence to be transposed into three one-dimensional components. The one-dimensional components will be the ones most directly used for the determination of aircraft loads. As far as possible these functions should be readily transferable from one stream velocity to another. Also they should be in a form that allows fairly simple calculation procedures to be used to estimate the distribution of energy at different wavelengths from direct measurements of the turbulence velocity.

9.3.1. *Correlation of Energy Distributions in Time and Space*

G. I. Taylor (1938) deduced that for homogeneous isotropic turbulence the distribution of energy at different wavelengths would be the same for measurements at a point over a period of time and for instantaneous measurements in a line through the point and in the direction of the stream passing the point provided the transformation

$$x = Ut \quad (9.1)$$

was made and that

$$\sigma_u^2/U^2 \ll 1 \quad (9.2)$$

where  $x$  = the coordinate along the direction of the stream

$U$  = the stream velocity

$\sigma_u$  = the root mean square of the turbulence velocity in the direction of the stream

$t$  = time.

In aircraft applications equation (9.2) will almost invariably hold and there is no restriction on the use of equation (9.1) other than the basic one that the turbulence may be assumed to be homogeneous and isotropic. Thus all turbulence can be quoted in terms of length rather than time. This simplifies the presentation considerably and is used throughout the Manual.

9.3.2. *Transformation from Three-dimensional Energy to the One-dimensional Energy Components*

The total turbulence energy per unit mass is  $\frac{1}{2}\sigma^2$ , where  $\sigma^2$  is the mean square of the turbulence velocity. As all measurements will be given in terms of turbulence velocity, rather than turbulence energy,  $\sigma^2$  will usually be quoted in preference to  $\frac{1}{2}\sigma^2$ . A function is required for the distribution of the energy over different inverse wavelengths. The function  $S(k)$  is chosen so that twice the energy per unit mass in the range of inverse wavelengths  $k$  to  $k + \delta k$  is

$$S(k) \delta k \quad (9.3)$$

With this definition  $S(k)$  will be twice the density with respect to inverse wavelength of the energy per unit mass. The component of twice the energy per unit mass between  $\kappa_1$  and  $\kappa_2$  will be given by

$$[\sigma^2]_{\kappa_1}^{\kappa_2} = \int_{\kappa_1}^{\kappa_2} S(k) dk \quad (9.4)$$

and the total will be

$$\sigma^2 = \int_0^{\infty} S(k) dk \quad (9.5)$$

( $Oxyz$ ) are taken as coordinate axes with  $Ox$  in the direction of the stream.\* The three-dimensional turbulence is given by equation (9.4) in terms of inverse wavelengths along the direction  $Ox$ .  $Ox$  could be chosen in any direction in homogeneous isotropic turbulence without changing the values. The turbulence could also be defined in terms of the three components  $S_u(k)$ ,  $S_v(k)$ ,  $S_w(k)$  along the three axes ( $Oxyz$ ). Because of symmetry all components at right angles to the stream direction  $Ox$  must be the same and in particular  $S_v(k) = S_w(k)$ . For those cases where the stream direction  $Ox$  is horizontal it is customary to make the axis  $Oz$  the vertical one thus making  $S_w(k)$  the vertical component. The third component  $S_u(k)$  is in the direction of the stream and will have a different form from the other two which are at right angles to the stream. This difference between the components does not imply any preferential direction to the turbulence itself as  $Ox$  could have been given any direction.

The relationship between  $S(k)$  and  $S_u(k)$  was examined by Heisenberg (1948a) and shown for homogeneous isotropic turbulence to be

$$S_u(\kappa_1) = \frac{1}{2} \int_{\kappa_1}^{\infty} \{S(k) (k^2 - \kappa_1^2)/k^3\} dk \quad (9.6)$$

The relationship between  $S_u(k)$  and  $S_w(k)$  is governed by the condition of continuity for incompressible fluids and it is deduced in paragraph 9.3.3 to be

$$S_w(k) = \frac{1}{2} S_u(k) - \frac{1}{2} k \frac{d}{dk} S_u(k) \quad (9.7)$$

### 9.3.3. Algebraic Functions for Calculation Purposes

The distribution of turbulence energy is defined completely by equations (9.6) and (9.7). However, estimates of the energy from direct measurements of the velocity require extensive manipulation of the basic data. These calculations are made easier by first estimating functions that are transforms of  $S_u(k)$  and  $S_w(k)$  and then transforming these functions to  $S_u(k)$  and  $S_w(k)$ . These transformations are essential also for the mathematical analysis that produces equation (9.7).

The total energy in the directions  $Ox$  and  $Oz$  are the summations over all inverse wavelengths. Thus

$$\sigma_u^2 = \int_0^{\infty} S_u(k) dk \quad (9.8)$$

$$\sigma_w^2 = \int_0^{\infty} S_w(k) dk \quad (9.9)$$

\* The term stream is used because of the validity of equation (9.1)  $x = Ut$  although for the case of instantaneous measurements along a straight line it would strictly be a direction of measurement and not a stream.

# THEORETICAL ANALYSIS OF TURBULENCE

where  $\sigma_u^2$  = the mean square of the turbulence velocity in the direction  $Ox$

$\sigma_w^2$  = the mean square of the turbulence velocity\* in the direction  $Oz$

Two new functions  $f_u(r)$ ,  $f_w(r)$  are introduced and are defined as the Fourier transforms of  $S_u(k)$ ,  $S_w(k)$  as follows:

$$\sigma_u^2 f_u(r) = (\frac{1}{2}\pi) \int_0^\infty S_u(k) \cos(2\pi kr) dk \quad (9.10)$$

$$\sigma_w^2 f_w(r) = (\frac{1}{2}\pi) \int_0^\infty S_w(k) \cos(2\pi kr) dk \quad (9.11)$$

The properties of Fourier transforms are such that

$$S_u(k) = 4\sigma_u^2 \int_0^\infty f_u(r) \cos(2\pi kr) dr \quad (9.12)$$

$$S_w(k) = 4\sigma_w^2 \int_0^\infty f_w(r) \cos(2\pi kr) dr \quad (9.13)$$

These functions  $f_u(r)$  and  $f_w(r)$  are usually called the longitudinal and lateral autocorrelation functions. The mathematical analysis of turbulence by von Kármán and Howarth (1938) was made on autocorrelation functions which were defined as

$$f_u(r) = \overline{u(x) \cdot u(x+r) / u^2(x)} \quad (9.14)$$

$$f_w(r) = \overline{w(x) \cdot w(x+r) / w^2(x)} \quad (9.15)$$

where  $u(x)$ ,  $w(x)$  are the components of the turbulence velocity in directions  $x$ ,  $z$  at a point  $x$  along the  $Ox$  axis and

$$\overline{u(x) \cdot u(x+r)} = \lim_{T \rightarrow \infty} \frac{1}{T} \int_0^T u(x) \cdot u(x+r) dx$$

Thus  $\overline{u^2(x)}$  and  $\overline{w^2(x)}$  are the mean squares of the turbulence velocity in directions  $Ox$  and  $Oz$  and are identical to  $\sigma_u^2$  and  $\sigma_w^2$ . G. I. Taylor (1938) introduced the transforms of  $f_u(r)$  and  $f_w(r)$  as defined in equations (9.14) and (9.15) and established equations (9.12) and (9.13) for the energy density per unit mass of air. It is usually more accurate with measured data starting with the distributions of  $u(x)$  and  $w(x)$ , to calculate first  $f_u(r)$  and

\* In isotropic turbulence  $\sigma_u^2 = \sigma_w^2$  but separate symbols are used as the formulae that ensue are not subject to much error if there is a small difference between them.

$f_w(r)$  by equations (9.14) and (9.15) and then determine  $S_u(k)$  and  $S_w(k)$  by equations (9.12) and (9.13) rather than calculate  $S_u(k)$  and  $S_w(k)$  direct from  $u(x)$  and  $w(x)$ .

Von Kármán and Howarth (1938) showed that the continuity equation for incompressible flow gave

$$f_w(r) = f_u(r) + (r/2) \frac{d}{dr} f_u(r) \quad (9.16)$$

By combining equations (9.12), (9.13) and (9.16) the following relationship between  $S_u(k)$  and  $S_w(k)$  can be obtained

$$S_w(k) = \frac{1}{2} S_u(k) - \frac{1}{2} k \frac{d}{dk} S_u(k) \quad (9.17)$$

This formula was quoted in equation (9.7).

#### 9.3.4. Scale of Turbulence

When analytical functions are used to describe the energy density they will include a parameter that has the dimension of length and will be proportional to the scale of turbulence. The actual value given to the scale could be chosen to be the value of  $1/k$  where  $kS(k)$  is a maximum or it could be chosen to be the value of  $1/k$  where there is an equal amount of energy above and below, or it could be chosen purely for analytical convenience. In fact the last alternative is usually made. The scale of turbulence  $L$  is defined as

$$L = \int_0^{\infty} f_u(r) dr \quad (9.18)$$

By virtue of the relationship of equation (9.16) this is identical to

$$L = 2 \int_0^{\infty} f_w(r) dr \quad (9.19)$$

This definition of scale of turbulence is used throughout this Manual.

#### 9.3.5. Distribution of Velocities of Turbulence

The property of turbulence that has been defined is the energy density at all wavelengths along the length of the stream. At every point on the stream there will be a combination of all the densities. It is assumed that the energy densities at different wavelengths will be combined in a random fashion but this of itself does not define the frequency with which different velocities will occur. There are only two possibilities, either the distribution must be assumed or it must be measured. Measurements are not very satisfactory as the extreme values occur very rarely and it would be necessary to have turbulence that maintained its properties for a long time. A Normal distribution is usually taken for the distribution of velocities, in any of the component directions, along the length of the stream. The root mean square of the distribution is the standard deviation and this is made equal

to the root mean square of the velocity as deduced from the energy measurements. Rice (1944) has shown that the number of times that different velocities are crossed is also a Normal distribution and is given by

$$\left. \begin{aligned} N_w &= N_0 \exp(-w^2/2\sigma_w^2) \\ N_0 &= (1/\sigma_w) \left[ \int_0^\infty k^2 S_w(k) dk \right]^{1/2} \end{aligned} \right\} \quad (9.20)$$

where  $N_w$  = number of crossings in one direction of velocity  $w$  per unit distance

$N_0$  = number of zero crossings in one direction per unit distance.

### 9.3.6. Two-dimensional Lateral Turbulence Energy

In general the main air stream will have a velocity parallel to the surface of the aircraft and the turbulence loads will be produced by the energy from the lateral component of the turbulence velocity. When the scale of the turbulence is large compared with the aircraft surface that is being loaded the turbulence velocity may be assumed to be the same at any instant over the whole surface. The one-dimensional energy density for lateral turbulence  $S_w(k)$  is then applicable. The mean square of the lateral turbulence velocity  $\sigma_w^2$  is given by equation (9.9). The scale of the turbulence  $L$  is given by equation (9.19) where  $f_w(r)$  is defined in terms of  $S_w(k)$  by equation (9.11). The number of times per unit distance that a velocity  $w$  is exceeded is given by equation (9.20).

When the scale of turbulence is not large compared with the dimensions of the aircraft surface equations (9.9), (9.11), (9.19), (9.20) need replacing by appropriate formulae for two-dimensional lateral turbulence. In the one-dimensional case the distance  $r$  is in the direction  $x$  only. In the two-dimensional case it will be assumed to have components  $(r_1, r_2)$  in the directions  $(xy)$ . Likewise  $k$  will be replaced by its components  $(k_1, k_2)$ . If there is the same scale of turbulence in all directions equation (9.19) shows that the autocorrelation functions remain the same for any direction. Thus  $f_w(r)$  will remain the same for two-dimensional turbulence and it is required to find  $S_w(k_1, k_2)$ . This two-dimensional energy density function will be given by an equation similar\* to that of equation (9.13) as

$$S_w(k_1, k_2) = \sigma_w^2 \int_{-\infty}^{\infty} \int_{-\infty}^{\infty} \cos(2\pi k_1 r_1 + 2\pi k_2 r_2) f_w \sqrt{r_1^2 + r_2^2} dr_1 dr_2 \quad (9.21)$$

By making the transformation

$$\begin{aligned} r_1 &= r \cos(\theta - \varepsilon) \\ r_2 &= r \sin(\theta - \varepsilon) \\ k_1^2 + k_2^2 &= k^2 \\ \tan \varepsilon &= k_2/k_1 \end{aligned}$$

\* In the two-dimensional case the integration is over the whole plane and the coefficient outside the integrals becomes  $\sigma_w^2$  instead of  $4\sigma_w^2$ .

this reduces to

$$S_w(k_1, k_2) = \sigma_w^2 \int_0^\infty \int_0^{2\pi} \cos(2\pi k r \sin \theta) f_w(r) r d\theta dr \quad (9.22)$$

Watson (1944) shows that  $\int_0^{2\pi} \cos(z \sin \theta) d\theta = 2\pi J_0(z)$ , where  $J_0$  is a Bessel function. Thus equation (9.22) becomes

$$S_w(k_1, k_2) = 2\pi \sigma_w^2 \int_0^\infty J_0(2\pi k r) r f_w(r) dr \quad (9.23)$$

The function  $S_w(k)$  is now a Hankel transform of  $f_w(r)$  and as in the Fourier transform for the one-dimensional case there is a corresponding inverse relationship

$$\sigma_w^2 f_w(r) = \int_0^\infty J_0(2\pi k r) k S_w(k) dk \quad (9.24)$$

#### 9.4 SPECIFIC ANALYTICAL DISTRIBUTIONS OF TURBULENCE ENERGY

The equations that have been given in paragraph 9.3 are general ones for any form of turbulence. Functions are needed to express measured turbulence. As the functions express the data from which the loads on the aircraft are determined it is an advantage if they can be given either in closed form or in terms of tabulated functions. Even in these circumstances the calculations would be extensive and it is doubtful if calculations of load from an energy density distribution in tabular form could be undertaken in any but the simplest structures, e.g. a single panel.

To some extent the functions have to be chosen by trial, making a compromise between the feasibility of the functions themselves and the feasibility of doing the integrations of the various equations that ensue. I am indebted to Mr. N. I. Bullen who has informed me of the following family for longitudinal autocorrelation functions that are simple to manipulate.

$$f_u(r) = [(r/a)^n / 2^{n-1} (n-1)!] K_n(r/a) \quad (9.25)$$

where  $a$  and  $n$  are parameters governing the shape and scale of the expression

$K_n$  are Bessel functions with imaginary argument

$(n-1)!$  are gamma functions when  $n$  is not a positive integer.

Substituting equation (9.25) in equations (9.18) and (9.16) gives the scale of turbulence as

$$L = [\sqrt{\pi} (n - \frac{1}{2})! / (n-1)!] a \quad (9.26)$$

and the lateral autocorrelation function as

$$f_w(r) = [(r/a)^n / 2^n (n-1)!] [2K_n(r/a) - (r/a) K_{n-1}(r/a)] \quad (9.27)$$



The energy density functions for longitudinal turbulence velocities and lateral turbulence velocities in one and two dimensions are obtained from equations (9.12), (9.13) and (9.23). The solutions reduce to

$$S_u(k) = 4\sigma_u^2 L / (1 + 4\pi^2 a^2 k^2)^{n+1} \quad (9.28)$$

$$S_w(k) = 2\sigma_w^2 L [1 + 8\pi^2 a^2 k^2 (n+1)] / (1 + 4\pi^2 a^2 k^2)^{n+3/2} \quad (9.29)$$

$$S_w(k_1, k_2) = 32\sigma_w^2 n(n+1)\pi^2 a^4 (k_1^2 + k_2^2) / [1 + 4\pi^2 a^2 (k_1^2 + k_2^2)]^{n+2} \quad (9.30)$$

where  $a = [(n-1)! / \sqrt{\pi}(n-\frac{1}{2})!] L$

The three-dimensional energy function  $S(k)$  that satisfies equations (9.5) and (9.6)

$$\left. \begin{aligned} S(k) &= 4(2n+3)(2n+1)\sigma_u^2 L (2\pi a k)^4 / (1 + 4\pi^2 a^2 k^2)^{n+5/2} \\ \sigma^2 &= 3\sigma_u^2 \end{aligned} \right\} \quad (9.31)$$

#### 9.4.1. Dryden's Model ( $n = \frac{1}{2}$ )

Equations (9.28) to (9.30) give the energy density distributions in terms of the scale of turbulence  $L$  and a shape parameter  $n$ . By assigning values to  $n$  a range of shapes can be obtained. If  $n$  is made equal to  $\frac{1}{2}$  the distribution for lateral turbulence becomes identical to the empirical formula proposed by Dryden (1938). Putting  $n = \frac{1}{2}$  in equation (9.26) gives  $L = a$  and equations (9.28) to (9.31) become

$$S_u^2(k) = 4\sigma_u^2 L / [1 + (2\pi k L)^2] \quad (9.32)$$

$$S_w(k) = 2\sigma_w^2 L [1 + 3(2\pi k L)^2] / [1 + (2\pi k L)^2]^3 \quad (9.33)$$

$$S_w(k_1, k_2) = 24\sigma_w^2 L^4 \pi^2 (k_1^2 + k_2^2) / [1 + 4\pi^2 L^2 (k_1^2 + k_2^2)]^{5/2} \quad (9.34)$$

$$\left. \begin{aligned} S(k) &= 32\sigma_u^2 L (2\pi k L)^4 / [1 + (2\pi k L)^2]^3 \\ \sigma^2 &= 3\sigma_u^2 \end{aligned} \right\} \quad (9.35)$$

The associated autocorrelation functions are

$$f_u(r) = \exp(-r/L) \quad (9.36)$$

$$f_w(r) = (1 - \frac{1}{2}r/L) \exp(-r/L) \quad (9.37)$$

#### 9.4.2. von Kármán's Model ( $n = \frac{1}{3}$ )

By putting  $n = \frac{1}{3}$  the distribution for three-dimensional turbulence becomes identical to the empirical formula proposed by von Kármán (1948). Putting  $n = \frac{1}{3}$  in equation (9.26) gives

$$\begin{aligned} a &= [(-\frac{2}{3})! / \sqrt{\pi}(-\frac{1}{3})!] L \\ &= 1.339 L \end{aligned} \quad (9.38)$$

and equations (9.28) to (9.31) become

$$S_u(k) = 4\sigma_u^2 L / [1 + \{2\pi(1.339L)k\}^2]^{5/6} \quad (9.39)$$

$$S_w(k) = 2\sigma_w^2 L [1 + (8/3)\{2\pi(1.339L)k\}^2] / [1 + \{2\pi(1.339L)k\}^2]^{11/6} \quad (9.40)$$

$$S_w(k_1, k_2) = (128/9) \sigma_w^2 \pi^2 (1.339L)^4 (k_1^2 + k_2^2) / [1 + 4\pi^2 (1.339L)^2 (k_1^2 + k_2^2)]^{7/3} \quad (9.41)$$

$$S(k) = (220/9) \sigma_u^2 L \{2\pi(1.339L)k\}^4 / [1 + \{2\pi(1.339L)k\}^2]^{17/6} \quad (9.42)$$

$$\sigma^2 = 3\sigma_u^2$$

The associated autocorrelation functions are

$$f_u(r) = 2^{\frac{1}{2}} (r/a)^{\frac{1}{2}} K_{\frac{1}{2}}(r/a) / (-\frac{3}{2})! \quad (9.43)$$

$$f_w(r) = 2^{\frac{1}{2}} (r/a)^{\frac{1}{2}} [K_{\frac{1}{2}}(r/a) - \frac{1}{2}(r/a)K_{-\frac{1}{2}}(r/a)] / (-\frac{3}{2})! \quad (9.44)$$

The turbulence models for any value of  $n$  will have  $S(k)$  proportional to  $k^4$  for low values of  $k$  and are all subject to the same limitations. At high values of  $k$ ,  $S(k)$  will be proportional to  $k^{-(2n+1)}$ . Theoretical reasons were given in paragraph 9.2 to justify a relationship of  $S(k)$  proportional to  $k^{-1}$  at high values of  $k$ . This corresponds to  $n = \frac{1}{2}$ , the von Kármán model, and this distribution should have the widest application.

#### REFERENCES

- |                               |                      |
|-------------------------------|----------------------|
| Batchelor (1948)              | Lin (1947)           |
| Dryden (1938)                 | Lin (1948)           |
| Heisenberg (1948)             | Loitsiansky (1939)   |
| Heisenberg (1948a)            | Rice (1944)          |
| von Kármán and Howarth (1938) | Taylor, G. I. (1938) |
| von Kármán (1948)             | Watson (1944)        |
| Kolmogoroff (1941)            | Zbrozek (1960)       |

**CHAPTER 10**  
**AIRCRAFT LOADS IN ATMOSPHERIC**  
**TURBULENCE**

**CONTENTS**

10.1 Introduction	205
10.2 The gust response factor	206
10.2.1 Response factor of the normal acceleration at the centre of gravity of the aircraft	208
10.2.2 Use of accelerometers on aircraft to determine atmospheric turbulence	210
10.3 Comparison of accelerometer measurements and direct measurements of vertical turbulence velocity on aircraft	213
10.4 Specific turbulence conditions	218
10.4.1 Clear air turbulence up to 1000 ft	219
10.4.2 Turbulence in and near cumulus clouds	222
10.4.3 Turbulence in thunderstorms	225
10.5 Atmospheric loads encountered by aircraft on normal opera- tional duties	228
10.5.1 Avoidance of turbulence	233
10.5.2 Seasonal variations	235
References	241

## CHAPTER 10

# AIRCRAFT LOADS IN ATMOSPHERIC TURBULENCE

### 10.1 INTRODUCTION

When an aircraft passes through atmospheric turbulence it receives some of the turbulence energy. The lateral components of the turbulence velocity, i.e. normal to the flight path, produce changes in incidence of the aircraft which in turn produce loads on the aircraft. If the turbulence were known precisely the aircraft loads could be predicted from the turbulence data provided the aerodynamic properties of the aircraft were also known. In practice most of the data on loads due to atmospheric turbulence are from measurements of the normal accelerations experienced by aircraft in turbulence. In this case the data from one type of aircraft can be used for another type if the accelerations can be transformed into turbulence data and then transformed back into accelerations for the second type. Normal acceleration data from different aircraft can be used to build up a turbulence model for the energy component normal to the wing surfaces. This will be predominantly vertical and is therefore usually referred to as vertical turbulence. All comparisons with direct measurements of turbulence are made for the vertical component. When the agreement is good the direct measurements of the other components can be used with confidence.

For the loading conditions that depend only on vertical turbulence, errors in the transfer functions from normal acceleration to gust velocity will immediately produce errors in the turbulence model. However, the errors in the normal accelerations predicted for other aircraft will be those due to the transfer functions of the two aircraft. In the trivial case of using the data to predict normal accelerations for the same aircraft on which the measurements were made the resulting error will be zero, and for aircraft with fairly similar configurations and size it should be small. For the data to have maximum value the transfer functions should be estimated as accurately as possible so that the data can be extrapolated to aircraft types appreciably different from those on which the measurements were made.

The atmospheric turbulence is defined in Chapter 2 in two parts, first there is the total energy per unit mass of air and its distribution at all wavelengths, secondly there is the distribution of the turbulence velocities, in terms of the root-mean-square value, along the length of the flight path. In describing turbulence attention has been mainly given to the energy distribution with the distribution of the turbulence velocity in a secondary role. In describing the turbulence model that is equivalent to the normal accelerations the distribution of the turbulence velocity is the more important. When the distribution along the length of the flight path is Normal, and the rate of change of velocity independent of the velocity, the distribution of the

number of times a velocity is exceeded will also be Normal. In the ideal case of Normal distribution the same result would be obtained by either method; however, for load assessment the crossings are more directly applicable. When the distribution is not Normal the correlation breaks down unless the distribution is a combination of Normal distributions with the same number of zero crossings for each distribution. Whilst for many purposes it is assumed that the distribution is such a combination the error is kept to a minimum by measuring the numbers of crossings rather than deducing them from measurements of the time at different levels.

Even if there were perfect correlation between aircraft normal accelerations and turbulence velocities the model of turbulence would differ appreciably from that of the atmosphere due to the discrimination exercised by the pilot on his own initiative, on information received from instruments and from other people. It is difficult to assess the extent of this discrimination, in terms of the turbulence avoided, either for the measurements that have been made or for particular forms of flying postulated for new designs. At one extreme there is the turbulence at low altitudes, near the landing airfield, that is only avoided on the very rare occasions that the aircraft is diverted. At the other extreme a single cumulo-nimbus cloud that protrudes above a cumulus layer can be avoided in almost all cases by an aircraft flying above the cumulus layer.

## 10.2 THE GUST RESPONSE FACTOR

The movement of the air in the atmosphere has been described in Chapter 2. It was shown that there are two distinct types of vertical movement, a quasi-steady flow and a continuous turbulence.

The quasi-steady flow may be due to flow of air over hills or due to the overall effects of convection. The overall velocities in a thunderstorm can be large and were shown diagrammatically in Fig. 2.3. For such a single profile of vertical velocity along the flight path it is appropriate to call it a single gust of that shape. This gust is then the applied load on all aircraft. The subsequent motion of an aircraft will depend on its aerodynamic form, mass, speed and the consequential action of the pilot. If a particular aircraft is flown repeatedly in the same manner through the same gust its complete motion will be repeated. Thus the motion of the aircraft can be used to predict the shape of the gust. In practice the single gusts never occur in isolation and it is almost impossible to assess the various contributions to the aircraft motion. For example the single gust of a thunderstorm will have continuous turbulence of varying intensity superimposed upon it and the aircraft motion will be mainly due to this continuous turbulence. Little is known about the actual dimensions of the gust but it is probably better to estimate them from direct measurements of typical storms, rather than from the aircraft motion, and then to assume that the remainder of the motion is due to the continuous turbulence.

In continuous turbulence the air velocity at every point is continuously changing and there is a steadily varying effective gust pattern. It was shown theoretically in Chapter 9 that this motion can be described statistically and the statistics of certain examples of the atmosphere were given in Chapter 2.

The motion of the aircraft can also be described statistically. For this motion to be used to describe the atmosphere it is necessary to introduce a Gust Response Factor to transform from one to the other. The aircraft response, either measured or predicted, will be functionally related to the atmospheric turbulence by equation (10.1), through  $|T_r(k)|^2$  with the assumption that the response of the aircraft at any wavelength is produced entirely by the turbulence energy at the same wavelength. Thus

$$S_r(k) = |T_r(k)|^2 \cdot S_w(k) \quad (10.1)$$

where  $S_r(k)$  = aircraft response density with respect to inverse wavelength  $k$

$S_w(k)$  = twice the vertical component of the turbulence energy density per unit mass

$T_r(k)$  = the frequency response function relating the required aircraft response to a steady sinusoidal turbulence at inverse wavelength  $k$

A choice has to be made of a parameter that will be suitable for determining the atmospheric load due to turbulence. It will usually be the normal acceleration at a point on the structure near to the aircraft centre of gravity. The total response will be given in two parts in the same way that the turbulence energy was given in two parts by equations (9.9) and (9.20), i.e. a measure of the magnitude by its r.m.s. value and the number of times the response crosses each level.

The magnitude of the response is given by

$$\sigma_r^2 = \int_0^\infty S_r(k) dk \quad (10.2)$$

where  $\sigma_r$  = the root mean square of the response.

The number of zero crossings in each direction per unit distance  $N_0$  is given by

$$N_0 = (1/\sigma_r) \left[ \int_0^\infty k^2 S_r(k) dk \right]^{1/2} \quad (10.3)$$

For the cases where it may be assumed that the patch of turbulence has a Normal distribution of crossings of velocity, the distribution of the aircraft response will also be Normal and

$$N_r = N_0 \exp(-r^2/2\sigma_r^2) \quad (10.4)$$

where  $N_r$  = number of crossings in each direction of response  $r$  per unit distance.

The equations (10.2), (10.3), (10.4) describe the particular response of the aircraft to the atmospheric turbulence. The factor by which  $\sigma_w$ , the root mean square of the turbulence velocity, has to be multiplied to obtain  $\sigma_r$  is the response factor of the aircraft. This same factor can be used to

obtain the value of  $w$  that has the same number of crossings as the response  $r$ . But there still remains the number of zero crossings, and equation (10.3) shows that this depends on  $k^2 S_r(k)$  as well as  $\sigma_r$ . Thus the number of zero crossings depends on the response that is being measured.

This number varies so much with the type of response that is being measured that there is little practical significance in its relationship to the atmospheric turbulence. The number of zero crossings of the actual atmospheric turbulence velocity is extremely large due to the components at very low wavelengths. For any aircraft response, whether it be normal acceleration or any other structural response, the very low wavelengths will be filtered out so thoroughly that they produce a negligible number of zero crossings. The number of zero crossings ( $N_0$ ) of the aircraft response is the characteristic inverse wavelength of that particular response. In the extreme case of the frequency response factor,  $T_r(k)$  of equation (10.1), being at only one inverse wavelength, the associated  $N_0$  would be that inverse wavelength.

#### 10.2.1. Response Factor of the Normal Acceleration at the Centre of Gravity of the Aircraft

The value to be given to  $N_0$  changes with the particular response that is examined but a simplification can be made by regarding the normal acceleration of the aircraft centre of gravity as the basic response and referring all other responses to it. The loads from atmospheric turbulence are then defined by the normal accelerations occurring at an average of  $N_0$  per unit distance and the magnitude is given as the relative frequency of occurrence of different accelerations. In order to keep the information more general the accelerations should be divided by the response factor so that the magnitudes are given as turbulence velocities.

Equations (10.1) and (10.2) may be re-written for the relationship between C.G. acceleration and turbulence as follows:

$$S_a(k) = |T_a(k)|^2 \cdot S_w(k) \quad (10.5)$$

$$\sigma_a^2 = \int_0^\infty S_a(k) dk \quad (10.6)$$

where the general subscript "r" in  $S_a(k)$ ,  $T_r(k)$ ,  $\sigma_r$ , is replaced by "a" to denote C.G. accelerations. General formulae can be obtained for the response factor by giving the functions  $T_a(k)$ ,  $S_w(k)$  algebraic form. In Chapter 9 algebraic forms are proposed for  $S_w(k)$ . J. Hall (1962) gives the following simple formula for  $T_a(k)$  for the case in which pitching and the effect of finite span on the lift due to atmospheric turbulence are neglected.

$$|T_a(k)|^2 = [(\rho S V_T m g / 2 W)^2 \{ \xi^2 / (a^2 + \xi^2) \}] \times [(B_1 / \alpha_1^2) / (1 + S_1^2 \xi^2) + (B_2 / \alpha_2^2) / (1 + S_2^2 \xi^2)] \quad (10.7)$$

where  $\rho$  = density of the air slugs/ft<sup>3</sup>

$\rho_0$  = density of the air at ground level slugs/ft<sup>3</sup>

# AIRCRAFT LOADS IN ATMOSPHERIC TURBULENCE

$S$  = wing area ft<sup>2</sup>

$V_T$  = aircraft velocity ft/sec

$m$  = lift slope per radian

$g$  = acceleration of gravity ft/sec<sup>2</sup>

$W$  = weight of aircraft lb

$\xi = 2\pi kL$

$L$  = scale of turbulence ft

$a = L/c\mu_0$

$c$  = wing mean chord

$\mu_0$  = aircraft mass parameter  $2W/\rho S c m g$

$A$  = aspect ratio

$M$  = Mach Number

$\alpha_1 = (0.26 + 2/A)/(1 + 0.83M + 0.95M^2)$

$\alpha_2 = (2 + 2/A)/(1 + 0.83M + 0.95M^2)$

$B_1/\alpha_1^2 = (\alpha_1 + 3\alpha_2)/(4\alpha_1 + 4\alpha_2)$

$B_2/\alpha_2^2 = (\alpha_2 + 3\alpha_1)/(4\alpha_1 + 4\alpha_2)$

$S_1 = (c/L)/\alpha_1$

$S_2 = (c/L)/\alpha_2$

The first factor is the acceleration that would occur if the lateral velocity produced lift instantaneously. The second factor is the coefficient for the unsteady lift functions. The scale of turbulence  $L$  is introduced for convenience later when  $T_a(k)$  is substituted in equation (10.5);  $L$  could be cancelled out completely in equation (10.7).

Combining equations (10.5), (10.6) and (10.7) gives

$$\sigma_a = K(\rho S V_T m g / 2 W) \sigma_w \quad (10.8)$$

where  $K$  = the Gust Response Factor and

$$K^2 = \int_0^\infty [\xi^2 / (a^2 + \xi^2)] [(B_1/\alpha_1^2)/(1 + S_1^2 \xi^2) + (B_2/\alpha_2^2)/(1 + S_2^2 \xi^2)] [S_w(k)/2\pi L \sigma_w^2] d\xi \quad (10.9)$$

Equation (10.8) makes it possible to deduce the magnitude of the turbulence from the magnitude of the normal acceleration at the centre of gravity of the aircraft.



For the Dryden model of turbulence quoted in equation (9.33)

$$S_w(k)/2\pi L\sigma_w^2 = (1/\pi) (1 + 3\xi^2)/(1 + \xi^2)^2 \quad (10.10)$$

For the von Kármán model quoted in equation (9.40)

$$S_w(k)/2\pi L\sigma_w^2 = (1/\pi) \{1 + (8/3) (1.339\xi)^2\} / \{1 + (1.339\xi)^2\}^{11/6} \quad (10.11)$$

Values of  $K$  are obtained by substituting equations (10.10) and (10.11) in equation (10.9) and integrating. Numerical integration is used for the von Kármán model but integration in closed form for the Dryden model is as follows:

$$\begin{aligned} K^2 = & (B_1/2\alpha_1^2) \{2 - 1/(1 + a) + 1/(1 + S_1)\} / (1 + a) (1 + S_1) (1 + aS_1) \\ & + (B_2/2\alpha_2^2) \{2 - 1/(1 + a) + 1/(1 + S_2)\} / (1 + a) (1 + S_2) (1 + aS_2) \end{aligned} \quad (10.12)$$

The simplification of neglecting the effect of finite span on the lift due to atmospheric turbulence in determining equation (10.7) makes it possible to give general values for gust response factors for the aircraft C.G. These are shown in Fig. 10.1 for a range of values of  $c\mu_g/L$  and infinite aspect ratio. The variation with aspect ratio is small.

Unfortunately the simplification of neglecting the effect of finite span on the lift due to atmospheric turbulence produces serious changes in the value of  $N_0$ , the number of zero crossings, given by equation (10.3). Thus general values cannot be given for  $N_0$  and specific values have to be calculated for each aircraft and the value of  $|T_a(k)|^2$  given by equation (10.7) has to be multiplied by  $1/(1 + 0.3b\xi/L)$ , where  $b$  = the span of the aircraft.

#### 10.2.2. Use of Accelerometers on Aircraft to Determine Atmospheric Turbulence

In practice the normal acceleration of an aircraft has to be measured at a point on the structure and, due to the flexibility of the structure, this point will move relative to the centre of gravity, and the normal acceleration will be the algebraic sum of that at the centre of gravity and that due to the structural distortion. An approximation to the C.G. acceleration is achieved by placing the accelerometer as near as possible to the C.G. and filtering the structural distortion in some way. All modes other than the fundamental one can be filtered by a cut-off in the response of the accelerometer. The fundamental mode will increase the number of crossings of all levels of acceleration and also the r.m.s. value. The number of crossings can be greatly reduced if they are made for a threshold of finite width, of acceleration, at each level. J. Taylor (1953) showed, for aircraft of the general type used for the measurements described in this chapter, that provided the width exceeded 0.1g the number of counts would remain the same for all widths up to counts being made only when the datum 1g was crossed. Thus the number of zero crossings estimated from an extrapolation from all other levels will be independent of the width of the threshold and it may be concluded that it is a good approximation to the number of zero crossings of the C.G. However the r.m.s. value will exceed the r.m.s. value of the C.G. J. Taylor (1953) suggested a dynamic overshoot of 15 per cent and Press and

# AIRCRAFT LOADS IN ATMOSPHERIC TURBULENCE

Steiner (1958) suggested 25 per cent as simple corrections for all flight conditions. There is wide variation for different aircraft and for different heights but as a rough correction to compare aircraft acceleration measurements with direct velocity measurements an overshoot factor of 1.20 will be assumed.

Most of the aircraft that have been used to measure turbulence have values of  $c\mu_g$  in the range 400–600 and for a scale of turbulence  $L$  of 1000 ft

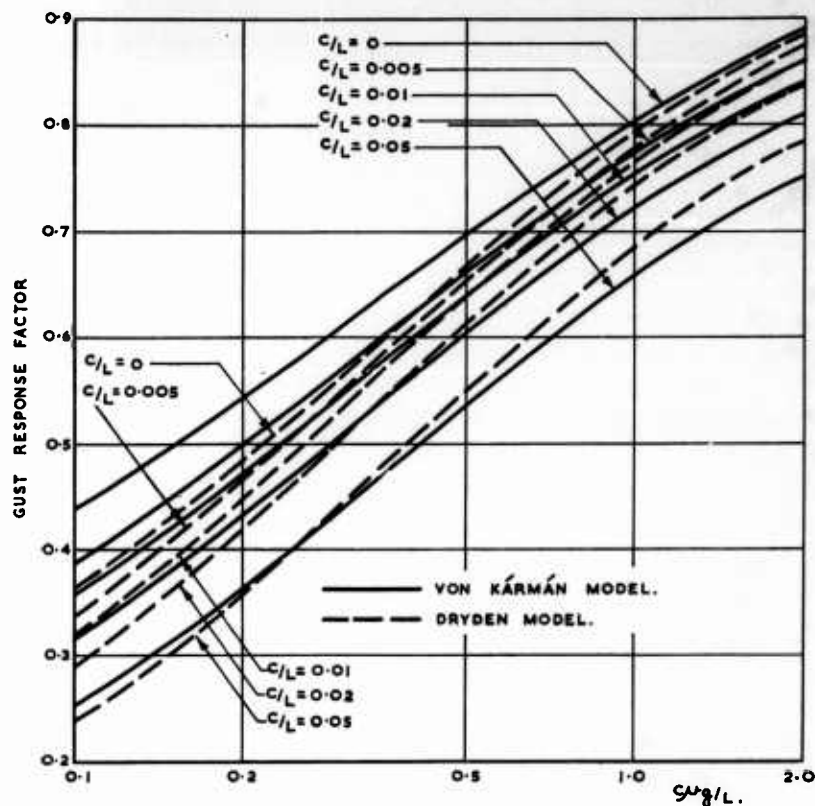


Fig. 10.1. Gust response factors for motion of aircraft C.G. in terms of  $c\mu_g/L$ . Pitching neglected and also the effect of finite span on lift due to atmospheric turbulence.  $c$  = wing mean chord,  $\mu_g$  = mass parameter,  $L$  = scale of turbulence.

or more (i.e.  $c\mu_g/L$  less than about 0.5) the gust response factor will change rapidly. Thus errors in the assumed  $L$  will produce an appreciable error in predicting the total r.m.s. vertical velocity of the turbulence. This is less important in predicting atmospheric loads on the aircraft as the aircraft respond little to the smaller inverse wavelengths and thus the turbulence energy density at higher inverse wavelengths is of more significance than the total turbulence energy. Furthermore the errors in predicting loads in other

aircraft in the same range for  $c\mu_g$  of 400-600 will be small even if the scale of turbulence that was assumed was vastly different from its true value; this is because approximately the same gust response factor is used to transform gusts to accelerations that had been used originally to transform accelerations to gusts. The discrepancies arise when the data are used for aircraft with different values of  $c\mu_g$ . The discrepancies will not be much for lower  $c\mu_g$ 's but they might become serious for larger ones.

As an illustration of the effect of assuming the wrong scale of turbulence when the energy density at high inverse wavelengths is known Fig. 10.2

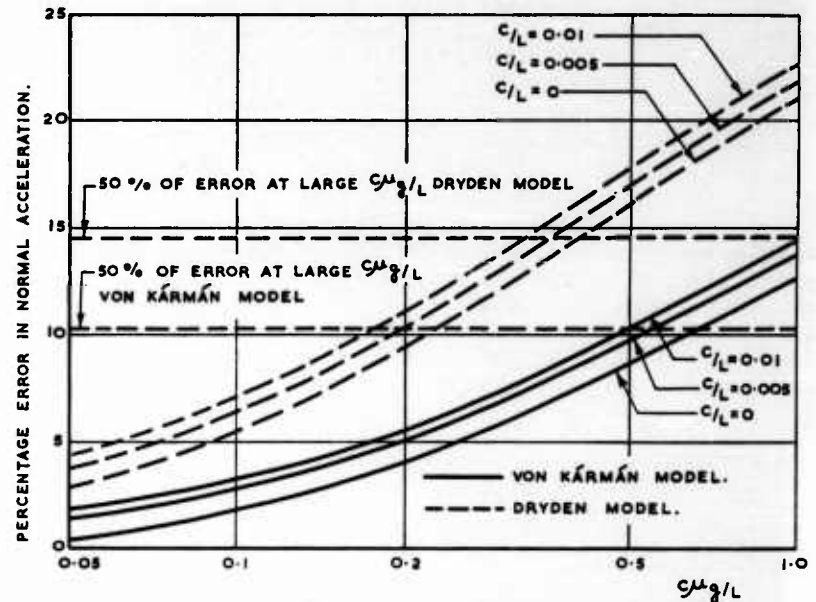


Fig. 10.2. Error in normal acceleration calculated for a scale of turbulence half the real value but with no change in the turbulence energy density at high inverse wavelengths.

$c$  = wing mean chord,  $\mu_g$  = mass parameter,  $L$  = scale of turbulence.

shows the error in acceleration that would result if the assumed scale of turbulence was half the true value. At very low values of  $c\mu_g$  the error is small and if  $c/L$  also is small the error is of the second order of smallness. As  $c\mu_g$  increases the error increases until at very high values the acceleration is proportional to the total energy of the turbulence rather than the energy density at high inverse wavelengths. At a value of  $c\mu_g/L = \frac{1}{2}$  the two have about equal importance.

The number of zero crossings for all the aircraft on which Bullen (1963) quotes measurements are discussed in paragraph 10.5 and the values for the Dryden model of turbulence are quoted in Table 10.5. For each aircraft  $N_0\sqrt{\rho_0/\rho}$  will be nearly constant for all heights. The range of  $N_0\sqrt{\rho_0/\rho}$  for

the different aircraft is 8.4 to 12.9 with a mean for all the flying of 9.9. Thus the operational data refer to aircraft with an average  $N_0 \sqrt{\rho_0/\rho}$  of 9.9 and the variation between the aircraft is so small that the error introduced by not weighting the data according to the  $N_0$  of each aircraft is negligible. The value of  $N_0$  will be slightly greater when calculated for the more representative von Kármán model of turbulence. The number does not vary much with scale of turbulence for either model of turbulence.

This simplification of treating all the aircraft as having the same  $N_0$  at each height means that as far as these measurements are concerned the number of gusts is not dependent on the aircraft encountering them and therefore is the same as a series of discrete gusts. Each gust has to be multiplied by the appropriate gust response factor for the aircraft that encountered it. When the original data were obtained a gust alleviation factor was used for each gust. An estimate of the true gust velocities will now be made by replacing these gust alleviation factors by the gust response factor for a von Kármán model of turbulence. For U.S. data the alleviation factor is that given by Pratt and W. G. Walker (1954)

$$K_g = 0.88\mu_g/(5.3 + \mu_g) \quad (10.13)$$

For U.K. data the alleviation factor  $K_z$  is that given by Zbrozek (1953) for a ramp-shaped gust rising to its maximum value in 100 ft.

Selected curves of alleviation factors are shown in Fig. 10.3 against  $c\mu_g/L$  so that their general shape can be compared with the gust response factors of Fig. 10.1. To facilitate this comparison the gust response factors for several scales of turbulence are also shown.

#### 10.3 COMPARISON OF ACCELEROMETER MEASUREMENTS AND DIRECT MEASUREMENTS OF VERTICAL TURBULENCE VELOCITY ON AIRCRAFT

K. D. Saunders (1961) made a series of flight tests on the B-66B in which the normal acceleration was measured at a point near the aircraft centre of gravity. During each flight the air velocity normal to the line of flight was also measured at a probe at the nose of the aircraft. In 25 flights over flat terrain at different heights the scale of the turbulence was estimated and the results are quoted in Table 2.6. By assuming the gust response factor appropriate to the scale of turbulence, the turbulence velocity can be estimated from the measurements of the normal acceleration of the aircraft. There were also 39 flights in groups of three at 200 ft, 600 ft, 1000 ft when the scale of turbulence was not measured. A comparison of the predicted turbulence velocity can be made at each height by assuming the same average scale of turbulence measured at each height in the 25 other flights.

Table 10.1 compares the r.m.s. vertical velocity measured directly with the r.m.s. vertical velocities deduced from normal acceleration measurements for the 25 flights over flat terrain. The conversion from normal acceleration of the aircraft to vertical velocity of the turbulence is made in the three following ways: firstly using the alleviation factor of equation (10.13) and then using the gust response factor of equation (10.9) combined successively with equations (10.10) and (10.11) with a dynamic overshoot factor of 1.2, at the position of the accelerometer, due to the flexibility of the

structure. Table 10.2 makes a similar comparison for the  $13 \times 3$  group of flights at different heights. The agreement between the turbulence velocity predicted directly and by means of the gust response factor is closer than

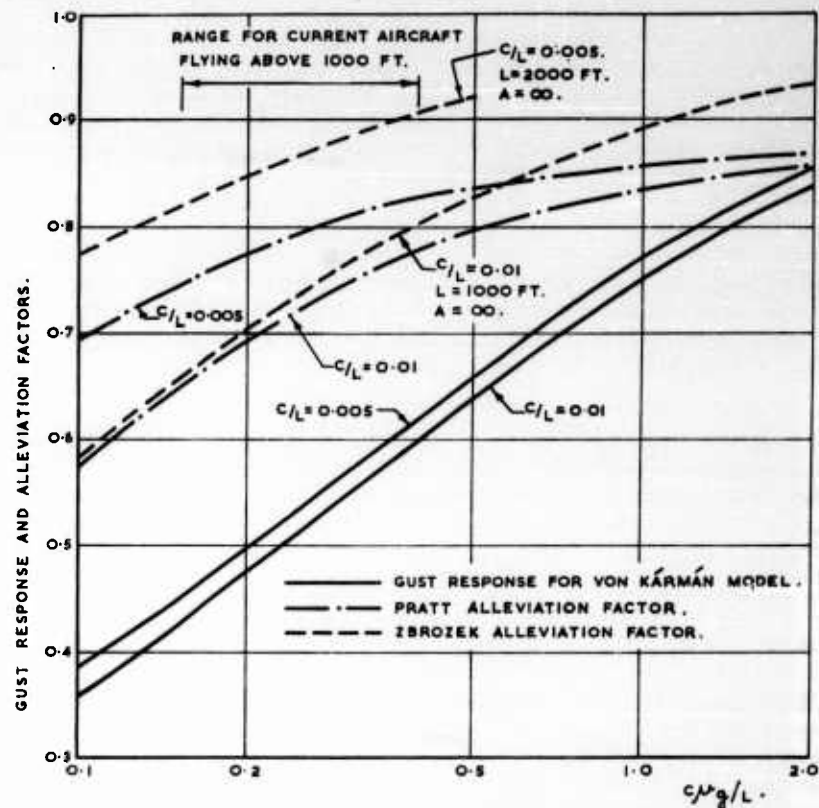


Fig. 10.3. Comparison of gust response and alleviation factors.

Pratt factor for all scales of turbulence and aspect ratios. Von Kármán factor for all scales of turbulence and aspect ratio infinite. Variation with aspect ratio is small and the curves for  $A = 5$  would be almost identical with those shown. Zbrozek factor varies with scale of turbulence and with aspect ratio. At finite aspect ratios the factor would be greater than those shown and for greater mean chords the factor would be less.

$A$  = aspect ratio,  $c$  = wing mean chord,  $\mu$  = mass parameter,  $L$  = scale of turbulence.

would have been expected, as an arbitrary dynamic factor of 1.2 was included. The relative agreement at different heights as brought out in Table 10.2 is more significant and gives confidence in the accuracy of using accelerometer readings to predict turbulence velocity when a good estimate can be made of the scale of turbulence. The accuracy of the data is not sufficient to discriminate between the Dryden and the von

# AIRCRAFT LOADS IN ATMOSPHERIC TURBULENCE

Table 10.1. Comparison of R.M.S. Vertical Velocity Measured Directly with that Deduced from Normal Acceleration Measurements

Run no.	Height ft	Scale of turbulence ft	r.m.s. vertical velocity ft/sec E.A.S.			
			Direct measurement	Using alleviation factor equation (10.13)	Using (gust response factor $\times 1.2$ )	
					Equations (10.9) and (10.10)	Equations (10.9) and (10.11)
1	200	277	1.45	1.67	1.37	1.44
4	600	359	1.71	2.19	1.85	1.92
6	200	220	1.89	1.36	1.10	1.15
7	600	834	2.09	1.93	1.86	1.88
9	200	414	1.95	2.40	2.06	2.13
10	400	640	3.67	3.54	3.23	3.32
12	600	675	3.51	3.08	2.84	2.91
13	200	480	3.72	3.64	3.04	3.14
14	600	511	3.27	4.15	3.66	3.77
17	200	374	3.23	4.01	3.40	3.53
18	1000	402	2.04	2.56	2.19	2.27
19	200	223	2.45	3.77	3.05	3.20
22	1000	739	2.21	2.34	2.20	2.24
24	600	570	2.88	3.37	3.02	3.10
25	200	410	3.19	4.24	3.64	3.76
26	600	413	2.64	3.12	2.68	2.77
27	600	510	2.71	3.21	2.82	2.92
30	600	383	4.76	5.30	4.51	4.67
31	200	153	3.14	4.52	3.56	3.70
32	200	167	3.16	4.48	3.56	3.71
34	600	649	5.12	4.57	4.19	4.30
35	200	349	3.35	4.21	3.55	3.68
36	1000	1327	4.05	3.66	4.02	3.98
40	200	252	2.71	3.56	2.91	3.04
42	200	499	4.68	3.66	3.22	3.32
Average		473	3.02	3.38	2.94	3.03

Kármán models of turbulence but the study of turbulence indicates that the von Kármán model should be more representative. Throughout the remainder of this chapter only the gust response factor corresponding to the von Kármán model will be used. The numerical values of r.m.s. vertical velocity for the 13 groups at heights of 200 ft, 600 ft and 1000 ft are combined with 32 other groups at heights of 200 ft, 400 ft and 600 ft in paragraph 10.4.1 to make an estimate of the variation with height up to 1000 ft.

Generally with accelerometer measurements reliance has to be placed on counting peaks rather than measuring r.m.s. values. The peaks were

Table 10.2. Comparison of R.M.S. Vertical Velocity Measured Directly with that Deduced from Normal Accelerations for Groups of Flights at 200 ft, 600 ft and 1000 ft

r.m.s. vertical velocity ft/sec E.A.S.

Height 200 ft assumed scale of turbulence 318 ft				Height 600 ft assumed scale of turbulence 545 ft				Height 1000 ft assumed scale of turbulence 823 ft			
Direct	Allev. equation (10.13)	(Response $\times 1.2$ )		Direct	Allev. equation (10.13)	(Response $\times 1.2$ )		Direct	Allev. equation (10.13)	(Response $\times 1.2$ )	
		Equations (10.9) and (10.10)	Equations (10.9) and (10.11)			Equations (10.9) and (10.10)	Equations (10.9) and (10.11)			Equations (10.9) and (10.10)	Equations (10.9) and (10.11)
4.09	3.34	2.79	2.90	3.51	3.08	2.73	2.82	3.46	2.88	2.76	2.80
3.72	3.64	3.04	3.16	4.41	3.76	3.33	3.44	4.11	3.44	3.30	3.35
4.10	4.00	3.34	3.47	4.00	3.64	3.22	3.33	3.77	2.92	2.80	2.84
2.85	3.41	2.85	2.96	3.23	3.84	3.40	3.52	2.33	3.24	3.11	3.16
3.01	3.69	3.08	3.20	3.27	4.15	3.68	3.80	3.10	3.73	3.58	3.63
3.23	4.01	3.34	3.48	3.40	3.97	3.51	3.64	2.81	3.37	3.23	3.28
3.23	3.80	3.18	3.30	4.47	4.40	3.90	4.03	4.76	4.55	4.36	4.44
3.69	4.10	3.45	3.56	5.12	4.57	4.05	4.19	4.94	4.36	4.19	4.25
3.35	4.21	3.52	3.66	4.67	4.29	3.80	3.92	5.15	4.45	4.26	4.34
3.37	4.21	3.52	3.66	4.53	4.33	3.83	3.96	4.56	4.05	3.88	3.94
2.74	3.80	3.18	3.30	3.85	4.05	3.59	3.71	4.05	3.66	3.51	3.56
2.76	3.52	2.94	3.06	3.90	3.88	3.44	3.56	4.44	3.82	3.66	3.72
3.55	4.56	3.81	3.96	3.56	4.48	3.96	4.10	3.91	3.66	3.51	3.56
Average	3.87	3.23	3.36	3.99	4.03	3.57	3.70	3.95	3.70	3.55	3.61
3.37											



measured for the series of 25 flights for both the turbulence velocity and for the normal acceleration. These are shown in Fig. 10.4. In both cases the number of peaks greater than a given value varies exponentially with the value, except for very low values when the actual number of peaks is a little less than the exponential distribution. Both distributions can be represented by

$$N/N_0 = \exp(-1.41 w/\sigma_w) \quad (10.14)$$

- DIRECT MEASUREMENTS
- x DEDUCED FROM MEASUREMENTS OF NORMAL ACCELERATION ASSUMING VON KÁRMÁN'S MODEL OF TURBULENCE AND DYNAMIC OVERSHOT FACTOR OF 1.2.

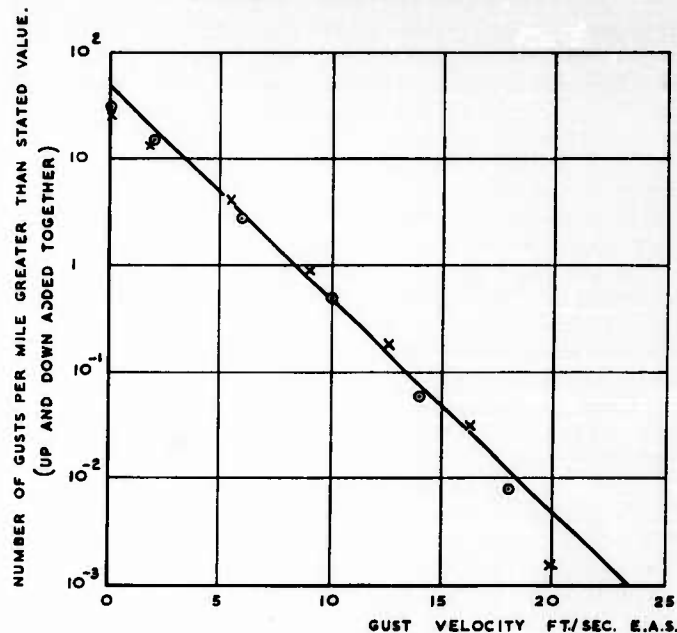


Fig. 10.4. Comparison of the number of gusts greater than given values as measured directly and deduced from measurements of normal accelerations.

where  $w$  are the velocities from direct measurements or from the normal acceleration measurements

$\sigma_w$  are the average of the r.m.s. values for each flight.

The 25 flights are the same as those used for Fig. 2.10. The distributions of crossings in Fig. 2.10 showed that for the individual flights they were more nearly exponential than Normal. So it would be expected that when all the flights were combined together that the number of high peaks would be greater than that expected from a Normal distribution for each flight.

It is fortuitous that the value of  $N_0$  is the same for direct measurements of



velocity and for that deduced from normal acceleration measurements as it has been shown in paragraph 10.2 that the number of zero crossings that occur will depend on the response that is being measured. Furthermore the values of  $N_0$  in equations (10.14) are the extrapolated values and are not the same as the measured ones.

#### 10.4 SPECIFIC TURBULENCE CONDITIONS

For the case of turbulence up to 1000 ft agreement was reached between direct measurements of turbulence velocity and estimates based on measurements of the normal acceleration at a point on the structure near to the centre of gravity of the aircraft. By assuming that agreement should be achieved for turbulence at greater heights separate results by the two methods can be grouped to give a better estimate of atmospheric turbulence than could be achieved from either group by itself.

For the most part the measurements of acceleration do not include any estimate of the scale of the turbulence. Moreover nearly all the aircraft that have been used have a value of  $c\mu_g$  less than 600 and the values of the normal accelerations are rather insensitive to the scale of turbulence above 1000 ft for the same value of energy density at a high inverse wavelength. As far as the normal accelerations are concerned the relative magnitudes for different values of  $c\mu_g$  below 600 will not vary much with the scale of turbulence that is assumed for the gust response factors for scales above 1000 ft. For a scale of turbulence below 1000 ft such as is the case up to a height of 1000 ft the normal accelerations do change appreciably with the scale: this is apparent in the results given in Tables 10.1 and 10.2 for the B-66B.

Some formula for the scale of turbulence at different heights had to be assumed. There is good evidence that the scale is roughly equal to the height up to 1000 ft but there is little direct evidence at heights above that. Such evidence as there is suggests that the scale will be more than 1000 ft at greater heights. Thus it cannot be expected that the normal acceleration measurements that have been made will show up any differences between the aircraft such as would verify the formula assumed. However, an indication of the accuracy can be obtained by comparing the total turbulence energy deduced from the normal accelerations with direct measurements of the total turbulence energy. In addition the total measurements of acceleration will give the distribution of energy at different heights associated with the assumed formula for scale of turbulence. This can be compared in a general way with overall meteorological data.

In considering specific forms of atmospheric turbulence twice the turbulence energy per unit volume will be regarded as the basic unit. This will be expressed in terms of the density of the air at ground level so that it becomes  $(\rho/\rho_0) \sigma_w^2$  which equals  $(\sqrt{\rho/\rho_0} \cdot \sigma_w)^2$ , i.e. the mean square of the turbulence equivalent velocity. Equivalent velocities not only provide a suitable basis for the study of the physical characteristics of turbulence but are almost invariably used to express aircraft loads.

The scale of turbulence has to be decided empirically. The earth's boundary layer in unstable air is about 1000 ft and measurements in this region have shown that the scale of turbulence is about equal to the height.

Outside the boundary layer the majority of the turbulence is of the convective type in which the turbulence is carried up by thermals. There is, in addition, clear air turbulence in the vicinity of jet streams but these occur very infrequently and attention is focused entirely on convective turbulence in the estimate of the scale of turbulence. If the turbulence activity covers an area with linear dimensions large compared with the scale of turbulence it seems to be not unreasonable to assume that to a first approximation the area at all heights of the turbulence activity will be substantially the same and the turbulence will move upwards in a cylinder. Ludlam's (1963) description of the main movement in a thunderstorm is given in Chapter 2 as being precisely that. However, due to the variation of the density of the air with height, the dimensions of any volume of turbulence will increase as it rises in the cylinder and will be inversely proportional to the density of the air at the height concerned. It seems therefore that it might be assumed that the scale of turbulence varies inversely as the air density. In the present treatment it will be assumed empirically that the scale of turbulence equals  $1000 \rho_0/\rho$  ft at all heights above 1000 ft. Using this scale of turbulence, which is equal to the height below 1000 ft and equal to  $1000 \rho_0/\rho$  above 1000 ft, the turbulence energy per unit volume will be examined for examples of the three following specific turbulence conditions

- (i) clear air turbulence up to 1000 ft
- (ii) turbulence in and near cumulus clouds
- (iii) turbulence in thunderstorms.

#### 10.4.1. *Clear Air Turbulence up to 1000 ft*

Extensive direct measurements of air velocity fluctuations at heights up to 1000 ft were described in Chapter 2. It was shown in paragraph 10.3 that deductions of the air velocity fluctuations from normal acceleration measurements gave the same results as those from direct measurements of velocity.

In one respect clear air turbulence below 1000 ft is more easily investigated than other forms of turbulence as it is present most of the time. Thus whenever visibility is good enough for flying at these heights it may be assumed that flights may be made to examine the turbulence. Bullen (1961) gives results from flights in quick succession in groups of three at 200 ft, 400 ft and 600 ft in North Africa and K. D. Saunders (1961) gives results from flights in quick succession in groups of three at 200 ft, 400 ft, 600 ft and at 200 ft, 600 ft, 1000 ft in America. K. D. Saunders gives direct measurements of the turbulence velocities and the deductions from normal acceleration measurements on the aircraft, but Bullen gives normal accelerations only. These experiments give a good indication of the character of the turbulence.

At such low heights the air stream carrying the turbulence flows roughly parallel to the ground surface. The measured vertical velocities will be the combination of the turbulence velocities and the vertical components of the stream velocity. It was shown in Chapter 2 that the scale of turbulence passing a fixed point is approximately equal to the height in flat terrain but the scale of turbulence measured along a horizontal line by an aircraft is

rather more than the height. This difference is more marked over hilly terrain but even over flat terrain it is large at 200 ft. In forming an opinion on this clear air turbulence below 1000 ft some attempt has to be made to remove qualitatively the apparent contribution of the stream flow. The turbulence itself is the same whether the measuring point is moving or stationary but the apparent change due to the stream flow is different. The characteristics of the stream flow do not satisfy the conditions of randomness, essential to the theory of turbulence. However, the deviation of the stream from uniform flow in a straight line can be regarded as a perturbation to the turbulence provided the energy is not too great a proportion of the total energy. The maximum equivalent scale of turbulence induced by the stream deviations seem to be about 1000 ft, even over hilly terrain, and over flat terrain the stream deviations seem to be completely negligible compared with the turbulence at heights above 600 ft. The lowest flights were made at 200 ft, where the average equivalent measured scale was 314 ft. It is doubtful if turbulence theory could be applied for aircraft flight below 200 ft.

Table 2.5 shows 14 groups of 3 flights at heights of 200 ft, 600 ft, 1000 ft. All these flights had an r.m.s. vertical velocity greater than 3 ft/sec at 600 ft. It also shows 32 groups of 3 flights at 200 ft, 400 ft, 600 ft which are made up of 23 groups with the r.m.s. vertical velocity at 600 ft below 3 ft/sec and 9 groups with it above. The 9 groups above 3 ft/sec showed a tendency, the same as did the other 14 groups above 3 ft/sec, for the r.m.s. value to be greater at 600 ft than at 200 ft. The 23 groups below 3 ft/sec had the same r.m.s. vertical velocity at 200 ft, 400 ft and at 600 ft. The variation in turbulence intensity with height is shown in Fig. 10.5. The curves that are drawn are made to have a constant r.m.s. velocity ( $\sigma_w$ ) at heights above 300 ft and a constant energy density at high inverse wavelengths (i.e. constant  $\sigma_w/L_{\frac{1}{2}}$ ) below 300 ft. Simultaneous measurements on towers given by Anon A.S.T.I.A. (1959a) show a marked drop in r.m.s. vertical velocity from 300 ft to 75 ft. The drop seems to be rather less rapid than constant energy density but the accuracy of the information does not warrant a more elaborate formula than the one quoted above for Fig. 10.5. The r.m.s. vertical velocities deduced from normal acceleration measurements on the aircraft during the same flights agree very closely with the direct measurements if a dynamic overshoot of 1.20 is assumed for r.m.s. values below 3 ft/sec and 1.13 above 3 ft/sec. Bullen's (1961) results for the average intensity over flat desert in May, June, July and November, December, January, have been transposed to r.m.s. vertical velocities; his alleviation factor has been replaced by a gust response factor with a scale of turbulence equal to the height and a dynamic overshoot factor of 1.20. The purpose of the diagram is to demonstrate the variation with height rather than give an absolute value of the intensity. It will be seen that all the data from K. D. Saunders (1961) and Bullen (1961) support the contention that the turbulence increases in intensity up to a height of a few hundred feet. K. D. Saunders' data strongly suggest that the intensity then remains sensibly constant up to 1000 ft.

Whilst it seems reasonable to assume that the atmospheric turbulence in clear air from 200 ft to 1000 ft is reasonably constant it has to be remembered that the earth's surface may influence the air stream directions and so impose

# AIRCRAFT LOADS IN ATMOSPHERIC TURBULENCE

loads on the aircraft. An indication of the effect can be obtained from an analysis of the measurements over hilly terrain by K. D. Saunders. It is assumed that the air motion relative to the aircraft is in two parts, atmospheric turbulence with a scale equal to the height and the stream direction changing along the flight path. The normal accelerations of the aircraft are transformed to turbulence velocities, on the basis of a gust response factor

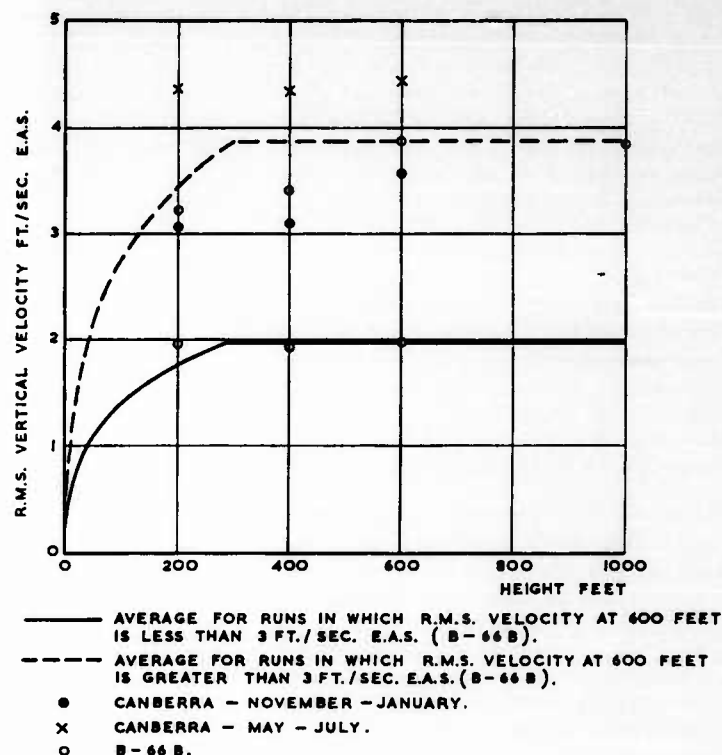


Fig. 10.5. Variation of intensity of clear air turbulence with height up to 1000 ft above flat terrain.

appropriate to the atmospheric turbulence alone. These derived turbulence velocities will differ from the direct measurements of air velocity, which give the equivalent turbulence intensity for the turbulence and stream effects combined. Up to a height of 600 ft the velocities, deduced from the normal accelerations of the aircraft with the same dynamic overshoot factor of 1.2 that was measured over the flat terrain, are 18 per cent lower than the velocities measured directly. The direct measurements over hills were shown in Chapter 2 to have an average r.m.s. velocity of 3.79 ft/sec compared with 2.73 ft/sec over flat ground. Thus the direct measurements of turbulence r.m.s. velocity over hills are 1.40 times the measurements over flat terrain.

The estimated velocities over hills from measurements of normal acceleration of the aircraft, being 18 per cent less than the direct measurements of velocity, are therefore 1.15 (i.e.  $0.82 \times 1.40$ ) times the measurements over flat terrain. This 15 per cent estimated increase in turbulence velocity from measurements of normal acceleration is based on the gust response factor being the same for the stream effects as for the turbulence. The stream effects, which includes the pilot's actions, will be predominantly at longer wavelengths than the main turbulence wavelengths and will be more alleviated. Data are not available to show whether the alleviation was sufficient to account for the difference between the two sets of measurements. At 1000 ft where the ground effects should be considerably attenuated the actual measurements of normal acceleration gave the same r.m.s. turbulence velocities as those measured directly; it is emphasized, though, that this is somewhat fortuitous as there were only 6 flights, which are much fewer than in the remainder of the analysis.

The best estimate of the r.m.s. vertical velocity of turbulence over flat terrain was given in Chapter 2 for any single flight as a mean of 2.73 ft/sec with a standard deviation of 1.1 ft/sec. Over hilly terrain the turbulence will be superimposed on stream motions of varying directions which must be treated separately. In the direct measurements of air velocity on the B-66B there was a 40 per cent increase in apparent r.m.s. value but the aircraft normal accelerations increased by only 15 per cent. No evidence is available to show the influence on other aircraft but it may be presumed that the increase in the normal acceleration would be greater for aircraft with larger values of mass parameter times mean chord.

#### 10.4.2. *Turbulence In and Near Cumulus Clouds*

At all heights below 1000 ft it could be assumed that the air density was the same as that at ground level. Cumulus clouds reach heights of more than 15,000 ft and the air density changes are important. Crane and Chilton (1956) quote a flight at 1700 ft in clear air in the vicinity of a storm centre. J. Taylor (1953) quotes a series of ten flights and a re-examination of the original data from which the paper was prepared shows that it included two moderately turbulent passages through cumulus at 3000 ft. Houbolt, Steiner and Pratt (1962) quote 9 traverses through cumulus clouds at 15,000 ft. In addition to these aircraft measurements Gorelic, Kostarev and Chernikov (1958) quote r.m.s. vertical velocities in cumulus at 10,000 ft measured along a vertical radar beam. For comparison purposes all the velocities are given as equivalent velocities (i.e. true velocity times  $\sqrt{\rho/\rho_0}$  where  $\rho$  is the air density and  $\rho_0$  the air density at ground level) and wherever a scale of turbulence is required it is assumed to be  $1000 \rho_0/\rho$  ft.

Houbolt *et al.* quote turbulence energy in wavelengths 10 to 5000 ft. By assuming a scale of turbulence these can be transformed into total energy. In nine flights at 15,000 ft they found a range of 4.3 to 11.5 ft/sec E.A.S. for the r.m.s. vertical velocity. This would be approximately equal to a mean of 7.6 ft/sec E.A.S. with a standard deviation of 30 per cent of the mean. J. Taylor measured crossings of normal acceleration and counted them at one-minute intervals. The flying was done in 4 min runs alternately at 120 knots E.A.S. and 180 knots E.A.S. with one minute without recording

between each run. The r.m.s. vertical velocity was calculated for each minute on the assumption that the Viking aircraft, that was used, had 8 crossings of the datum  $1g$  acceleration, in each direction, per mile and that over 1 min the distribution of crossings of different levels was Normal. The calculated r.m.s. vertical velocities were not significantly different whether they were based on  $0.1g$  or  $0.2g$  increment at 180 knots E.A.S. or on a  $0.1g$  increment at 120 knots E.A.S. During 10 flights, each of approximately 100 min at 3000 ft, two storms in cumulus clouds were encountered each extending to a flight distance of about 60 miles. One had a mean r.m.s. vertical velocity of  $4.6$  ft/sec E.A.S. and the other  $4.9$  ft/sec E.A.S. Both had standard deviations, for the velocities averaged over  $3\frac{1}{2}$  miles, of 20 per cent and the maximum r.m.s. vertical velocity over a distance of  $3\frac{1}{2}$  miles was  $7$  ft/sec E.A.S. Crane and Chilton measured the turbulence energy at all wavelengths in one flight of 170 miles at 1700 ft and obtained an r.m.s. vertical velocity of  $4.9$  ft/sec E.A.S. for the complete flight. Gorelic *et al.* used vertical radar beams to measure the r.m.s. vertical velocity in cumulus at about 10,000 ft. These differ in two respects from the aircraft measurements. The effective path is vertical instead of horizontal and the effective speed along the path the speed of light instead of the speed of the aircraft. They found a range from  $1.7$  to  $4.8$  ft/sec E.A.S. over a number of clouds and a range of  $3.2$ – $4.3$  ft/sec E.A.S. over one storm. The number of readings is not quoted but the mean and scatter seem to be of the same order as those encountered by J. Taylor and Crane and Chilton. It would be expected that the radar measurements would be a little lower as the total extent in a vertical direction of the turbulence would be too little to include all the longer wavelengths and in any case the radar measurements would be limited to scales of turbulence of about 500 ft.

J. Taylor's measurements are of the number of crossings of selected normal accelerations and give an opportunity of comparing the distribution of crossings with the distribution of r.m.s. values. The combined counts for the two storms are shown in Fig. 10.6. The distribution of counts greater than a stated value of vertical velocity is close to an exponential distribution and is given by

$$N/2N_0 = \exp(-1.38 w/\sigma_w) \quad (10.15)$$

where  $N/2N_0$  is used instead of  $N/N_0$  because the number of up and down velocities are added together. The coefficient 1.38 is nearly the same as the 1.41 given for the B-66B in paragraph 10.3. Once again the distribution shows that the distribution of crossings for a constant r.m.s. value is more nearly exponential than Normal. The constancy of the coefficient is to a large degree due to both examples including turbulence with relatively little scatter: the standard deviation for the Viking is 20 per cent and that for the B-66B 30 per cent.

Little error will occur if turbulence in a small patch of cumulus is assumed to be homogeneous and isotropic. However, the distribution of crossings is not known. This introduces a difficulty if a complete storm is examined. The two storms from J. Taylor (1953) include continuous turbulence for the duration of the measurements. Each of the 24 patches  $3\frac{1}{2}$  miles long can be represented reasonably well by a Normal distribution of crossings with



8 per mile zero crossings in each direction: the number of crossings of a velocity of 8 ft/sec E.A.S. and more in each patch are rather few but such as there are tend to be more than would be expected from Normal distributions. When the counts from all the patches are added together the distribution is close to exponential from 5 to 20 ft/sec (the highest velocity

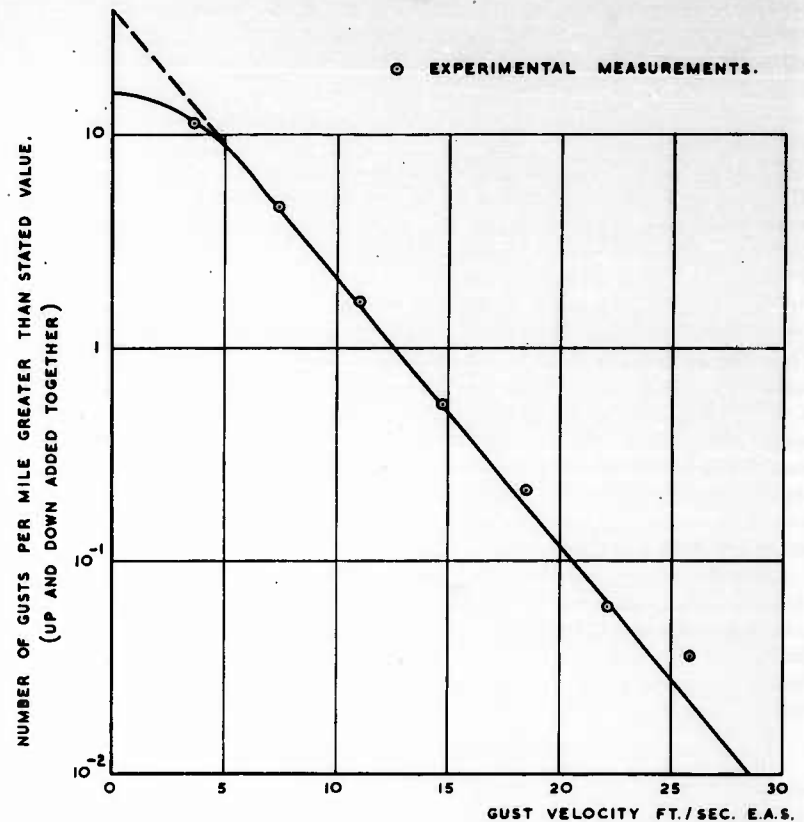


Fig. 10.6. The number of gusts greater than different levels in cumulus at 3000 ft. Measurements made on Viking in 120 miles flying. r.m.s. vertical velocity in lengths of 3.5 miles had an average of 4.78 ft/sec with a standard deviation of 20 per cent.

recorded in the total length of 120 miles). A Normal distribution that fits the number of crossings at 3.70 ft/sec and 7.4 ft/sec gives a r.m.s. velocity of 4.75 ft/sec and 8.0 zero crossings compared with an average of 4.78 ft/sec for the individual patches with 8.0 zero crossings for each. This agreement in zero crossings will be lost when flights in the absence of cumulus turbulence are added. Also it cannot be assumed that the extrapolated value of  $N_0$  from the exponential distribution will always be  $2\frac{1}{2}$  times the actual zero

crossings that occurs in this one example but it will be assumed that in any particular storm the ratio of the extrapolated  $N_0$  to the actual will be the same for all aircraft.

#### 10.4.3. Turbulence in Thunderstorms

Tolefson (1956) gives an extensive survey of thunderstorms by means of counts of peak normal accelerations. At the levels that he measured there would be a negligible difference between the number of peaks exceeding a given level and the number of crossings, in one direction, of that level. Houbolt, Steiner and Pratt (1962) quote 15 traverses through thunderstorms and for one traverse give the turbulence energy density at wavelengths 10-5000 ft and the proportion of time above different velocities.

In the survey by Tolefson (1956) a P-61 was flown 12,616 miles and a C-35 905 miles. The alleviation factors used by Tolefson are replaced by gust response factors to estimate the real velocities of the turbulence. Table 10.3 gives the parameters used in the original calculations and those required

Table 10.3. Values used for Calculations

Altitude in 1000 ft	Mass para- meter	Mean chord ft	Response factors				
			$K$	$K_g$	$K_g/1.2K$	$N_0$	$N_0\sqrt{\rho_0/p}$
1941-42 investigations by C-35							
5-10	18.7	9.25	0.429	0.686	1.30	16.6	18.6
10-15	23.6	9.25	0.449	0.718	1.31	14.7	17.9
15-20	27.5	9.25	0.455	0.738	1.35	13.6	17.9
20-25	32.1	9.25	0.460	0.755	1.37	12.5	17.9
25-30	37.7	9.25	0.463	0.771	1.39	11.4	17.8
30-34	44.0	9.25	0.466	0.785	1.41	10.6	18.0
1946-47 investigations by P-61							
5-6	26.4	10.5	0.510	0.733	1.20	12.2	13.2
10-11	30.0	10.5	0.514	0.748	1.21	11.4	13.3
15-16	34.6	10.5	0.518	0.763	1.23	10.5	13.3
20-21	41.1	10.5	0.526	0.779	1.24	9.6	13.3
25-26	48.6	10.5	0.531	0.793	1.25	8.8	13.3

for the conversion. The gust response factor  $K$  is based on von Kármán's model of turbulence and a scale of turbulence of 1000  $\rho_0/\rho$ . The sixth column is the ratio of the alleviation factor  $K_g$  to the gust response factor  $K$  times a dynamic overshoot factor of 1.2 and is the conversion factor from the gust velocities given by Tolefson to the present ones.  $N_0$  is the calculated number of zero crossings. Purely for simplicity of the calculations these have been done for the Dryden model of turbulence instead of the von Kármán



model. The relative values will be approximately the same for the two models but the absolute values will be different. In either case there may be considerable error in the absolute value and until much more information is available on measured values only relative values of  $N_0$  are significant.

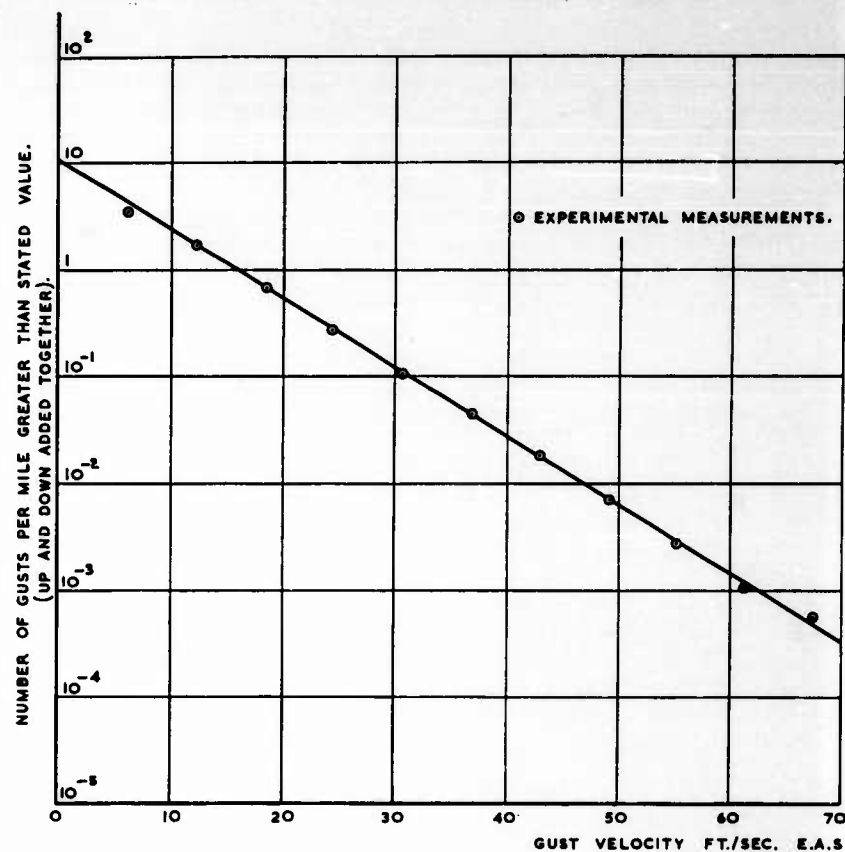


Fig. 10.7. The frequency of occurrence of gusts of different velocity in thunderstorms. Measurements made in 12,616 miles flying in thunderstorms at heights from 5000 to 26,000 ft.

The number of gusts greater than different values is shown in Fig. 10.7 for the 12,616 miles flown by the P-61 in thunderstorms. The distribution is represented closely, over the whole range of velocities measured, by

$$N/2N_0 = \exp(-w/6.72) \quad (10.16)$$

where  $N_0 = 5.5$ .

The distributions at different heights, taken separately, can also be represented well by exponential distributions. The plotted experimental points

# AIRCRAFT LOADS IN ATMOSPHERIC TURBULENCE

for the different heights, up to velocities of 55 ft/sec E.A.S., lie as close to a straight line as those shown in Fig. 10.7. The values of  $N_0$  and exponential decay with gust velocity are shown in Table 10.4. The measured values of

Table 10.4. Variation of Turbulence Intensity with Height in Thunderstorms

Height in 1000 ft	No. of miles recorded	No. of miles per gust greater than stated value and given by the formula $N/2N_0 = \exp(-w/w_0)$	
		$w_0$ ft/sec E.A.S.	$N_0$ number per mile
5-6	1750	6.20	6.3
10-11	2905	6.41	6.7
15-16	3328	7.03	5.5
20-21	2630	6.72	5.4
25-26	2003	6.72	4.0
	12,616	6.72	5.5

$N_0$  show the same tendency as the calculated ones to reduce with height and are close to 50 per cent of the calculated ones at each height.

The thunderstorms surveyed by the C-35 were for a total of only 905 miles. The results show the same trends as those given in Table 10.4 but the values of  $w_0$  and  $N_0$  for the whole 905 miles taken together are  $w_0 = 8.60$ ,  $N_0 = 10.0$ . The intensity of the turbulence  $w_0$  is rather more than the average of the more extensive recordings on the P-61 and the measured  $N_0$  is about 70 per cent of the calculated value compared with 50 per cent for the P-61.

No measurements were taken in this survey of the r.m.s. velocity. A rough approximation can be obtained by assuming that the factor 1.4, found in the survey of low-level turbulence in clear air and in the flights in cumulus and given in equations (10.14) and (10.15), applies. The variation in r.m.s. velocity with height is shown in Fig. 10.8. A curve is drawn to show an increase in turbulence energy per unit volume up to 15,000 ft and thereafter constant. Some speculation is needed to give values at 40,000 ft. However, the 15 flights by Houbolt *et al.* (1962) confirm that high intensity thunderstorms can be encountered at 40,000 ft. They quote the turbulence energy in wavelengths 1000-5000 ft. By assuming a scale of turbulence of  $1000 \rho_0/\rho$  ft this can be transformed into total energy. The 15 flights had a range from 6.6 to 17.2 ft/sec E.A.S. for the r.m.s. vertical velocity. This would be approximately equal to a mean of 11.9 ft/sec E.A.S. with a standard deviation of 27 per cent of the mean. In one traverse, in which the intensity was about 20 per cent above the average, the scale of turbulence was estimated. It is quoted as 5600 ft, which is not much different from the empirical value of 4100 ft used in the present analysis. For this traverse the proportion of time above different levels was measured. As with other forms of turbulence

the proportion for the higher velocities is greater than would be expected for a Normal distribution. Thus the same difficulty again arises in deciding the relationship between the extrapolated value of  $N_0$  from the exponential distribution and the actual number of zero crossings.

#### 10.5 ATMOSPHERIC LOADS ENCOUNTERED BY AIRCRAFT ON NORMAL OPERATIONAL DUTIES

Typical samples of the three types of atmospheric turbulence, most frequently met by aircraft, were quoted in paragraph 10.4. There is a fourth type of turbulence which occurs in the vicinity of jet streams and therefore

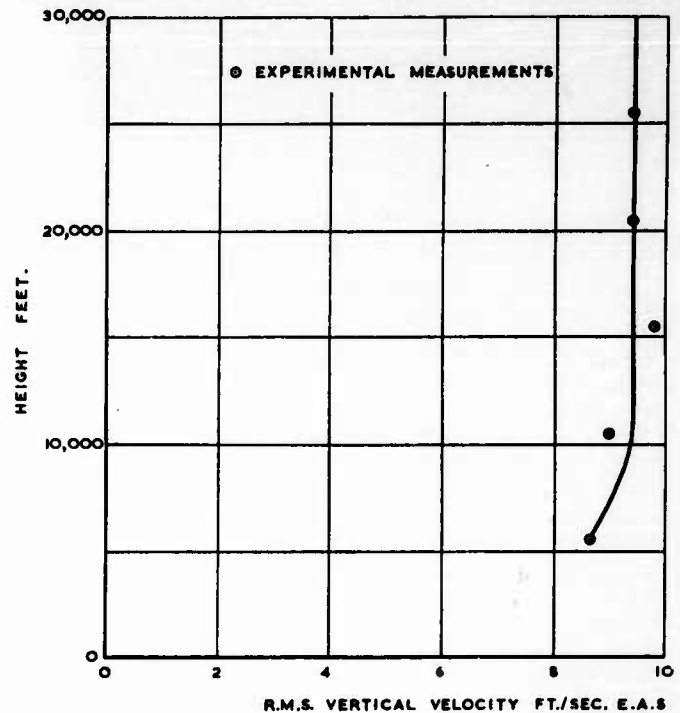


Fig. 10.8. The variation with height of r.m.s. vertical velocity in thunderstorms.

occurs less frequently and is less amenable to a detailed survey. It would be impracticable to fly aircraft solely to establish the average values for the various types of turbulence. The flying time required would involve a prohibitive cost and there are many patches of turbulence that cannot be catalogued with certainty into one particular category. Even if the average values could be obtained for the atmosphere itself and, in addition, the proportion of time in each was known, extensive information on the flying procedures would be required to establish the atmospheric loads on aircraft.

The apparent atmosphere, deduced from aircraft encounters, will differ appreciably from the real atmosphere in several respects. Low flying will be mainly in the vicinity of aerodromes: the height and the direction of the cruise is subject to considerable adjustment to avoid turbulence, the amount depending on the operation: the climb and descent will not be adjusted much for atmospheric conditions except that they will generally start or terminate at an aerodrome: the density of air traffic will depend on the geographical position, the time of day, the season and on restrictions placed on take-off and landing. Generally it may be stated that the apparent atmosphere is the one required and the best assessment of this can be made from operational flying. The present data are based almost entirely on civil aircraft operations and although very extensive it is doubtful if a correction could be made with much accuracy to give the apparent atmosphere for military aircraft or for civil aircraft that had little choice of route or height.

Bullen (1963) quotes measurements from 5.3 million flying miles on a variety of aircraft. Details of the aircraft and their operating conditions are given in Table 10.5. It is shown in Table 10.5 that for the aircraft used in the experiment the average number ( $N_0$ ) of gusts in each direction per mile, when in turbulence, is  $9.9 \sqrt{\rho/\rho_0}$ . The original data were given for an alleviation factor  $K_z$  for each gust. Table 10.5 shows that the gust response factor has an average of  $K_z/1.21$  below 25,000 ft and the difference between aircraft is not great; nearly all the data above 25,000 ft are from Comet 1 and 2, which have a gust response factor of  $K_z/1.44$  and  $K_z/1.48$  respectively at those heights. The frequency of occurrence of gusts of different velocities and at different heights is given in Fig. 10.9; the data from the Comet 2 are omitted as this aircraft was the only one that used cloud collision warning radar. The original data were transposed to true velocity (E.A.S.) by assuming an average gust response factor of  $K_z/1.21$  below 25,000 ft and  $K_z/1.44$  above. The frequency of occurrence of gusts is given as the number of gusts per mile for an aircraft with  $N_0 = 9.9 \sqrt{\rho/\rho_0}$ . It is done this way so that the diagram may be used directly for aircraft of similar type to those used in the experiments. The absolute value of  $N_0$  is uncertain and the information can be used for other aircraft only by calculating  $N_0$  from the same formula. The distribution of gusts does not seem to vary much with height so that the results from all heights may be added together. This distribution is also shown in the diagram; the curve that is drawn is calculated from the following formula

$$\left. \begin{aligned} \text{down-gusts } N &= \rho N_0 [0.984 \exp(-w/2.87) \\ &\quad + 0.016 \exp(-w/5.74)] \\ \text{up-gusts } N &= \rho N_0 [0.984 \exp(-w/3.10) \\ &\quad + 0.016 \exp(-w/6.20)] \end{aligned} \right\} \quad (10.17)$$

where  $N$  = number of gusts per mile with velocities greater than  $w$  ft/sec E.A.S.

$\rho N_0$  = 0.58 for the particular proportion of flying at different heights that happened to be used.

Table 10.5. Operating Details of Aircraft used for Measurements given by Bullen (1963)

Aircraft	Airline	No. of miles recorded in millions	Average cruising height	Mass parameter	Response factors			
					$K$	$K_z$	$K_z/1.2 K$	$N_0$
Ambassador	B.E.A.	0.20	11,000	28.8	0.504	0.756	1.25	9.5
Comet 1*	B.O.A.C.	0.70	35,000	35.5	0.500	0.865	1.44	5.9
Comet 2*	R.A.F. Lynchem	0.34	40,000	46.9	0.502	0.888	1.48	5.1
Freighter	S.A.F.E.	0.09	2000	12.3	0.411	0.676	1.38	12.2
	S.C.A.	0.06	1000	11.4	0.400	0.661	1.38	12.7
	W.A.A.C.	0.06	6000	12.8	0.408	0.682	1.39	11.8
Hermes 4	Airwork	0.48	9000	33.3	0.558	0.812	1.21	8.3
	B.O.A.C.	0.42	12,000	36.6	0.564	0.820	1.21	7.9
Stratocruiser	B.O.A.C.	0.86	14,000	44.5	0.590	0.826	1.17	6.8
Superconstellation	Qantas	0.99	14,000	41.3	0.586	0.830	1.18	7.0
Viking	B.E.A.	0.12	7000	25.0	0.486	0.759	1.30	11.4
Vicount	Aer Lingus	0.59	16,000	48.4	0.572	0.854	1.25	8.2
	B.E.A.		21,000	58.3	0.580	0.880	1.26	7.4
	C.A.A.C.	0.42	17,000	51.9	0.579	0.856	1.23	7.9
	Total	5.33				Average excluding Comet	1.21	Average
								9.9

\* Allowance has been made for the effects in compressibility on the slope of the lift curve and on the indicial lift functions. The same allowance is used for  $K$  and  $K_z$ .

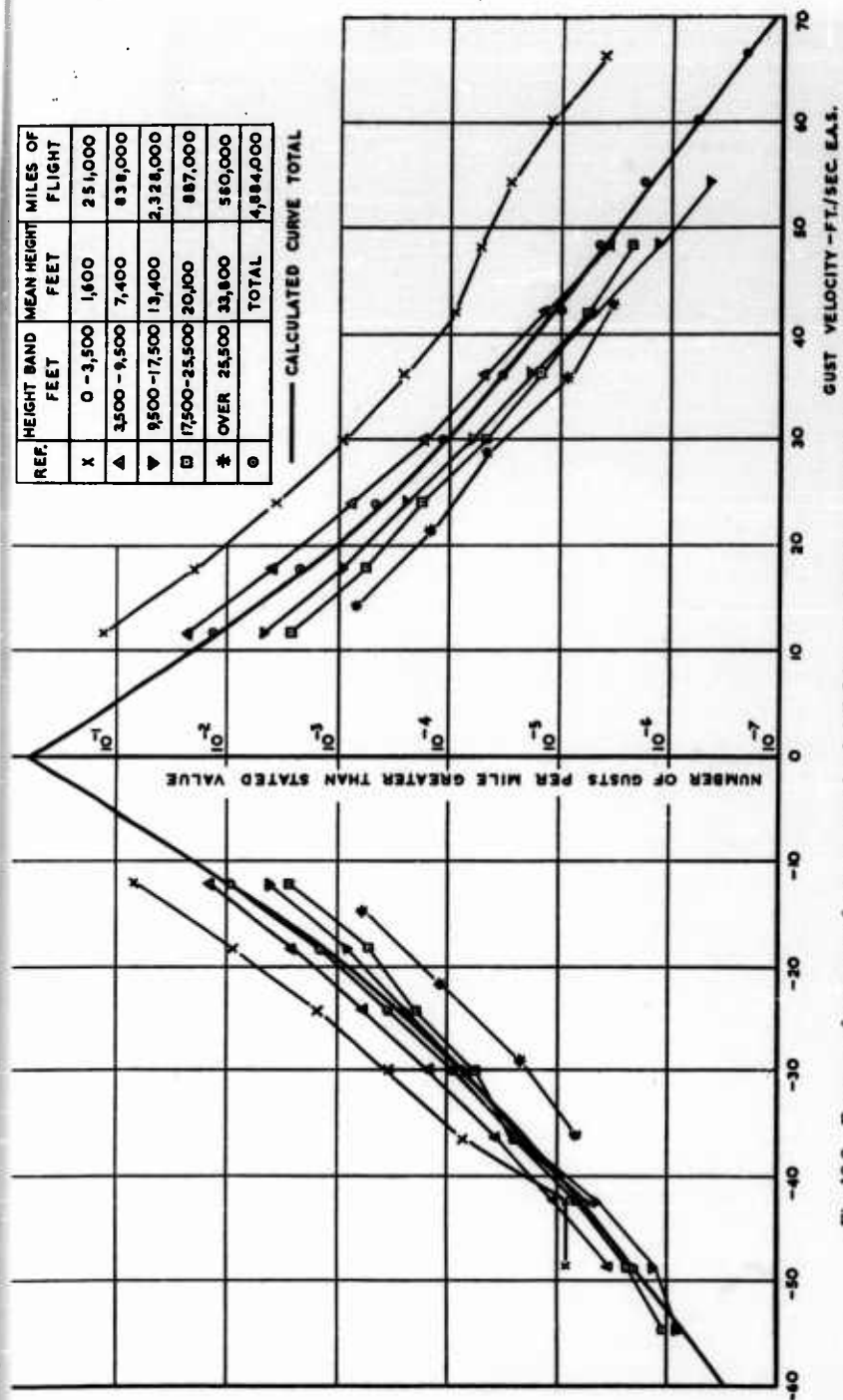


Fig. 10.9. Frequency of occurrence of gusts on operational civil flying. Deduced from measurements given by Bullem (1963).

Total compared with the formula

down-gusts  $N = 0.58 [0.984 \exp(-w/2.87) + 0.016 \exp(-w/5.74)]$

up-gusts  $N = 0.58 [0.984 \exp(-w/3.10) + 0.016 \exp(-w/6.20)]$

where  $N$  = number of gusts per mile with velocity greater than  $w$  ft/sec E.A.S.

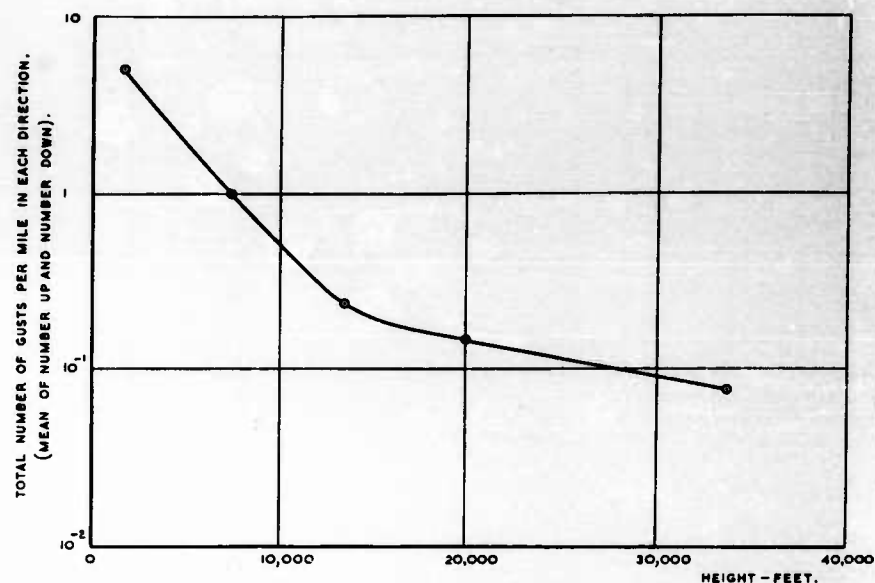


Fig. 10.10. Variation in total number of gusts with height.

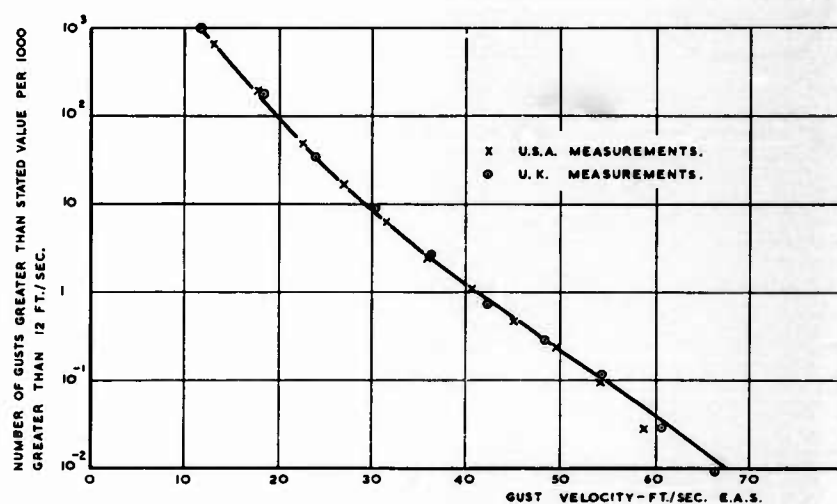


Fig. 10.11. Comparison of U.S.A. and U.K. data on relative frequency of occurrence of gusts of different magnitude.

U.S.A. data based on measurements from 4.8 million miles of flying by W. G. Walker and Copp (1959) and 0.5 million by Copp and Fetner (1959).

U.K. data based on measurements from 4.9 million miles of flying by Bullen (1963).



The formula (10.17) may be used to give the number of gusts at any height if the appropriate  $pN_0$  is known. The values on the curves at a velocity of 12 ft/sec E.A.S. are used to estimate  $pN_0$  for each height and these are shown in Fig. 10.10.

W. G. Walker and Copp (1959) quote measurements from 4.8 million miles of flying on civil airlines. They added the number of up-gusts and down-gusts at each velocity so that a comparison is only possible by first adding those from Bullen (1963). The two distributions are shown in Fig. 10.11 for the same number of gusts\* of 12 ft/sec E.A.S. It will be seen that both sets of experimental points fit the same curve.

#### 10.5.1. Avoidance of Turbulence

Bullen (1963) splits the data up into climb and descent and into cruise so that Fig. 10.10 can be presented in more detail. Estimates of  $pN_0$  are based on the number of gusts exceeding 12 ft/sec E.A.S. and are shown in Fig. 10.12. The cruise condition of each of the aircraft is compared with the combined climb and descent for all the aircraft. The climb and descent data are from all the aircraft combined and are therefore approximately appropriate for an aircraft with  $N_0 = 9.9 \sqrt{\rho/\rho_0}$ . The cruise data are from each aircraft separately and have been amended to make them also appropriate for an aircraft with  $N_0 = 9.9 \sqrt{\rho/\rho_0}$ . It will be seen that the number of gusts encountered per mile is less in the cruise than in the climb and descent. This is due to the deliberate avoidance of turbulence.

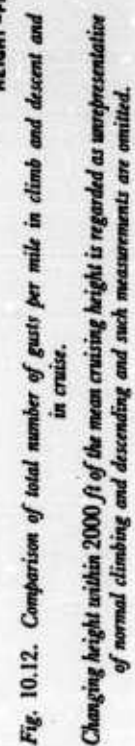
The formula (10.17) for the distribution of gusts, each consist of two exponentials. It would seem likely that they are due to different forms of turbulence and a comparison with the results of paragraph 10.4 on measurements in specific turbulence conditions confirms this conjecture.

The exponential distribution of gusts in 12,616 miles of thunderstorms gave a variation of  $\exp(-w/6.72)$ , which is 8 per cent more severe than the second exponential,  $\exp(-w/6.20)$  of the up-gusts of equation (10.17). The exponential distribution in the typical examples of cumulus of J. Taylor and Crane and Chilton are  $\exp(-w/3.45)$  and  $\exp(-w/3.55)$ , the average of which is 13 per cent more severe than the first exponential  $\exp(-w/3.10)$  of the up-gusts of equation (10.17). This agreement strongly suggests that the two exponentials of equation (10.17) are mainly for flights in cumulus and in thunderstorms. The numerical value achieved on the operational flights and given in equation (10.17) is more reliable than the 3 typical flights in cumulus but the amount of flying in thunderstorms is much the same in the controlled experiment in thunderstorms and in the whole of the 5 million miles of operational flying. On the other hand the operational flying will be on the fringes of the storms, rather than through the centre, wherever possible and an 8 per cent reduction in intensity seems not unreasonable.

The thunderstorm survey indicated a drop of intensity below about 15,000 ft and meteorological considerations would suggest that the intensity is rarely fully developed below 5000 ft. Thus there seems to be a justification

\* The conversion factor from alleviation factor to gust response factor is 1.12 for W. G. Walker and Copp's data compared with 1.21 for Bullen's.





for regarding the larger exponential of equation (10.17) as rather severe below 5000 ft. On the other hand the operational measurements have a greater proportion of large gusts at heights below 5000 ft. This is presumably due to the relative difficulty of avoiding turbulence at low levels by change of route. These two effects seem roughly to cancel out and the equations (10.17) can be used at all heights. Below 1000 ft the controlled experiments in clear air turbulence show that turbulence with an average distribution  $\exp(-w/1.95)$  is present at all times and in addition there are ground effects. Whilst it may be assumed that the fully developed thunderstorm turbulence is rarely present there is little information on the ground effects. The operational measurements actually give rather more high velocities than at higher altitudes and until further data are available the best estimate seems to be to assume the same distribution (10.17) holds at all heights but with  $N_0 \exp(-w/1.95)$  in addition to cover clear air turbulence.

The distribution of large gusts shows a preponderance at low altitudes and, even allowing qualitatively for the fact that thunderstorms will reach different heights, it seems that a large proportion are avoided at high altitudes and few are avoided below 10,000 ft. Thus any advantage that were sought for radar detection of turbulence would have to be the avoidance of storms that would not have been avoided by pilots without the radar aid.

#### 10.5.2. Seasonal Variations

A small counting accelerometer, which is referred to as a fatigue load meter, is carried on a large number of British aircraft. These include Viscounts of the British European Airways fleet and the Trans Australian Airways fleet. R. H. Taylor (1962) has analysed the records of 163,000 flying hours by B.E.A. for 4 years from mid 1957 and 41,000 flying hours by T.A.A. for 3 years from mid 1957.

In all cases the number of occurrences of increments of 0.25g, 0.55g, 0.95g up and down from straight and level flight were tabulated. The totals on a monthly basis are given in Tables 10.6 and 10.7 for B.E.A. and T.A.A. respectively. These occurrences of normal acceleration are mainly due to atmospheric turbulence but some of them are due to manoeuvres. The average frequency of occurrence of manoeuvres on a large amount of flying by civil aircraft was shown in Fig. 5.6. These values for the amount of flying done by the Viscounts are shown in Tables 10.6 and 10.7. Thus the number of accelerations due to gusts will be the total less those due to manoeuvres.

By assuming a distribution for the frequency of occurrence of gusts of different intensities it is possible to estimate the average conversion factor from normal acceleration to gust velocity. In paragraph 10.5 it is suggested that the frequency of occurrence of gusts may be represented by the sum of two exponential distributions, one that is predominantly in cumulus cloud conditions and one that is predominantly in thunderstorms. In the distribution of equation (10.17) the two exponents differ by a factor of 2, the down-gusts are 92 per cent of the size of up-gusts for the same frequency of occurrence and the number of gusts in thunderstorm conditions are 1.6 per cent of the total. By assuming that the two exponents are always in the ratio of two to one, two parameters, the total number of gusts per mile

Table 10.6. Number of Occurrences of Normal Accelerations at the Aircraft C.G. of Viscounts on British European Airways Service 1957-1961

Month	Flying hours	Total number of occurrences, quoted by R. H. Taylor (1962), at various normal accelerations					Estimated number of occurrences due to manoeuvres, from Fig. 5.6, at various normal accelerations						
		0.05g	0.45g	0.75g	1.25g	1.55g	1.95g	0.05g	0.45g	0.75g	1.25g	1.55g	1.95g
January	10,751	1	224	12,404	28,088	851	19		10	310	1027	132	9
February	8119	1	194	9464	21,808	616	15		8	234	775	100	7
March	8877	5	178	10,160	25,920	586	19		9	256	848	109	7
April	10,788	2	209	14,284	35,992	755	9		10	311	1030	133	9
May	12,869	7	275	17,103	40,779	909	25		12	371	1229	158	11
June	15,102	10	344	17,835	42,492	902	39	1	14	435	1442	186	13
July	17,915	13	409	20,725	48,770	1127	22	1	17	516	1711	220	15
August	19,985	17	451	21,495	49,394	1286	49	1	19	576	1909	246	17
September	19,764	7	323	18,361	44,469	1047	43	1	19	569	1887	243	17
October	16,090	10	320	15,320	36,413	989	35	1	15	463	1537	193	14
November	10,087	9	275	10,696	24,784	703	26		11	316	1047	135	9
December	11,715	12	320	14,457	31,261	928	33		11	337	1119	144	10
Total	162,940	94	3522	182,304	430,170	10,789	334	5	155	4693	15,561	2004	138

Table 10.7. Number of Occurrences of Normal Accelerations at the Aircraft C.G. of Viscounts on Trans Australian Airways Service 1957-1960

Month	Flying hours	Total number of occurrences, quoted by R. H. Taylor (1962), at various normal accelerations						Estimated number of occurrences due to manoeuvres, from Fig. 5.6, at various normal accelerations					
		0.05g	0.45g	0.75g	1.25g	1.55g	1.95g	0.05g	0.45g	0.75g	1.25g	1.55g	1.95g
January	5114	5	266	13,121	23,382	762	30		5	147	488	63	4
February	2313	2	122	5383	10,200	322	9		2	66	221	28	2
March	3022	2	111	5131	9605	263	9		3	87	288	37	3
April	3294	2	74	4767	10,213	315	12		3	95	315	41	3
May	3166	1	61	3371	7496	185	8		3	91	302	39	3
June	2960	0	67	3775	8154	230	13		3	85	283	37	2
July	3330	4	130	6072	11,630	354	21		3	96	318	41	3
August	3496	0	90	5908	10,807	289	8		3	101	334	43	3
September	2959	0	104	5681	10,063	267	13		3	86	283	36	2
October	3205	2	222	11,419	17,640	547	22		3	92	306	39	3
November	3049	8	225	9033	14,511	518	25		3	88	292	38	3
December	5205	15	514	15,453	28,746	1055	44	1	5	150	496	64	4
Total	41,113	41	1986	89,114	162,447	5107	214	1	39	1184	3926	506	35

in each direction and the proportion of gusts that are associated with thunderstorm conditions, are required to give the distribution for either up-gusts or down-gusts. A further parameter is needed to convert the data from normal accelerations into data for gust velocities.

The measurements of normal accelerations given in Tables 10.6 and 10.7 are at 3 levels above and 3 levels below  $1g$  (i.e. straight and level flight). If there were no relationship between the numbers of up and down gusts there would be just sufficient information to give the gust distributions. As there is a relationship there is redundant information and a best estimate

Table 10.8. *Total Number of Gusts, Estimated from the Frequency of Occurrence of Normal Accelerations in Table 10.6 for Viscounts on British European Airways Service*

The assumptions made are:

- (i) An increment of  $1g$  corresponds to a gust velocity of  $44.8$  ft/sec E.A.S.
- (ii) The average speed is  $270$  statute miles per hour.
- (iii) The number of gusts per mile greater than  $w$  ft/sec E.A.S. is given by

$$pN_0 [(1 - x) \exp(-w/2.79) + x \exp(-w/5.58)] \text{ for down-gusts}$$

$$pN_0 [(1 - x) \exp(-w/3.10) + x \exp(-w/6.20)] \text{ for up-gusts.}$$

- (iv) The values of  $pN_0$  and  $x$  are determined from the frequency of occurrence of increments of normal acceleration of  $0.25g$  and  $0.55g$  but the conversion from acceleration to gust velocity of assumption (i) was previously chosen so that the values of  $pN_0$  and  $x$  for the total flying gave a good estimate of the frequency of occurrence of increments of normal acceleration of  $0.95g$ .

Month	$pN_0$			$x\%$		
	Down	Up	Mean	Down	Up	Mean
January	0.208	0.309	0.259	1.77	2.48	2.12
February	0.205	0.324	0.264	2.29	2.07	2.18
March	0.208	0.371	0.290	1.64	1.03	1.44
April	0.250	0.430	0.340	1.09	0.81	0.95
May	0.247	0.404	0.325	1.38	1.02	1.20
June	0.210	0.362	0.286	2.03	0.75	1.39
July	0.205	0.344	0.275	2.13	1.09	1.61
August	0.187	0.304	0.246	2.40	1.56	1.98
September	0.168	0.283	0.226	1.65	1.00	1.32
October	0.166	0.276	0.221	2.37	1.71	2.04
November	0.160	0.263	0.211	3.51	2.72	3.11
December	0.212	0.317	0.265	2.67	2.37	2.52
Total	0.199	0.328	0.264	2.03	1.43	1.73
Average values given in equation (10.17)			0.58	1.60		

has to be made. In addition, the number of increments of  $0.95g$  is small and can only be used practically when grouped together.

In the first place the totals for Table 10.6 are taken to estimate one gust distribution for the up-gusts and one gust distribution for the down-gusts. Similar totals are obtained from Table 10.7. The relative size of the down-gust and up-gust is estimated for both groups and the average of the two groups shows that down-gusts are 90 per cent of the size of the up-gusts for the same frequency of occurrence. This average value is assumed to hold generally. The totals for Tables 10.6 and 10.7 are next taken separately to

Table 10.9. Total Number of Gusts, Estimated from the Frequency of Occurrence of Normal Accelerations in Table 10.7 for Viscounts on Trans Australian Airways Service

The assumptions made are:

- (i) An increment of  $1g$  corresponds to a gust velocity of  $41.2$  ft/sec E.A.S.
- (ii) The average speed is  $270$  statute miles per hour.
- (iii) The number of gusts per mile greater than  $w$  ft/sec E.A.S. is given by  
 $pN_0 [(1-x) \exp(-w/2.79) + x \exp(-w/5.58)]$  for down-gusts  
 $pN_0 [(1-x) \exp(-w/3.10) + x \exp(-w/6.20)]$  for up-gusts
- (iv) The values of  $pN_0$  and  $x$  are determined from the frequency of occurrence of increments of normal acceleration of  $0.25g$  and  $0.55g$  but the conversion from acceleration to gust velocity of assumption (i) was previously chosen so that the values of  $pN_0$  and  $x$  for the total flying gave a good estimate of the frequency of occurrence of increments of normal acceleration of  $0.95g$ .

Month	$pN_0$			$x\%$		
	Down	Up	Mean	Down	Up	Mean
January	0.347	0.421	0.384	1.42	2.08	1.75
February	0.308	0.407	0.358	1.88	1.88	1.88
March	0.226	0.304	0.265	1.66	0.94	1.30
April	0.203	0.287	0.245	0.53	1.55	1.04
May	0.145	0.229	0.187	0.96	0.26	0.61
June	0.176	0.261	0.218	0.91	0.98	0.94
July	0.244	0.325	0.284	1.63	1.55	1.59
August	0.239	0.296	0.267	0.49	0.80	0.64
September	0.264	0.326	0.295	1.03	0.83	0.93
October	0.488	0.512	0.500	1.26	1.86	1.56
November	0.385	0.428	0.406	2.34	2.71	2.52
December	0.354	0.493	0.423	4.21	2.99	3.60
Total	0.287	0.364	0.326	1.80	1.80	1.80
Average values given in equation (10.17)			0.58	1.60		

estimate the conversion factor from normal acceleration of the aircraft to vertical velocity of gusts. A different conversion factor can be calculated for up-gusts and for down-gusts. The average of the two is then assumed to hold for the individual months.

In examining the variation between months only the numbers of gusts at

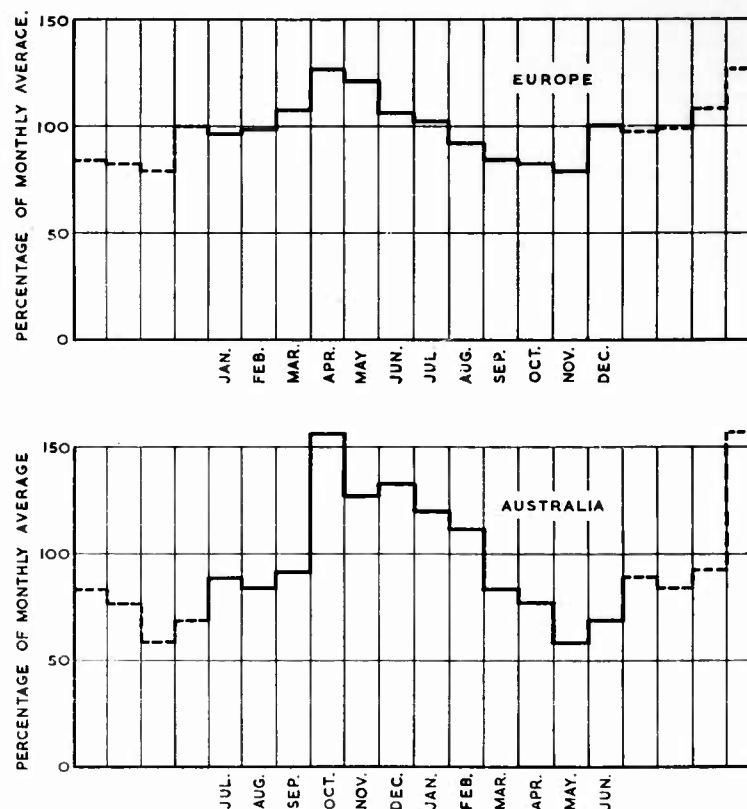


Fig. 10.13. Seasonal variation in frequency of occurrence of gusts encountered by Viscounts.

increments of  $\pm 0.25g$  and  $\pm 0.55g$  are used. The up-gusts and down-gusts are taken separately and the following parameters are calculated

- (i) the total number of gusts per mile ( $pN_0$ )
- (ii) the proportion of gusts that are associated with thunderstorm conditions ( $x$ ).

The calculated values of  $pN_0$  and  $x$  are given in Tables 10.8 and 10.9.

The total number of gusts per mile is rather less than the average of the flying from a variety of aircraft as given in equation (10.17). This is not

surprising as it depends markedly on the average flight plan of the particular aircraft. The difference between European and Australian flying is probably mainly due to the longer flights in Europe, 1.8 hr compared with 1.5 hr, with correspondingly greater time at higher altitudes. In the absence of a detailed average flight plan the numerical value of the total number of gusts cannot be used but the variation with the seasons can. The monthly variation of the total number of gusts is shown in Fig. 10.13. The frequency of occurrence is a maximum in the spring and a minimum in the autumn in both Europe and Australia but the difference between the two extremes is greater in Australia.

The overall proportion of thunderstorm type of condition is roughly the same in Europe and in Australia and each is close to the average given in equation (10.17). There is, however, a seasonal variation and thunderstorms occur most frequently in mid-summer and mid-winter. In Australia the summer activity is by far the more pronounced. In Europe the variation is not very marked but the mid-winter tends to be the more frequent. The accuracy of predicting the proportion of thunderstorms to the total is not high but it does give an indication of the relative frequency of occurrence of large and small gusts. The number of occurrences of 0.95g increments, predicted from those of 0.25g and 0.55g for each month, agree reasonably well with the measured values having regard to the fact that the numbers involved are rather small.

## REFERENCES

- |  |                                |
|--|--------------------------------|
| Anon ASTIA (1959a)                     | Pratt and Walker, W. G. (1954) |
| Bullen (1961)                          | Press and Steiner (1958)       |
| Bullen (1963)                          | Saunders, K. D. (1961)         |
| Copp and Fetner (1959)                 | Taylor, J. (1953)              |
| Crane and Chilton (1956)               | Taylor, R. H. (1962)           |
| Gorelic, Kostarev and Chernikov (1958) | Tofelson (1956)                |
| Hall, J. (1962)                        | Walker, W. G., and Copp (1959) |
| Houbolt, Steiner and Pratt (1962)      | Zbrozek (1953)                 |
| Ludlam (1963)                          |                                |



**CHAPTER 11**  
**BUFFETING TURBULENCE**

**CONTENTS**

11.1 Introduction	245
11.2 Flight in the wake of other aircraft	245
11.2.1 Trailing vortices	246
11.2.2 Refuelling	249
11.3 Wake of dive brakes	251
11.4 Turbulence near cavities such as bomb-bays	256
11.5 Wing buffeting	259
References	260

## CHAPTER 11

### BUFFETING TURBULENCE

#### 11.1 INTRODUCTION

The passage of any part of an aircraft through the air produces turbulence in its wake. Any turbulence so produced that influences the structural loads on the aircraft itself, or on other aircraft, is referred to as buffeting. This buffeting turbulence is influenced in varying degrees by the aircraft structure. The turbulence that is least influenced by structural parts is the complete wake of one aircraft that is encountered by another aircraft. In buffeting of an aircraft due to itself it is most difficult, in general, to break down the combined motion of the air and the aircraft structure into air turbulence and the resultant structural loads. This reaches an extreme when the buffeting turbulence is generated by the structural part that is most affected structurally, e.g. control surface and bomb-bay buffeting.

It is possible to describe the turbulent wake of an aircraft at distances of thousands of feet behind it in terms that are independent of the following aircraft. As the distance between the aircraft is reduced the interaction becomes appreciable and when the aircraft are very close to each other such as during refuelling the data are insufficient to determine the loads on the following aircraft in terms of a wake and a transfer function. A limiting case of one aerofoil surface following in the vicinity of the wake of another surface is that of a tailplane. In some ways this is more amenable to separation into a buffeting turbulence and a transfer function to give the structural loads, as the two aerofoils are structurally connected through the fuselage.

Wings frequently produce buffeting turbulence of such magnitude that the wing itself is said to be buffeting. The turbulence at particular points of the wing can be described but it will be so closely associated with the aerodynamic and structural features of the wing itself that it is hardly amenable to extrapolation to other aircraft. Dive brakes and open cavities, such as bomb-bays, also produce buffeting turbulence but in these cases the forms for different aircraft are sufficiently near that some general features can be described.

#### 11.2 FLIGHT IN THE WAKE OF OTHER AIRCRAFT

The wake behind an aircraft consists essentially of the following three components:

- (i) Turbulence from the engines.
- (ii) Turbulence from the boundary layer surrounding the airframe surface.
- (iii) Trailing vortices.

Andrews (1954) investigated each of these three components separately for the wake behind a Meteor aircraft. He showed that the turbulence in the neighbourhood of the jets from the engines decayed rapidly and was negligible about 250 ft behind the jet exit at 10,000 ft. The turbulence produced behind the fuselage and other drag producing bodies was much less than that behind the jets of the engines and decayed more rapidly. Thus the disturbances at large distances beyond a turbo-jet aircraft will be predominantly due to the trailing vortices. It may be expected that this would apply to propeller driven aircraft also. Even for aircraft undergoing refuelling the trailing vortices are likely to produce more loads than the turbulence.

#### 11.2.1. *Trailing Vortices*

Classical aerodynamic theory predicts that a wing lifting surface will shed a vortex sheet from its trailing edge. This sheet rapidly rolls up into two vortices near the wing tips which then pass downstream as trailing vortices. For an elliptic spanwise wing loading the circulation for each of the vortices is

$$K = 4W/\pi\rho bU \quad (11.1)$$

where  $K$  = the circulation (ft<sup>2</sup>/sec)

$W$  = the aircraft weight (lb)

$\rho$  = the air density (slugs/ft<sup>3</sup>)

$b$  = the wing span (ft)

$U$  = the aircraft true velocity (ft/sec)

and the centres of the vortices are at a distance  $\pi b/8$  from the centre line of the aircraft. Kaden (1931) made a theoretical investigation of the phenomena and estimated that, for elliptic spanwise wing loading, each trailing vortex is essentially rolled up at a distance  $0.280 Ab/C_L$  behind the wing

where  $A$  = the wing aspect ratio

$b$  = the wing span

$C_L$  = the lift coefficient

The time corresponding to this distance is  $0.280 AbU/C_L$ , which, by using equation (11.1), can be given as

$$Kt_0/(\pi b/4)^2 = 0.289 \quad (11.2)$$

where  $t_0$  = the time the aircraft has flown past any point before the trailing vortices are essentially rolled up.

As the trailing vortices pass further downstream they will decay. Various writers including Lamb (1932) have shown that for practical purposes the decay of turbulent flow may be represented in a similar manner to that used for laminar flow by replacing the air viscosity by an empirical eddy viscosity. Squires (1954) suggests that the eddy viscosity may be assumed to be proportional to  $K$ . Thus the laminar viscosity  $\nu$  should be replaced by

$(\nu + aK)$  where  $a$  is a constant. Practical values of  $aK$  are so much greater than  $\nu$  that  $\nu$  may be neglected in studying the decay of the vortices.

A rigorous solution is possible if it is assumed that

- (i) the vortices start as line vortices immediately behind the wing,
- (ii) the flow in each of the two vortices is independent.

Assumption (i) cannot hold whilst the vortex sheet behind the wing is rolling up into two trailing vortices, but the time taken is so short (equation (11.2)) that for most purposes it may be ignored. However, the diameter of the rolled up vortex may be somewhat different from that given by the rigorous solution. An adjustment could be made for the time of the rolling up process, either by assuming a much higher viscosity than subsequently or by assuming a longer time, whilst retaining the two basic assumptions for the rigorous solution. In the analysis that follows no adjustment is made as there is insufficient evidence to suggest the amount.

The solution given by Lamb (1932) for each trailing vortex is

$$\zeta = (K/4\pi aKt) \exp(-r^2/4aKt) \quad (11.3)$$

$$w_r = (K/2\pi r) [1 - \exp(-r^2/4aKt)] \quad (11.4)$$

where  $\zeta$  = the circulation at a radius  $r$

$w_r$  = the circumferential velocity at a radius  $r$

$t$  = time

The velocity of the air at any point will be the sum of the velocities due to the two vortices. Measurements of the vertical velocity along a straight line through the two axes of the vortices can be used to estimate the eddy viscosity of an aircraft wake. On traversing a wake the vertical velocity will increase to a maximum followed by either one or two minima (peak downward velocity) between the two axes and a final maximum before leaving the wake. Kraft (1955) made measurements of the wake of a small propeller-driven fighter aircraft span 37.3 ft by flying another aircraft as near as possible at right angles to the wake and through the axes of the trailing vortices. For each traverse it is possible to determine the value of the constant  $a$  that would give the same difference between the maximum and minimum vertical velocities measured. These ranges of velocity have been estimated from Kraft's original paper and are given in Fig. 11.1. Rose and Dee (1963) have made measurements of the range of vertical velocity of a number of traverses in the wake of a Comet 3B. These are also shown in Fig. 11.1. In order that curves for different values of  $a$  may be shown the velocities and times are given in the non-dimensional forms  $(w_{\max} - w_{\min})(\pi b/4)/K$  and  $Kt/(\pi b/4)^2$ .

Qualifications to these data are essential before they can be used generally. In both sets of flight tests an attempt was made to assess the persistence of trailing vortices on calm days. Any atmospheric turbulence that might have been present would reduce the persistence and the equivalent eddy viscosity would be correspondingly increased. Unfortunately in addition the actual flights would not be precisely through the axes of the vortices and this error

must always produce an apparent eddy viscosity that is also too high. The experimental points in Fig. 11.1 that are most likely to be in serious error due to the flights not being precisely through the axes of the vortices are those for the shorter times when the size of the vortices is smaller: this is especially so for the wakes of the small fighter.

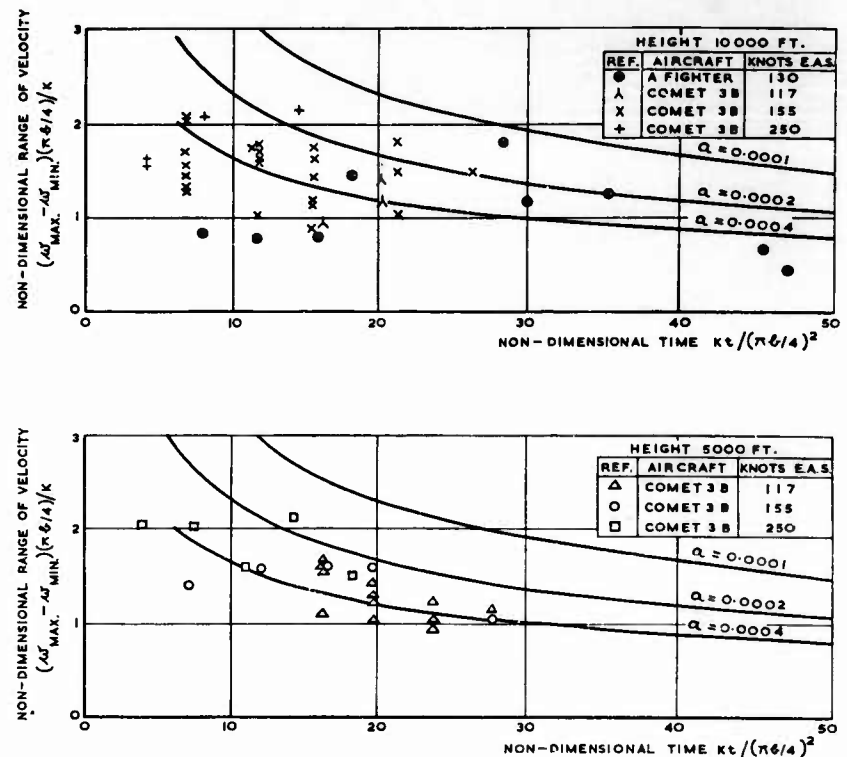


Fig. 11.1. Range of vertical velocity across trailing vortices of an aircraft. Measurements on Comet 3B by Rose and Dee (1963) and on a propeller-driven fighter by Kraft (1955) are compared with calculations based on two vortices at distances  $\pi b/8$  from the aircraft centre-line each with a circumferential velocity  $w_r$  at a radius  $r$  given by

$$w_r = \frac{K}{2\pi r} [1 - \exp(-r^2/4aKt)]$$

where  $K$  = the circulation;  $aK$  = eddy viscosity;  $t$  = time.

The theory, on which the curves for different values of  $a$  have been based, will break down when the motions of the two vortices can no longer be assumed to be independent. When mixing is appreciable it is likely that the effective eddy viscosity will increase rapidly and the vortices will collapse. Some empiricism is necessary, but it seems reasonable to suppose that the mixing will depend on the proximity of the minima vertical velocities of the two vortices. The minima will approach each other as the vortices travel

downstream and, even on the theory that the motions of the vortices are independent, they will coincide when

$$Kt/(\pi b/4)^2 = 1/16\pi a \quad (11.5)$$

Kerr and Dee (1959b) estimated the intensity of the vortices of a 4 piston-engined bomber (Lincoln) by flying a small 2 piston-engined transport (Devon) through them at a slight angle to the direction of the axes and finding the maximum aileron angle that was necessary to compensate for the change in vertical velocity along the span of the Devon. It was found that the vortices from the Lincoln persisted for about 120 sec with the flaps down at 110 knots E.A.S. and 200 sec with the flaps up at 130 knots E.A.S. In both conditions the rate of decay was rapid just before final collapse of the vortices. In the clean condition the vortices were so intense that full aileron was required on the Devon flying behind the Lincoln up to 160 sec after the vortices had been initiated by the Lincoln. There was a rapid decay for all longer separation times. In the flaps down condition full aileron was required on the Devon up to a separation of 60 sec. The necessary aileron angles decreased slowly between 60 and 100 sec separation but between 100 sec and 120 sec the decay is of the order of ten times more rapid.

A rough estimate has been made of the persistence of vortices of a number of aircraft. These are compared with the times given by equation (11.5) in Table 11.1. The value of eddy viscosity cannot be estimated very accurately and it is assumed somewhat arbitrarily from Fig. 11.1, on the assumption that all experimental errors will give higher values for eddy viscosity, that  $0.0002 K$  is a reasonably representative value.

It should be appreciated that the comparison of measured and calculated times in Table 11.1 is based on a small amount of data. The time at which final decay occurs is probably related to the time given in equation (11.5) but no evidence is available on the relationship. However, the measured values of the estimated duration are from about 30 to 50 per cent of the calculated values, with no marked differences between aircraft. As all experimental errors will tend to produce measured times that are low it seems reasonable on present evidence to use equation (11.5) as an upper limit for the duration of the trailing vortices.

There are several conditions that will reduce the duration of trailing vortices. Whenever atmospheric turbulence is present it will reduce the time. Near the ground there will be a further reduction due to friction of the vortex system with the ground. Also the aircraft generating the vortices will normally be flying with flaps down and the effective axes of the vortices will be closer together and will therefore begin to mix sooner.

#### 11.2.2. Refuelling

When an aircraft is being refuelled in the air it must fly close to the tanker and is therefore in the vicinity of its wake. The separation time is of the same order as that required for the trailing vortices to become essentially rolled up. The idealized solution (equation (11.4)) for circumferential velocity gives the radius  $r_c$  at which the velocity is a maximum as

$$r_c/(\pi b/4) = \sqrt{[1.26 \times 4aKt/(\pi b/4)^2]} \quad (11.6)$$

Table 11.1. Persistence of Trailing Vortices from Aircraft without Flaps Down

Reference	Aircraft	Speed knots E.A.S.	Height ft	Span b ft	Circulation K ft <sup>2</sup> /sec	Time	
						Calculated by equation (11.5) with $a = 0.0002$ sec	Max. measured sec
Kerr and Dee (1959b)	Lincoln	130	6000	120	1470	608	200
Kraft (1955)	Propeller- driven fighter	130	10,000	37.3	669	127	60
Andrews, D. R. (1954)	Meteor	248	15,000	37.3	702	120	17*
Andrews, D. R. (1954)	Meteor	188	32,000	37.3	1247	68	17*
Rose and Dee (1963)	Comet 3B	155	5000	115	1930	414	115
Rose and Dee (1963)	Comet 3B	117	5000	115	2550	314	90
Rose and Dee (1963)	Vulcan	200	3000	99	1870	324	115
Rose and Dee (1963)	Vulcan	175	10,000	99	2400	254	105

\* The trailing vortices were strong after 17 sec but no measurements were made at greater times.

This reduces, for a time for roll-up given by equation (11.2) and for the typical value of  $a = 0.0002$ , to

$$r_c/(\pi b/4) = 0.017 \quad (11.7)$$

The experimental evidence given in paragraph 11.2.1 indicates that  $a = 0.0002$  is a typical value for long separation times, but this is not strictly applicable to the rolling up process. A higher value of  $a$  should presumably be used in equation (11.6) to obtain an estimate of  $r_c$ . The tankers used for refuelling will have a span of the order of 150 ft so equation (11.7) gives  $r_c$  a value of 2 ft, which is probably rather lower than would be found in practice. Thus the depth of the wake due to the trailing vortices is of the order of 4 ft or a little more.

The rest of the wake is either turbulence from the jets of the engines or turbulence from the boundary layer. Both types of turbulence can be considered as homogeneous isotropic turbulence with perturbations. In this way the scale of the turbulence may be defined in the manner described in

Chapter 9. It is shown in Chapter 12 that the scale of the turbulence in the immediate vicinity of the jets from the engines is about  $\sqrt{x D}/5$ , where  $D$  is the exit diameter of the jet and  $x$  is the distance downstream. This gives a scale of turbulence of about 4 ft. There is less direct evidence of the scale of turbulence in the wing or fuselage boundary layer but a rough indication of the order of the scale should be obtained by replacing the diameter of the jet by the diameter of the fuselage. This should give a scale of turbulence of about 12 ft.

Thus the salient dimensions of the three components of the wake, trailing vortices, turbulence from the engines, turbulence from the airframe are all of the order of 5–12 ft. It seems, therefore, that as far as the aircraft that is being refuelled is concerned the scale of the turbulence in the wake is so small that it will be greatly alleviated by the aircraft gust response factor. However, the loads due to flying in and out of the wake may be quite large.

Wallace (1961) points out that "most of the loads during refuelling are caused, at least on the B-52, by pilot input rather than by a turbulent effect from tanker wash. The pilot is constantly manoeuvring, trying to keep the large, flexible airplane in position". The analysis given above suggests that the turbulent effect of the tanker wash should not be significant for any except small aircraft. It is proposed, therefore, to treat loads during refuelling as one would those of manoeuvres. Data are available on normal accelerations experienced during refuelling on the B-52 from Wallace (1961) and Kelly and Broom (1962) and on the B-47E from Durkee (1961). Figure 11.2 gives the frequency of occurrence of these normal accelerations. The data from the B-52 are from 237.8 flying hours of refuelling compared with only 9.4 flying hours on the B-47E. The curves shown for the B-47E are plotted for each frequency of occurrence at 75 per cent of the increment of acceleration of the B-52. In both cases the curves are the same at low increments for up and down accelerations but at high increments the down accelerations occur more frequently than the up accelerations. The flights on the B-52 cover the range of marks B-52B to B-52G at a variety of bases. There does not seem to be any significant difference in the measurements due to height, speed or all-up weight and consequently all the data are grouped together in the one diagram.

### 11.3 WAKE OF DIVE BRAKES

Dive brakes are incorporated in aircraft to increase the total drag. This is achieved by deliberately introducing turbulence into the airstream round the aircraft. Fail, Owen and Eyre (1955) have examined the air flow round flat plates and the measurements on the turbulence is of general value in studying any buffeting turbulence. Their work on flat plates in isolation shows up the characteristics of turbulence in the absence of other bodies. Some experiments on plates attached to a solid fuselage shape indicate the interaction of two aerodynamic forms in the absence of appreciable structural flexibility.

A square flat plate 5 in.  $\times$  5 in. was tested in a wind tunnel at airspeeds of the order of 100 ft/sec. The airflow was examined in a plane about 15 in.



downstream of the plate for different angles of incidence of the plate to the airstream. In the present analysis attention is confined to incidences that are sufficiently high to produce a turbulent flow behind the plate. A survey was made of the mean square of the fluctuating velocity in the direction of the stream, i.e. twice the longitudinal component of the energy of turbulence per unit mass. A point was then chosen in the neighbourhood of maximum

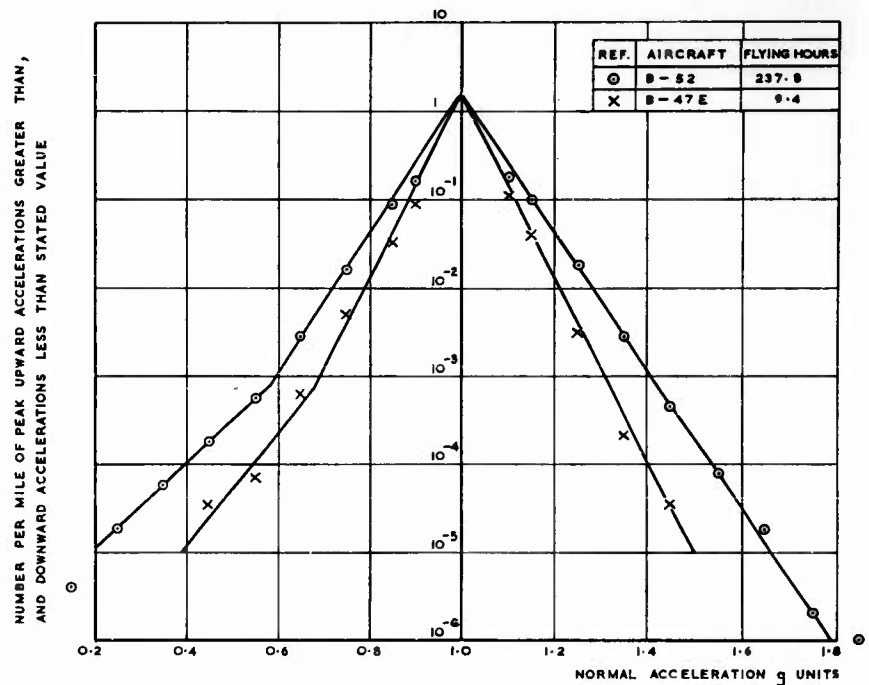


Fig. 11.2. Normal accelerations on aircraft whilst being refuelled in flight.

energy and the distribution of this energy at different wavelengths was determined. For convenience of presentation the fluctuating velocity is given as a proportion of the stream velocity. The concept of energy at different wavelengths is the same as that used for atmospheric turbulence moving in a stream past a given point. Distances are measured as the length of stream passing the point. Provided the change in turbulence with distance is not too great compared with its scale there should be little error in regarding the turbulence at the point in the plane of measurement as isotropic and homogeneous. This is equivalent to a stream extending for a great distance each side of the point without change of character. Of course the equivalent stream will be different for each measuring point.

In order to define the turbulence by means of a few parameters only, it will be given in two parts, one the equivalent homogeneous isotropic turbulence

and the other the additional turbulence necessary to produce the total. The homogeneous isotropic turbulence will be estimated on the assumption that it may be represented by the formulae of Chapter 9 for the von Kármán model (equations (9.38) to (9.42)). All the measurements by Fail, Owen and Eyre (1955) were of the longitudinal component of turbulence energy density. The corresponding equation for von Kármán's model is

$$S_u(k) = 4 \sigma_u^2 L / [1 + \{2\pi (1.339L)k\}^2]^{5/6} \quad (9.39)$$

(repeated)

where  $\sigma_u$  = r.m.s. longitudinal velocity

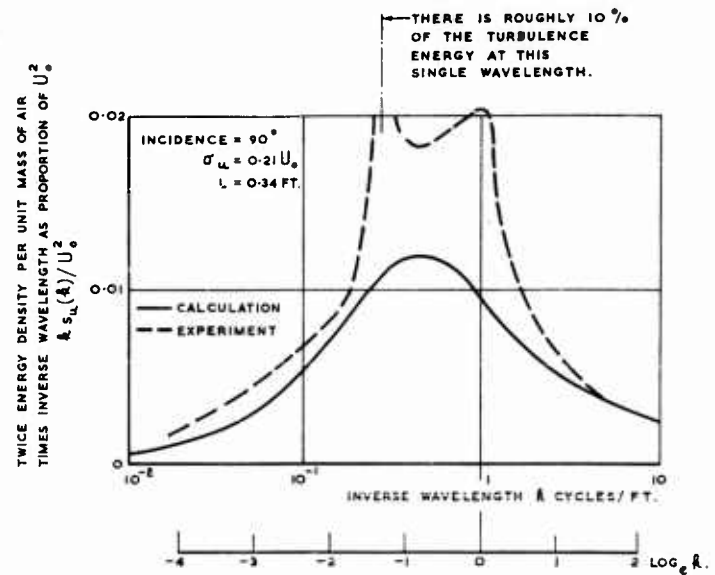
$L$  = scale of turbulence      ft

$k$  = inverse wavelength      cycles/ft

$S_u(k)$  = longitudinal component of energy density with respect to inverse wavelength.

Figure 11.3 shows the distribution of energy of turbulence for different angles of incidence of the plate. The calculated distribution that is shown is that given in equation (9.39) with the measured total r.m.s. longitudinal velocity used for  $\sigma_u$  and the scale of turbulence  $L$  selected by inspection to give the best fit between the calculated and experimental curves. It was shown in Chapter 2 by means of equation (2.5) that the total energy is the area under the curve  $kS_u(k)$  and the axis  $\log_e k$ . In the practical measurements the energy will be within a band of wavelengths dependent on the limitations of the instruments used, whereas the calculated curve is the energy from zero to infinite wavelengths. On the other hand the practical measurements will include all turbulence, not merely that that may be regarded as homogeneous and isotropic turbulence. It is evident from Fig. 11.3 that the measured turbulence at each incidence consists of two parts, (i) energy at a single wavelength and (ii) a continuously varying energy density at all wavelengths measured. Fail, Owen and Eyre (1955) observed that the energy at a single wavelength was produced by a regular shedding of vortices. In the present analysis it is assumed that all very sharp peaks in the original curves were due to energy at single frequencies and a rough assessment of the amount of this energy is 10 per cent for  $90^\circ$  incidence, 20 per cent for  $60^\circ$  and small for  $40^\circ$ . No measurements were made at different positions and an assessment of the rate of breakdown of the vortices is not possible. The data are not extensive and so the general agreement of shape at both high and low inverse wavelengths may not be of wide application to other buffeting; it should be appreciated in making the comparison that in the calculated curves a change in  $\sigma_u$  increases all the amplitudes in the same proportion and a change in the only other parameter  $L$  moves the curves, as drawn, bodily to right or left without change of shape. The scale of turbulence is of the same order as the dimensions of the plate exposed to the air stream.

The distribution of energy of turbulence downstream of a similar plate hinged to a body of typical fuselage shape with maximum diameter 7 in. is



(Part 1)

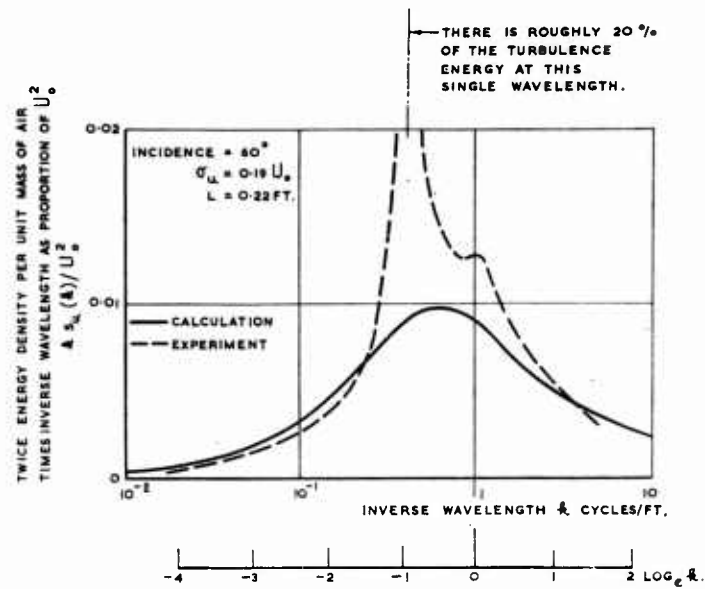
Fig. 11.3. Distribution of energy of turbulence per unit mass of air  $\{ \frac{1}{2} S_u(k) \}$  at different wavelengths behind a  $5 \times 5$  in. flat plate.

Measurements by Fail, Owen and Eyre (1955) of longitudinal component of energy are compared with

$$S_u(k) = 4\sigma_u^2 L / [1 + \{2\pi(1.339L)k\}^2]^{5/6}$$

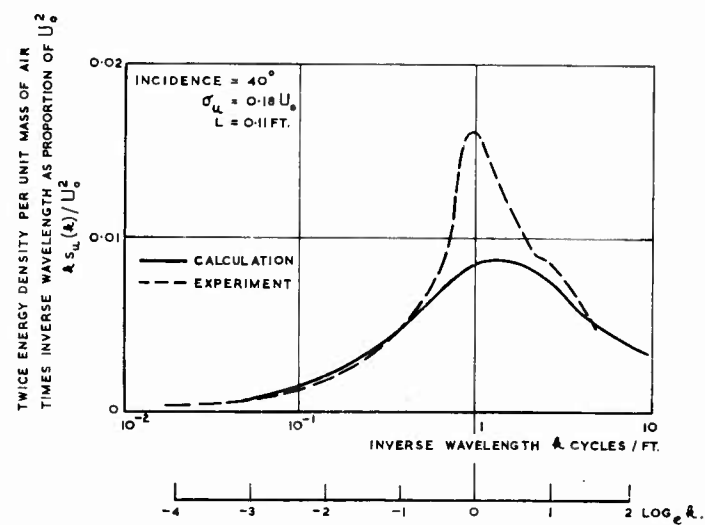
where  $\sigma_u$  = measured r.m.s. longitudinal velocity;  $U_0$  = stream velocity;  $L$  is chosen by inspection to give the best fit between the calculated and experimental curves. The distribution was determined at a point near to the position of maximum turbulence in a plane 15.3 in. downstream for incidences of  $40^\circ$  and  $60^\circ$  and 11 in. downstream for an incidence of  $90^\circ$ .

# BUFFETING TURBULENCE



(Part 2)

Fig. 11.3. (continued)



(Part 3)

Fig. 11.3. (continued)

shown in Fig. 11.4. The general characteristics of the distribution remain the same. About 10 per cent of the energy due to a regular shedding of vortices and the scale of the turbulence is a little higher than that for a plate isolated from a body. Figure 11.5 shows the distribution of energy when the flat plate is replaced by a cascade of 11 vanes forming a plate of 3.54 in.  $\times$  3.54 in. with an effective thickness of about  $\frac{1}{2}$  in. With this configuration

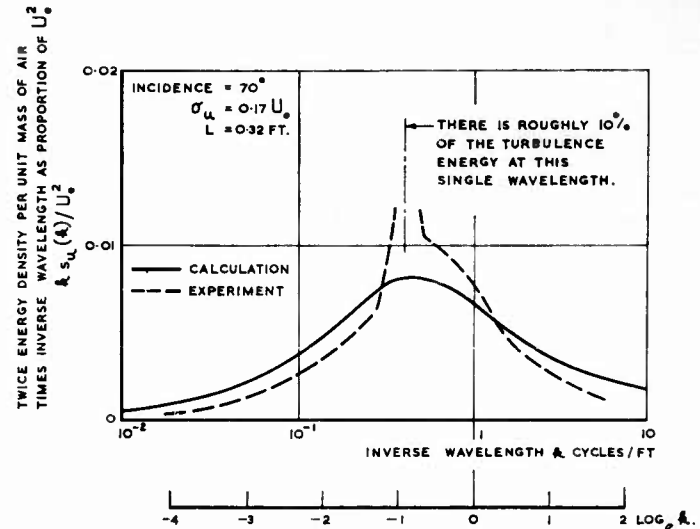


Fig. 11.4. Distribution of energy of turbulence per unit mass of air  $\{ \frac{1}{2} S_u(k) \}$  at different wavelengths behind a  $5 \times 5$  in. flat plate below a fuselage-type body with maximum diameter 7 in.

Measurements by Fail, Owen and Eyre (1955) of longitudinal component of energy are compared with

$$S_u(k) = 4\sigma_u^2 L / [1 + \{2\pi(1.339L)k\}^2]^{5/4}$$

where  $\sigma_u$  = r.m.s. longitudinal velocity;  $U_0$  = stream velocity; value of  $\sigma_u$  was not measured so  $\sigma_u$  and  $L$  were chosen by inspection to give the best fit between the calculated and experimental curves.

The distribution was determined at a point 9.8 in. below centre-line of body and 15 in. downstream of the hinge attaching the plate to the body.

the energy due to shedding of vortices is not apparent at the position of the measurements and the measured distribution is roughly the same as the calculated one. The scale of the turbulence is rather less than that of the flat plate attached to the body.

#### 11.4 TURBULENCE NEAR CAVITIES SUCH AS BOMB-BAYS

The presence of a cavity, such as a bomb-bay, in a fuselage interferes with the air flow over the fuselage and turbulence is set up in and around the

cavity. Quantitative measurements have been made only on the surface of the body. As the primary interest has been to determine the loads on the structure the measurements have mainly been of pressure and the data have been used to predict the air motion. One of the consequences of this procedure is that the formulae of Chapter 9 cannot be compared directly with the experimental results.

Rossiter (1962) has made a systematic study of rectangular holes in flat plates and given a few comparisons with representative models of typical

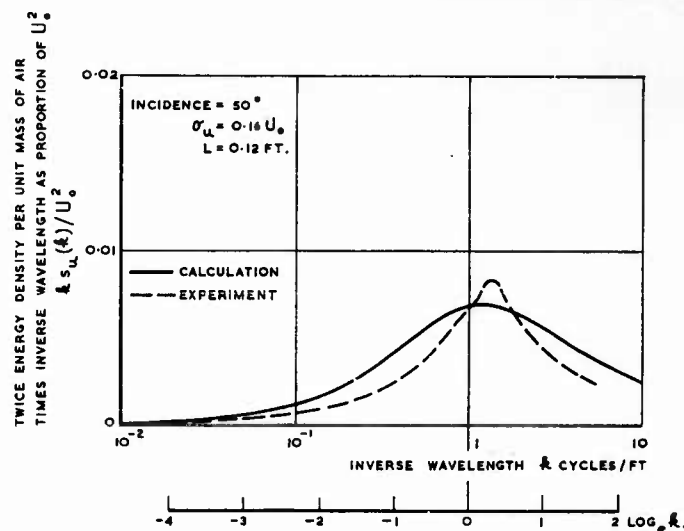


Fig. 11.5. Distribution of energy of turbulence per unit mass of air  $\{ \frac{1}{2} S_u(k) \}$  at different wavelengths behind a cascade of 11 vanes forming a plate  $3.54 \times 3.54$  in. below a fuselage-type body with maximum diameter 7 in.

Measurements by Fail, Owen and Eyre (1955) of longitudinal component of energy are compared with

$$S_u(k) = 4\sigma_u^2 L / [1 + \{2\pi(1.339L)k\}^2]^{5/6}$$

where  $\sigma_u$  = measured r.m.s. longitudinal velocity;  $U_0$  = stream velocity;  $L$  is chosen by inspection to give the best fit between the calculated and experimental curves.

The distribution was determined 15 in. downstream of the hinge at a point on the centre line of the plate and body near to the position of maximum turbulence.

aircraft designs. Measurements were made along the centre line of the cavity on the roof, the front and rear walls and a short distance downstream. The distribution of the mean square of the pressure at different wavelengths was determined at each point. The analyser that was used determines the mean square of the pressure over a band of inverse wavelengths and the width of the band is a constant fraction  $\epsilon$  of the mid inverse wavelength  $k$  of the band. Thus for small values of  $\epsilon$  it may be assumed that the density of the

mean square pressure is constant over the bandwidth and that the measurement is

$$\epsilon k \cdot S_p(k)$$

where  $S_p(k)$  is the density of the mean square pressure at inverse wavelength  $k$ .

The measurements are quoted in non-dimensional form as

$$\sqrt{k \cdot S_p(k)/q_D}$$

where  $q_D$  is the tunnel kinetic pressure.

At each point  $S_p(k)$  is a function of  $k$  but it will not be the same function as  $S_u(k)$ . No attempt is made in the present analysis to determine the relationship of  $S_u(k)$  and  $S_p(k)$  even in the flow region at a distance from the surfaces of the fuselage and cavity. Thus there is no theoretical formula for  $S_p(k)$ .

Rossiter (1962) found that the distribution of  $k \cdot S_p(k)$  was of two parts,

- (i) a continuously varying density of (pressure)<sup>2</sup> at all the inverse wavelengths measured,
- (ii) a number of pressure levels at discrete inverse wavelengths.

Rossiter deduced the following empirical formula to give the inverse wavelengths at which discrete pressures occur.

$$k = (m - \gamma_1)/(L_c/\gamma_2 + L_c M) \quad (11.8)$$

where  $m = 1, 2, 3 \dots$

$L_c$  = length of the cavity

$M$  = Mach number

$\gamma_1, \gamma_2$  = constants that depend on the cavity.

For deep cavities, i.e. depth at least  $\frac{1}{2}$  length,  $\gamma_1 = 0.25$  and for shallower ones  $\gamma_1$  is greater. Average values, over a speed range  $M = 0.4$  to  $1.2$ , for rectangular cavities in flat plates are given in Table 11.2.

Table 11.2. Values of Constant  $\gamma_1$  in Equation (11.8) for Rectangular Cavities in Flat Plates

Ratio of length to depth	$\gamma_1$
1	0.25
2	0.25
4	0.25
6	0.38
8	0.54
10	0.58

The values of  $\gamma_2$  are approximately 0.6 for all ratios of length to depth. This value must be regarded as empirical as the flow within the cavity is quite different for the deep and shallow cavities. The dominant frequencies that were present depended on the Mach Number but integer values of  $m$  from 1 to 4 were found for most of the cavities. Unfortunately these data and other data by Norton (1952) are not sufficient to make general estimates of the magnitude of these pressures.

The shape of the distributions of the continuously varying density are fairly similar at all points measured along the centre line of the cavity. It is difficult to make general conclusions. Until further data become available it may be inferred from Rossiter (1962) and Owen (1958) that at least up to  $M = 1.2$  the pressure fluctuations are most intense near the rear wall of the cavity and decrease rapidly downstream: that the density with respect to inverse wavelength of (pressures)<sup>2</sup> is proportional to the external stream kinetic pressure. The value of  $kS_p(k)/q^2$  has a maximum of about  $10^{-4}$  for deep cavities (i.e. length less than twice depth) and about  $2 \times 10^{-3}$  for shallow cavities. This maximum occurs roughly at an inverse wavelength of  $1/10D_c$  for the shallow cavities and at  $1/L_c$  for the deep cavities, where  $D_c, L_c$  are the depth and length of the cavities. For lower inverse wavelengths  $S_p(k)$  is approximately constant and for the higher ones  $S_p(k)$  is approximately proportional to  $k^{-10/3}$ .

### 11.5 WING BUFFETING

The turbulence of a wing that initiates buffeting of the wing itself is more complex than any of those forms of turbulence that have been considered so far. The available data are all concerned with the combined effect of the aerodynamic and structural characteristics of wings. T. B. Owen (1958) and Pearcey (1958) each regard the onset of buffeting as the stage at which the turbulence influences appreciably the circulation round the wing. T. B. Owen (1958) concentrates on measurements of the mean square pressure at different inverse wavelengths and notes that this onset of buffeting is associated with a sudden rise of mean square pressure at low inverse wavelengths with gradually increasing incidence. He arbitrarily chooses the pressure fluctuations at an inverse wavelength of  $5l$ , where  $l$  is a representative aerodynamic length, as a basis for comparing the onset of buffeting; he states that the frequency associated with this wavelength and buffeting speed of full-scale aircraft is roughly equal to the natural frequency of the wing structure. Pearcey notes that this onset of buffeting is conveniently marked by a distinct divergence in the variation of mean static pressure at the trailing edge.

Both methods have a limited application in that they depend on measurements at isolated points and in addition do not give a quantitative estimate of the magnitude of the turbulence. More data are essential before an assessment can be made of their full usefulness. Pearcey and Holder (1962) suggest that work in progress by C. L. Bore might help to make quantitative estimates on the basis that the magnitude of the buffeting loads are related to the mean divergence of the trailing edge pressure. Fail (1962) gives a number of measurements of mean square pressures, including those of



T. B. Owen (1958). This method can be applied to an assessment of the local pressures and is applicable to cases such as the local effects on panels beneath a steady vortex flow. The estimates should be amenable to quantitative assessment for these local areas.

## REFERENCES

- |                                    |                           |
|------------------------------------|---------------------------|
| Andrews, D. R. (1954)              | Owen, T. B. (1958)        |
| Durkee (1961)                      | Pearcey (1958)            |
| Fail, Owen, T. B., and Eyre (1955) | Pearcey and Holder (1962) |
| Fail (1962)                        | Rossiter (1962)           |
| Kaden (1931)                       | Rose and Dee (1963)       |
| Kelly and Broom (1962)             | Spreiter and Sacks (1951) |
| Kerr and Dee (1959b)               | Squires (1954)            |
| Kraft (1955)                       | Wallace (1961)            |
| Lamb (1932)                        | Wetmore and Reeder (1963) |
| Norton (1952)                      |                           |

CHAPTER 12  
NOISE TURBULENCE

CONTENTS

12.1 Introduction	263
12.2 Turbulence in a subsonic air jet	264
12.3 Pressures in the near field of a jet engine	266
12.3.1 Effect of jet velocity on pressure distributions	271
12.4 Use of models	273
12.5 Rockets	274
12.6 Pressure fluctuations in flight	275
12.7 Test facilities	276
References	277

## CHAPTER 12

### NOISE TURBULENCE

#### 12.1 INTRODUCTION

Loads are developed in the aircraft structure in the neighbourhood of the jets from the engines. The air is expelled from the jet pipe at a velocity relative to the neighbouring air. In the jet itself the energy of the turbulence is high and the resulting local loads that would be imposed on a structure would be high also. At the boundary of the jet there is a region where there is extensive mixing of this highly turbulent air of the jet and the surrounding air. In the jet itself the turbulence is carried downstream at the stream velocity and is estimated from measurements of the turbulence velocity. In the mixing region measurements are available of the velocities and pressures of the turbulence. With increasing distance from the jet the stream velocity reduces and the pressure disturbances are transmitted as sound. The subsequent loading on a structure is affected by the presence of the structure. The turbulence velocities are modified by the structure and the sound pressures are reflected by the surface of the structure.

The problem of defining jet noise loads can be reduced to that of defining the distribution of turbulence velocities or pressures in the near field of typical or idealized jet engines in the absence of any other objects, then estimating its interaction with the structure and finally determining the load on the structure. This last step is so closely concerned with the actual design that it need only be considered in the present context to the extent needed to obtain a better understanding of the earlier steps. Attention will actually be concentrated mainly on the distribution of pressure fluctuations in the near field of jet engines when uninfluenced by the aircraft structure. It should be emphasized, however, that the interaction between the jet noise and the structure is highly complex and at present theoretical bases for calculation are very limited. It is possible that a fully satisfactory theory might require more details on the jet noise than is currently available. On present knowledge the important parameters that influence the loads are the overall mean square pressure, its distribution over different frequencies and the correlation between pressures at neighbouring points. The dimensions over which the correlation is of interest depend on the form of structure that might be encountered. It is shown in paragraph 12.3 for the region of the jet boundary that the wavelength, at which an octave band of pressure or velocity fluctuations is a maximum, is about  $1.33 D\sqrt{Z}$  where  $D$  is the jet exit diameter and  $Z$  is the ratio of distance downstream of the jet exit to the jet exit diameter. So for a typical jet engine of about 2 ft diameter the wavelength of peak intensity will be 2 ft at one diameter distance rising to 8 ft at 9 diameters distance from the jet exit. At a jet velocity of 1800 ft/sec these correspond to 900 c/sec and 225 c/sec. These frequencies are of the same

order as the natural frequencies of panels commonly used in aircraft structures.

Turbulence of the same order of scale also occurs in the boundary layers surrounding an aircraft surface. Much less data are available on this form of turbulence but two small sets of flight data are available that make it possible to compare the intensity of turbulence in the boundary layer and in the near field of a jet engine.

## 12.2 TURBULENCE IN A SUBSONIC AIR JET

Measurements have been made by Laurence (1956) of the turbulence velocities of a small subsonic jet. The jet exit diameter was 3.5 in. A range of velocities was investigated and it is possible to form general opinions on

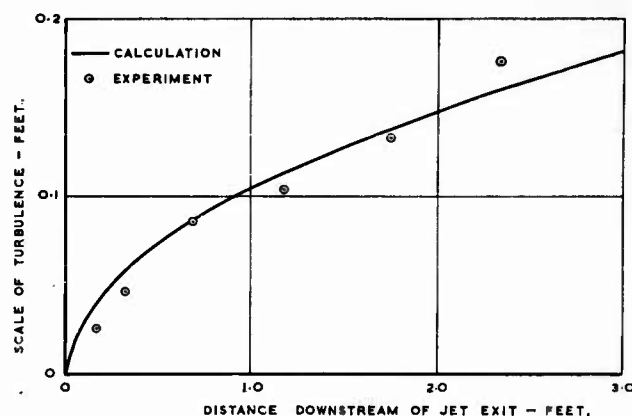


Fig. 12.1. Scale of turbulence in a subsonic jet at various distances downstream. Measurements (Laurence, 1956) at a distance from the jet centre line equal to half the exit diameter are compared with

$$L = 0.194 \sqrt{x D}$$

where  $L$  = scale of turbulence

$x$  = distance downstream of jet exit

Jet velocity = 342 ft/sec

$D$  = jet exit diameter = 3.5 in. (i.e. 0.292 ft)

the turbulence in jets from a series of the tests at 342 ft/sec. All available measurements in the near field of jet engines are of pressure fluctuations along or outside the jet boundary. A direct comparison of these subsonic jet measurements and the jet engine pressure measurements is not possible. However measurements at a radial distance  $\frac{1}{2}D$  from the jet axis for a range of distances downstream should give an indication of the conditions arising in the vicinity of the jet boundary. The longitudinal velocity  $u$  was measured, the density of twice the turbulence energy per unit mass  $S_u(k)$  (i.e. mean

square longitudinal turbulence velocity) was estimated and also the scale of turbulence  $L$  using the formula (9.18). These calculated values of scale of longitudinal turbulence are given in Fig. 12.1, and the distribution of mean square longitudinal velocity at different inverse wavelengths  $k$  is given in Fig. 12.2.

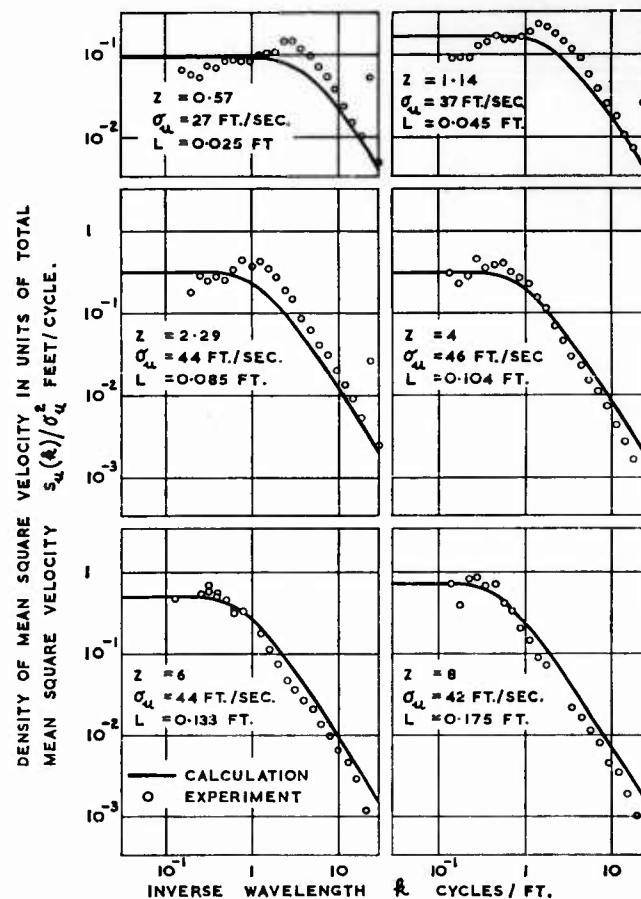


Fig. 12.2. Distribution of mean square longitudinal velocity  $S_u(k)$  at different inverse wavelengths  $k$  in a subsonic jet.

Measurements (Laurence, 1956) made at various distances downstream and at a distance from the jet centre line equal to half the exit diameter are compared with

$$S_u(k) = 4L\sigma_u^2/[1 + \{2\pi(1.339L)k\}^2]^{5/8}$$

where  $\sigma_u$  = measured total r.m.s. longitudinal velocity

$L$  = measured scale of turbulence

$Z$  = distance downstream of jet exit in units of jet exit diameter

Jet exit diameter = 3.5 in.; jet velocity = 342 ft/sec

The measurements of the scale of turbulence are compared with

$$L = 0.194 \sqrt{x} D \quad (12.1)$$

where  $x$  = distance downstream of jet exit ft

and the measurements of  $S_u(k)$  are compared with

$$S_u(k) = 4L\sigma_u^2/[1 + \{2\pi (1.339 L)k\}^{5/6}] \quad (9.39)$$

(repeated)

where  $\sigma_u$  = measured total r.m.s. longitudinal velocity ft/sec

$L$  = measured scale of turbulence ft  
(as given in Fig. 12.1)

for the range of positions downstream.

The value of the coefficient in equation (12.1) of 0.194 was chosen so that the maximum value of  $kS_u(k)$ , for  $S_u(k)$  given by equation (9.39), would occur at

$$kD = 0.75/\sqrt{Z} \quad (12.2)$$

where  $Z = x/D$

The agreement between the calculated and measured scale of turbulence is good. However, the other measurements by Laurence (1956) show considerable variation across the jet and also he suggests that beyond  $Z = 8$  there may be a different form of turbulence along the line at a radial distance  $\frac{1}{2}D$  from the jet axis. For the purpose for which it is now being used, i.e. to indicate the conditions along the jet boundary, it seems inappropriate to consider positions for  $Z$  much greater than 8 as they will be rather far from the jet boundary and will be more representative of the jet stream than of the mixing zone.

The measurements that are quoted in Fig. 12.2 are for  $S_u(k)/\sigma_u^2$ . Thus any errors that might be present in the estimates of  $\sigma_u^2$  will result in an error in  $S_u(k)/\sigma_u^2$  at all values of  $k$ . Also if the turbulence consisted in part only of the form, given by equation (9.39), there would be a difference at all values of  $k$ . There is a moderate scatter, between the different positions, in the overall measured values of  $S_u(k)$  but at high values of  $k$ ,  $S_u(k)$  varies approximately with  $k^{-5/3}$  as does the calculated curve. There is a considerable difference at low values of  $k$  between the measured and calculated values particularly near the jet exit where turbulence is being fed into the stream. The measured values of  $\sigma_u^2$  are also in agreement with the concept that turbulence energy is being fed into the stream near the jet exit. At distances beyond  $4D$  the turbulence energy per unit mass begins to reduce gradually.

### 12.3 PRESSURES IN THE NEAR FIELD OF A JET ENGINE

Investigations have been made of the near field of jet engines by Howes *et al.* (1957) and by Wolfe (1957). In both cases pressure measurements only

were made. As in the measurements of pressure, quoted in paragraph 11.4 for turbulence near bomb-bay cavities, the analysers determine the mean square pressure over a band of inverse wavelengths and the width of the band is a constant fraction  $\epsilon$  of the mid-inverse wavelength  $k$  of the band. In all the results quoted the pressures were for either  $\frac{1}{3}$  octave bands (i.e.  $\epsilon$  approximately 0.246) or the whole band of the pressures measured. The mean square pressures are all quoted in decibels, this being the normal scale for investigations of sound pressures. Thus the overall mean square pressure is  $10 \log_{10} (\sigma_p/2 \times 10^{-4})^2$  decibels, where  $\sigma_p$  = root mean square pressure in dynes/cm<sup>2</sup>. The measurements of  $\frac{1}{3}$  octave bands are in decibels and as  $\epsilon$  is small they will be equal to

$$\epsilon k \cdot S_p(k)$$

where  $S_p(k)$  is the density of the mean square pressure at inverse wavelength  $k$ .

As the relationship between  $S_u(k)$  and  $S_p(k)$  has not been obtained the distribution for  $S_p(k)$  cannot be compared with a theoretical formula even in the turbulent jet stream.

The contours of the overall mean square pressure in the near field of a jet engine, and outboard of the jet boundary, are given in Fig. 12.3. The coordinates of the field are distance downstream of the jet exit and radial distance from the jet axis and in both cases the distances are given in units of jet exit diameter. There is good agreement between the shapes of the contours from Jet engine A and those from Jet engine B. Jet A has a slightly higher exit diameter and exit velocity and the resultant pressures are somewhat higher especially near the jet boundary. However, it is suggested that the measurements for Jet A, which are over a larger field than those for Jet B, may be regarded as typical for any jet engine with exit velocity 1850 ft/sec. If the scaling procedure described in paragraph 12.4 were used, the estimated contours for Jet B would be a reasonable representation.

The overall pressure level is of only limited value in determining the loads that would be applied on any structure in the near field. The components of the mean square pressure also need to be known. Howes *et al.* (1957) and Wolfe (1957) both give the contours of the  $\frac{1}{3}$  octave bands. Howes *et al.* (1957) have analysed their results at selected positions along the jet boundary and give the distribution of  $\frac{1}{3}$  octave band mean square pressures for different frequencies in cycles per second. The distributions are plotted on log-log scales and "best" straight lines are plotted above and below the frequency at which the  $\frac{1}{3}$  octave band mean square pressure is a maximum. The slopes of these lines are used to estimate the values of  $m$  that correspond to distributions  $kS_p(k)$  proportional to  $k^m$ . These are given in Table 12.1. Similar estimates are deduced from Wolfe's data for three distances downstream. For low values of  $k$ , the average value of  $m$  is 2 and for high values of  $k$  it is close to  $-\frac{5}{3}$ . The scatter on the results is rather high for low values of  $k$  but for high values of  $k$  there is not much scatter. This value of  $S_p(k)$  being proportional to  $k^{-8/3}$  (i.e.  $kS_p(k)$  proportional to  $k^{-5/3}$ ) at high inverse wavelengths does not differ much from Batchelor's (1953) prediction that  $S_p(k)$  should be proportional to  $k^{-7/3}$  when  $S_u(k)$  is proportional to  $k^{-5/3}$ .

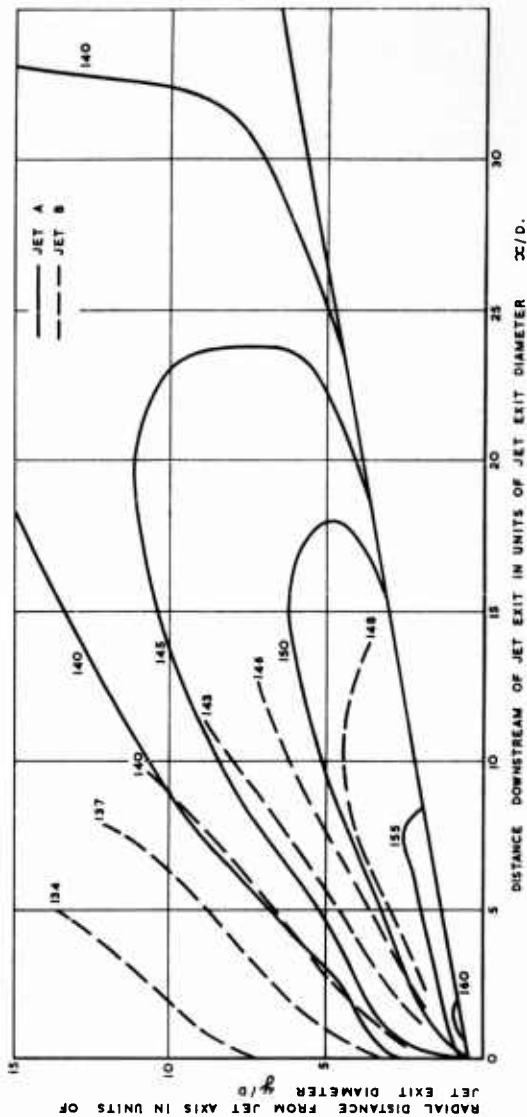


Fig. 12.3. Contours of overall mean square pressure in the near field of jet engines.

	Jet exit diameter ft	Jet exit velocity ft/sec	Maximum thrust lb
Jet A. Howes et al. (1957)	1.85	1850	9600
Jet B. Wolfe (1957)	1.75	1800	5000

Pressures given in decibels, which are defined as  
 $10 \log_{10} (\sigma_p / 2 \times 10^{-4})^2$  where  $\sigma_p =$  r.m.s. pressure in dynes/cm<sup>2</sup>.



Table 12.1. *Distribution of Density of Mean Square Pressures  $S_p(k)$  at Different Inverse Wavelengths  $k$  for Various Distances along the Jet Boundary*  
*Estimates are made of the values of  $m$  that give a good fit for a distribution  $kS_p(k)$  proportional to  $k^m$*

Basic data	Distance from jet exit in units of exit diameter $Z$	Value of $m$ for $k$ below position of max $kS_p(k)$	Value of $m$ for $k$ above position of max $kS_p(k)$
Howes <i>et al.</i> (1957)	0.44	2.3	-1.3
	1.31	2.6	-1.5
	2.44	2.6	-1.9
	3.56	2.2	-1.7
	4.69	2.0	-1.6
	8.34	1.3	-1.7
	10.8	1.7	-2.1
	14.1	1.8	-2.3
	16.7	1.1	-2.1
	25	2.3	-1.7
	33.4	2.0	-1.7
	Average	2.0	-1.7
Wolfe (1957)	5	insufficient data	-1.6
	10	insufficient data	-1.8
	15	insufficient data	-1.9
	Average		-1.7

The values of frequency in cycles per second can be changed to inverse wavelength by the relationship

$$k = f/U$$

where  $f$  = frequency c/sec

$U$  = jet velocity ft/sec

$k$  = inverse wavelength cycles/ft

In the jet itself the stream velocity is  $U$  and the wavelengths have a direct physical meaning. The inverse wavelengths can be given in non-dimensional form  $kD$ , which is a suitable way for comparing distributions in the near field but its meaning is not directly obvious at points away from the jet where the stream velocity is not  $U$ . The values of  $kD$  at which  $kS_p(k)$  is a maximum in Howes *et al.* (1957) investigation along the jet boundary are shown in Fig. 12.4 for various distances downstream. The values of  $kD$  at which  $kS_u(k)$  is a maximum in Laurence (1956) investigation, at a radial

distance of  $\frac{1}{2}D$  of a subsonic air jet, is also shown for various distances downstream. The pressure measurements on the supersonic jet boundary of a jet engine and the longitudinal velocity measurements in the subsonic air jet both agree well with the formula that the value of  $kD$ , at which  $kS_p(k)$  or  $kS_u(k)$  is a maximum, is

$$kD = 0.75/\sqrt{Z} \quad (12.2)$$

(repeated)

Figure 12.4 and Table 12.1 can be combined to give the distribution of  $kS_p(k)$  for all values of distance downstream. This is done in Fig. 12.5,

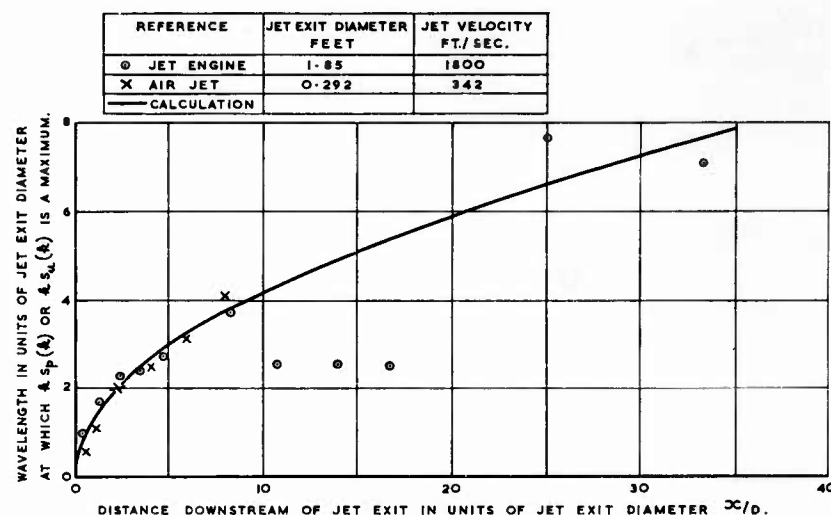


Fig. 12.4. The variation with distance downstream of the inverse wavelength at which  $kS_p(k)$  or  $kS_u(k)$  is a maximum.

Pressure measurements on a jet engine (Howes et al., 1957) along the jet boundary and longitudinal velocity measurements on an air jet (Laurence, 1956) at a distance from the jet centre line equal to  $\frac{1}{2}D$  are compared with

$$r = kD = 0.75\sqrt{D/x}$$

In the velocity measurements the maxima are those corresponding to the curves of  $S_u(k)$  plotted in Fig. 12.2.

which gives the distribution of mean square pressure levels at different inverse wavelengths for all positions along the jet boundary. The distribution is given in terms of the overall mean square pressure which can be deduced from Fig. 12.1. This simple distribution gives a good representation of the density of the mean square pressure for values of  $k/(0.75/\sqrt{x}D)$  greater than unity, for all distances downstream up to the extent of the measurements  $33.4D$ . For values lower than unity there will be considerable departure from this average distribution and the departures do not seem to

be related to the distance downstream. There is also considerable variation in the distribution near the position of maximum density of mean square pressure. Usually the peak would be less pronounced than the curves indicate but the data are not sufficiently consistent to justify recommending an adjustment to the distributions of the figure.

### 12.3.1. Effect of Jet Velocity on Pressure Distributions

So far all the experimental results that have been quoted are for jet velocities of about 1800 ft/sec. Greatrex (1955) has proposed that the overall

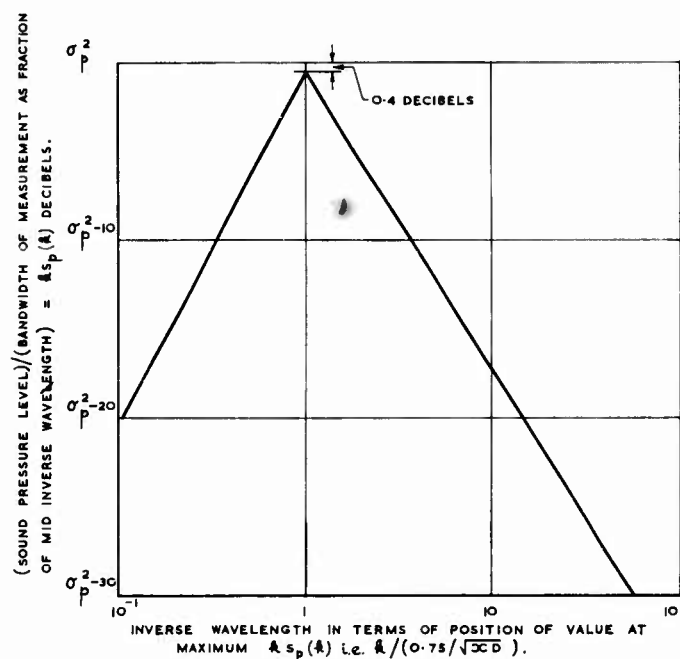


Fig. 12.5. Distribution of mean square pressure levels at different inverse wavelengths for all positions along the jet boundary.

The shape of the distribution is the average of Table 12.1 for all distances downstream. The maximum value is that given in Fig. 12.4.

r.m.s. pressure should vary as (jet velocity)<sup>n</sup> and that the value of *n* should depend on the form of the jet and on the position in the field. Extensive measurements have been quoted by Wolfe (1957) and Clarkson (1960) of overall pressures for a range of jet speeds and the contours of values of *n* deduced. These are shown in Fig. 12.6 for the two different jet engines. Estimates for three isolated positions are available from Howes *et al.* (1957) and are shown also. It is found for all three engines that *n* approximates to 4 at a large distance from the jet exit. This agrees with the theoretical estimate

of Lighthill (1952), by dimensional analysis, that the overall sound intensity at a given point in the neighbourhood of a jet should be given by

$$\text{Intensity proportional to } \rho_0 U^8 a_0^{-5} D^2 \quad (12.3)$$

where  $\rho_0$  = ambient density outside the jet stream

$U$  = jet exit velocity

$a_0$  = speed of sound external to jet stream.

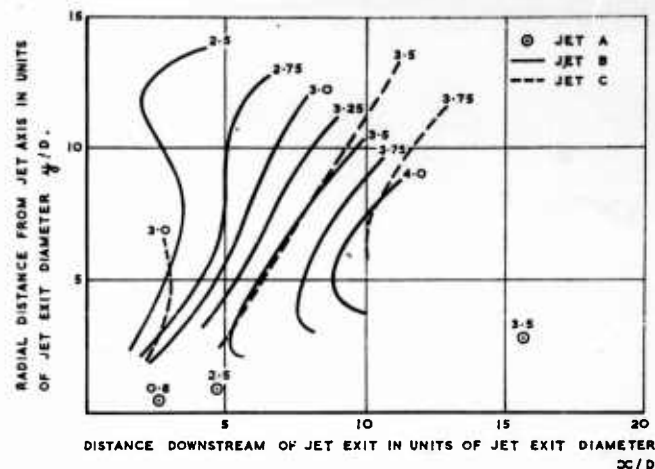


Fig. 12.6. Variation of velocity index  $n$  in the near field of a jet engine.

	Jet exit diameter ft	Jet exit velocities ft/sec	Maximum thrust lb
Jet A. Howes <i>et al.</i> (1957)	1.85	1000–1800	9600
Jet B. Wolfe (1957)	1.75	1660–1900	5000
Jet C. Clarkson (1960)	1.73	1300–1985	10,000

Value of  $n$  determined on assumption that overall root mean square pressure varies as (jet exit velocity) $^n$ .

Figure 12.6 shows that the value of  $n$  is much less than 4 in the near field. The variation in contours of  $n$  from one jet to another may be fairly large but for small changes of jet exit velocity it should be possible to use Fig. 12.6 to predict the change in the contours of overall mean square pressure.

This diagram does not give any information regarding a possible change, in the distribution of density of mean square pressure with inverse wavelength, due to change in jet velocity. Howes *et al.* (1957) examined the longitudinal

correlation of pressure at a distance  $2.16D$  downstream for a range of jet velocities from 630 to 1780 ft/sec. The longitudinal correlation on a distance basis of overall pressure varied very little for velocities of 1290, 1620, 1780 ft/sec and the change was small even for 630 ft/sec. The correlation function  $f_p(r)$  is related to  $S_p(k)$  by

$$S_p(k) = 4\sigma_p^2 \int_0^{\infty} f_p(r) \cos(2\pi kr) dr \quad (12.4)$$

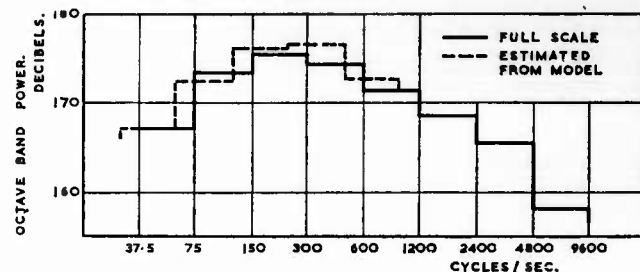
and therefore the distribution of  $S_p(k)$  remains the same. It is more accurate practically to make the comparison on  $f_p(r)$  than on  $S_p(k)$  as large changes in  $f_p(r)$  usually correspond to smaller changes in  $S_p(k)$ .

#### 12.4 USE OF MODELS

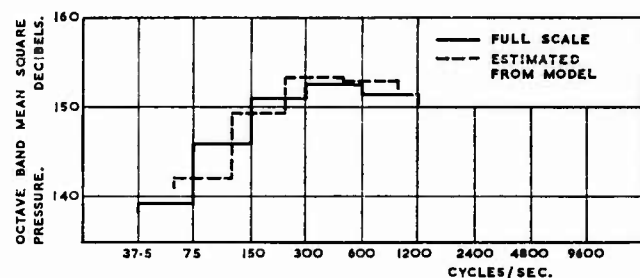
There is good evidence in Figs. 12.1 and 12.2 that the longitudinal turbulence in the jet stream of a small subsonic air jet can be represented by equation (9.39), where the scale of the turbulence is given by equation (12.1). This representation is non-dimensional provided the overall mean square pressure  $\sigma_p^2$  can be given non-dimensionally. There is further evidence in Fig. 12.4 that equation (12.1) can be used to give the scale of turbulence on the jet boundary of a jet engine with supersonic stream velocity. Furthermore the pressure distributions on the jet boundary of the jet engine indicate that the scale of turbulence remains the same for jet velocities from 630 to 1780 ft/sec. Thus it is to be expected that for the stream itself the value of  $kS_p(k)/\sigma_p^2$  at every point will be the same for a model or for full-scale, where the coordinates of each point are given in units of  $D$  and hence corresponding  $k$ 's are inversely proportional to  $D$ . Outside the jet boundary the turbulence has different characteristics and the evidence quoted is not so directly applicable.

Sutherland and Morgan (1961) made model tests on the B-52 to see whether these scaling laws apply in the near field outside the jet boundary. It was shown in Fig. 12.6 that the overall mean square pressure is proportional to  $U^{2n}$  but that  $n$  varies over the whole field. Sutherland and Morgan (1961) conducted their model tests at the same air density and jet velocity as full scale thus the speed of sound remains the same and it would be expected that  $\sigma_p^2$  should be proportional to  $l^2$ , where  $l$  is a typical length of the aircraft or its model. Figure 12.7 shows a comparison between the pressure measurements on a B-52 and on a  $1/10$ th scale model. As all the readings were made of octave band measurements they have been shown as histograms with the frequency in octaves. The actual measurements are quoted for the full-scale tests and the values, estimated on the basis of the above similarity conditions, are quoted from the model tests. This series of experiments is on jets with structures present in the near field so that structural scaling effects are included together with the turbulence and sound effects. The agreement is good for the overall sound power radiating from the jet and for the distribution of power at different frequencies in full-scale cycles per second. Mean square pressure distributions are compared in matched pairs at 52

test points on the model and on the full-scale wing. There was a standard deviation of about 2 decibels between the individual readings of the octave band mean square pressures. The average of the 52 points is shown in Fig. 12.7 and the estimates from the model tests agree well with the full scale measurements.



A. POWER LEVELS.



B. PRESSURE LEVEL ON WING.

Fig. 12.7. Comparison of sound measurements on a model and full scale.

Measurements (Sutherland and Morgan, 1961) on a B-52 are compared with scaled estimates from a  $\frac{1}{50}$  scale model. Total power is estimated from measurements 200 ft from the jet exit. Full-scale overall power is 180.6 decibels and that estimated from the model 181.2 where the decibels are  $10 \log_{10} (\text{power}/10^{-13} \text{ watts})$ .

The pressures are the average from 52 test points on model and on full-scale wing. Pressure decibels are  $10 \log_{10} (\text{r.m.s. pressure}/2 \times 10^{-4} \text{ dynes/cm}^2)^2$ .

## 12.5 ROCKETS

The information that is available on rockets is much less than that for jet engines. A few general features may, however, be noted.

The noise generation is of the same form in both cases, turbulence is set up downstream of the exit and this in turn produces noise. The speed of the jet is higher and the flow at the nozzle usually more stable. Both these effects tend to delay the start of the turbulence. In a jet engine turbulence normally seems to start at the nozzle whereas in a rocket it may be delayed for a number of diameters. Some model tests by Mull and Erickson (1957)

have given a delay of about 20 diameters. The overall sound-pressure-level along the jet boundary displays the same corresponding delay in build up. At about 20 diameters the  $\frac{1}{3}$  octave band mean square pressure is fairly uniform up to about  $kD = 0.05$  and thereafter decays roughly as  $k$  to the power  $-\frac{5}{3}$ .

This displacement of the commencement of the turbulence in the jet makes the design of nozzle even more important for rockets than for jet-engines. In consequence prediction of the near-field noise distribution in advance of measurements on an actual motor is of even less value than for a jet-engine.

## 12.6 PRESSURE FLUCTUATIONS IN FLIGHT

Noise measurements have been made by Shattuck (1961) on a fighter aircraft on the ground and in flight. The microphones were placed on the side of the fuselage at about  $4\frac{1}{2}$  diameters downstream and  $4\frac{1}{2}$  diameters inboard from the jet engine exit nozzle. The noise level on the ground was 135 decibels at an engine rating of 99 per cent power. The jet velocity is not given, nor is the jet noise compared with the values on the free-field side. However the overall value is probably reasonably compatible with the values that could be predicted from paragraph 12.3.

The noise measured in flight is much closer to the noise that would be expected from boundary layer noise than noise from a jet even though the microphones were placed in a position where the jet noise was probably the most intense for any place on the structure. Under steady flying conditions the ratio of sound pressure to dynamic pressure did not change much with Mach No. between 0.4 and 0.8 and did not change much with height between 10,000 ft and 30,000 ft. These are shown in Fig. 12.8 and compared with boundary layer noise measurements by Mull and Algranti (1960) near the nose of another aircraft.

When power is taken from the engines in excess of that required to overcome drag, such as in a climb or in accelerated flight, there is an increase in the sound pressure level. The density of mean square pressure is fairly constant over a wide range of frequencies in the level flight condition, but the increase due to excess power tends to be over a small bandwidth of frequencies at a mean of about 200 c/s for small excesses and changing to a mean of about 600 c/s for large excesses. In the actual numerical example given by Shattuck there was a change of overall noise level of 2 decibels on increasing engine power from idling (64 per cent maximum power) to 99 per cent maximum power at 20,000 ft. It is implied that the engine was put into an idling condition and then increased to 99 per cent maximum power whilst the aircraft was flying at a Mach No. of 0.55. The steady speed level flight condition corresponding to 99 per cent maximum power is greater than a Mach No. of 0.8, and the final change in noise level would be at least 6 decibels increase on the steady state value of about 126 decibels at Mach No. 0.55. As far as aircraft structural loads are concerned the jet noise contribution in flight is not great. Account could probably be taken of it merely by assuming that the full value of the boundary layer noise was achieved a little faster than the aircraft achieved its speed.

## 12.7 TEST FACILITIES

The description of jet noise has been concentrated mainly on that in the free-field in the neighbourhood of the engine run on the ground. The flight work is somewhat limited but it does indicate that the contribution

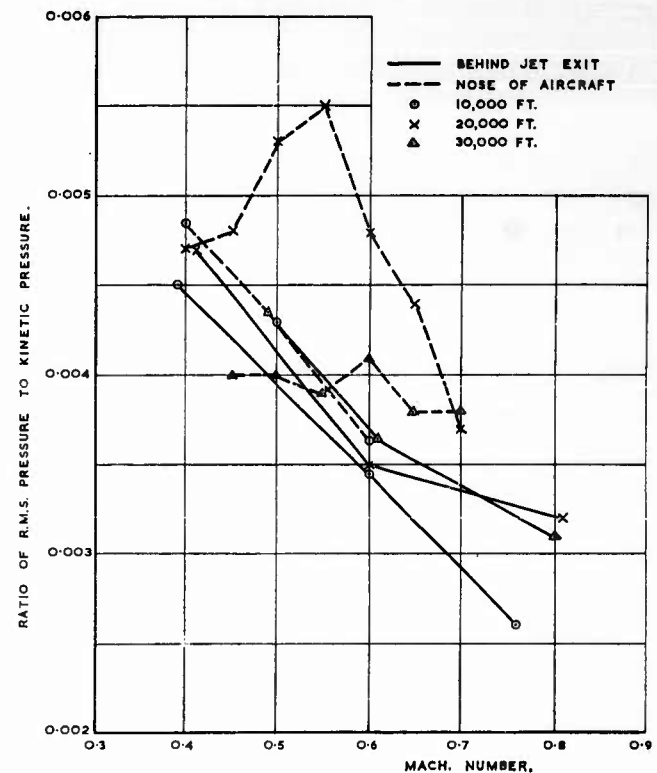


Fig. 12.8. Comparison of mean square pressures in flight on fuselage nose and behind jet exit.

Measurements (Shattuck, 1961) behind jet exit of a twin engined aircraft are compared with measurements (Mull and Algranti, 1960) near nose of another aircraft of similar size.

of jet noise in the air is so small that it can be neglected. Thus the total effect can be accounted for if full representation is made of the engine running in the aircraft on the ground. The aircraft structure itself will influence the noise but if the environment were fully represented as a free-field, then the load on a structure placed in that environment would also be fully represented. The local pressures on the structure would not be known unless further measurements were made.



Howes *et al.* (1957) have shown that if small panels are placed in the neighbourhood of the jet boundary near to the exit nozzle that the sound pressure levels on the panels are about 2 or 3 decibels greater than the corresponding free-field values. The actual magnitude of the increase is only of direct interest if the components are to be tested in a manner markedly different from a jet engine exhaust.

The knowledge of the stresses set up in structures in the near field of jet engines is so limited that it seems probable that the pressure distributions that have been described should be reproduced experimentally on representative structures rather than attempt to calculate directly the behaviour of the structure in such a pressure field. For small components of the structure the noise will consist essentially of sound pressure levels at a range of frequencies as given from paragraph 15.2 with appropriate spacial correlation. The sound pressure levels at a range of frequencies can be represented fairly well by a series of loudspeakers with an appropriate input feed but the spacial correlation can only be represented by loudspeakers if the pressure field is the equivalent of a number of stationary sources of sound. Fortunately at many places the sound is the equivalent of a plane wave impinging at an angle to the structure. Thus for much early design work it should be possible to use sound waves produced by any convenient method. Where the velocity of the turbulent stream in which the sound is generated is a major parameter and has to be represented, the engine itself is probably simpler than any analogue.

For many years it will be advisable to do confirmatory tests on the complete structure with fully representative engines. No matter how well noise distributions can be represented on individual components it will be necessary to check the interaction of one part of the structure on another, the reflections of sound from one part to another and also the combined interaction of sound, structure and turbulent air stream on each other.

## REFERENCES

- |   |                              |
|---|------------------------------|
| Batchelor (1953)                        | Lighthill (1952)             |
| Clarkson (1960)                         | Mull and Erickson (1957)     |
| Greatrex (1955)                         | Mull and Algranti (1960)     |
| Howes, Callaghan, Coles and Mull (1957) | Shattuck (1961)              |
| Laurence (1956)                         | Sutherland and Morgan (1961) |
|   | Wolfe (1957)                 |

CHAPTER 13  
DESIGN PHILOSOPHY

CONTENTS

13.1 Introduction	281
13.2 General considerations	282
13.3 Static strength	287
13.4 Applied static loads	295
13.5 Reliability of structures under static loads	300
13.6 Fatigue strength	311
13.7 Applied fatigue loads	313
13.8 Reliability of structures under fatigue loads	316
13.8.1 Permissible residual strength after fatigue failure	319
13.8.2 Inspection and reliability	322
13.9 Achievement of design strength	325
13.9.1 Static test strength and fatigue test strength when failure is catastrophic	327
13.9.2 Residual strength after fatigue failure	329
References	331

## CHAPTER 13

### DESIGN PHILOSOPHY

#### 13.1 INTRODUCTION

The purpose of all philosophies of structural design is to produce reliability and reliability may be defined as the certainty with which the structure should withstand the loads that may be applied to it. Differences between philosophies only occur in the way the reliability is achieved and whether the degree of reliability is given a numerical value directly or indirectly.

When the structure is for a completely new purpose, such as the Wright Brothers aeroplane, and only one of its type exists it is appropriate that the reliability should be given as at least a certain value. The Wright Brothers decided that their aeroplane should withstand five times the loaded weight and that all parts should be tested to that value. In this particular case, as the actual aeroplane that was flown was strength tested, it may be stated that its strength was greater than that to which it was tested. If there are a number of aircraft to the same design and the measured static strength of one is used to predict that of another the concept of probability must be introduced. For fatigue strength loads applied in the laboratory merely reduce the operational life of that particular structure and reliance must be placed on tests on laboratory specimens even if only one operational structure is envisaged.

As soon as there were a number of designs of aircraft it was possible to take advantage of former designs and soon the procedure, common to many forms of structural design, of designing to a prescribed applied load with a prescribed margin between it and the design static strength was adopted. This leads immediately to a design static strength, this being the product of the applied load and a factor which provides the required margin. Concurrently with this development it became impracticable to test the actual operational structure and reliance had to be placed on calculation or on the measured strength of a laboratory specimen. Where only one operational structure is involved it is necessary to know, within some confidence limit, that there is some prescribed high probability that its strength is above the design strength. Supposing it is decided that there shall be 95 per cent confidence that there is at least a 99.9 per cent probability that the strength is greater than the design strength, this means that in 95 per cent of the times that the procedure is used there would be at least a 99.9 per cent probability that the strength is greater than the design strength but it reveals nothing in respect of the 5 per cent outside the 95 per cent confidence.

In the case of a single operational structure this probability statement gives a good impression of the reliability of the structure but if the procedure is used repeatedly for a large number of structures of the same design it

becomes important to know what happens in the 5 per cent of cases outside the 95 per cent confidence. What happens in these 5 per cent depends on the strength variation between the different structures to the same design. At one extreme the 5 per cent outside the 95 per cent confidence could mean a certainty that the strength was below the design strength, giving a total of almost exactly 5 out of 100 below that value, at the other extreme it could mean a certainty that the strength was above the value giving a total that might have only a small fraction of 1 out of 1000 below the value. With practical values for strength variation neither of these extremes is reached.

When there are a large number of structures to the same design a better impression is given by stating that on average each structure has some prescribed high probability of having a strength above the design value. However, a problem still remains in that the factor relating applied load to design strength has a series of discrete values between about  $1\frac{1}{2}$  and 2. Thus if there is an applied loading condition in which there is a borderline decision between adjacent values there would be a significant difference in the degree of reliability depending on which one was chosen.

This difficulty can be overcome by defining the applied load in terms of its frequency of occurrence and thus replacing the concept of a single applied load by a functional relationship of all loads and their frequency of occurrence. This function is then combined with the functional relationship of the proportion of structures at all strength levels to give a measure of reliability. Finally the design strength is chosen for each design case to correspond to the same prescribed standard of reliability. Methods of forming the functions for loads and strengths and their combination are given in this chapter. The procedure is applicable equally well for Static and Fatigue Strengths. The refinement that is introduced by this procedure is that the applied loads and design strengths are, after manipulation, related by one single numerical value. This is a direct measure of reliability; however it has been obtained from formulae for frequencies of occurrence of loads and strengths that are extrapolated far beyond practical experience. Thus the engineering judgment that was used to estimate the factor between applied load and design strength is transferred to estimating the appropriate formulae for extrapolation.

### 13.2 GENERAL CONSIDERATIONS

The process of design can be regarded as falling into the three distinct phases of Load, Strength and the relationship between Load and Strength. All these are to some extent interrelated, but by treating them separately a better understanding of how they fit into the complete pattern ensues.

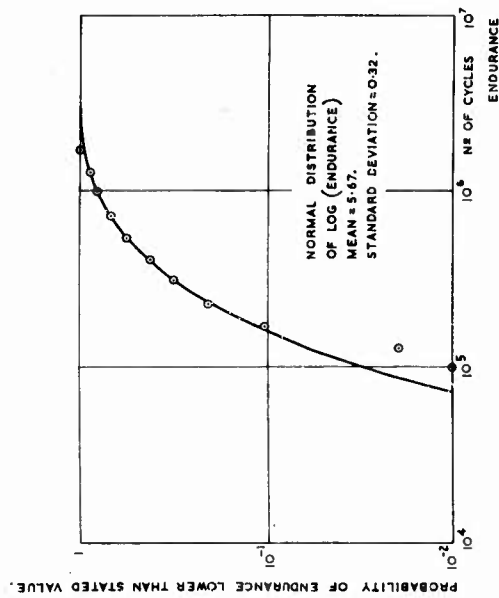
The basic knowledge of the strength of a structure is based on the strength of a small number of typical structures or parts thereof. Thus even in the simplest of components, this knowledge will be limited to about the range of strength that would be expected with 10 structures made to that design. The mathematical tools that are used to estimate the frequency of occurrence of strengths outside this range are merely those thought to be the most suitable for the purpose. It must be remembered that the process is most

definitely extrapolation once it is outside the limits of measurement. A decision has to be taken either quantitatively or qualitatively on how much margin should be allowed on a structural strength, somewhere near the average, at the time of manufacture to allow for scatter in strength between different specimens and also to account for deterioration with time and use. If a quantitative method is used the average strength and the scatter within the experimental range would be measured; mathematical functions would be used to interpolate within this experimental range and the same function or others would be used to extrapolate to lower strengths.

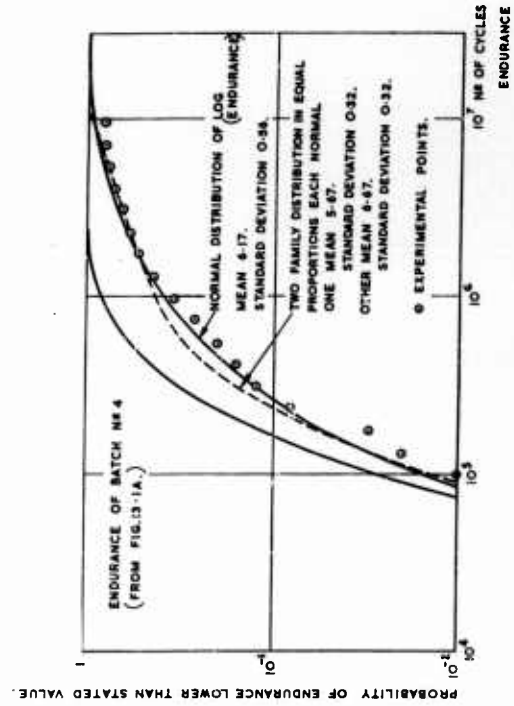
The basic strength data, from which the function of distribution of strength is deduced, will usually be from average sorts of structure in a new condition. In deciding what is the whole distribution an estimate has to be made of the frequency of occurrence of low strengths that might occur in new structures before account is taken of the deterioration with time and use. There will be a scatter in strength that should be apparent if several specimens are tested and may be presumed to extend in a fairly orderly manner outside the experimental range. The number of test specimens of any particular design will usually be too small to estimate satisfactorily the magnitude of its scatter but by grouping experience on a number of designs, that are structurally and materially fairly similar, useful estimate can be made. The structures that make up this distribution will be the main family to that design. However, some structures may be weak due to the manufacturing processes that are used at any stage from the raw materials to the finished product or due to any human fallibility, also at any stage. With a good design these weaker structures will occur in such relatively small numbers that they will not normally be apparent in the basic data. Thus they form a weaker family that has to be added to the main family, deduced from the basic data. Far more guesswork is required to estimate the numbers in, and the distribution of, this weaker family than was required to estimate the distribution of the main family.

One means whereby a weak family can be produced is illustrated by an examination of some tests by Cox (1959) on bolts. He has a number of batches, each of 100 specimens, the thread of each bolt being cut by the same die after different amounts of use. The tests were in fatigue but the discussion should be applicable to static strength, although the discrimination might be less sensitive. The distribution of the endurances at one load level of batch No. 4,\* which had the threads cut with a relatively new die, are plotted in Fig. 13.1A; apart from the two points at an endurance of  $10^6$  and  $1.3 \times 10^6$  which are for 2 specimens only the experimental points lie on a Normal distribution. Figure 13.1B gives a corresponding distribution of endurance for batch No. 5 after the die has become worn. From physical reasoning Cox decided that the strength of a number of the bolts is improved as the die becomes worn and it can be seen that the average is in fact appreciably greater. For comparison, a curve corresponding to batch No. 5 being made up of half the original family and the other half being improved ten-fold on endurance is shown; a "best" estimate for a single Normal

\* The results for this particular batch were not quoted in the published paper and have been supplied privately.



A - BATCH NO 4. DIE NO 1 OF COX (1959)



B - BATCH NO 5. DIE NO 1 OF COX (1959)

Fig. 13.1. Distribution of fatigue endurance of a 10BA nut and bolt assembly.  
All specimens tested at the same mean and alternating loads.

distribution is also shown. With roughly equal sizes of family the "best" single Normal distribution would tend to predict a greater proportion of weak specimens and in the example just quoted, the curves cross at the 1 in 30 failure rate. In a design in which the weaker family has only a small proportion of the total, and this is probably by far the more common case, there is a possibility of there being no weak samples present amongst the test specimens, and in this case the best single Normal distribution would be less severe.

In estimating the strength of complete structures the number of tests on similar elements will be very small and the weaker family will not in general be apparent, and in the rare case that it is, it will frequently be regarded as a rogue. Most engineers can cite cases where structural parts have cracked before or during assembly and subsequently it has been established that it was due to wrong heat treatment. A more insidious type of apparent weakness was experienced with aluminium-zinc alloys. There was a suspicion that rogues of very much reduced strength were appearing in structural elements (tested in fatigue) of the order of once in  $10^2$  to once in  $10^3$  specimens. A controlled series of tests covering about 500 specimens was described in an unpublished report by the Ministry of Aviation, England, and showed up no defect, but even if all 500 specimens were from completely independent material, there would have been a little under an equal chance that it would show up a phenomenon that occurred on 1 in  $10^3$  occasions.

The examples quoted show that in new structures the distribution of strength of new structures may be regarded as made up of a main family and a weaker family. In deciding on the distribution of strength that will be used for design, account must be taken of the deterioration due to wear, creep, fatigue, corrosion and accidental damage. These can be included by an overall reduction in the strength of all the structures together with a change in the relative distribution of different strengths. In many practical cases it should be simpler to group many of these deteriorations with the initial weaknesses and use a distribution that is applicable to the end of the operational life and add to this any deterioration, such as some fatigue failures, that might be the subject of separate and special investigation.

The function relating the applied loads and their frequency of occurrence is of equal importance to the function for strengths. As with strength there is a strong indication that for many, if not all, loading conditions there is a main family, that will be the average sort of conditions that an aircraft meets during its operational life, and a subsidiary family of rare severe conditions. In several instances direct evidence of the severe conditions has been noted. In Chapter 5 it was noted that the very high normal accelerations in manoeuvres appear to be from a different family from the medium to high accelerations, in Chapter 7 it was noted that there appear to be occasional high vertical velocities at touchdown in clear non-squally conditions and in Chapter 10 attention was drawn to the severe family of atmospheric turbulence loads. The first two of these are likely to be due in part to the human fallibility of the pilot and the third due to thunderstorms. In the case of loads, the extreme family may be less severe than would be indicated by an

extrapolation of the main family. An example of this is given in Chapter 8 where it is shown that the time spent at very high airspeeds is less than would be expected from extrapolation from lower speeds. This is almost certainly due to pilots deliberately trying to avoid exceeding the Service Limit of speed.

In loading conditions, in which the measurements are on a limited scale, similar care must be taken to that recommended for strength conditions as there will be a strong possibility that the measurements will be only from the main family. Thus a subsidiary family will need to be postulated for the severe conditions, basing it on evidence from other types of loading conditions in which the extreme conditions have been experienced.

Finally the distributions of frequency of occurrence of load and strength must be combined to give a measure of reliability. The numerical value, that ensues, for reliability is the reciprocal of the combined frequency that the load is greater than the strength. It will have the dimensions of time per failure but it cannot be emphasized too strongly that the object of structural design is to obtain a design that is reliable. It is accurate to say that a structure is reliable if it has a negligible frequency of failure. As the frequency of failure is negligible its value is the same as the chance of failure. The absolute value of the chance is quite unmeasurable. Lusser (1958) gives a rule of thumb for a fixed load and a variation in strength. He states that the number of specimens required to estimate the chance of failure, with 90 per cent confidence, is ten times the reciprocal of the chance, i.e. to measure a chance of 1 in 1000 would require 10,000 specimens. In the general case it is necessary also to determine the remote chance of the loads occurring. Attention has already been drawn to the added complication that the exceptionally high loads and the exceptionally low strengths may well be from families that are subsidiary to the two main ones. The contribution from the subsidiary families to the calculated probability of failure will be a large proportion of the total, which will consequently be subject to considerable error. Although the absolute value of reliability is most inaccurate, its calculated value must nevertheless be of immense value as a means of comparison.

A decision must be taken of what value shall be given to the reliability. It must inevitably be the number of hours per failure, i.e. the reciprocal of the probability of failure per hour. Because of the inherent inaccuracies it is probable that the number of hours selected will be 10 to some power. In order to appreciate what 10 to some power means it must be remembered that in our present era of nearly 2000 years there have been less than  $1.8 \times 10^7$  hr. However it must be remembered also that one particular aircraft has many parts and loading conditions. To obtain the full failure rate of the particular design it would be necessary to add the failure rates of all parts for each loading condition and then add the failure rates of all the loading conditions. In considering any particular loading condition, in the ideal case there would be a large number of parts that would be equally likely to fail but in a practical design the number that might fail is small. There are several reasons for this, the stress distribution under the assumed applied loads will not be uniform, some parts will have to be so strong for one loading condition that they have excess strength for all others, the



actual load distribution will differ from the assumed one. As a small excess of strength is accompanied by a large increase in reliability of that part relative to the others the contributions to the failure rate are likely to be concentrated in a very small number of parts. Similar reasoning may be applied to the summation of the effects of the different loading conditions. In practice any particular design of aircraft will be more susceptible to failure under one or two of its loading conditions than under all others. In those cases where a number of static failures have occurred in service with a particular type of aircraft it is almost invariable that they have been under the same loading condition and the same part has failed. Such occurrences have been on aircraft with inadequate reliability for one reason or another and more uniformity would be expected with a reliable structure. However it should be conservative to assume that the weakest part under the most severe loading condition will contribute at least 10 per cent of the total chance of structural failure under all loading conditions. There is no need to know in advance which is the weakest point, the procedure would be to allow a factor of 10 on reliability for all parts so that the one that happened to be the critical one, which might not necessarily be the one predicted by design, would have its required margin. There are naturally reservations to be made in the above argument. If there were a row of bolts, for example, that all have substantially the same load, it is the strength of the whole row that has to be taken and not that of one bolt only.

It has just been shown that to achieve an overall reliability of a structure it is necessary to design each individual part to that reliability, multiplied by some factor. It was suggested that a factor of 10 would be conservative with current knowledge of applied loads and strengths. This would allow for improvements in this knowledge but if there were a major refinement it might be necessary to assess what the factor should be rather than taking an arbitrary value such as 10.

### 13.3 STATIC STRENGTH

In any considerations of strength it is worthwhile studying the Normal distribution noting the conditions under which it is applicable and even more, noting where it is not applicable. There are many physical phenomena including the strength of structures that, within the limits of observation have this distribution. The main interest usually lies in the strengths outside the limits of observation, but first the characteristics of a hypothetical family of structures with a Normal distribution of strength will be examined and afterwards possible departures at the extreme values. Figure 13.2 gives the distribution, the ordinate being the probability that the strength is lower than the stated value and the abscissa being the strength in the non-dimensional form of multiples of the standard deviation ( $\sigma$ ) from the mean strength. The point that is noticed at once is that the chance of a particular strength appearing reduces very rapidly beyond three standard deviations from the mean. Nevertheless most designers would be reluctant to design a structure that had only a strength margin of about  $3\sigma$  above loads that they knew would be applied.

The concept of a weaker family was introduced in paragraph 13.2 to overcome this intuitive objection. Figures 13.3, 13.4 and 13.5 show a series of curves of distribution of strength of a double family with 1, 2 and 5 per cent of the specimens respectively from a weaker family and the mean of the weaker families up to  $5\sigma$  below the mean of the main family. Taking Fig. 13.3 as an illustration the curves for this double family with 1 per cent

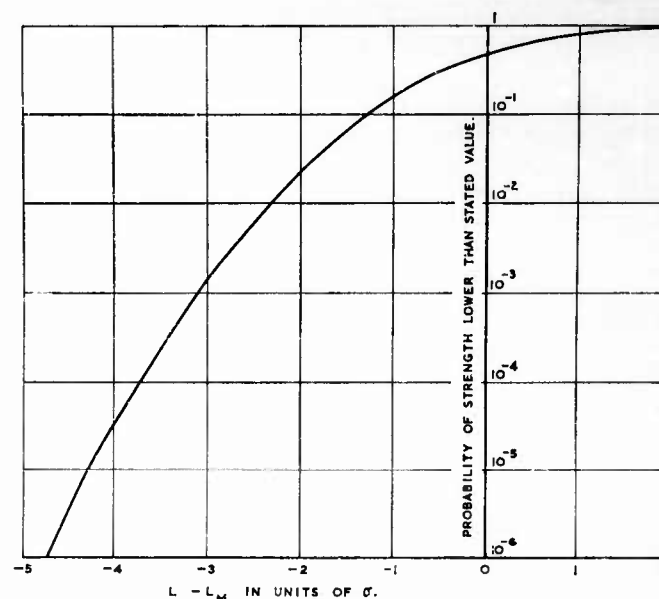


Fig. 13.2. Normal distribution of strength.

$L$  = strength

$L_M$  = average strength

$\sigma$  = standard deviation of strength

specimens in the weaker family are cross-plotted in Fig. 13.6 to show the proportions of failures from the two families at different total failure rates and a range of reductions of strength of the weaker families. For loads that give failure rates as high as 1 in 1000 the mean of the weaker family need only be  $2.5\sigma$  weaker than the mean of the main family for the failures to be almost entirely in the weaker family (say 95 per cent, which is a figure often used in statistics to give boundaries of significance). Thus if the applied load is known and there is a weaker family of as few as 1 per cent of the total, it is necessary, for all practical purposes of low failure rates, only to consider the weaker family as a source of failure provided the two families differ in strength by  $2.5\sigma$ , i.e. 10 per cent for  $\sigma$  as low as 4 per cent.

The curves of Figs. 13.3, 13.4 and 13.5 are replotted in Fig. 13.7 to show

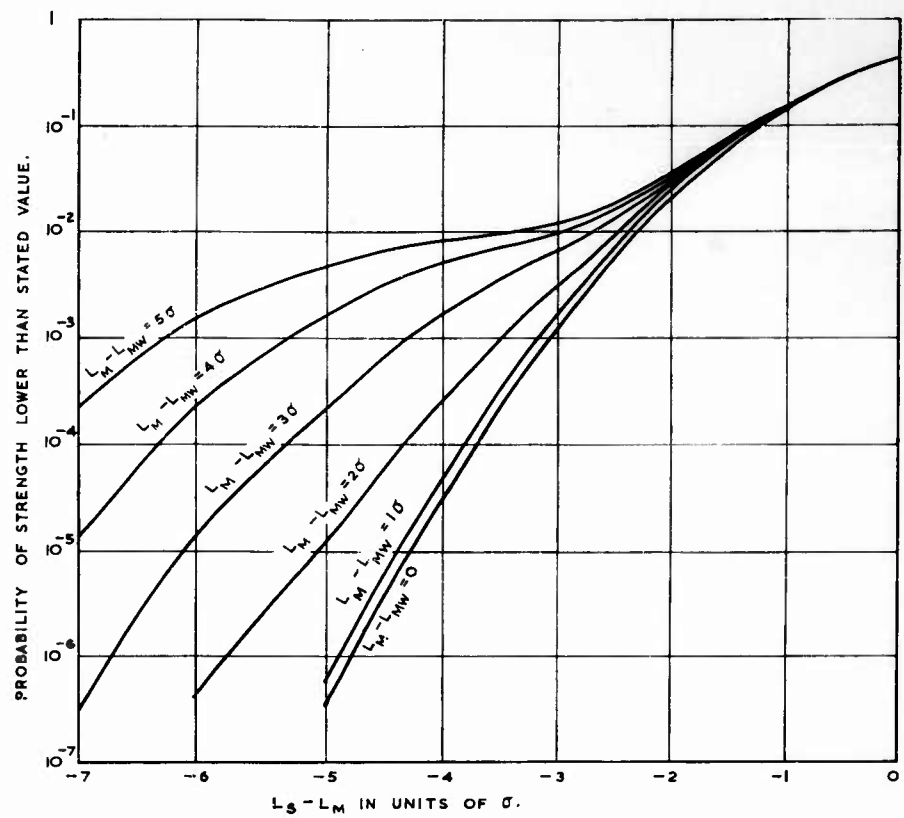


Fig. 13.3. Probability distribution of strength of double family each with normal distribution.

Weaker family consists of 1 per cent of total.

$L$  = strength

$L_M$  = average strength of main family

$L_{MW}$  = average strength of weaker family

$\sigma$  = standard deviation of strength in both families

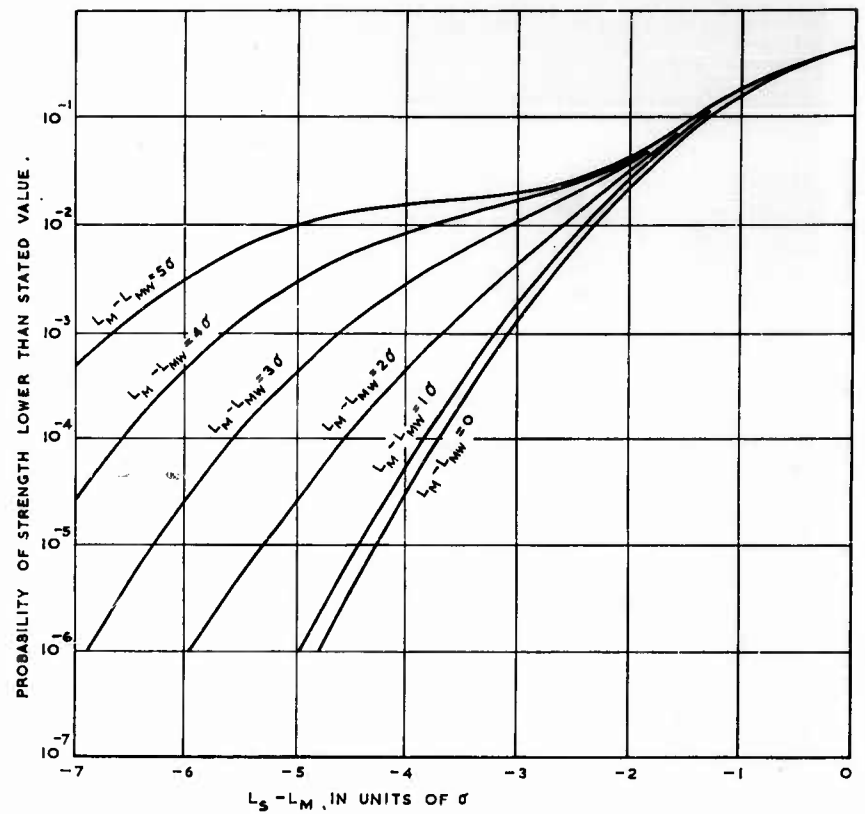


Fig. 13.4. Probability distribution of strength of double family each with normal distribution.

Weaker family consists of 2 per cent of total.

$L$  = strength

$L_M$  = average strength of main family

$L_{MW}$  = average strength of weaker family

$\sigma$  = standard deviation of strength in both families

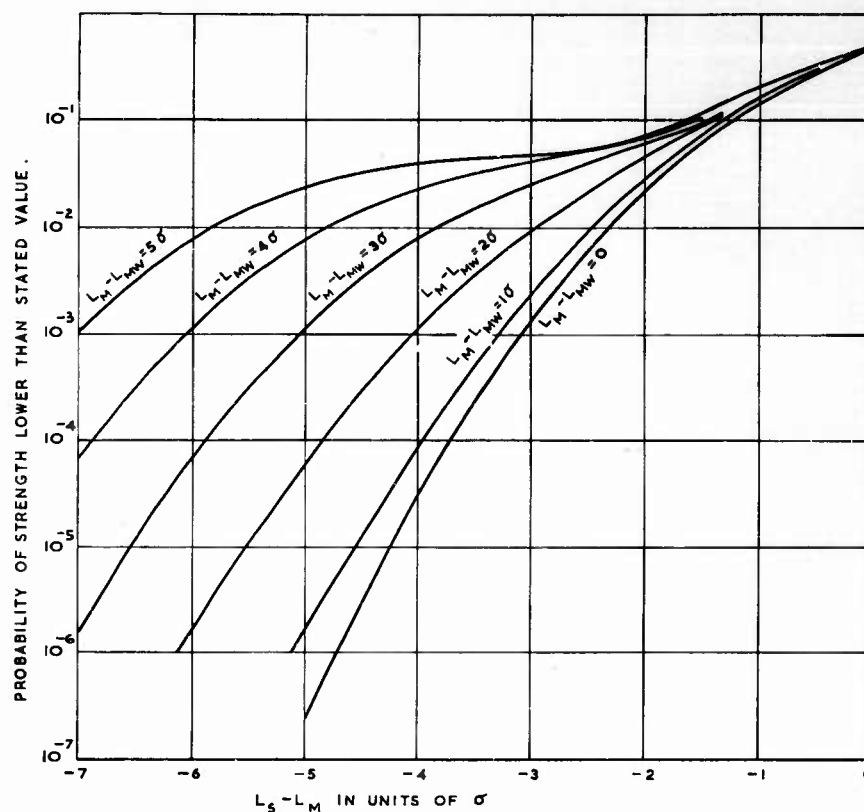


Fig. 13.5. Probability distribution of strength of double family each with normal distribution.

Weaker family consists of 5 per cent of total.

$L$  = strength

$L_M$  = average strength of main family

$L_{MW}$  = average strength of weaker family

$\sigma$  = standard deviation of strength in both families

the reduction of strength values that occur at various probability levels. The median value is not shown but it is hardly affected for the whole range considered, i.e. up to 5 per cent of specimens from a weak family whose mean may be up to  $5\sigma$  below the mean of the main family. The strengths that are not attained on average once in ten specimens ( $P = 0.1$ ) are hardly affected when 2 per cent are from a weak family and even for 5 per cent it is only  $\frac{1}{2}\sigma$  at the lowest strength considered. This is roughly the

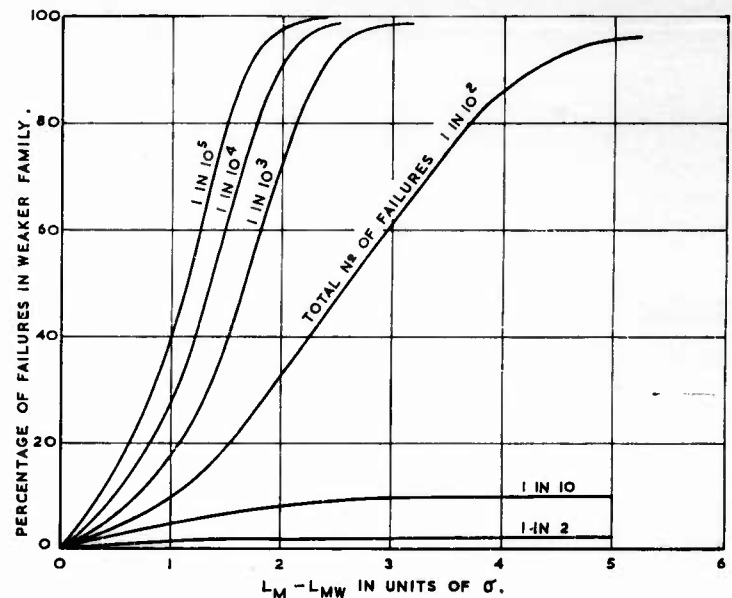


Fig. 13.6. Proportion of failures in weaker family for a range of relative strengths of the two families and for various total failure rates.

Weaker family consists of 1 per cent of total.

$L_M$  = average strength of main family

$L_{MW}$  = average strength of weaker family

$\sigma$  = standard deviation of strength in both families

extent to which experimental evidence might be available and such experimental information could not be used to discriminate between the various curves.

From a reliability standpoint it is the lower probabilities that are of interest. Figure 13.7 is general for all standard deviations, but for illustration an example is taken of a standard deviation of 4 per cent and shown in Table 13.1 for strengths that are not attained on average once in 1000 specimens.

This table indicates that if it is known that a particular load but none greater will be applied to all the structures, then for the idealized structures under examination 1 in 1000 would fail if the load was made equal to the mean strengths multiplied by the per cent values quoted in the table. The

88 per cent value given in the top line is the well-known value of 3 standard deviations below the mean for a single family of Normal distribution, but if weaknesses are present or are allowed to develop from any cause, then some appropriate value on one of the lower lines should be taken. Allowance must

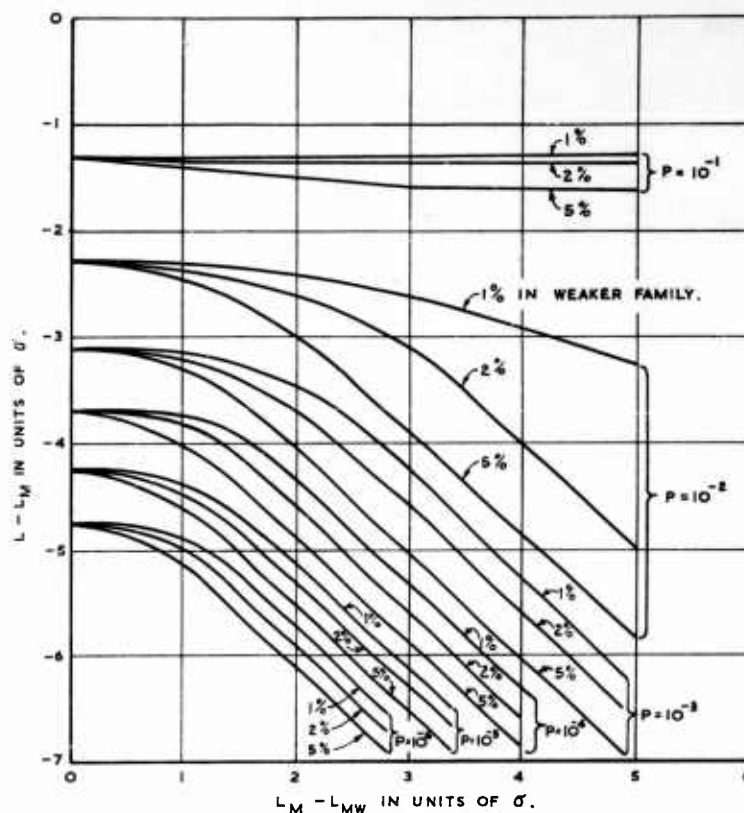


Fig. 13.7. Variation of strength with reduction in mean strength of weaker family at different probability levels.

- $L$  = strength
- $L_M$  = average strength of main family
- $L_{MW}$  = average strength of weaker family
- $\sigma$  = standard deviation of strength of both families
- $P$  = probability of strength being lower than  $L$

be made immediately for those weaknesses that may be present when the structure is put into service and for those weaknesses like accidental damage that may occur at any time in the life of the aircraft, but those weaknesses that are dependent on time, either flying or absolute, should be allowed for at the appropriate time.

Table 13.1. *Strengths of Double Family each with Normal Distributions and Standard Deviation 4 Per Cent*  
(Strengths given as Percentage of Mean Strength of the Main Family)

Mean strength of weaker family	Strength that 1 in 10 <sup>3</sup> specimens do not attain		
	Proportion in weaker family		
	1%	2%	5%
100	88	88	88
96	87	87	87
92	86	85	84
88	83	82	80
84	79	78	76
80	75	74	72

In practical loading conditions the maximum load will not be a fixed value and there will be a range of loads to be examined. In such cases a range of strengths must also be examined and the shape of the curve of strength distribution rather than its value at a selected point becomes important. In the discussion so far the sum of two Normal distributions has been considered because a physical representation of this ideal case could easily be made. It may often be appropriate to take a single distribution to represent a continuously varying distribution of weaknesses. In such a case a "best" curve of an exponential distribution\* below the mean strength with a Normal distribution above might be as good as any and is easy to manipulate. When there are less than 20 experimental points the best exponential curve of frequency up to the mean will not differ much from  $(1/2\sigma) \exp(x/\sigma)$ ,

where  $\sigma^2 = \sum x_r^2 / (n - 1)$

$x$  = strength relative to mean

$x_r$  = experimental readings

$n$  = total number of experimental readings

and the best Normal distribution above the mean will be  $(1/\sigma\sqrt{2\pi}) \exp(-x^2/2\sigma^2)$ . This particular exponential has the advantage of simplicity

\* If it were thought that the departure from normal were due to scatter rather than weakness a Normal distribution  $(1/\sigma\sqrt{2\pi}) \exp(-x^2/2\sigma^2)$ , with the standard distribution  $\sigma$  itself distributed as  $(\sigma/\rho^2) \exp(-\sigma^2/2\rho^2)$ , becomes  $(1/2\rho) \exp(x/\rho)$  below the mean and  $(1/2\rho) \exp(-x/\rho)$  above it. This does not seem to be as likely a physical explanation as the one given and consequently it would be more difficult to assess values for  $\rho$ .



that the same value of  $\sigma$  can be used for both parts of the distribution. If it is felt that it is too severe at the extreme values, or not severe enough, in any particular application adjustments can be made in the choice of the value of  $\sigma$ .

#### 13.4 APPLIED STATIC LOADS

Throughout the Manual the applied loads that occur in aircraft have been described. In order to build up a design philosophy it is an advantage to examine the general characteristics of these loads and if possible use only one or two formulae to represent them. The absolute value of the frequencies of occurrence of the loads vary greatly with different types of load, but the relative frequencies are more consistent.

Unlike strength characteristics, which are based on very few experimental points per type, measurements of loads can be collected in large numbers even though this is not done frequently. The fields in which loads have been collected in large numbers are notably atmospheric turbulence loads, normal accelerations and forward velocities in manoeuvres and landing loads. The characteristics of the distribution of frequency of occurrence of different applied loads will depend on the characteristics of the loads themselves. Three distinct and different types are illustrated in Fig. 13.8: Fig. 13.8A is the distribution of up gusts extracted from Chapter 10, Fig. 13.8B is the proportion of time spent at different speeds extracted from Chapter 8 and Fig. 13.8C is the distribution of normal accelerations on landing (the distribution is similar to those of Fig. 7.8 but not identical to any one). In each of these three cases the distributions have two distinct families and a physical explanation is available as to why this should be so. It will be noticed that in two cases the families at the higher loads are more severe than those at lower loads but in the third the opposite condition ensues.

Turbulence loads have received very much attention and the numbers of measurements taken of the normal acceleration is prodigious. It is well established that there are a variety of conditions of atmospheric turbulence that produce the loads, and that the distribution of loads in light forms of turbulence is quite different from that in severe turbulence such as in thunderstorms. In Chapter 10 it is suggested that the frequency of occurrence of gusts greater than stated values has a distribution that consists of two exponential decays. In Fig. 13.8A attention is confined to the up gusts. The experimental points are shown and compared with a distribution which is the sum of two exponential distributions. In addition the two exponential distributions are also shown separately. Extrapolated values to zero velocity show that 98.4 per cent of all the gusts are from the less severe family but that the gusts with velocities above 42 ft/sec are predominantly from the more severe family. A total number of 50 gusts with velocities above 42 ft/sec were encountered in the 5 million miles (19,000 flying hours) recorded. It would be expected that 5 of these were from the less severe family. It is only the distribution of the magnitude of these 50 gusts that is of interest in predicting the higher gusts of interest in design for static strength. As a variety of pairs of exponential distributions could have been used to

fit reasonably well the experimental data it is evident that there would be greater confidence in the predictions of the frequency of occurrence of the higher gusts if there were other evidence to support the contention that 1.6 per cent of all gusts encountered were from the severe family. In order

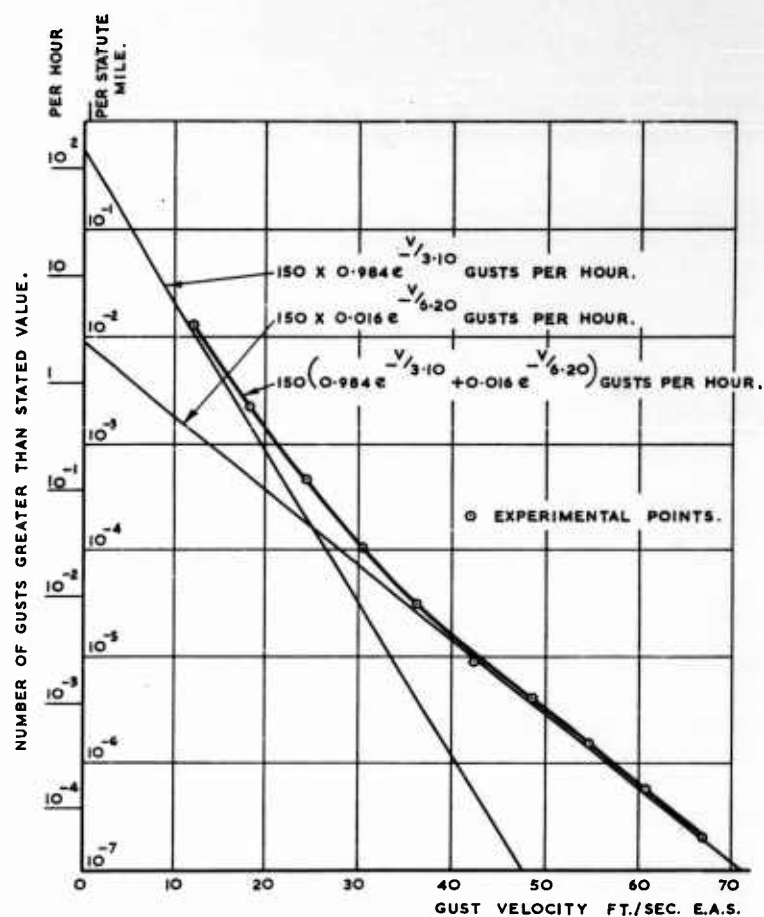


Fig. 13.8. Typical examples of double family loading conditions.

A—Distribution of up gusts for all altitudes combined.  
5 million statute miles in 19,000 flying hours.

to test the validity of this contention it is necessary to estimate the proportion of the total distance travelled that is in severe turbulence. It was shown in Chapter 10 that the total number of gusts encountered by an aircraft in continuous turbulence depends mainly on the characteristics of the aircraft although their magnitude will vary with the severity of the turbulence. For the aircraft used for the measurements quoted the number would be 4 to 5

up gusts per mile. The total number shown in Fig. 13.8A for severe turbulence is 0.009 gusts per mile. Thus the proportion of the total distance that is spent in severe turbulence is 0.009 divided by about 4.5, i.e. 0.2 per cent. This does not seem an unreasonable value for thunderstorms that cannot be avoided.

In Fig. 12.8B, which is extracted from Chapter 8, measurements of the proportion of time spent at different speeds give the opportunity to study a distribution with a different type of double family. Sufficient data for a good

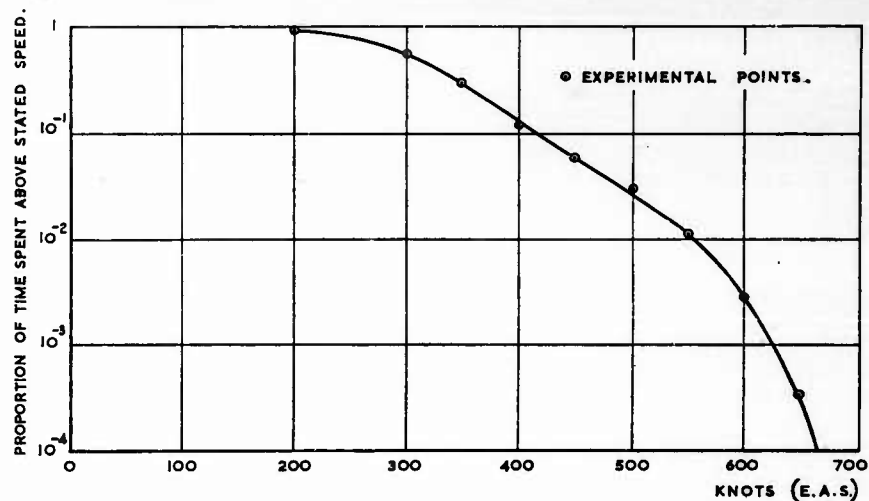


Fig. 13.8. Typical examples of double family loading conditions.

B—Proportion of time spent above different speeds by F-100 class fighters in 6050 flying hours combined duties.

assessment of the distribution at high speeds is available from 6050 flying hours of recording on the F-100 class of aircraft. The figure shows that the proportion of time at relatively low speeds varies exponentially from the speeds, that are exceeded half the time, up to those speeds that are exceeded 1 per cent of the time. At speeds of about 0.8 times the design diving speed there appears to be a discontinuity above which the variation is a much more rapid exponential decay. The physical reasons for these two distributions are discussed in Chapter 8 where it is suggested that the cut-off to the distribution for lower speeds is due to the pilot deliberately avoiding speeds near to the design diving speed. This type of distribution differs from that for turbulence in that an extrapolation from frequently occurring phenomena would give a more severe loading condition than the actual conditions measured.

The data on the behaviour of aircraft at touchdown is more limited and more reliance must be put on physical reasoning to decide to what extent there are different families of landing conditions. The main body of information given in Chapter 7 supports the contention that aircraft of particular types normally land with the approach speed, the vertical velocity at

touchdown and the increment of normal acceleration, all having distributions that are substantially Normal for values in excess of their median values. The problem of design is to decide whether there are a group or groups of severe types of landing that form separate families.

A specific example is taken from unpublished N.A.S.A. data and plotted in Fig. 13.8C to illustrate the problem that arises in deciding the design load

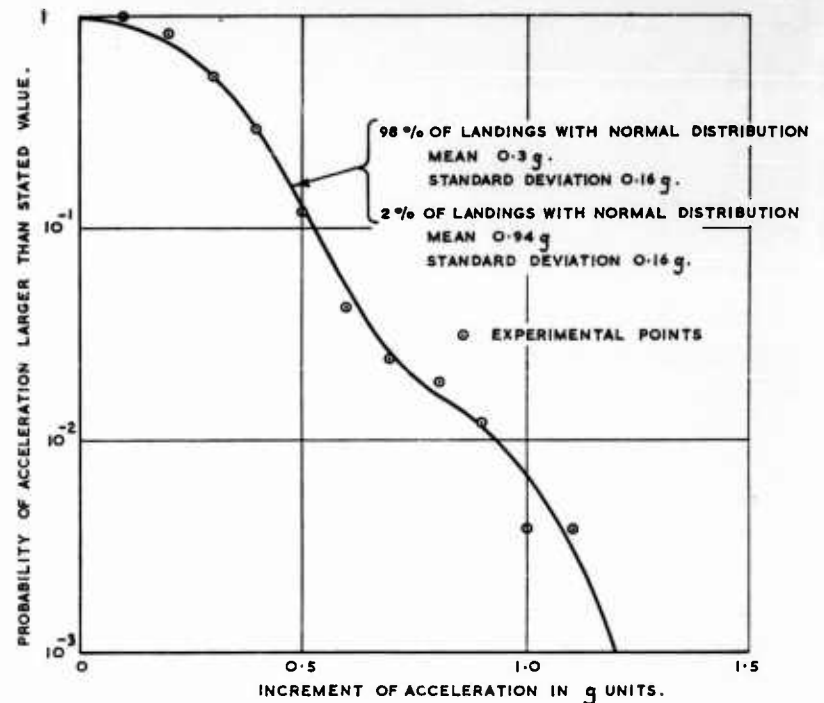


Fig. 13.8. Typical examples of double family loading conditions.

C—Normal acceleration on landing of turbo-jet aircraft.  
320 landings.

from a limited amount of data. A set of 320 landings was taken and the increment of normal acceleration noted. This particular example is very similar to those given in Fig. 7.8 of Chapter 7 but not identical with any of them. The probability of accelerations greater than the stated value is shown. It can be seen that the experimental points can be represented well by a distribution consisting of two Normal distributions, a main family for 98 per cent of all landings of mean 0.3g with a standard deviation 0.16g, and a subsidiary but more severe family of 2 per cent of all landings having a mean of 0.94g, i.e.  $0.3 + (4 \times 0.16)g$  and the same standard deviation. This suggests strongly that under normal landing conditions the increment of normal acceleration at touchdown has a Normal distribution with a mean

of about  $0.3g$  with a standard deviation of about  $0.16g$ , at any rate for values of the increment of  $0.3g$  and more. From the point of view of fatigue loads this distribution is the more important one. From the point of view of static loads it is the family of more severe landing conditions that is significant. Whilst there is little doubt that there is such a family of severe loads, the amount of experimental evidence available is inevitably rather small and even if the above distribution were fully representative it means that the subsidiary curve would have to be determined from about 6 landings. The actual landings include 8 with an increment above  $0.7g$  of which 6 were above  $0.8g$ , 4 above  $0.9g$  and 1 above  $1.1g$ . The mathematical analysis suggests that all the landings above  $0.8g$  increment were probably from the severe family, and also that there were probably none of the severe family with an increment less than  $0.8g$ . If the severe landings were taken in isolation from the main family, extrapolation to a frequency of 1 in 1000 landings could easily give an increment anywhere between  $1.1g$  and  $2g$ .

The best compromise seems to be to take the experimental points for the severe loads and use the main family of landings as background information. As the main family can be well represented by a Normal distribution, it seems reasonable to assume that the severe family has also a Normal distribution, but the question to be asked is whether it is reasonable to assume the same scatter and whether there might be a succession of severe families. Having regard to the scantiness of the information and drawing on experience of other loading conditions such as atmospheric turbulence, there seems little to be gained from starting other than with the experimental point at  $0.8g$  and deciding on some exponential decay for all values above. It will be appreciated that the rate of decay is of much greater significance than the absolute value at  $0.8g$ , and also that it is of little significance that the decay curve can be drawn on Fig. 13.8C and fitted smoothly to the curve for the main family of landings which are accepted as arising from a different set of conditions.

The three examples that have been given in Fig. 13.8 may be regarded as typical of all applied loading conditions. In each case it is shown that there were two families of loads and that the severe one, which is of major interest for design for static strength, appears to be present only a small fraction of the time. The distributions of frequency of occurrence of the loads of the two families are probably only loosely connected and in each case attention has been drawn to the importance of extrapolating for static design purposes mainly from the severe family. Furthermore it was shown that in two of the three examples larger loads of the severe family occurred more frequently than would have been expected from an extrapolation of the distribution of the main family but in the third example the larger loads of the severe family occurred less frequently than would have been expected from an extrapolation of the main family.

It seems probable that every loading condition should be split up into a main family and a severe family. In view of the inevitable scarcity of information on the severe family it should be adequate to define the frequency of occurrence of its loads by a Normal distribution or Exponential distribution using Engineering judgment to decide which one is to be used in any particular loading condition.

## 13.5 RELIABILITY OF STRUCTURES UNDER STATIC LOADS

The purpose of the present proposals for producing reliability of structures is to give a refinement to conventional methods and not to revolutionize them. In conventional design for static strength a high load that occurs reasonably infrequently is selected and defined as the applied load. This load is multiplied by a factor, the resulting value being taken as the design strength. In aircraft design this factor for ultimate usually has values varying from about  $1\frac{1}{2}$  to 2; higher values are sometimes taken such as for the pressure cabins, but this is done almost certainly as an indirect means of obtaining satisfactory fatigue strength. The factor that is used to correlate the applied load and the design strength is not of itself a measure of reliability. In fact the same design strength could be regarded as having any factor whatsoever provided the value given to the applied load were changed in the appropriate manner. In the present proposals it is suggested that an applied load that occurs with about the same frequency as the applied loads used in conventional design be chosen as the datum load. Thus the refinement lies in estimating a frequency of occurrence of this load and a formula for the relative frequency of occurrence of other loads.

The reliability of the structure under static loads is calculated using the following three parameters:

- (i) An applied load and its frequency of occurrence, with a function giving relative frequencies of occurrence of other and particularly higher load values.
- (ii) Mean static strength with a function giving the proportion of structures at other and particularly lower values of strength.
- (iii) The resultant reliability as the average number of hours per failure.

An applied load is selected in the neighbourhood of that which will occur once in the lifetime of an aircraft and the frequencies of occurrence of all other loads given relative to it. The distribution of static strengths is given relative to the mean strength. In determining reliability the most significant range is between this applied load and the mean strength. Even the smallest load in this range occurs only about once in the lifetime of the aircraft so that it will most likely be from the severe family of any double family of loads. It was shown in paragraph 13.4 that this severe family could be represented adequately either by a Normal distribution or by an exponential distribution. It was suggested in paragraph 13.3 that the distribution of static strength should be represented by a main and a weaker family each of Normal distributions.

In order to give the maximum scope in the selection of shapes to the load and strength distributions, the reliability formulae will be determined for all the above combinations and for completeness of presentation the case of load and strength varying exponentially is also included.

The first case to be examined is that in which (i) the frequency of occurrence of the applied loads greater than stated values varies exponentially and (ii) the distribution of the strength of the structure is Normal. One advantage of discussing this first is that it brings out certain interesting physical attributes of the problem.

Throughout the analysis the probability of failure will be determined as the sum of the probability of failure at each strength. Mathematically this is identical to the sum of the probability of failure at each applied load, but physically it is more realistic to think in terms of structures that broke because the load surpassed their strength than in terms of loads that caused failure.

The probability of failure is given by

$$P = \int_{L_A}^{\infty} f_L a_L dL \quad (13.1)$$

where  $L_A$  is the lowest value of applied load being represented by the formula

$P$  = probability of failure per flying hour

$L$  = load

$f_L$  = frequency of occurrence per flying hour of loads greater than  $L$

$a_L \delta L$  = proportion of structures with strength between  $L$  and  $L + \delta L$ .

In this first case the distributions of  $f_L$  and  $a_L$  are given by

$$f_L = f_0 \exp(-L/\sigma_A) \quad (13.2)$$

$$a_L = (1/\sigma_S \sqrt{2\pi}) \exp[-(L - L_S)^2/2\sigma_S^2] \quad (13.3)$$

where  $f_0$ ,  $\sigma_A$ ,  $\sigma_S$ ,  $L_S$  are constants, the product  $f_L a_L$  can be simplified to become

$$f_L a_L = f_{L_S} - \frac{1}{2} \sigma_S^2 / \sigma_A \cdot (1/\sigma_S \sqrt{2\pi}) \exp[-(L - L_S + \sigma_S^2/\sigma_A)^2/2\sigma_S^2]$$

$$\text{where } f_{L_S} - \frac{1}{2} \sigma_S^2 / \sigma_A = \text{the value of } f_L \text{ at } L = L_S - \frac{1}{2} \sigma_S^2 / \sigma_A \quad (13.4)$$

Equation (13.4) shows the distribution density of the strength of the structures that fail. The strength distribution ( $a_L$ ) is Normal, with mean  $L_S$  and standard deviation  $\sigma_S$ . The frequency of occurrence of failures distribution ( $f_L a_L$ ) is also Normal with a mean of  $(L_S - \sigma_S^2/\sigma_A)$  and the same standard deviation  $\sigma_S$ . This is equivalent to displacing the mean by  $\sigma_S^2/\sigma_A$  and saying that the mean strength of the structures that fail is  $\sigma_S^2/\sigma_A$  less than the mean strength of all the structures.

Provided that the value of  $\sigma_A$  and  $L_A$  are such that

$$(1/\sigma_S \sqrt{2\pi}) \int_{-\infty}^{L_A} \exp[-(L - L_S + \sigma_S^2/\sigma_A)^2/2\sigma_S^2] dL$$

is negligible, and this will normally be the case due to the extreme rarity of such low strengths, then

$$P = \int_{L_A}^{\infty} f_L a_L dL = \int_{-\infty}^{\infty} f_L a_L dL = f_{L_S} - \frac{1}{2} \sigma_S^2 / \sigma_A \quad (13.5)$$

Thus the frequency of occurrence of failures is equal to the frequency of occurrence of applied loads that are greater than  $L_S - \frac{1}{2} \sigma_S^2 / \sigma_A$ .

Van der Neut (1957) discusses this case in detail and points out that if there is a range of designs with different  $\sigma_S$  they will all have the same failure rate if they have the same value of  $L_S - \frac{1}{2}\sigma_S^2/\sigma_A$ . In the present treatment the notation has been changed for convenience in comparing the results with other distributions of load; in Van der Neut's notation

$$L_S - \frac{1}{2}\sigma_S^2/\sigma_A = 1 = \text{"standard" load}$$

$$\sigma_S = \sigma$$

$$\sigma_A = 1/\beta$$

$$\frac{L_S}{L_S - \frac{1}{2}\sigma_S^2/\sigma_A} = j$$

He discusses scatter in terms of  $p$ , rather than  $\sigma_S$ , which he defines as follows

"If we count the aircraft whose actual strengths are smaller than  $(1 - p)$  times the design load, these aircraft form 1% of the total number of aircraft."

This means that  $p = 2.3 \sigma_S$  and as he takes values of  $p$  up to 0.20, it is the same as taking  $\sigma_S$  up to 8.6 per cent. He shows that for  $\sigma_S = 8.6$  per cent,  $\sigma_A = 4.3$  per cent (i.e.  $p = 0.20$ ,  $K = 10$  on his notation) that

$$j = 1.1$$

It is generally accepted that metal aircraft structures have a  $\sigma_S$  of less than half this value. If it is taken at half (i.e.  $\sigma_S = 4.3$  per cent) and a third (i.e. 2.9 per cent) the corresponding values are respectively

$$j = 1.022 \text{ and } 1.015$$

Engineers feel intuitively that the margins purely for scatter on strength should be much greater than 2.2 per cent. One possibility is that there is a weak family within the main family as was suggested in paragraph 13.2. Suppose that the weak family consists of a proportion  $\epsilon$  of the total and that it has a mean of  $L_S - \lambda\sigma_S$  and the same standard deviation  $\sigma_S$ . Equation (13.5) becomes

$$P = (1 - \epsilon)f_{L_S - \frac{1}{2}\sigma_S^2/\sigma_A} + \epsilon f_{L_S - \lambda\sigma_S - \frac{1}{2}\sigma_S^2/\sigma_A} \quad (13.6)$$

which simplifies to

$$P = f_{L_S - \frac{1}{2}\sigma_S^2/\sigma_A} \cdot [(1 - \epsilon) + \epsilon \cdot \exp(\lambda\sigma_S/\sigma_A)] \quad (13.7)$$

$$= f_{L_S - \frac{1}{2}\sigma_S^2/\sigma_A - \mu\sigma_S} \quad (13.7A)$$

$$\text{where } \exp(\mu\sigma_S/\sigma_A) = (1 - \epsilon) + \epsilon \exp(\lambda\sigma_S/\sigma_A) \quad (13.8)$$

Figure 13.9 shows the proportion of failures in the weak and the main families for a range of values of  $(\lambda\sigma_S/\sigma_A)$  and  $\epsilon$ . Figure 13.10 gives a plot of  $(\mu\sigma_S/\sigma_A)$  against  $(\lambda\sigma_S/\sigma_A)$  for different  $\epsilon$ . Figure 13.11 is deduced from Fig. 13.10 and shows a plot of  $(\frac{1}{2}\sigma_S^2/\sigma_A + \mu)\sigma_S$  against  $\lambda\sigma_S$  for the three conditions  $\sigma_S/\sigma_A = \frac{1}{2}, 1$ , and 2. Taking as a typical example  $\sigma_S = \sigma_A = 4$



per cent, then with a weak family of 2 per cent of the whole having a mean of 84 per cent (i.e.  $4\sigma_s$  below that of the main family) and the same standard deviation as the main family, the increase in strength of the whole that is required for scatter in strength is 5 per cent (i.e.  $1\frac{1}{4}\sigma_s$ ) compared with the

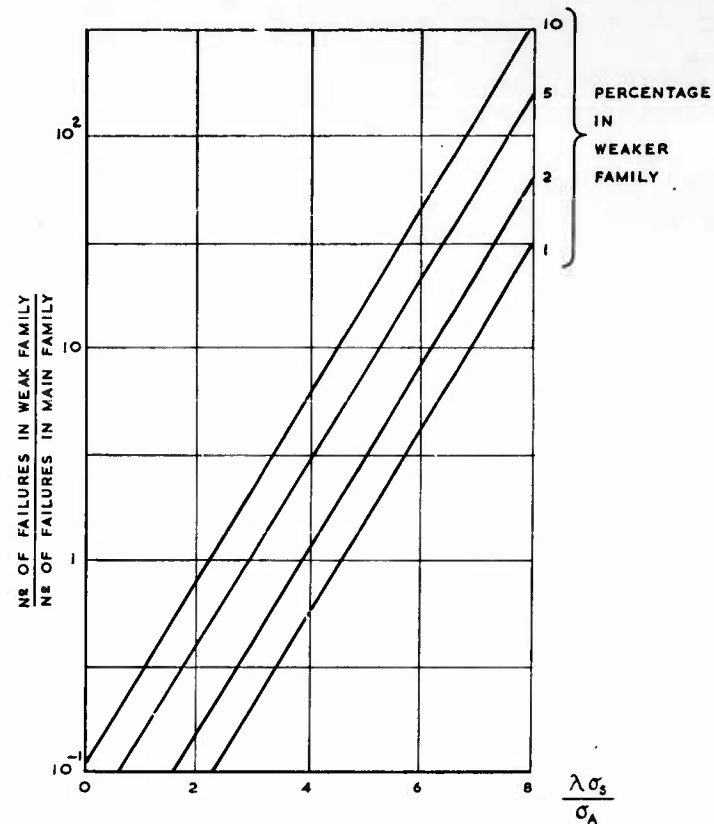


Fig. 13.9. Distribution of failures between weak family and main family.

Frequency of occurrence of loads greater than  $L$  is given by  $f_L = f_0 \exp(-L/\sigma_A)$

Both families have normal distribution of strength

$L_s$  = average strength of main family

$L_s - \lambda\sigma_s$  = average strength of weaker family

$\sigma_s$  = standard deviation of strength in both families

2 per cent that would be required if there were no weak family; the failures are about equally divided between the weak and the main family. This is not a very big change, but if there were only half the exponential decay ( $\sigma_A$ ) in the applied loads the increase in strength that would be required for scatter would be 12 per cent.

The values of probability of failure already obtained will now be compared with those that would be required if other distributions for the extreme values of strength and load are assumed. The case of both load and strength having Normal distributions and the case of both load and strength

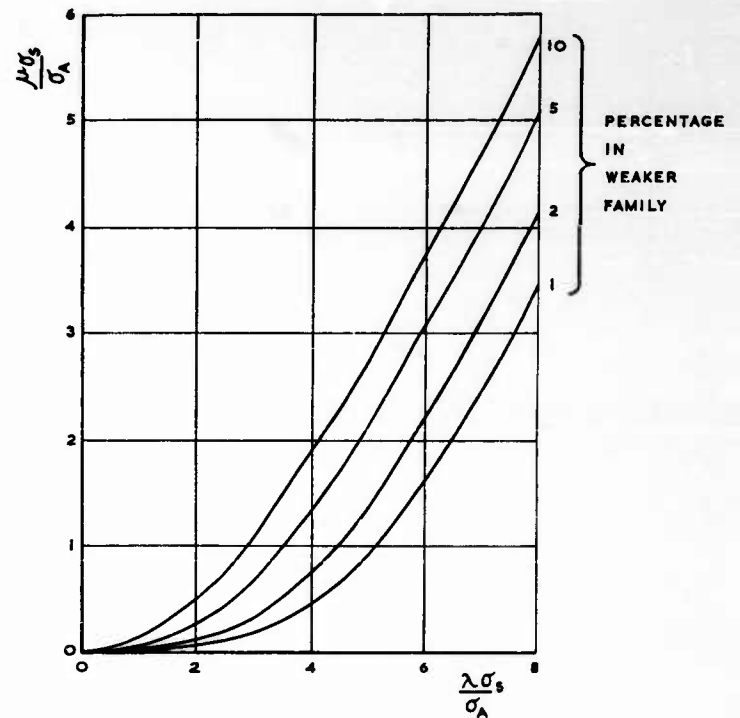


Fig. 13.10. Comparison of strengths of main family and weak family for the standard of reliability.

Frequency of occurrence of loads greater than  $L$  is given by  $f_L = f_0 \exp(-L/\sigma_A)$

Both families have normal distribution of strength

$L_s$  = average strength of main family

$L_s - \lambda\sigma_s$  = average strength of weaker family

$\sigma_s$  = standard deviation of strength in both families

$\mu\sigma_s$  = necessary increase in strength of both families to compensate for weak family

having exponential decays will be examined. When there is a Normal distribution of frequency of occurrence of loads greater than a stated value it will be given by

$$f_L = 2f_{L_A} \cdot (1/\sigma_A \sqrt{2\pi}) \int_L^{\infty} \exp[-(L - L_A)^2/2\sigma_A^2] dL \quad (13.9)$$

In practical distributions of applied load that approach that of Normal, the departures are likely to be greatest below  $L_A$  and the algebra can be simplified by splitting up the integration into values of  $L$  above and below  $L_A$ . The strength distribution remains

$$a_L = (1/\sigma_S \sqrt{2\pi}) \exp [-(L - L_S)^2 / 2\sigma_S^2] \quad (13.10)$$

as before.

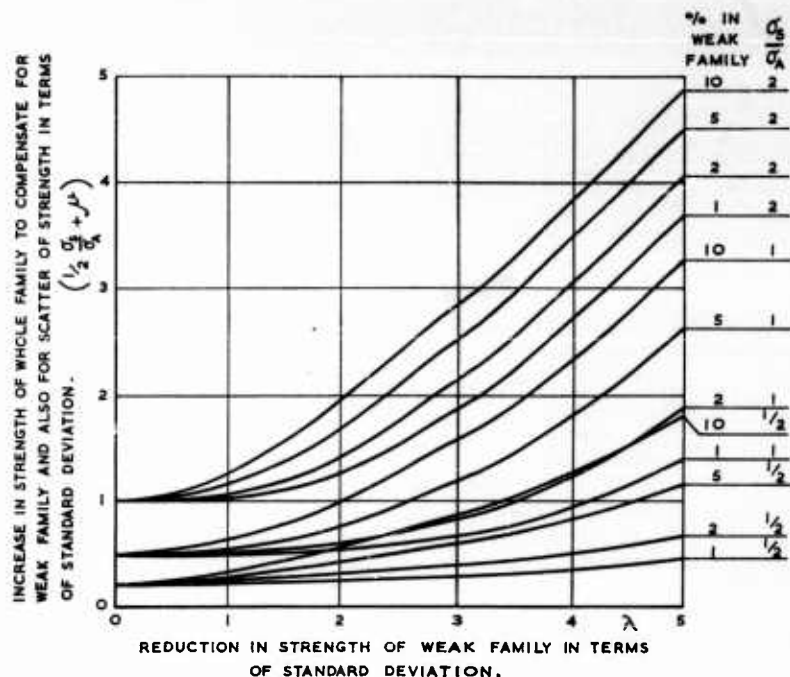


Fig. 13.11. Comparison of strengths of main family and weak family for the same standard of reliability and  $\sigma_s/\sigma_A$  equal to  $\frac{1}{2}$ , 1 or 2.

Frequency of occurrence of loads greater than  $L$  is given by  $f_L = f_0 \exp (-L/\sigma_A)$   
Both families have normal distribution of strength

$L_S$  = average strength of main family

$L_S - \lambda\sigma_A$  = average strength of weaker family

$\sigma_s$  = standard deviation of strength in both families

$\mu\sigma_s$  = necessary increase in strength of both families to compensate for weak family

The frequency of occurrence of failures ( $f_{La}$ ) is no longer a Normal distribution. It is not necessary to obtain this distribution to calculate the total failure rate but they have been determined for three examples to show how they compare with a Normal distribution. The margin between  $L_S$  and  $L_A$  is slightly different in each case, this has no significance as it was merely

for ease of calculation. A plot of the failure distribution is given in Fig. 13.12 for values of  $\sigma_S/\sigma_A = 1, \frac{1}{2}$  and  $\frac{1}{4}$  for  $L_S - L_A = 3.7\sigma_A, 3.75\sigma_A$  and  $3.725\sigma_A$ .

In the case  $\sigma_S/\sigma_A = 1$  the distributions of frequency of occurrence of applied loads and of strengths are the same but the procedure for determining the strength of the structures that failed shows that the mean value of the

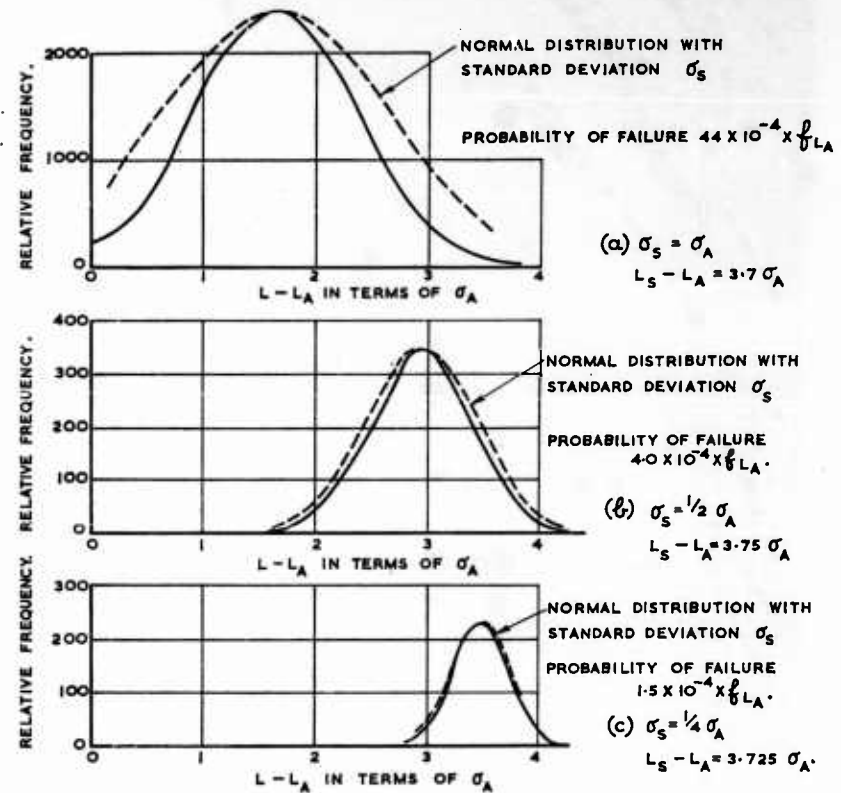


Fig. 13.12. Distribution of failures for a normal distribution of load and a normal distribution of strength.

$L_A$  = average load

$L_S$  = average strength

$\sigma_A$  = standard deviation of load

$\sigma_S$  = standard deviation of strength

$f_{L_A}$  = frequency of occurrence of loads greater than  $L_A$

static strength at which failure occurs is  $0.21 \sigma_S$  below the half-way position between mean load and mean strength. With the alternative approach the mean value of the applied loads that would cause failure would be  $0.21 \sigma_S$  above the half-way position and all other failure rates would be transposed in like manner.

To obtain the total failure rate it is not necessary to integrate numerically the values of Fig. 13.12. The probability of failure is given as before by

$$P = \int_{L_A}^{\infty} f_L a_L dL \doteq \int_{-\infty}^{\infty} f_L a_L dL \quad (13.11)$$

By combining (13.9), (13.10) and (13.11) and recasting the integrand (Hilton and Feigen (1960)) this reduces to

$$P = f_{L_A} \cdot (1/\sqrt{2\pi}) \int_{\tau}^{\infty} \exp(-z^2) dz \quad (13.12)$$

where  $\tau = (L_S - L_A)/(\sigma_S^2 + \sigma_A^2)^{1/2}$

The final combination of loads and strengths that will be examined is the one in which  $f_L$  and  $a_L$  each have an exponential distribution. In this case bounds must be put to the loads over which the distributions apply, otherwise frequencies of occurrence become completely unrealistic and the integration for failure rate would tend to infinity. It is assumed that these bounds for the applied loads and the strengths are respectively  $L = L_A$  and  $L = L_S$  and that the applied loads below  $L_A$  and the strengths above  $L_S$  are each Normal distributions. The contributions from these parts should be small but it is advisable to keep them in the integration to check that they are in fact small.

The distribution of the applied load becomes

$$\left. \begin{aligned} \text{for } L < L_A, f_L &= 2f_{L_A} \cdot (1/\sigma_A \sqrt{2\pi}) \int_L^{\infty} \exp[-(L - L_A)^2/2\sigma_A^2] dL \\ \text{for } L > L_A, f_L &= f_{L_A} \exp[-(L - L_A)/\sigma_A] \end{aligned} \right\} \quad (13.13)$$

and the distribution of the strength becomes

$$\left. \begin{aligned} \text{for } L < L_S, a_L &= (1/\sigma_S) \exp[(L - L_S)/\sigma_S] \\ \text{for } L > L_S, a_L &= (1/\sigma_S \sqrt{2\pi}) \exp[-(L - L_S)^2/2\sigma_S^2] \end{aligned} \right\} \quad (13.14)$$

Between  $L_A$  and  $L_S$  the frequency of occurrence of failures is given by

$$f_L a_L = (f_{L_A}/2\sigma_S) \exp(L_A/\sigma_A - L_S/\sigma_S) \exp[-(1/\sigma_A - 1/\sigma_S)L] \quad (13.15)*$$

This distribution is an exponential decay from  $L_A$  or from  $L_S$ , depending on which of  $\sigma_A$  and  $\sigma_S$  is the greater, except for the limiting case of  $\sigma_A$  being equal to  $\sigma_S$  when it has a constant value between  $L_A$  and  $L_S$ .

\* The slight lack of symmetry is due to  $f$  being a frequency of occurrence greater than a stated value of  $L$  whereas a  $\delta L$  is a proportion in a range  $\delta L$ .

The probability of a failure between  $L_A$  and  $L_S$  is

$$P = \int_{L_A}^{L_S} f_L a_L dL$$

which simplifies to

$$P = \sigma_A/2(\sigma_A - \sigma_S) [-f_{L_A} \exp \{-(L_S - L_A)/\sigma_S\} + f_{L_S}] \quad (13.16)$$

If  $\sigma_A$  is appreciably greater than  $\sigma_S$  this approximates to  $f_{L_S} \sigma_A/2(\sigma_A - \sigma_S)$ . If in addition  $\sigma_S/\sigma_A$  is small the contribution to the failure for  $L > L_S$  is very important and is obtained by using the formula of equation (13.4) to give an integrand. If  $\sigma_S$  is appreciably greater than  $\sigma_A$  the probability approximates to  $f_{L_A} [\sigma_A/2(\sigma_S - \sigma_A)] \exp [-(L_S - L_A)/\sigma_S]$  and for small values of  $\sigma_A/\sigma_S$  the contribution below  $L_A$  becomes important.

Table 13.2 gives the contributions in the three ranges of

- (i) failure less than  $L_A$
- (ii) failure between  $L_A$  and  $L_S$
- (iii) failure greater than  $L_S$ .

Table 13.2. *Distribution of Failures.*

*Load and Strength Distributions given by Equations (13.13) and (13.14)*

$\sigma_S/\sigma_A$	Strength of the structure that fails		
	Less than $L_A$	Between $L_A$ and $L_S$	More than $L_S$
small	negligible	50% of the failures	50% of the failures
$\frac{1}{2}$	negligible	60% of the failures	40% of the failures
$\frac{1}{3}$	negligible	72% of the failures	28% of the failures
$\frac{1}{4}$	negligible	86% of the failures	14% of the failures
$(n-1)/n$	negligible*	100/(1 + 0.52/n)% of the failures	100/(1 + n/0.52)% of the failures

Because of the similarity of the distributions for load and for strength it is possible to calculate for values of  $\sigma_S/\sigma_A$  greater than unity the distribution of the loads that cause failure instead of the strength of the structures that failed.

\* Negligible provided  $(L_S - L_A)/\sigma_A$  is greater than  $3/n$ , in other cases equation (13.4) must be used.

A numerical example is taken to show how the various distributions of load and strength might be used. The loading condition of Fig. 13.8 is taken and the strength selected to give a failure rate of one in  $10^7$  landings for the different distributions. For scatter of strength a value of  $\sigma_S = 0.04L_S$  is taken and wherever a weak family is postulated it is taken to consist of

# DESIGN PHILOSOPHY

2 per cent of the whole and to have a mean of  $0.84L_s$  and a standard deviation of  $0.04L_s$ .

The five different conditions are given in Table 13.3.

Table 13.3. Loading and Strength Conditions to give a Reliability of  $10^7$  Landings Per Failure.

All Loads and Strengths are given in Units of Acceleration  $g$

Condition	Applied load	Static strength
A	Normal distribution $L_A = 1.94g$ $\sigma_A = 0.16g$ $f_{L_A} = 0.0083$ of the landings	Normal distribution $L_s = 2.80g$ $\sigma_s = 0.112g$
B	Normal distribution as A	Normal distribution with 2% weak* $L_s = 3.16g$ $\sigma_s = 0.126g$
C	Normal distribution as in A and B for $L < L_A$ Exponential for $L > L_A$ $L_A = 1.94g$ $\sigma_A = 0.16g$ $f_{L_A} = 0.0083$ of the landings	
D	Distribution as C	Normal distribution with 2% weak* $L_s = 3.95g$ $\sigma_s = 0.158g$
E	Distribution as C	Exponential for $L < L_s$ Normal for $L > L_s$ $L_s = 4.10g$ $\sigma_s = 0.164g$

\* The weak family has mean  $0.84L_s$  standard deviation of  $0.04L_s$ .

The distributions of the loads strengths, and failures for each of the 5 conditions are given in Fig. 13.13. In conditions A and E the load and strength have about equal importance, in condition C the load is much the more important, in conditions B and D the changes from A and C are entirely due to the postulation of a weak family and its constitution. The change from A to B (12.7 per cent) is much more significant than the change from

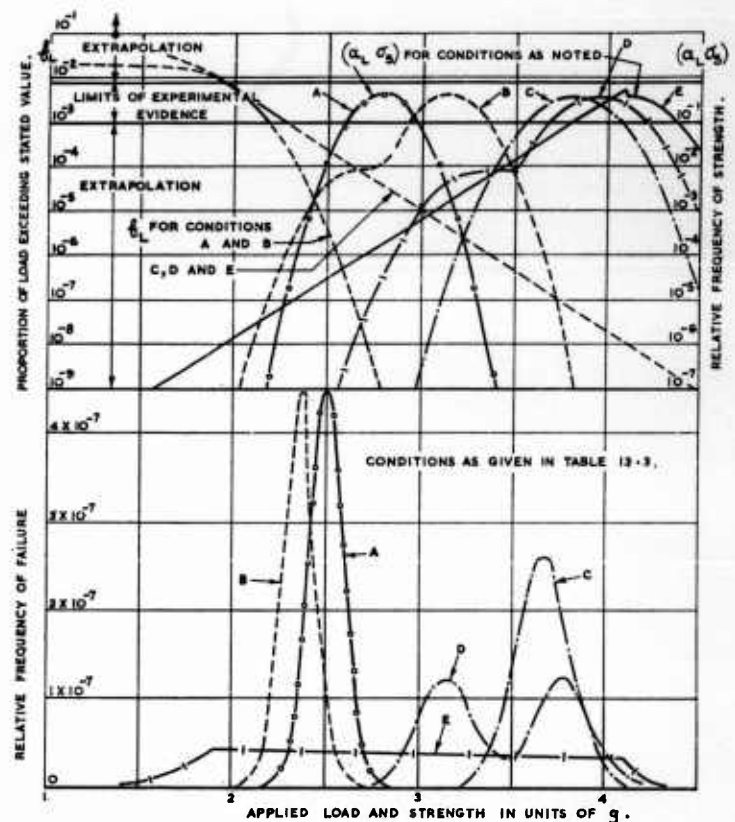


Fig. 13.13. Various loading and strength conditions which give a reliability of ten million landings per failure.

C to D (2.9 per cent). A rough check is made of the order of the factor, between applied load and design strength, that would be required in these numerical examples using conventional methods. This is roughly equal to the mean strength divided by the load expected to occur once in  $10^4$  landings (i.e. once per life-time of one aircraft). The equivalent ultimate factors are as follows:

$$\begin{aligned} A &= 1.19 \\ B &= 1.35 \\ C &= 1.43 \\ D &= 1.48 \\ E &= 1.53 \end{aligned}$$

Had conditions A and B had no scatter on load the cases would degenerate into these given in the table of paragraph 16.3 and the corresponding factors



would be 1.14 and 1.29. In this limiting case the effect of the weak family is to increase the ultimate factor by 13.1 per cent whereas between case A and B it is 12.7 per cent and between C and D 2.9 per cent. Thus the postulation of a weak family in design provides a safeguard such that when the maximum load is known and will occur on all the structures, there has to be 13 per cent margin to allow for the weak family. This is of the same order as the fixed margin of 10 per cent suggested by the Institution of Structural Engineers (1955) for the idealized case in which the load and strength are known precisely. When there is only a small chance of a high load, such as in C and D, the extra margin for the weak family is only 3 per cent.

The loading condition that has been used in this illustration is typical of the amount of data that is likely to be available for static strength estimates. It is a small group of about 6 rough landings taken from the total group of 320 landings. These 6 are, of course, plotted in the region of  $10^{-2}$  landings and the extrapolation is taken to  $10^{-7}$  landings. Whilst there may be a justification on general reasoning to assume an exponential decay for the frequency with which the loads are exceeded, the actual rate of decay has to be estimated and the knowledge of frequencies of the main family of landings is of little help. In the distribution of strengths it is unlikely that more than 10 values will ever be available, even for the main family, and if there is a weak family of less than about 5 per cent of the total with an unknown source of weakness, this cannot reasonably be detected at all unless it produces failure rates that would be prohibitive in operational use.

There is no hope of producing experimental data that will give the distributions of the extreme values used in the above calculations, but there is hope at least on the load side of extending the knowledge of some of the families of severe loads and reduce the amount of extrapolation. It seems possible in certain cases, e.g. turbulence in thunderstorms, that measurements are in fact made of the severe family of loads that will be the design case. Here then the extrapolation is within the actual family and does not have to make a discontinuous jump into another more extreme family.

### 13.6 FATIGUE STRENGTH

In dealing with the design philosophy for static strength it was possible to examine it under three nearly unrelated phases of applied loads, design strength, and reliability. In dealing with the design philosophy for fatigue there is much more interrelation between the three phases and constant reference will have to be made to the relationships. The main difference arises because of the cumulative effect of loads on the fatigue strength and the virtual independence of previous loading on static strength. The fatigue strength of a structure under any specified type of applied load is the magnitude of that load that the structure can withstand a specified number of times. The number of times any applied load occurs is directly related to the period of service. Thus fatigue strength must be given for the service life of the structure. Whilst the philosophy of design will be to determine the design strength for a specified service life, the relationship between fatigue strength and life allows for the actual strength to be quoted also as a service life for a specified applied loading condition.

Reliability of a structure under fatigue loads is determined in terms of a load history of the structure and the strength to withstand the loads. The principles that should be used in designing for reliability under fatigue loads will be described with the aid of simple formulae for the loads and for the strengths. For many purposes these simple formulae are adequate, but whenever greater accuracy is required more representative formulae may be used.

Many types of applied load can be represented by a series of terms of the form

$$E = \alpha \exp(-L/L_{AF}) \quad (13.17)$$

where  $E$  is the number of cycles of applied loads of amplitude greater than  $\pm L$  about a mean  $M$ ,  
 $\alpha, L_{AF}$ , are constants.

In this formula  $\alpha$  is the total number of load cycles since it is the extrapolated value of the number of loads of amplitude greater than zero. It is therefore directly proportional to time. This parameter  $\alpha$  will usually be the most suitable for defining the life of a structure. To make the analysis manageable the strength must also be given in terms of a formula. Heywood (1955) has shown that for a large variety of structural elements that the following relationship holds for endurance  $N$  between  $10^4$  and  $10^7$  cycles.

$$N = 10^6 \frac{L_{SF}}{(L - L_{SF})^2} \quad (13.18)$$

where  $N$  = the number of cycles to produce failure at a load of amplitude  $\pm L$  about a mean value  $M$

$L_{SF}$  = a constant.

This formula, which is a special case of one given by Weibull (1961), will be used in the present analysis. It has the advantage of implicit definition of fatigue strength by a single parameter  $L_{SF}$ . In particular cases either of equations (13.17) and (13.18) could be replaced by more representative ones. For a single loading condition  $M \pm L_1$  which fails in  $N_1$  cycles it may be presumed that after  $n_1$  cycles that  $n_1/N_1$  of the fatigue life has been consumed. If the effects of loadings at different amplitudes were cumulative then

$\sum_{r=1}^m n_r/N_r$  would be the proportion of fatigue life consumed by  $m$  different loads, where  $n_r$  are the number of applications of the  $r$ th load which would require  $N_r$  applications to produce failure. When the applied loads are of substantially the same magnitude this simple formula is a fair representation of reality. It will be assumed throughout the analysis that the fatigue life will be consumed in accordance with this cumulative formula. In those cases in which there are serious departures a correction should be made empirically to the life so calculated. In practical cases the applied loads will not be at discrete levels and the formula should be used in the integral form

$$\text{Proportion of life consumed} = D = - \int_0^{\alpha} \{(dE/dL)/N\} dL \quad (13.19)$$

For applied loads of a single type as given by equation (13.17) the main contributions to the life consumed will be from a small range of loads and it would be expected that the cumulative formula could be used with confidence. It would, however, be necessary for many structures to make a correction to the life to account for the permanent effect of relatively large loads applied occasionally. In substituting equation (13.18) into equation (13.19) the calculated values outside the band  $10^4$  to  $10^7$  cycles will usually be negligible; the realistic loads to produce failure outside this band will probably be smaller than those given by equation (13.18) and therefore the calculated value of the damage due to them will also be negligible.

The combination of equations (13.17), (13.18) and (13.19) gives

$$D = (2\alpha/10^6) \cdot \{\exp(-L_{SF}/L_{AF})\}/(L_{SF}/L_{AF})^2 \quad (13.20)$$

The purpose of formula (13.20) is to determine when failure will occur and this happens when the proportion of life consumed is unity. Thus substituting  $D = 1$  in the equation gives the fatigue strength of the structure as follows:

$$1 = (2\alpha/10^6) \{\exp(-L_{SF}/L_{AF})\}/(L_{SF}/L_{AF})^2 \quad (13.21)$$

Because of the simple formulae used for the applied loads and fatigue strength, the life is characterized by  $\alpha$ , the strength by  $L_{SF}$  and the loads by  $L_{AF}$ . Equation (13.21) may be regarded as giving the fatigue strength  $L_{SF}$  for a life of  $\alpha$  under the applied loads  $L_{AF}$ . If a number of structures were made to the same design there would be scatter in their fatigue strength. More experimental information is available on the scatter in fatigue strength than on static strength: Keppert and Payne (1955) give an extensive series of tests on complete aircraft wings, each test being at a fixed load cycle. A variety of amplitudes of the load cycle were used and the resultant endurance ranges ranged from  $5 \times 10^3$  to  $10^6$  cycles. Equation (13.18) is used to calculate the fatigue strength  $L_{SF}$  for each loading condition and it is found that at all load levels the standard deviation of the fatigue strength is about 10 per cent of the mean strength.

There are insufficient data to assess the actual distribution of the fatigue strengths but the analysis will be based on a Normal distribution. The arguments that were put forward for a weak family in static strength apply equally well in fatigue strength. The significance will not be so great for the same reduction in mean strength because the scatter in fatigue is so much more.

When there are a number of loading conditions that are significant the right-hand side of equation (13.21) becomes a series of terms with different values of  $\alpha$ ,  $L_{SF}$ ,  $L_{AF}$ .

### 13.7 APPLIED FATIGUE LOADS

The discussion of fatigue strength in paragraph 13.6 involved the use of equation (13.17) to define the applied loads. This equation was quite adequate for the purpose but there still remains the problem of scatter between the applied loads that occur in the specified life of a structure. The scatter will be examined for loads that can be defined in the form of equation (13.17) and the parameter  $\alpha$  will be retained as a measure of life. If the occurrence of an applied load greater than any particular magnitude was

completely random, the distribution of the number of occurrences of that particular load in a given time would be a Poisson distribution. So if the number of occurrences of a load is  $E$  there should be a standard deviation about  $E$  of  $\sqrt{E}$ . Bullen (1956) has shown that for atmospheric turbulence a scatter of about  $4\sqrt{E}$  could be expected because of the tendency for turbulent conditions to be clustered together. In the case of atmospheric turbulence,  $\alpha$  is the total number of up gusts in the life of the aircraft. This depends on the proportion of time spent at different altitudes but the average of those shown in Fig. 13.8A was 150 per hour so that  $\alpha = 10^7$  corresponds to about 65,000 hr and is the order of the operational life for transport aircraft. For loading conditions other than turbulence  $\alpha = 10^6$  or  $10^7$  should be the order of the number of loads in the life of an aircraft. Scatter on applied load can only be examined for loadings with numerical values included. To do this a typical loading due to atmospheric turbulence is taken for which  $\alpha = 10^7$  and the standard deviation for a number  $E$  of loads is  $4\sqrt{E}$ .

The analysis that will be done will show that the scatter on the applied loads is negligible and great simplifications can be made on this account. Conservative assumptions will be made so that an upper limit is established for the scatter. It will then be shown that this upper limit of scatter will have a negligible effect in all practical cases. The procedure for obtaining this upper limit is illustrated first for the typical case of atmospheric turbulence. In Fig. 13.14 the average loading condition together with those corresponding to departures of 1, 2 and 3 standard deviations from the mean are shown. The departures from the mean are so small that the loads have to be drawn as 2 components. The load is given in non-dimensional terms by giving it as a percentage of the load that occurs on average  $10^4$  times in the life of the aircraft. Loads occurring fewer times than  $10^4$  are not considered because the basis for the whole analysis, as mentioned in connection with equation (13.18), is that they consume a negligible amount of life compared with the more frequently occurring loads. The distributions for the applied loads which give the rigorous calculations for scatter are in an unsuitable form for general conclusions to be formed. A much simpler form can be produced by introducing a constant  $\sigma_{AF}$  and choosing it so that  $2\sigma_{AF}$  is two standard deviations from the mean value for the loads that occur  $10^4$  times. Lines of the form

$$E = \alpha \exp [-L/(L_{AFm} \pm r\sigma_{AF})] \quad (13.22)$$

where  $r$  is a factor

$\sigma_{AF}$  is a constant

$L_{AFm}$  is the mean value of  $L_{AF}$

will give greater scatter than the real scatter and will be conservative. Values for  $r = 1, 2$  and  $3$  are plotted in Fig. 13.14 for comparison with the more rigorous estimates of departure of 1, 2 and 3 standard deviations.

The simple formula of equation (13.22) identifies all the applied loads by a single load and the load that is  $r$  standard deviations from the mean as  $L_{AFm} \pm r\sigma_{AF}$ . Figure 13.14 was deduced for atmospheric turbulence but it would apply equally well for any other loading of the form

$$L = L_{AFm} \log_e (E/\alpha)$$

# DESIGN PHILOSOPHY

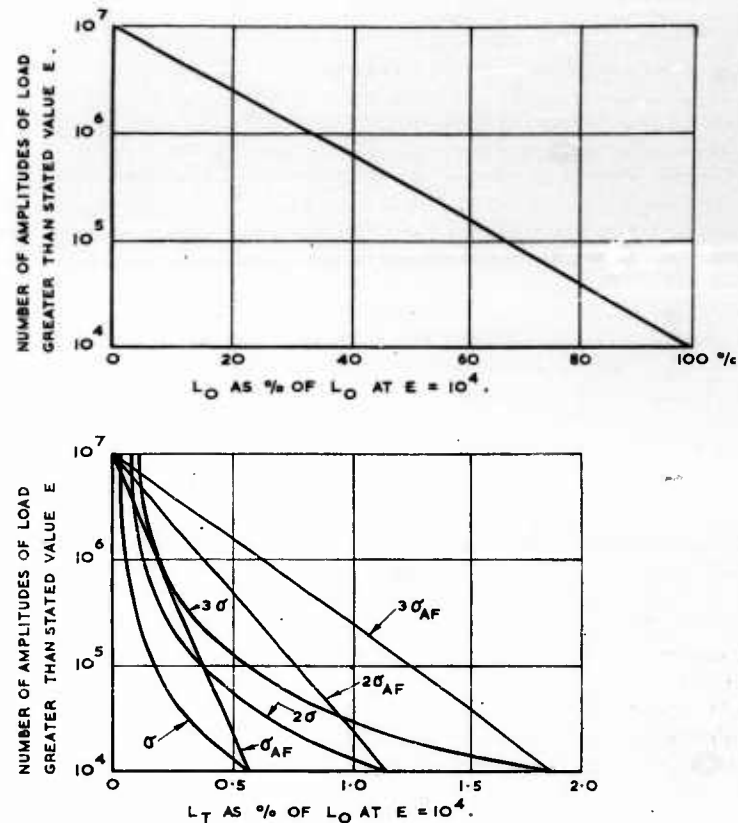


Fig. 13.14. Scatter on loading conditions typical of atmospheric turbulence.

The load is given as the sum of two components  $L_0$  and  $L_r$ , where

$$L_0 = L_{AFm} \log_e (E/10^7)$$

$L_r$  = the component for  $r$  standard deviations from  $L_0$

$\sigma = 4\sqrt{E}$  = the standard deviation for atmospheric turbulence loads observed by Bullen (1956)

$\sigma_{AF}$  = empirical constant as defined in equation (13.22) and the adjacent text

where  $\alpha = 10^7$ , with a standard deviation of  $4\sqrt{E}$ . It seems likely that there will tend to be clustering for other loading conditions as well, but it is probably conservative to assume that all loadings have clustering as severe as that for atmospheric turbulence. The general case can be calculated by allowing  $\alpha$  to have a general value, then  $\sigma_{AF}$  is given by

$$\sigma_{AF}/L_{AFm} = 0.0174/\log (\alpha/10^4) \quad (13.23)$$

The fatigue load condition for a life given by  $\alpha$  has now been reduced to a form identifiable by the two coefficients  $L_{AFm}$  and  $\sigma_{AF}$ ; the total number of

loads is  $\alpha$  and the relative frequency of different loads is  $\alpha \exp(-L/L_{AF})$ , where  $L_{AF}$  has a Normal distribution with mean  $L_{AFm}$  and standard deviation  $\sigma_{AF}$ . The scatter on applied load is evidently quite small, but its full significance can only be appreciated by combining it with the scatter on fatigue strength. Doing this has the added advantage that it can be introduced as an adjustment to the scatter on strength.

The fatigue strength condition can be given by two coefficients  $L_{SFm}$  and  $\sigma_{SF}$ ; the endurance at different loads is  $10^6 [L_{SF}/(L - L_{SF})]^2$ , see equation (13.18), where  $L_{SF}$  has a Normal distribution with mean  $L_{SFm}$  and standard deviation  $\sigma_{SF}$ . It was shown in equation (13.21) that the fatigue life is given in terms of  $L_{SF}/L_{AS}$ . It is assumed that  $L_{SF}$ ,  $L_{AF}$  are each distributed Normally and have respectively means of  $L_{SFm}$ ,  $L_{AFm}$  and standard deviations  $\sigma_{SF}$ ,  $\sigma_{AF}$ . The distribution of the ratio  $L_{SF}/L_{AF}$  can be shown, using either Geary (1930) or Hilton and Feigen (1960) to be as follows:

The proportion of the times that  $(L_{SF}/L_{AF})/(L_{SFm}/L_{AFm})$  is less than  $x$  is given by

$$\varepsilon = 1/\sqrt{2\pi} \int_{-\infty}^a [\exp(-\frac{1}{2}z^2) dz] \quad (13.24)$$

where  $a = (1 - x)/v_S(1 + x^2 v_A^2/v_S^2)^{1/2}$

$$v_S = \sigma_{SF}/L_{SFm}$$

$$v_A = \sigma_{AF}/L_{AFm}$$

So the distribution of the ratio of strength to applied load is the same as the distribution of strength alone with the standard deviation multiplied by the factor  $(1 + x^2 v_A^2/v_S^2)^{1/2}$ . For strengths below average  $x$  is less than unity so that substituting  $x = 1$  and the value of  $\sigma_{AF}/L_{AFm}$  from equation (13.23) gives an upper limit for the factor as

$$\{1 + [0.0174/v_S \log(\alpha/10^6)]^2\}^{1/2}$$

This upper limit is plotted in Fig. 13.15 for  $\alpha$  greater than  $10^6$ . It can be seen that the error on strength by ignoring the scatter of the applied loads is less than 1 per cent of the scatter on strength over most of the range examined, which should include the majority of the practical range. As the mathematical simplification used gives higher scatters than the real values the correction for scatter on load is quite infinitesimal and should be neglected; however if it is thought that it may be important in some exceptional case the equations (13.21) and (13.24) are easily usable on the conservative basis described. The most likely circumstance would be that of a fatigue condition in which loads occurring less than  $10^6$  times were important and in this case the formula for strength would also have to be re-examined.

### 13.8 RELIABILITY OF STRUCTURES UNDER FATIGUE LOADS

In considering the reliability of structures for static conditions it is possible to regard the applied loads and the static strength of a structure as independent and reliability is achieved by having a negligible chance that the applied load exceeds the strength. In fatigue the strength is a function of the applied

loads and if no life is imposed the number of applications must become sufficient eventually to break the part. Reliability may be achieved by one of two practices. Either the margin between the number of applications that are applied and the number that the part could withstand shall be sufficiently great, or alternatively local failure of the structure may be permitted but in such a way that static reliability is retained through adequate residual strength.

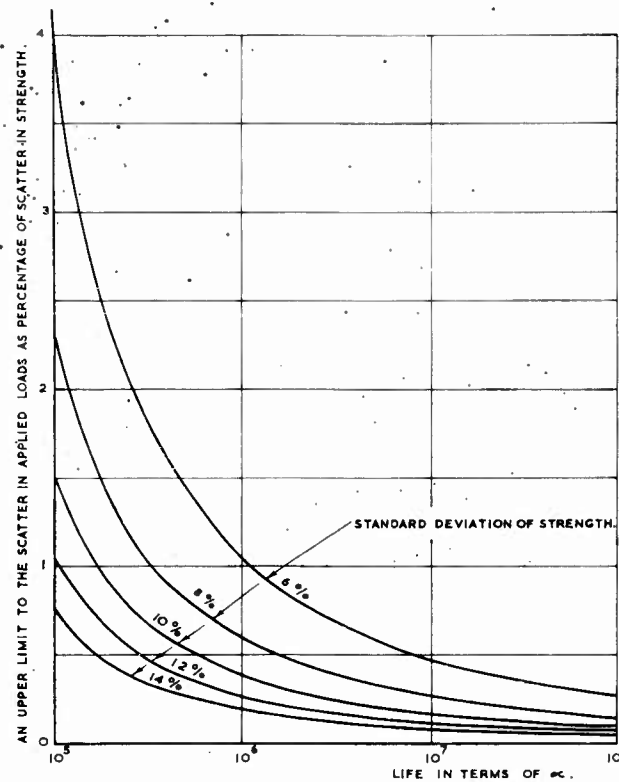


Fig. 13.15. Upper limit for scatter of applied fatigue loads.

If the reliability is achieved by a margin between applied loads and strength, the case is identical in substance with reliability of static strength. Every structure will have a margin of strength above the loads that are applied to it in its life-time. For an average structure with average loads the margin in conventional aircraft design is of the order of 50 per cent for both static strength and fatigue strength. This is somewhat fortuitous, as the static condition is usually one of high scatter on load and low scatter on strength whereas the fatigue condition is one of low scatter on load and high scatter on strength.

Equation (13.24) was deduced to show the relative values of scatter on load and on strength. In fact the equation gives the proportion of structures that have strengths less than the applied loads and can also be used to give a direct measure of reliability. The distribution is Normal and reliability can be achieved by selecting a margin of a multiple of the standard deviation below the mean for the parameter  $a$  that will give a negligible probability of failure. In general the scatter on applied loads is negligible, so that a multiple of the standard deviation of  $a$  is equivalent to the same multiple of the standard deviation margin on fatigue strength. The numerical value for the probability of failure is the proportion of the structures that fail but the assessment of reliability requires a knowledge of the rate at which they are failing. This increases as the life is consumed and will be at its greatest at the end of the life. Reliability in fatigue is achieved by ensuring that the numerical value of hours per failure is high at the end of the life of the structural part.

Values for the reliability can be determined from equations (13.21) and (13.24). A typical value for the scatter on strength is 10 per cent, so that the margin corresponding to 4 standard deviations is a factor of  $1\frac{1}{2}$  on strength, which can be shown from equation (13.21) to be a factor of 4 on life. There is a mathematical probability of 1 in  $3 \times 10^{-5}$  of the structure failing and for a design life of 10,000 hr the rate at which the hypothetical failures occur is zero at the beginning of operational service of the structural part and building up to  $2.5 \times 10^7$  flying hours per failure on completion of the 10,000 hr design life.

Fatigue failures differ greatly from static failures in that it is much more common for them not to be immediately catastrophic. On the other hand it is a more insidious form of failure and gives little indication that a loading condition is near to that which will cause failure; a static load a little below the ultimate strength will usually produce visible distortion. Should this occur it will be a warning that the applied loads might be greater than had been assumed in design or that the design strength is lower. This acts as a safeguard against human fallibility or ignorance. In fatigue a premature failure would take the form of one member of the structure failing and in good design an attempt is made whenever possible to utilize several members to carry vital loads, even when the design is such that fatigue failure should not occur.

In those cases where fatigue failures are not immediately catastrophic reliability does not depend solely on strength margins of safety. In certain circumstances, but by no means all, the fatigue failure can be detected by inspection. If the failure is always found immediately after the aircraft lands and if the aircraft has full design static strength with the part broken, then there is reliability. This was the case in some early bi-planes that had to have design static strength with any one of the wires connecting the two wings broken. The structures of modern aircraft are not nearly so easily inspected, but nevertheless if they retain their full design static strength after a particular fatigue failure, static reliability is retained. Fatigue reliability is reduced only in so far as the time required to produce other failures may become shorter than it otherwise would have been. As fatigue damage is cumulative, this latter condition can be included in design by



insisting that the structure shall be capable of withstanding these additional loads for a period less than the maximum time that the failure might go undetected.

The period that may elapse with an undetected failure depends on a number of things including detection methods and accessibility, and the inspection period does not necessarily put an upper limit to the time. If, however, the time of an undetected failure is controllable it is possible to take advantage of this information in design. In the case just cited the time for which the aircraft (damaged by fatigue but retaining full design static strength) has to carry the additional fatigue loads may be stipulated as part of the design.

Other information that becomes available by inspection of a particular part is the frequency with which that part fails in service. From this it should be possible to estimate the average number of aircraft that are in a damaged condition at any one time, so that if the residual strength is known a numerical value can be put on the reliability of a group of aircraft of a given type taken together. In the analysis of the reliability of static strength in paragraph 13.5 it was assumed that there were a number of aircraft of different strengths and the value given to the reliability was an average of the failure rates of all the aircraft. As far as the mathematical formula is concerned it is possible to retain the same reliability whilst deliberately increasing the proportion of structures that are below average strength provided that there is an appropriate increase in strength of the remainder. The purpose of the inspection procedure must be to find weakened structures (i.e. those that are broken) and remove them. When deciding to what extent aircraft can be damaged in service care must be taken not to violate the basic assumption of design philosophy that every aircraft must be reliable as it is no consolation when considering one particular aircraft to know that it is below standard but that many others are very much above it.

#### 13.8.1. *Permissible Residual Strength after Fatigue Failure*

An examination of the philosophy behind allowing fatigue failures will reveal roughly to what extent the process of reducing strength can be tolerated. Two fleets, one with some aircraft that have suffered fatigue damage and the other with no aircraft that have been damaged, can have the same numerical value for reliability provided the average strength of the aircraft in the fleet containing damaged aircraft is greater initially. It is not necessary for the damage to be very great for the total risk to be concentrated almost entirely in the aircraft that have suffered damage and there is no loss of generality in the physical reasoning by assuming it to be so. Thus if there is a fraction  $\epsilon$  of the aircraft in one fleet damaged, and all to the same extent, then the probability of failure of each one of the damaged aircraft is  $1/\epsilon$  times the probability of failure of each one of the aircraft of the other fleet. Whilst it is true to say that a negligible quantity can be multiplied by a small number and remain negligible, this cannot be continued indefinitely, and care must be taken that the probability of failure of the damaged aircraft remains negligible. The probability of failure will increase with the reduction in strength due to the fatigue failure and the residual strength that must be retained depends on the probability of failure, which in turn

will depend on the value of  $\varepsilon$  that is allowed to occur. For the procedure to be used with any confidence the actual value of  $\varepsilon$  needs to be known fairly accurately. In general the accuracy will not be good enough for very small  $\varepsilon$ 's and this itself will prevent the process being used where the failure rate of an individual aircraft may not be regarded as negligible.

The phenomena that has to be examined is in two phases, in the first phase fatigue damage is sustained by some aircraft and in the second phase these aircraft are subjected to all the normal flying loads at reduced static strength. For the first phase equations (13.21) and (13.24) can be used to give the rate at which the parts would fail in fatigue. As the reliability of the damaged aircraft is being compared with undamaged ones a formula is required for the relative frequency of occurrence of the static loads which need not be the same loading condition that caused fatigue damage. As it is only the relative frequency of occurrence over a fairly small range of loads that is involved it may be represented by a simple formula such as

$$f_L = f_0 \exp(-L/\sigma_A) \quad (13.2)$$

(repeated)

It was shown in paragraph 13.5 that for a frequency of occurrence per flight hour of loads greater than  $L$  given by this equation the probability of failure  $P$  per flight hour of a fleet of aircraft with a Normal distribution of strength with an average strength  $L_S$  and a standard deviation  $\sigma_S$  is given by

$$P = f_{L_S - \frac{1}{2}\sigma_S^2/\sigma_A} \quad (13.4)$$

(repeated)

Thus if there is a fleet with the same standard deviation, but consisting of a fraction  $\varepsilon$  of the structures with a strength  $(L_S - \mu\sigma_A)$  and the remainder  $(1 - \varepsilon)$  with a strength  $(L_S + \lambda\sigma_A)$ , the probability of failure  $P_D$  per flight hour is

$$P_D = \varepsilon f_{L_S - \mu\sigma_A - \frac{1}{2}\sigma_S^2/\sigma_A} + (1 - \varepsilon) f_{L_S + \lambda\sigma_A - \frac{1}{2}\sigma_S^2/\sigma_A} \quad (13.25)$$

If the probability of failure of the two fleets is the same  $P_D = P$  and equation (13.25) can be equated to (13.4). Then using equation (13.2) this simplifies to

$$\exp(\lambda) - 1 = \varepsilon \{ \exp(\mu) - 1 \} \quad (13.26)$$

This is plotted in Fig. 13.16 showing the increased static strength of the undamaged aircraft that is required to compensate for a reduction in static strength of various fractions of the total number of aircraft. It is evident both from equation (13.26) and the graph that after the fatigue damage has reached a certain level any further drop in fatigue strength must be compensated for by an identical increase in initial static strength. (In the limiting case of all aircraft damaged the residual strength must remain the same as an undamaged fleet.) Thus no matter how strong the structure was initially there is a maximum permissible drop below the basic design strength in residual strength, and so for any stated fraction of the structures damaged their residual strength must be greater than some definite and related value. This case will be considered further and is equivalent to considering the

risk to a structure that is damaged by fatigue in isolation from other risks in much the same way that individual static strengths were considered in paragraph 13.5. With this simplification equation (13.26) reduces to

$$\varepsilon = \exp(\lambda - \mu) \quad (13.27)$$

Equations (13.21), (13.24) and (13.26) can be combined to give the number of failures that have occurred after different periods of time and

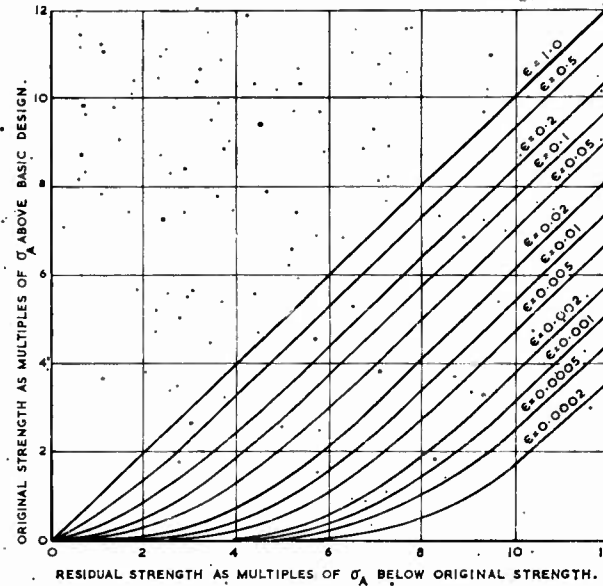


Fig. 13.16. Comparison of original static strength with the residual strength after fatigue damage for the same total reliability of fleet.

$\varepsilon$  = the proportion of the fleet that have sustained fatigue damage

$f_0 \exp(-L/\sigma_A)$  = the frequency of occurrence of loads greater than  $L$  where  $f_0$  and  $\sigma_A$  are constants

the residual strength that must remain in those damaged structures if none of them were repaired or removed from service. Figure 13.17 shows the variation in permissible drop in residual strength below the static design strength with service time in terms of the average life of the part of the structure under examination. (The time in hours would have to be used if the scatter on applied loads was not negligible.) One of the first difficulties that is encountered in using this diagram is the meaning to be given to design static strength as it should not include excess strength that has been included for improved fatigue resistance. Another feature is the scatter on life of individual structures. The actual magnitude of the scatter needs to be known fairly accurately if aircraft of reduced strength are to be tolerated; whereas in static design or fatigue design where failures are not tolerated a

structure that happened to have very much lower scatter than anticipated would have excess reliability, in fatigue design that permits failures there would be a longer period before failures commenced but it would be followed by failures at a greater frequency with a corresponding increased risk to the fleet as a whole. A further feature is the meaning of the numerical value of reliability. In the diagram the residual strength is shown that will ensure that the static reliability of the group of structures taken as a whole is the same regardless of the proportion that are damaged. This means that it is the reliability at a given moment in time rather than the average reliability over the whole life; the difference in design strength that would ensue if average reliability over the whole life was taken is not much with the formulae that have been used in the present study.

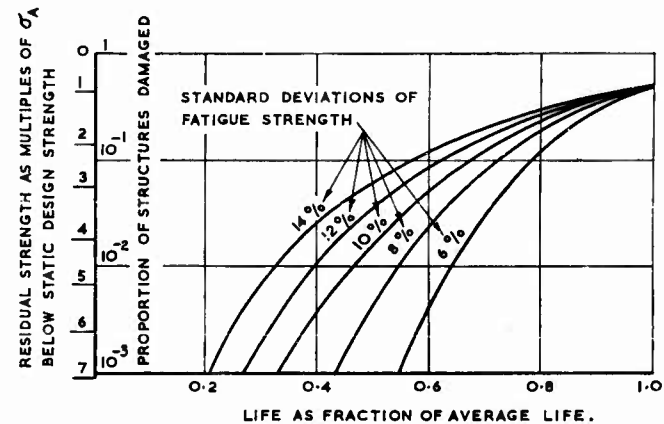


Fig. 13.17. Comparison of number of failures and permissible residual strength with life when no parts are removed from service.

In the case that the applied load is known fairly precisely, such as the pressure in a cabin,  $\sigma_A$  is small and the permissible drop in residual strength is small. If  $\sigma_A$  is zero no failures that involve a residual strength below the static design strength can be tolerated; this is in keeping with standard engineering practice. For most loading conditions  $\sigma_A$  is of the order of 4 per cent of the static design strength, so if half the aircraft were damaged they could have a residual strength 3 per cent below design strength; this is the order of superficial damage that is allowed more or less indiscriminately in almost all engineering practice.

#### 13.8.2. Inspection and Reliability

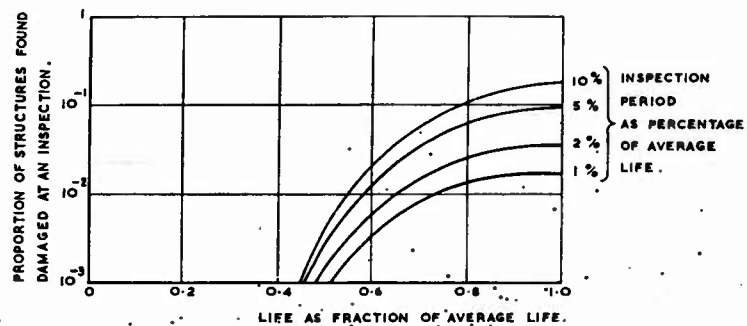
Figure 13.17 shows the proportion of structures that will become damaged due to fatigue as the life proceeds. If none are removed from service a group of structures with the fatigue strengths as shown in the diagram, would have the proportion damaged that are shown. The diagram also shows the residual strength, associated with the proportion damaged, that shall be maintained to ensure that the reliability does not drop below the

design level. Thus if the residual strength is known for a structure that has sustained some particular fatigue damage, the proportion of structures that may be so damaged is also known. The diagram also shows the life that may be permitted for various standard deviations of fatigue strength. If it is intended that all parts, that may be damaged in this way, are removed from service at some specified life without any prior inspection a margin for error must be made to avoid the permitted proportion of damaged structures being exceeded. If the part is in such a position in the structure that inspection of the area that might become damaged is possible, the proportion of damaged structures may be kept below the specified level by periodic inspection and removal or repair of parts found damaged. The inspection that is being discussed is one that might be used for specific parts to determine whether they have suffered fatigue damage that is already known to be a possibility. It is therefore supernumerary to general routine inspections of the structure for unpredicted fatigue, wear or accidental damage; these general inspections also assist in maintaining reliability but are not a subject of discussion in the present context.

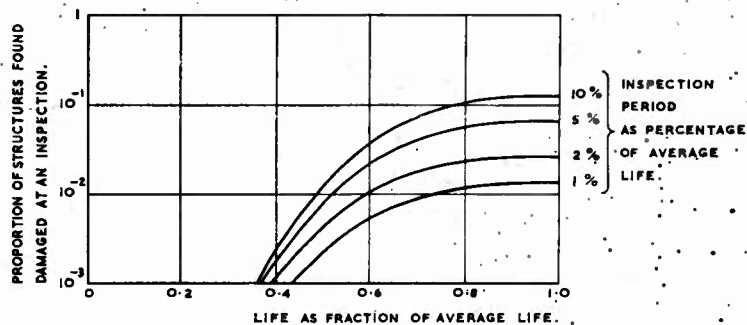
For the inspection procedure to be effective in controlling the proportion of particular parts of the structure that are damaged it is necessary to know fairly well the rate at which they should be damaged and to select the inspection period accordingly. If the rate at which the failures occur is not known accurately the inspection period must be shorter to compensate.

The required number of inspections will increase as the permitted drop in strength is increased. There are two reasons for this, first the corresponding proportion of structures that may be damaged is less and second the error that can be made in estimating this proportion is more. As a first step in estimating the required number of inspections can be made by deducing from Fig. 13.17 the average number of failures that would be present at an inspection. Figure 13.18 shows the average number of failures that should be detected per inspection of a complete fleet for different intervals between inspections, all of which are assumed to be 100 per cent efficient; Fig. 13.18 A, B and C are for standard deviations of 8, 10 and 12 per cent on strength. Diagrams of this type give an indication of when the first failures should be expected in a fleet of a given size and also can be used to check whether there are sufficient inspections to keep the number of damaged structures in the fleet at any one time down to the design level. If this data is collected by some central body it would be possible to regard a fleet as the total number of a given type in service and not merely those operated by one airline.

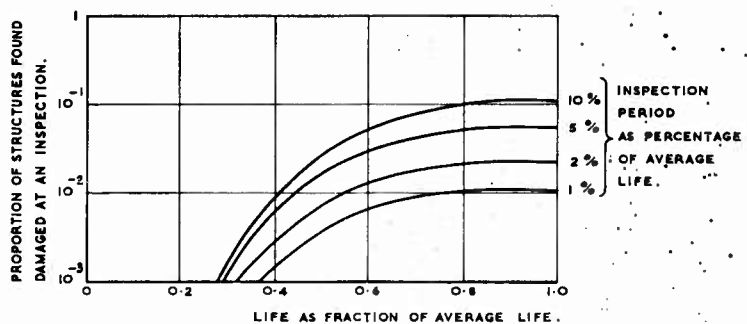
There are several difficulties involved in the use of these diagrams. All the lives are given in terms of the average life of the part concerned. The laboratory tests on typical specimens should give a fairly good estimate but a conservative value would be used for the prediction of inspection periods. Conservatism for scatter cannot be defined in a straightforward manner. For example, if a part had a 10 per cent standard deviation of fatigue strength it would be more conservative to assume a 12 per cent standard deviation at low lives but assume an 8 per cent standard deviation at high ones. In practical applications, a record of the lives at which damaged parts were found would be indispensable to an effective use of inspection. Furthermore



A - STANDARD DEVIATION OF FATIGUE STRENGTH = 8%



B - STANDARD DEVIATION OF FATIGUE STRENGTH = 10%



C - STANDARD DEVIATION OF FATIGUE STRENGTH = 12%

Fig. 13.18. Average number of failures detected at 100 per cent efficient inspections of different period.

an estimate must be made of the chance of not finding a failure at an inspection.

For any specific structural member an assessment could be made of the total cost of inspection. This will become prohibitive when the residual strength is too low, the actual value of the limit will, of course, depend on the weight penalty and increased cost of a replacement part and on the complexity of the inspection procedure. There is another limit to the number of inspections that can be made profitably. This can be illustrated by examining the case when the distribution of strength is known precisely; there is no loss of generality by so doing but in a practical case an allowance for error would be needed. If there is a fleet of  $N_A$  aircraft and  $P_A$  is the proportion of structures that are found damaged at an inspection, then the actual number of damaged aircraft is  $P_A N_A$  which must be a whole number. An estimate can be made of the lowest value that can be given to  $P_A$  by a study of  $P_A N_A$ . The curves of Fig. 13.18 give the average values of  $P_A$  with various inspection periods for a number of precise values of fatigue strength from which can be interpolated to give average values of  $P_A$  for any other prescribed inspection period (which may be variable) and fatigue strength.  $P_A N_A$  will be the average number of aircraft found damaged per inspection. Average numbers of damaged aircraft less than one have little meaning so that values of  $P_A$  less than  $1/N_A$  should not be considered. Even if  $P_A N_A = 1$ , there would be a lot of variation in the actual numbers found per inspection and the risk to the fleet as a whole would be very variable. Values of  $P_A N_A$  of 10 (i.e.,  $P_A = 10/N_A$ ) would produce much more consistency and would generally be preferred. It was shown in paragraph 13.8.1 that the risk to a whole fleet of aircraft was carried almost entirely by the damaged ones. If the number of aircraft of one type were large there would be a strong reluctance to designing deliberately to have all the risk to the type carried by a single aircraft that happened to be damaged at one particular point. Moreover there would be a feeling that that risk to the one aircraft might have ceased to be negligible. If the residual strength after damage were such that the permissible number of failures per inspection were 10, the risk could on average be spread over 10 aircraft. In such a case it is unlikely that the number of aircraft to one design would even be so large that the risk the damaged aircraft were undergoing had ceased to be negligible.

### 13.9 ACHIEVEMENT OF DESIGN STRENGTH

The principles that have been developed show how to define the design strength but there remains the problem of deciding how this design strength shall be achieved. In principle it is common practice to allow margins for error and for ignorance, but an important part of the practice is to reduce these to a minimum whilst ensuring that the margin is adequate in each case. For example, if there are two sources of error that always occur together for a particular feature of design, then the maximum error of the combination rather than the product of the two maxima taken separately would be taken. The determination of the structural temperature due to kinetic heating is a typical example. The maximum temperature that can be attained is the combined result of speed and ambient temperature

but the engine characteristics are such that at the higher ambient temperatures the maximum attainable speed is less than it would be at lower ambient temperatures.

On the load side there are possible sources of error in the overall load and also in the local distribution of load over the structure. One of the doubts that is always present at the design stage is that the loads are being extrapolated from information gained on other aircraft, from wind tunnel tests or from calculation. The applied loads that are decided upon will in general be the best estimates from all sources coupled with appropriate margins for error. These margins may be reduced once the aircraft has been flown and measurements have been taken on it, this is especially the case for fatigue loads.

On the strength side there are all the errors of stressing, material properties, manufacturing, deterioration in service and accidental damage. Having included appropriate margins, the design strength will finally be defined for a new structure or for one that has had some specified treatment, such as accelerated corrosion or heat treatment.

In the philosophy that has been described the design strength is given as a mean strength together with a distribution of strengths about this mean. When the strength is determined by calculation, allowances are made with the intention of ensuring that the strengths are greater at every level of probability. The margins for error that must be allowed are frequently unacceptably high and the strength is determined by test.

A margin must still be allowed as the estimate of the distribution of strengths of all structures to one design will be made from tests on samples. The number of samples that are tested will almost invariably be so small that the results cannot be used directly to estimate the whole distribution and reliance will have to be made on general experience from tests on similar types of structures and materials. For the purpose of comparing test strengths and design strengths it should be adequate to assume that the test specimens are taken from a group of structures which have a Normal distribution of strength. The mean is estimated from the tests but the scatter is usually estimated from general experience.

On these assumptions it is possible to calculate the most probable distribution of strength based on the tests on samples. This distribution will vary with the number of specimens that are tested and the estimate will increase in accuracy with number of specimens and be asymptotic to the distribution for an infinite number of tests. The best estimate of the mean value will be that given by the test as there is no more likelihood of it being above than below. The best estimate of the scatter at any probability level will be greater if there are fewer tests as it may be due to errors in the mean as well as due to variation between specimens. Bullen (1956b) has shown that if the group from which the specimens are taken has a Normal distribution of strength with a standard deviation  $\sigma$  times the mean, the proportion of specimens with strength lower than  $L$  will be given by

$$\epsilon = \int_{-\infty}^{\frac{L}{\sigma}} - [\exp(-\frac{1}{2}z^2)] dz \quad (13.28)$$



where  $a = (1 - L/L_m)/v (1 + L^2/nL_m^2)^{\frac{1}{2}}$

$L_m$  = mean strength of  $n$  specimens

This distribution is plotted for  $v = 3, 5, 10$  per cent in Fig. 13.19.

The error due to sampling is the margin between the strengths from the limited number of tests and the strengths from an infinite number. This margin varies with the probability level of the strength at which the comparison is made. There shall be no loss of reliability when test strengths are used instead of design strengths. A rigorous calculation would involve

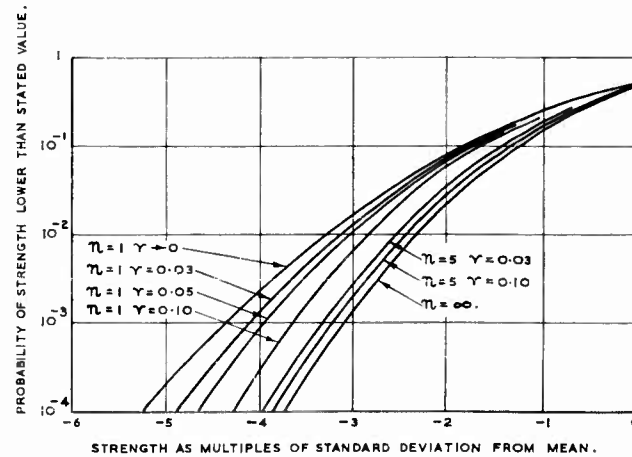


Fig. 13.19. Distribution of strength relative to experimental mean.

$n$  = number of tests

$v$  = standard deviation as fraction of mean strength

replacing the design strength distribution by the test strength distribution and determining the mean test strength that would be necessary to maintain the specified reliability. The required mean test strength will be equal to the mean design strength multiplied by a factor. This factor is the test factor.

#### 13.9.1. Static Test Strength and Fatigue Test Strength when Failure is Catastrophic

When the strength is determined by test it is measured on a small number of typical specimens. Even if the design strength has a double-family distribution it may be assumed that the proportion in the weaker family is so small that the test specimens are all from the main family and that the distribution is Normal. This allows a number of simplifications to be made when equating reliability of the design strength and of the test strength.

It was shown in paragraph 13.7 that the effective scatter on applied loads is negligible as far as fatigue reliability is concerned. For this condition, equation (13.28) may be used directly to equate the reliabilities of the design and test strengths. As there is no scatter on the applied loads the two reliabilities will be the same if the probability of the applied load producing

failure is the same in both cases. The test factor depends on the numerical value put on the reliability, the reciprocal of the probability of failure, and reduces gradually as the standard of reliability is increased. The minimum reliability likely to be contemplated is for the mean design strength 3 standard deviations of strength above the applied load. The test factors for this case are shown in Fig. 13.20 for different numbers of specimens and a range of standard deviations. This illustrates the benefit to be gained from

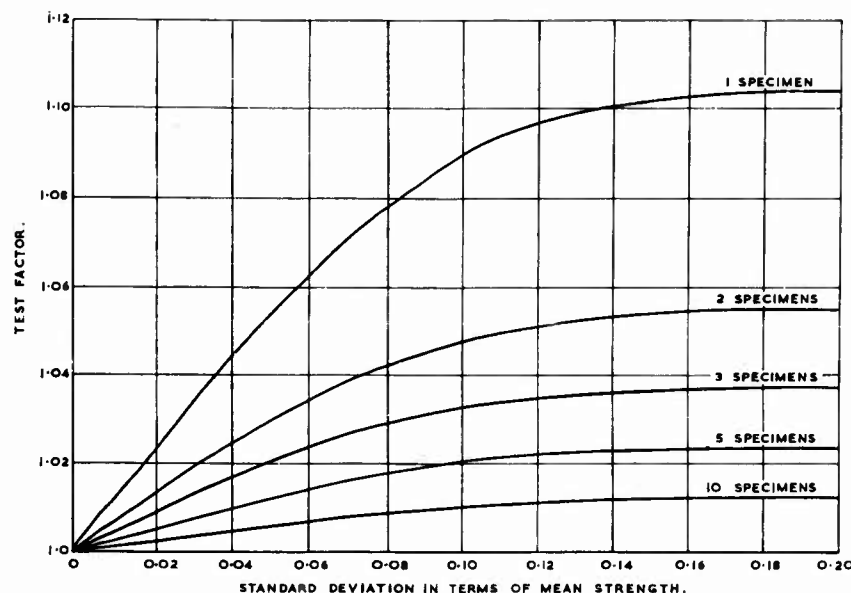


Fig. 13.20. Test factors for fatigue strength.

Calculated for applied load 3 standard deviations below the mean strength: the factors are less for higher reliability.

doing fatigue tests on a number of identical specimens. At a standard deviation of 10 per cent of the mean a test factor of 1.09 would be required for one specimen, but this drops steadily with increase in number of specimens down to 1.02 for 5 and 1.01 for 10 specimens; beyond 10 it reduces slowly to the asymptotic value of 1.00 for an infinite number of specimens.

For conditions in which the scatter on the applied loads is important, such as is the case for most static strengths, the distribution of strengths has to be combined with the distribution of applied loads. It was shown in paragraph 13.5 that, for the case in which the frequency of applied loads decayed exponentially, the most frequent strength at failure was  $(\sigma_S/\sigma_A)\sigma_S$  below the mean. For the purpose of determining the test factors it should be sufficiently accurate to replace those applied load distributions that are not exponential decays by the "best" estimate of an exponential decay at a load about  $(\sigma_S/\sigma_A)\sigma_S$  below the mean strength. A simplification can be made to the

test strength distribution, which are shown for selected values of numbers of specimens in Fig. 13.19, by making "best" estimates of Normal distributions. At very low values of  $\sigma_S$  the distribution is Normal with a standard deviation of  $\sigma_S(1 + 1/n)^{1/2}$ . At higher values a "best" estimate of the Normal distribution has to be made. The mean value is the same for both distributions and the Normal distribution will be fixed if it is given a strength for which there is a specified probability of it being exceeded. The reliability associated with the two strength distributions should be approximately the same if the strength chosen is  $(\sigma_S/\sigma_A)/\sigma_S$  below the design mean; this strength will be the one at which the failures are the most frequent for both distributions.

In the case of very low values of  $\sigma_S$  the standard distribution of the test strengths ( $\sigma_{ST}$ ) is given by

$$\sigma_{ST} = \sigma_S (1 + 1/n)^{1/2} \quad (13.29)$$

This will always be a good approximation for any practical values of  $\sigma_S$  and the more accurate value for  $\sigma_{ST}$  will always be less than that given by equation (13.29).

Paragraph 13.5 shows that the frequency of failure will be equal to the frequency of applied loads at  $L_{ST} = \frac{1}{2}(\sigma_{ST}^2/\sigma_A)$ . The test factor is determined by making this calculated frequency of failure for the test strength equal to that for the design strength. Thus  $L_S = \frac{1}{2}\sigma_S^2/\sigma_A = L_{ST} = \frac{1}{2}\sigma_{ST}^2/\sigma_A$  and the test factor becomes

$$F = 1 + \frac{1}{2}(\sigma_S/L_S)(\sigma_S/\sigma_A)[(\sigma_{ST}/\sigma_S)^2 - 1] \quad (13.30)$$

When equation (13.29) can be used the test factor simplifies to

$$F = 1 + \frac{1}{2}(\sigma_S/L_S)(\sigma_S/\sigma_A)(1/n) \quad (13.30A)$$

Figure 13.21 gives the test factors for values of  $n = 1, 2, 3, 5$  and  $\sigma_A/\sigma_S = 0.2, 0.4, 0.6$  for a range of values of  $\sigma_S/L_S$  up to 0.10. The calculated values using the simplified equation (13.30A) are shown for comparison with the more rigorous solutions using equation (13.30). It can be seen that for values of  $\sigma_S/L_S$  less than 0.04 the test factor is small; it only reaches 1.04 even for  $\sigma_S/L_S = 0.04$  and  $\sigma_A/\sigma_S = 0.02$ . For values of  $\sigma_S/L_S$  of the order of 10 per cent the importance of doing more than one test becomes apparent. At values appreciably above 10 per cent the simplifying assumptions that have been made for the strength and the load distributions are not justified and it is probably necessary to supplement the method described by some empiricism as is currently used for castings and transparencies.

### 13.9.2. Residual Strength after Fatigue Failure

For those structural parts that will be allowed to sustain fatigue damage in service the design has two parts; the first part is the fatigue strength and the second is the residual static strength of the whole structure after the fatigue failure. The procedure for determining the fatigue strength is exactly the same as that already described and tests of component parts can be used in the same way. The determination of the residual strength

is the same in principle as that for an undamaged structure and is subject to all the same simplifications and complications.

The practical implications are that for every fatigue failure that is contemplated the whole structure must be re-stressed for all the static cases. Many simplifications are possible and it will be self-evident that certain

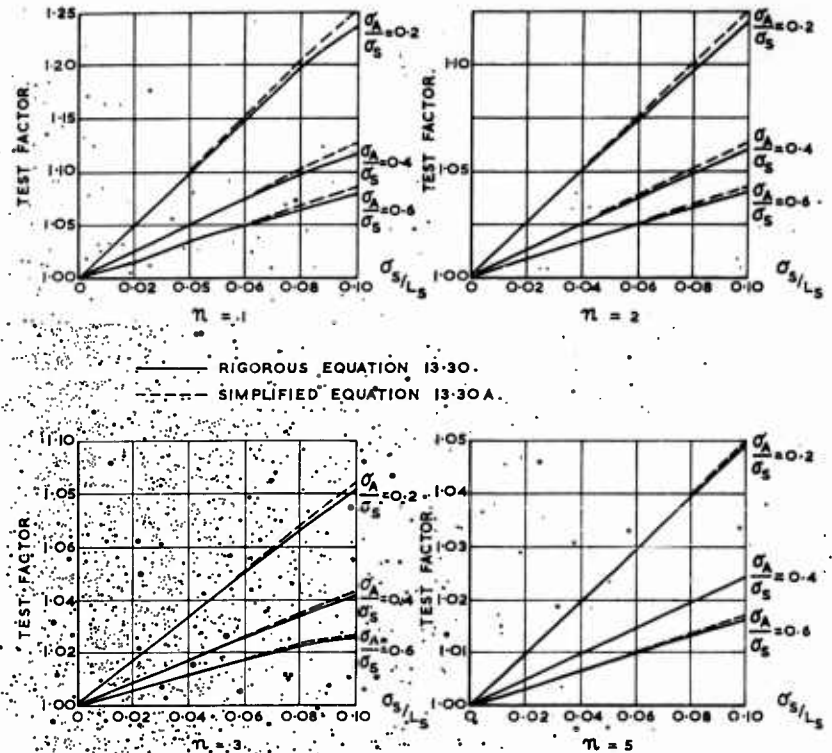


Fig. 13.21: Test factors for static strength.

$n$  = number of tests  
 $L_s$  = average strength  
 $\sigma_s$  = standard deviation of strength  
 $f_0 \exp(-L/\sigma_s)$  = frequency of occurrence of loads greater than  $L$ , where  $f_0$  and  $\sigma_A$  are constants.

parts will be unaffected by the failure. However, difficulties will arise in the representation of the fatigue damage either for calculation or for test. If reliance is made on calculation greater conservatism will be needed than for design of complete structures, as structures with damaged parts are far more complex and often they will have characteristics that would not have been countenanced in an original design.

An inspection procedure on the lines described in paragraph 13.8.2 is an

essential part of the achievement of design strength. If the inspections show that more failures are occurring than had been allowed by the design it means that the part is below strength and a reappraisal of the design has to be made. If the inspections show that fewer failures are occurring, it should be possible to reconsider the necessity for the number of inspections specified.

## REFERENCES

- |                          |  |
|--------------------------|--|
| Bullen (1956b)           | Institution of Structural Engineers (1955) |
| Cox (1959)               | Keppert and Payne (1955)                   |
| Geary (1930)             | Lusser (1958)                              |
| Heywood (1955)           | van der Neut (1957)                        |
| Hilton and Feigen (1960) | Weibull (1961)                             |

## NOTATION

THE notation for the whole Manual is given in alphabetical order taking first the Roman capitals followed by the Roman small letters, then the Greek capitals and Greek small letters. For each letter the order is roughly by chapter numbers.

For each symbol the chapter, or chapters, in which it occurs are given together with the meaning of the symbol. In each chapter there is no duplication of notation but there is a little duplication between the notation of different chapters but with little ambiguity. It is considered that a departure from well-established notation to avoid this duplication would have resulted in less clarity.

<i>Symbol</i>	<i>Chapters</i>	<i>Meaning</i>
$A$	4	Moment of inertia of the aircraft about axis $x$
$A$	10, 11	Wing aspect ratio
$B$	4	Moment of inertia of the aircraft about axis $y$
$B_1$	10	$\alpha_1^2(\alpha_1 + 3\alpha_2)/(4\alpha_1 + 4\alpha_2)$ equation (10.7)
$B_2$	10	$\alpha_2^2(\alpha_2 + 3\alpha_1)/(4\alpha_1 + 4\alpha_2)$ equation (10.7)
$^{\circ}\text{C}$	2	Centigrade degree of temperature
$C_0$	2	Speed of sound in atmosphere at $288.16^{\circ}\text{K}$ , 1116.89 ft/sec
$C$	4	Moment of inertia of the aircraft about axis $z$
$C_L$	4, 11	Lift coefficient of aeroplane
$C_{L0}$	4	Datum value of $C_L$
$C'_L$	4	Lift coefficient of tailplane
$D$	4	$d/d\tau$
$D$	11, 12	Exit diameter of a jet or nozzle ft
$D_c$	11	Depth of a cavity ft
$D$	13	Proportion of fatigue life consumed
$E$	4	Defined by equation (4.37)
$E_1$	4	Defined by equation (4.45)
$E'$	4	Defined by equation (4.46)
$E$	13	Number of cycles of applied loads of amplitude greater than $\pm L$ about a mean $M$
$F(\tau)$	4	Defined by equation (4.34)
$F$	13	Test factor
$G_0 G_1 G_2 G_3 G_4 G_5$	4	Coefficients of $D$ in equation (4.55)
$J$	4	Dimensionless frequency of the short-period oscillation of an aeroplane
$J_n$	9	Bessel function
$^{\circ}\text{K}$	2	Absolute degree of temperature
$K_n$	9	Bessel function with imaginary argument

MANUAL ON AIRCRAFT LOADS

<i>Symbol</i>	<i>Chapters</i>	<i>Meaning</i>
$K$	10	Gust response factor
$K_g$	10	Gust alleviation factor used by Pratt and W. G. Walker (1954)
$K_z$	10	Gust alleviation factor used by Zbrozek (1953)
$K$	11	Circulation round a wing ft <sup>2</sup> /sec
$L$	2, 9, 10, 11	Scale of turbulence ft
$L_1$	2	1.339 (2 $\pi$ $L$ )
$L$	4	Moment clockwise about direction $x$
$L_a$	4	Total aerodynamic couple about direction $x$
$L_c$	11	Length of a cavity ft
$L$	13	Used generally for static loads and strengths and for amplitude of fatigue loads and strengths
$L_A$	13	Datum load to which static loads are referred
$L_S$	13	Datum strength to which static strengths are referred
$L_{AF}$	13	Datum load to which amplitude of fatigue loads are referred
$L_{SF}$	13	Datum strength to which amplitude of fatigue strengths are referred
$L_{AFm}$	13	Mean value of $L_{AF}$ when there are a number of aircraft to the same design
$L_{SFm}$	13	Mean value $L_{SF}$ when there are a number of aircraft to the same design
$L_m$	13	Mean static strength of $n$ specimens
$\vec{M}$	4	Vector of applied couple
$M$	4	Moment clockwise about direction $y$
$M$	10	Mach number
$M$	13	Used in general terms for mean fatigue load
$M_a$	4	Total aerodynamic couple about direction $y$
$N$	4	Moment clockwise about direction $z$
$N$	13	Number of cycles to produce failure at a load of amplitude $\pm L$ about a mean value $M$
$N_a$	4	Total aerodynamic couple about direction $z$
$N_n$	5	Number per flying hour of peak normal accelerations greater than $ng$
$N'_0$	5	Parameter used in equation (5.1) to give a distribution for $N_n$
$N_V$	5	Number per flying hour of peak forward velocities greater than $V$
$N''_0$	5	Parameter used in equation (5.2) to give a distribution for $N_V$
$N_{Vn}$	5	Number per flying hour of peak normal accelerations greater than $ng$ at forward velocities greater than $V$

# NOTATION

Symbol	Chapters	Meaning
$N_w$	9	Number of crossings in each direction of velocity $w$ per unit distance
$N_r$	10	Number of crossings in each direction of response $r$ per unit distance
$N_0$	9, 10	Number of zero crossings in each direction per unit distance
$N_i$	13	Number of aircraft in a fleet
$O$	4, 9	Origin for coordinates axes $xyz$
$P$	2	Atmospheric pressure
$\bar{P}$	13	Probability of failure per flying hour
$\vec{P}$	4	Vector of the applied load to an aeroplane
$P_a$	4	Total incremental aerodynamic load on the tailplane
$P_{\bar{a}}$	13	Probability of failure per flying hour of a fleet of aircraft containing a fraction $\epsilon$ of the aircraft with a prescribed lower strength
$P_d$	13	Proportion of structures that are found damaged at an inspection
$R$	4	Dimensionless damping factor
$R_0$	2	95.984 ft lb/lb °K equation (2.1)
$R_i$	2	Richardson number equation (2.4)
$S$	4, 10	Wing area ft <sup>2</sup>
$S_0$	2	110.4 equation (2.3)
$S'$	4	Tailplane area ft <sup>2</sup>
$S(k)$	9	Twice the density with respect to inverse wavelength $k$ of turbulence energy
$S_x(k)$	9, 11	Component of $S(k)$ in direction $x$
$S_y(k)$	9	Component of $S(k)$ in direction $y$
$S_z(k)$	2, 9, 10	Component of $S(k)$ in direction $z$
$\bar{S}(k)$	10	Density with respect to $k$ of aircraft response to atmospheric turbulence
$\bar{S}'(k)$	10	Density with respect to $k$ of aircraft acceleration response to atmospheric turbulence
$\bar{S}_x(k)$	10	$(\bar{c}/L)/\alpha_1$ equation (10.7)
$\bar{S}_y(k)$	10	$(\bar{c}/L)/\alpha_2$ equation (10.7)
$\bar{S}_z(k)$	10, 12	Density with respect to $k$ of mean square pressure
$T$	10	Absolute temperature °K
$T_0$	10	288.16 °K equation (2.2)
$T(k)$	10	Response function relating aircraft response to a steady sinusoidal turbulence at inverse wavelength $k$
$T'(k)$	10	Response function relating aircraft acceleration response to a steady sinusoidal turbulence at inverse wavelength $k$
$U$	2, 9, 12	Velocity of stream of turbulence in direction $x$ sometimes referred to as horizontal
$U_x$	4, 11	Velocity of aircraft in direction $x$
$V$	4	Velocity of aircraft in direction $y$



# MANUAL ON AIRCRAFT LOADS

Symbol	Chapters	Meaning
$V$	5	Forward velocity knots E.A.S.
$V_D$	5	Design diving velocity knots E.A.S.
$V_T$	6, 10	True forward velocity ft/sec
$V_m$	5	Mean forward velocity at which peak normal acceleration manoeuvres are made
$V_v$	7	Vertical velocity at touchdown ft/sec
$W$	4	Velocity of aircraft in direction $z$
$W$	10, 11	Weight of aircraft lb
$\bar{W}_1$	4	Datum value of $W/U$
$X$	4	Force in direction $x$
$Y$	4	Force in direction $y$
$Y_a$	4	Total aerodynamic force in direction $y$
$Y_g$	4	Total gravity force in direction $y$
$Z$	2	Height
$Z$	4	Force in direction $z$
$Z$	12	Distance downstream of jet nozzle in terms of exit diameter
$Z_a$	4	Total aerodynamic force in direction $z$
$Z_g$	4	Total gravity force in direction $z$
$a$	4	$\partial C_L / \partial \alpha$ where $\alpha$ is in radians
$a$	9	A parameter used in equation (9.25)
$a$	10	$L/c\mu$ , equation (10.7)
$a$	11	Eddy viscosity in terms of circulation $K$
$a$	13	A limit of integration in equations (13.24) and (13.28)
$a_1$	4	$\partial C_L' / \partial \alpha_{eff}$ where $\alpha_{eff}$ is in radians
$a_2$	4	$\partial C_L' / \partial \eta$ where $\eta$ is in radians
$a_0, a_1, a_2, a_3, a_4$	4	Functions in equation (4.54)
$a_0$	12	Speed of sound external to jet stream
$a_L, \delta_L$	13	Proportion of structures with strengths between $L$ and $L + \delta L$
$b$	10, 11	Span of a wing ft
$b_1, b_3, b_5$	4	Functions in equation (4.54)
$c$	10	Mean chord of a wing ft
$f$	12	Frequency c/s
$f_u(r)$	9, 12	Longitudinal autocorrelation function as defined in equation (9.10)
$f_w(r)$	2, 9	Lateral autocorrelation function as defined in equation (9.11)
$f_{L*}$	13	Frequency of occurrence per flying hour of loads greater than $L$
$f_{L_A}$	13	Frequency of occurrence per flying hour of loads greater than $L_A$
$f_{L_S}$	13	Frequency of occurrence per flying hour of loads greater than $L_S$
$g$	Throughout	Acceleration due to gravity
$k$	2, 9, 10; 11, 12	Inverse wavelength cycles/ft
$k_1, k_2$	9	Components of $k$ in directions $xy$
$l$	4	Distance of the reference point of the tail from the centre of gravity of the aircraft
$l$	11, 12	Aerodynamic representative length

# NOTATION

Symbol	Chapters	Meaning
$l_p$	4	Derivative of angular velocity $p$ for a couple $L_a$
$l_\xi$	4	Derivative of aileron angle $\xi$ for a couple $L_a$
$m$	4	Mass of the aircraft
$m$	10	$\partial C_L / \partial \alpha$ where $\alpha$ is in radians
$m$	11	integers 1, 2, 3, . . . in equation (11.8)
$m_a, m_\eta, m_\psi, m_W$	4	Derivatives of $q, \eta, W, (W - W_0)$ respectively for a couple $M_a$
$n$	3	Parameter relating density of runway roughness with reduced frequency in Tables 3.1 and 3.2
$n$	4, 5	Normal acceleration in $g$ -units except that in Chapter 4 it is incremental normal acceleration
$n$	9	A parameter used in equation (9.25)
$n$	13	Number of specimens
$n_r, n_\xi, n_V, n_\nu$	4	Derivatives of $r, \xi, \dot{V}, V$ respectively for a couple $N$
$n_T$	4	Incremental normal acceleration at the tail in $g$ units
$n_T$	6	Transverse acceleration in $g$ units
$n_\infty$	4	Steady circling value of $n$ after an elevator angle $\eta_\infty$ has been held for a long time
$n_{max}$	4	Maximum value of $n$ when the elevator angle is increased linearly for time $\tau_1$ to a value $\eta_\infty$ and thereafter kept constant
$n_{T\infty}$	4	Steady circling value of the normal acceleration $n$ increment at the tail after an elevator angle $\eta_\infty$ has been held for a long time
$n_s$	5	Parameter used in equation (5.1) to give a distribution for $N_n$
$n_1$	13	Total number of experimental readings
$\dot{p}$	4	Angular velocity clockwise about direction $x$
$\dot{p}$	4	$\partial p / \partial t$
$\bar{p}$	11, 12	Fluctuating pressure in turbulence
$p_0, p^*$	4	Parameters introduced in equation (4.19) such that $p = p_0 + p^*$ where $p_0$ is a constant
$\bar{p}$	4	$\bar{p}$
$\bar{p}_0$	4	$\bar{p}_0$
$0, \pm \bar{p}_1, \pm \bar{p}_2$	4	Solutions of equation (4.54) for $\xi = \zeta = \eta = 0$
$\bar{p}_{00}, \pm \bar{p}_1, \pm \bar{p}_{11}, \pm \bar{p}_2, \pm \bar{p}_{22}$	4	Solutions of equation (4.54) for $\eta = 0$ and $a_0, a_2, a_4$ all small
$p N_{\sigma}$	10	Total number of gusts per mile in all operational flying combined
$q$	4	Angular velocity clockwise about direction $y$

Symbol	Chapters	Meaning
$\dot{q}$	4	$\partial q / \partial t$
$\bar{q}$	4	$Iq$
$q_D$	6	Dynamic pressure $\frac{1}{2} \rho V_T^2$ lb/ft <sup>2</sup>
$r$	4	Angular velocity clockwise about direction $z$
$\dot{r}$	4	$\partial r / \partial t$
$\bar{r}$	4	$Ir$
$r$	2, 9	Distance along direction $x$ at which auto-correlation of turbulence velocity is made
$r_1 r_2$	9	Components of $r$ in directions $x y$ for two-dimensional case
$r$	10	Response
$r$	11	radius ft
$r_c$	11	Radius at which circumferential velocity of a vortex is a maximum
$r$	12	Non-dimensional sound frequency = $fD/U = kD$
$t$	Throughout	Time seconds
$\bar{t}$	4	$m/(\rho S U)$
$t_0$	11	Time an aircraft has flown past any point before the trailing vortices are essentially rolled up
$u$	9	Turbulence velocity in direction $x$
$v$	9	Turbulence velocity in direction $y$
$v$	4	$V/U$
$w$	4	Increment of $W$
$\bar{w}$	4	$w/U$
$w$	2, 9, 10	Turbulence velocity in direction $z$
$w_r$	11	Circumferential velocity at a radius $r$ from the axis of a vortex
$x$	4	Forward and the principal axis of inertia of an aircraft most nearly along the centre line of the fuselage
$x$	9	Coordinate along direction of stream
$x$	10	Proportion of gusts that are associated with thunderstorm conditions
$x$	11	Distance downstream from the exit nozzle of a jet
$y$	4, 9	Principal axis of inertia of an aircraft to the right of a person facing forward in the fuselage
$y_V$	4	Derivative of $V$ for a force $Y_a$
$y_v$	4	Non-dimensional derivative of $v$ for a force $Y_a$
$z$	4	Principal axis of inertia of an aircraft at right angles to $x$ and $y$ and forming a right-handed system of axes
$z$	9	Coordinate forming right-hand system of axes with $x$ and $y$
$z_w$	4	Derivative of $W - W_0$ for a force $Z_a$
$\bar{z}_w$	4	Non-dimensional derivative of $\bar{w}$ for a force $Z_a$

## NOTATION

Symbol	Chapters	Meaning
$\Gamma$	2	Lapse rate to give neutral conditions in dry air
$\alpha$	4	Wing incidence, incremental value
$\alpha'_{\text{eff}}$	4	Effective tail incidence, incremental value
$\alpha'_{\text{eff}\infty}$	4	Steady state value of $\alpha'_{\text{eff}}$ after an elevator angle $\eta_{\infty}$ has been held for a long time
$\alpha_1$	10	$(0.26 + 2/A)/(1 + 0.83M + 0.95M^2)$ equation (10.7)
$\alpha_2$	10	$(2 + 2/A)/(1 + 0.83M + 0.95M^2)$ equation (10.7)
$\alpha$	13	Total number of load cycles, extrapolated value from equation of type (13.17)
$\beta$	6	Sideslip angle
$\gamma$	2	Lapse rate
$\gamma_1 \gamma_2$	11	Constants in equation (11.8) that depend on the dimensions of a cavity
$\delta$	4	Non-dimensional derivative of $\eta$ for a couple $M_a$
$\delta_v$	4	Non-dimensional form of $A - C$
$\delta_z$	4	Non-dimensional form of $B - A$
$\delta_{l\xi}$	4	Non-dimensional derivative of $\xi$ for a couple $L_a$
$\delta_{n\xi}$	4	Non-dimensional derivative of $\xi$ for a couple $N$
$\delta_{n\zeta}$	4	Non-dimensional derivative of $\zeta$ for a couple $N$
$\varepsilon$	4	Downwash angle at the tail
$\varepsilon$	4	Width of band, over which an analyser measures mean square pressures, in terms of mid inverse wavelength $k$ of the band
$\varepsilon$	13	Proportion that are from the weak family in a group of structures consisting of a main family and a weak family
$\zeta$	4, 6	Rudder angle
$\zeta$	5	Skewness of a distribution, third moment
$\zeta$	11	Circulation of air round vortex at radius $r$
$\eta$	4, 6	Angular deflection of the elevator from the position for straight and level flight
$\eta_{\infty}$	4	Elevator angle that is held indefinitely
$\theta$	4	Angle axis $x$ makes with the horizontal
$\lambda$	4	$(1 + d\varepsilon/dx)/\mu(1 - d\varepsilon/dx + a/2\mu)$ equation (4.44)
$\lambda$	13	Mean strength of the weak family of structures is $L_N - \lambda\sigma_N$
$\mu_0$	2	Air viscosity at Absolute temperature 288.16 K, $3.719 \times 10^{-7}$ slugs/ft sec
$\mu$	4	$m/(\rho SI)$
$\mu_v$	10	Aircraft mass parameter $2W/(\rho S c \bar{a} g)$
$\mu$	13	Defined by $\exp(\mu\sigma_N/\sigma_A) = (1 - \varepsilon) + \varepsilon \exp(\lambda\sigma_N/\sigma_A)$ , equation (13.8)

Symbol	Chapters	Meaning
$\nu$	4	Non-dimensional derivative of $q$ for a couple $M$
$\nu_l$	4	Non-dimensional derivative of $p$ for a couple $L$
$\nu_{lr}$	4	Non-dimensional derivative of $r$ for a couple $L$
$\nu_{np}$	4	Non-dimensional derivative of $p$ for a couple $N$
$\nu_n$	4	Non-dimensional derivative of $r$ for a couple $N$
$\nu$	11	Air viscosity
$\nu$	13	Standard deviation in terms of mean
$\nu_s$	13	$\sigma_{SF}/L_{SFm}$
$\nu_A$	13	$\sigma_{AF}/L_{AFm}$
$\xi$	4, 6	Aileron angle
$\xi$	10	$2\pi kL$
$\rho$	4, 6, 10, 11	Air density slugs/ft <sup>3</sup>
$\rho_0$	10	Air density at ground level slugs/ft <sup>3</sup>
$\sigma_n \sigma_m$	4	Functions introduced to simplify expressions in equation (4.46)
$\sigma$	5, 7, 13	Standard deviation of a distribution
$\sigma$	9	Root Mean Square of turbulence velocity
$\sigma_V$	5	Standard deviation of forward velocity
$\sigma_u$	9, 11	r.m.s. of turbulence velocity in direction $x$ of stream
$\sigma_v$	9	r.m.s. of turbulence velocity in direction $y$ with stream in direction $x$
$\sigma_w$	2, 9, 10	r.m.s. of turbulence velocity in direction $z$ with stream in direction $x$
$\sigma_r$	10	r.m.s. of aircraft response
$\sigma_a$	10	r.m.s. of aircraft acceleration response
$\sigma_p$	12	r.m.s. pressure
$\sigma_A$	13	Function of scatter of applied loads used in equation (13.2) or standard deviation of Normal distributions of applied loads
$\sigma_S$	13	Standard deviation of static strength with Normal distribution
$\sigma_{AF}$	13	Function of scatter of fatigue loads used in equation (13.22)
$\sigma_{SF}$	13	Standard deviation of fatigue load $L_{SF}$
$\sigma_{ST}$	13	Standard deviation of test strengths
$\tau$	4	Non-dimensional time $t/l$
$\tau_1$	4	Non-dimensional time for which elevator angle is increased linearly
$\tau_m$	4	Non-dimensional time at which normal acceleration of the aircraft reaches a maximum
$\tau_n$	4	Non-dimensional time at which $n_{Tmax}$ occurs
$\tau_n'$	4	Non-dimensional time at which $\alpha'_{eff max}$ occurs
$\tau$	12	Time at which autocorrelation function of jet pressure fluctuations are maximum

# NOTATION

Symbol	Chapters	Meaning
$\phi$	4	Angle $y$ axis makes with the horizontal
$\phi_0$	4	Value of $\phi$ at zero time
$\chi$	4	Non-dimensional derivative of $D\bar{w}$ for a couple $M$
$\chi_n$	4	Non-dimensional derivative of $D\bar{v}$ for a couple $N$
$\omega$	4	Non-dimensional derivative of $\bar{w}$ for a couple $M$
$\omega_l$	4	Non-dimensional derivative of $\bar{v}$ for a couple $L$
$\omega_n$	4	Non-dimensional derivative of $\bar{v}$ for a couple $N$

## REFERENCES

THE following is a list of all the papers to which reference is made in the text. A fuller bibliography is in preparation for publication by A.G.A.R.D. as *Bibliography of Aircraft Loads* by James Taylor. To avoid ambiguity all references in this Manual use the same identification as the Bibliography for the same paper. The list in both cases is in alphabetical order by first authors and wherever there are two or more papers by the first author in the same year the second and subsequent papers are identified by a, b, etc., after the year. Wherever there are two authors with the same name in the fuller bibliography all references in the text of this Manual include their initials.

The chapters in which the references are made are shown in square brackets [ ].

The following abbreviations are used

### (a) Organizations

A.G.A.R.D.	Advisory Group for Aeronautical Research and Development	International
A.R.C.	Aeronautical Research Council	U.K.
A.R.L.	Aeronautical Research Laboratory	Australia
A.S.D.	Aeronautical Systems Division	U.S.A.
A.S.T.I.A.	Armed Services Technical Information Agency	U.S.A.
C.A.A.R.C.	Commonwealth Advisory Aeronautical Research Council	International
H.M.S.O.	Her Majesty's Stationery Office	U.K.
I.A.S.	Institute of Aeronautical Sciences	U.S.A.
N.A.C.A.	National Advisory Committee for Aeronautics	U.S.A.
N.A.S.A.	National Aeronautics and Space Administration	U.S.A.
N.L.L.	Nationaal Luchtvaartlaboratorium	Netherlands
N.R.C.	National Research Council	Canada
O.N.E.R.A.	Office Nationale d'Etudes et de Recherches Aeronautiques	France
R.A.E.	Royal Aircraft Establishment	U.K.
R.Ae.S.	Royal Aeronautical Society	U.K.
Roy. Met. Soc.	Royal Meteorological Society	U.K.
W.A.D.C.	Wright Air Development Center	U.S.A.
W.A.D.D.	Wright Air Development Division	U.S.A.

### (b) Literature

Aero.	Aerodynamics
C.P.	Current Paper
J.	Journal
Memo.	Memorandum
Q.J.	Quarterly Journal
R.M.	Research Memorandum
R. and M.	Reports and Memoranda

Rept.	Report
T.M.	Technical Memorandum
T.N.	Technical Note
T.R.	Technical Report

- ANDREWS, D. R. (1954). A Flight Investigation of the Wake behind a Meteor Aircraft, with some Theoretical Analysis. A.R.C. C.P.282. [11]
- ANON, A.S.T.I.A. (1959a). Analysis of Turbulence Data Measured in Flight at Altitudes up to 1600 feet above three different types of Terrain. A.S.T.I.A. AD-212 231. [2, 10]
- ANON, INSTITUTE OF NAVIGATION (1960). Fuel reserves for aircraft. Symposium. *J. Inst. Nav.* Vol. 13, No. 3, July, 1960, pp. 273-287. [2]
- ANON, INSTITUTE OF NAVIGATION (1961). Fuel reserves for aircraft. *J. Inst. Nav.* Vol. 14, No. 1, January 1961, pp. 97-98. [2]
- ANON, INSTITUTION OF STRUCTURAL ENGINEERS (1955). Report on structural safety. *J. Struct. Eng.* Vol. 23, May 1955. [13]
- ANON, STAFF OF LANGLEY AIRWORTHINESS BRANCH, N.A.S.A. (1962). Operational Experiences of Turbine-Powered Commercial Transport Airplanes. N.A.S.A. T.N. D-1392. [7]
- BANNON, J. K. (1963). Turbulence in the Stratosphere and in the Upper Troposphere. R.A.E. Symposium, 16th November 1961, on Atmospheric Turbulence and its relation to Aircraft. H.M.S.O. [2]
- BATCHELOR, G. K. (1948). Recent developments on turbulence research. Seventh International Congress for Applied Mechanics. [9]
- BATCHELOR, G. K. (1953). *Theory of Homogeneous Turbulence*, p. 183. Cambridge University Press. [12]
- BULLEN, N. I. (1956b). A Note on Test Factors. R.A.E. Report Structures 215. [13]
- BULLEN, N. I. (1961). Gusts at Low Altitudes in North Africa. R.A.E. T.N. Structures 304. [10]
- BULLEN, N. I. (1963). Gust Loads on Aircraft. R.A.E. Symposium, 16th November 1961, on Atmospheric Turbulence and its relation to Aircraft. H.M.S.O. [10]
- BYERS, H. R. and BRAHAM, R. R. (1949). The thunderstorm. Wash. D.C.; U.S. Dept. of Commerce. [2]
- CLAY, L. E. and BERENS, A. P. (1963). Structural flight loads data from F-106A aircraft. Report No. ASD-TDR-63-653. [5, 8]
- CLARKSON, B. L. (1960). *Structural Aspects of Acoustic Loads*. A.G.A.R.D. Pergamon Press. [12]
- COLEMAN, T. L. and HALL, A. W. (1963). Implications of recent investigations on runway roughness criteria. A.G.A.R.D. Meeting, January 14th-18th, 1963. [3]
- COPP, M. R. and FETNER, M. W. (1959). Analysis of Acceleration, Airspeed, and Gust-Velocity Data from a Four-Engine Turboprop Transport Operating over the Eastern United States. N.A.S.A. TN D-36. [5, 10]
- COX, H. L. (1959). Reproducibility of Results in Fatigue Testing. Chapter XVII of *Metal Fatigue*, Editor J. A. Pope. Chapman and Hall, London. [13]
- CRANE, H. L. and CHILTON, R. G. (1956). Measurements of Atmospheric Turbulence over a Wide Range of Wavelength for One Meteorological Condition. N.A.C.A. TN 3702. [2, 10]
- CZAYKOWSKI, T. (1955). Loading Conditions of Tailed Aircraft in Longitudinal Manoeuvres. A.R.C.R. and M. 3001. [4]
- CZAYKOWSKI, T. (1962). Longitudinal Manoeuvre Loads. A.G.A.R.D. Conference 3rd July 1962, unpublished. [4]
- DREHER, R. C. (1956). A Method for Obtaining Statistical Data on Airplane Vertical Velocity at Ground Contact from Measurements of Center-of-Gravity Acceleration. N.A.C.A. TN 3541. [7]



# REFERENCES

- DREHER, R. C. and BATTESON, S. A. (1958). Landing and Taxiing Tests over Various Types of Runway Lights. N.A.C.A. RM L58C28a. [7]
- DRYDEN, H. L. (1938). Turbulence Investigation at the National Bureau of Standards. Fifth International Congress for Applied Mechanics. [9]
- DUNN, W. P. (1962). Dynamic Load Aspects of Runway Roughness and Alighting Impact. A.G.A.R.D. Conference 3rd-6th July 1962, unpublished. [3]
- DURKEE, E. D. (1961). Structural Flight Loads Data from B-47E Bomber Operations. W.A.D.D. TN-61-7. [5, 8, 11]
- FAIL, R., OWEN, T. B. and EYRE, R. C. W. (1955). Preliminary Low Speed Wind Tunnel Tests on Flat Plates and Air Brakes: Flow, Vibration and Balance Measurements. A.R.C. C.P. 251. [11]
- FAIL, R. (1962). Wind Tunnel Investigations of Buffeting. A.G.A.R.D. Conference 3rd-6th July 1962, unpublished. [11]
- FISHER, W. A. P. (1964). Aircraft manoeuvre loads. To be published by A.G.A.R.D. [5]
- GEARY, R. C. (1930). The frequency distributions of the quotient of two normal variables. *J. Roy. Stat. Soc.* Vol. 93, p. 442. [13]
- GERLACH, D. O. (1963). B-66B Summer Low Level Gust Study: Technical Analysis. Report No. ASD-TDR-62-1036, Vol. 1. [2]
- GORELIK, A. G., KOSTAREV, V. V. and CHERMIKOV, A. A. (1958). (Translated by Valda Dreimanis, edited by David Atlas) *Radar Measurement of Turbulent Motions in Clouds.* (*Radiolokatsionnoe Izmerenie Turbulentnykh Dvizhenii v Oblakakh*) A.S.T.I.A. AD-211 790. [10]
- GRAY, F. P. (1955). Maneuver Load Data from Jet-Fighter Combat Operations. W.A.D.C. TN-55-12. [5, 8]
- GREATREX, F. B. (1955). Jet Noise. Fifth International Aero. Conference, Los Angeles (Calif.), June 1955, pp. 415-448. [12]
- GRIMES, C. K. (1957). Development of a Method and Instrumentation for Evaluation of Runway Roughness Effects on Military Aircraft. A.G.A.R.D. Report 119. [3]
- HALL, J. (1962). A Re-Analysis of Existing Gust Data Using the Power Spectrum Method. Hatfield College of Technology Conference, 16th February 1962, unpublished. [10]
- HAMER, H. A. and MAYER, J. P. (1960a). Statistical Data on Control Motions and Airplane Response of a Republic F-84F Airplane during Operational Training Missions. N.A.S.A. TN D-386. [6]
- HARRIN, E. N. (1956). Comparison of Landing-Impact Velocities of First and Second Wheel to Contact from Statistical Measurements of Transport Airplane Landings. N.A.C.A. TN 3610. [7]
- HEISENBERG, W. (1948). *Proc. Roy. Soc.* Vol. A.195, pp. 402-406. [9]
- HEISENBERG, W. (1948a). *Zur Statistischen Theorie der Turbulenz. Zeitschrift für Physik*, Vol. 124, 1948. [9]
- HEYWOOD, R. B. (1955). Correlated Fatigue Data for Aircraft Structural Joints. R.A.E. Report Structures 184, June 1955. [13]
- HILTON, H. H. and FEIGEN, M. (1960). Minimum Weight Analysis Based on Structural Reliability. *J. Aerospace Sci.* Vol. 27, No. 9, September 1960. [13]
- HITCH, H. (unpublished 1960). [3]
- HOUBOLT, J. C. (1961). Runway Roughness Studies in the Aeronautical Field. *J. Air Transport Division*, American Society of Civil Engineers (March 1961). [7]
- HOUBOLT, J. C., STEINER, R. and PRATT, K. G. (1962). Flight Data and Considerations of the Dynamic Response of Airplanes to Atmospheric Turbulence. A.G.A.R.D. Conference 3rd-6th July 1962. Unpublished. A revised version is due to be issued as an N.A.S.A. Technical Note entitled "Dynamic response of

- airplanes to atmospheric turbulence including flight data on input and response." [2, 10]
- HOWES, W. L., CALLAGHAN, E. E., COLES, W. D. and MULL, H. R. (1957). Near Noise Field of a Jet-Engine Exhaust. Conger, C.C., and Berg, D. F. Appendix B: Correlation Computer. N.A.C.A. Report 1338. [12]
- IDRAC, P. (1923). Etude sur les conditions d'ascendance du vent favorable au vol à voile. Mem. de l'Office Nat. Mét. de France. [2]
- INSTITUTION OF STRUCTURAL ENGINEERS (1955). Report on Structural Safety. *J. Structural Engineers*, Vol. 23, May 1955. [13]
- JOYNER, U. T., HORNE, W. B. and LELAND, T. J. W. (1963). Investigations on the ground performance of aircraft relating to wet runway braking and slush drag. A.G.A.R.D. Conference 14th-18th January 1963. Unpublished. [7]
- KADEN, H. (1931). *Aufwicklung einer unstablen Unstetigkeitsfläche*. Ing. Archiv. II Band, pp. 140-168, 1931. [11]
- VON KÁRMÁN, TH. and HOWARTH, L. (1938). *Proc. Roy. Soc.* Vol. A.164, pp. 192-215. [9]
- VON KÁRMÁN, TH. (1948). Sur la Théorie Statistique de la Turbulence. *Collected works of Theodore von Kármán*, Vol. IV, pp. 357-359. [9]
- KELLY, L. G. and BROOM, C. A. (1962). Structural Flight Loads Data from B-52G Aircraft. A.S.D. TDR-62-634. [5, 8, 11]
- KEPPERT, J. L. and PAYNE, A. O. (1955). Interim Report on Fatigue Characteristics of a Typical Metal Wing. Aeronautical Research Laboratories, Melbourne. Report SM 207, January 1955. [13]
- KERR, T. H. and DEE, F. (1959b). A Flight Investigation into the Persistence of Trailing Vortices behind Large Aircraft. A.R.C. C.P. 489. [11]
- KOLMOGOROFF, A. N. (1941). The local structure of turbulence in incompressible viscous fluid for very large Reynolds numbers. *C.R. Acad. Sci. U.S.S.R.* [9]
- KOLNICK, J. J. and MORRIS, G. J. (1955). Statistical Measurements of Landing Contact Conditions of the Boeing B-47 Airplane. N.A.C.A. RM L55H24. [7]
- KRAFT, C. C. (1955). Flight Measurements of the Velocity Distribution and Persistence of the Trailing Vortices of an Airplane. N.A.C.A. TN 3377. [11]
- LAMB, H. (1932). *Hydrodynamics*. 6th edition, Cambridge University Press. [11]
- LAURENCE, J. C. (1956). Intensity, Scale and Spectra of Turbulence in Mixing Region of Free Subsonic Jet. N.A.C.A. Rept. 1292. [12]
- LEWIS, D. R. (1956). *V-g* Records from Sea Hawk Aircraft. Unpublished Ministry of Aviation Report. [5]
- LEWIS, D. R. (1956a). *V-g* Records from Sea Fury Aircraft. Unpublished Ministry of Aviation Report. [5]
- LEWIS, D. R. (1957). *V-g* Records from Provost T.1 Aircraft. Unpublished Ministry of Aviation Report. [5]
- LIGHTHILL, M. J. (1952). On Sound Generated Aerodynamically. Part 1. *Proc. Roy. Soc.* Vol. 211A. [12]
- LIN, C. C. (1947). Remarks on the Spectrum of Turbulence. First symposium of Applied Mathematics A.M.S. 1947. [9]
- LIN, C. C. (1948). On the Law of Decay and the Spectrum of Isotropic Turbulence. Seventh International Congress of Applied Mechanics. 1948. [9]
- LIN, C. C. (1953). On Taylor's hypothesis and the acceleration terms in the Navier-Stokes equation. *Q.A.M.* Vol. X, 1953. [2]
- LOITSIANSKY, L. G. (1939). Some basic laws of isotropic turbulent flow. Rep. Cent. Aero-Hydrodyn. Ist. Moscow. No. 440, 1939. [9]
- LUDLAM, F. H. and SCORER, R. S. (1953). Convection in the atmosphere. *Quart. J. R. Met. Soc.* Vol. 79, p. 317, 1953. [2]
- LUDLAM, F. H. (1963). Air Flow in Cumulonimbus. R.A.E. Symposium, 16th November, 1961, on Atmospheric Turbulence and its relation to Aircraft. H.M.S.O. [2, 10]

# REFERENCES

- LUSSER, R. (1958). Reliability through Safety Margins. A.S.T.I.A. AD-212 476. [13]
- MATRANGA, G. J. (1959). Roll Utilization of an F-100A Airplane during Service Operational Flying. N.A.S.A. Memo. 12-1-58H. [6]
- MAYER, J. P., HAMER, H. A., and HUSS, C. R. (1954). A Study of the Use of Controls and the resulting Airplane Response during Service Training Operations of Four Jet Fighter Airplanes. N.A.C.A. RM L53L28. [6]
- MAYER, J. P. and HARRIS, A. E. (1955). Analysis of *V-g* Records from Ten Types of Navy Airplanes in Squadron Operations during the period 1949 to 1953. N.A.C.A. RM L54G23. [5, 8]
- MAYER, J. P. and HAMER, H. A. (1955a). A Study of Means for Rationalizing Airplane Design Loads. N.A.C.A. RM L55E13a. [5]
- MCNAUGHTAN, I. I. (1958). Maximum and Minimum Atmospheric Temperatures for Aircraft Design Purposes. Unpublished Ministry of Aviation Report. [2]
- MEYER, C. H. (1957). Flight Testing for Inertial Coupling Characteristics. A.G.A.R.D. Report 124. [4]
- MILWITZKY, B. and COOK, F. E. (1953). Analysis of landing-gear behaviour. N.A.C.A. Ref. 1154. [7]
- MORGANS, W. R. (1931). Relation between Ground Contours, Atmospheric Turbulence, Wind Speed and Direction. A.R.C. R. and M. 1456. [2]
- MORRIS, G. J. and STICKLE, J. W. (1960). Response of a Light Airplane to Roughness of Unpaved Runways. N.A.S.A. TN D-510. [3]
- MORRIS, B. R. (unpublished 1962). [7]
- MULL, H. R. and ERICKSON, J. C., JR. (1957). Survey of the Acoustic Near Field of Three Nozzles at a Pressure Ratio of 30. N.A.C.A. TN 3978. [12]
- MULL, H. R. and ALGRANTI, J. S. (1960). Flight Measurement of Wall-Pressure Fluctuations and Boundary-Layer Turbulence. N.A.S.A. TN D-280. [12]
- MULLINS, D. W. (1961). Maneuver Load Data from F-104A Aircraft. A.S.T.I.A. AD-253 639. [5, 8]
- MULLINS, D. W. (1962). Maneuver Load Data from F-104C and D Aircraft. ASD-TDR-62-363. [5, 8]
- NETHAWAY, J. E. and CLARK, J. (1960a). Inertia Cross-Coupling Effects during Rolling of a Delta Aircraft (Boulton-Paul IIIA). R.A.E. T.N. Aero 2674. [4]
- NEUMARK, S. (1958). Simplified Loading Formulae for Pull-Out Manoeuvres of Tailed Aeroplanes. R.A.E. Report Aero 2608. [4]
- VAN DER NEUT, A. (1957). Some Remarks on the Fundamentals of Structural Safety. A.G.A.R.D. Report 155. [13]
- NORTON, D. A. (1952). Investigation of B-47 Bomb-bay Buffet. Boeing Airplane Co. Document No. D12675. [11]
- OWEN, E. M. (1954). *V-g* Records from Meteor 8 Aircraft (January 1952—May 1953) R.A.E. Tech. Note No. Structures 134. [5]
- OWEN, E. M. (1955). *V-g* Records from Vampire 5 Aircraft (March 1951—April 1953). Unpublished Ministry of Aviation Report. [5]
- OWEN, E. M. (1955a). *V-g* Records from Meteor 8 Aircraft. Unpublished Ministry of Aviation Report. [5]
- OWEN, E. M. (1955b). *V-g* Records from Meteor NF.11 Aircraft. Unpublished Ministry of Aviation Report. [5]
- OWEN, E. M. and SELLERS, M. J. (1956). *V-g* Records and Fatigue Meter Results from Venom F.B.1 Aircraft. Unpublished Ministry of Aviation Report. [5]
- OWEN, E. M. (1957). *V-g* Records from Wyvern S.4 Aircraft. Unpublished Ministry of Aviation Report. [5]
- OWEN, E. M. (1957a). *V-g* Records from Jet Provost Aircraft. Unpublished Ministry of Aviation Report. [5]

- OWEN, E. M. and SELLERS, M. J. (1958). *V-g* Records from Hunter 4 Aircraft. Unpublished Ministry of Aviation Report. [5, 8]
- OWEN, E. M. (1958a). *V-g* Records from Canberra B6 Aircraft. Unpublished Ministry of Aviation Report. [5]
- OWEN, E. M. (1958b). *V-g* Records from Javelin Mk. 1 Aircraft. Unpublished Ministry of Aviation Report. [5]
- OWEN, E. M. and MALCOM, M. A. (1959). *V-g* Records from Gannet A/S Mk. 1 Aircraft. Unpublished Ministry of Aviation Report. [5]
- OWEN, T. B. (1958). Techniques of Pressure-Fluctuation Measurements Employed in the R.A.E. Low-Speed Wind-Tunnels. A.G.A.R.D. Report 172. [11]
- PANOFSKY, H. A. and MCCORMICK, R. A. (1959). The Spectrum of Vertical Velocity near the Surface. Institute of Aeronautical Sciences. Report 59-6. [2]
- PEARCEY, H. H. (1958). A Method for the Prediction of the Onset of Buffeting and other Separation Effects from Wind Tunnel Tests on Rigid Models. A.G.A.R.D. Report 223. [11]
- PEARCEY, H. H. and HOLDER, D. W. (1962). (Unpublished), Simple Methods for the Prediction of Wing Buffeting Resulting from Bubble Type Separation. A.G.A.R.D. Conference 3rd-6th July 1962. [11]
- PEMBO, C. and MATRANGA, G. J. (1958). Control Deflections, Airplane Response, and Tail Loads Measured on an F-100A Airplane in Service Operational Flying. N.A.C.A. RM H58C26. [6]
- PERRY, E. and RIEVELY, J. (1961). Structural Flight Loads Data from Jet-Tanker Operation. A.S.T.I.A. AD-259 391. [5]
- PHILLIPS, L. (1961). Maneuver Load Data from C-130 Aircraft. A.S.T.I.A. AD-255 752. [5, 8]
- PHILLIPS, W. H. (1948). Effect of steady rolling on longitudinal and directional stability. N.A.C.A. T.N. No. 1627. [4]
- PICKEN, J. (1960). Free-Flight Measurements of Pressure and Heat Transfer in Regions of Separated and Reattached Flow at Mach Numbers up to 4. Unpublished Ministry of Aviation Report. [8]
- PICKEN, J. and WALKER, D. (1961). Techniques for the Investigation of Aerodynamic Heating Effects in Free Flight. Unpublished Ministry of Aviation Report. [8]
- PINSKER, W. J. G. (1955). Preliminary Note on the Effect of Inertia Cross-coupling on Aircraft Response in Rolling Manoeuvres. A.R.C.C.P.435. [4]
- PLANTEMA, F. J. and BUHRMAN, J. (1960). Roughness measuring systems for runways and taxi tracks. NLL Note MS-60-45, 15-7-1960. (Included as Appendix C to Report of the Working Party on runway roughness, June 6-7 1960.) [3]
- POCKELS (1901). Zur Theorie der Niederohlagobildung an Gebirgen. *Ann Phys.* (4). Vol. IV, 1901, pp. 459-480. [2]
- POTTER, D. M. (1957). Measurements of Runway Roughness of Four Commercial Airports. N.A.C.A. RM L56I26. [3]
- PRATT, K. G. and WALKER, W. G. (1954). A Revised Gust-Load Formula and a Re-Evaluation of *V-g* Data Taken on Civil Transport Airplanes from 1933 to 1950. N.A.C.A. Report 1206. [10]
- PRESS, H. and STEINER, R. (1958). An Approach to the Problem of Estimating Severe and Repeated Gust Loads for Missile Operations. N.A.C.A. TN 4332. [10]
- RHODE, R. V. (1937). Gust Loads on Airplanes. *S.A.E. J.* March 1937. [5]
- RICE, S. O. (1944). Mathematical analysis of random noise. *Bell System Tech. J.* Vol. 23, 282, 1944 and 24, 46, 1945. [2, 9]
- ROSE, R. and DEE, F. W. (1963). Aircraft vortex wakes and their effects on aircraft. R.A.E. Tech. Note Aero 2934. [11]
- ROSSITER, J. E. (1962). The Effect of Cavities on the Buffeting of Aircraft. A.G.A.R.D. Conference 3rd-6th July 1962. [11]

# REFERENCES

- RUMSEY, C. B., PILAND, R. O. and HOPKO, R. N. (1960). Aerodynamic-Heating Data Obtained from Free-Flight Tests between Mach Numbers of 1 and 5. N.A.S.A. TN D-216. [8]
- SAUNDERS, K. D. (1961). B-66 Low Level Gust Study. (14 Vol., 89 Parts) Vol. I. Technical Analysis. W.A.D.D. TR-60-305. [2, 10]
- SAUNDERS, P. M. (1961). An Observational Study of Cumulus. *J. Met.* Vol. 18, p. 451, 1961. [2]
- SCORER, R. S. (1957). Experiments on convection of isolated masses of buoyant fluid. *J. Fluid Mech.* Vol. 2, p. 583. [2]
- SCORER, R. S. (1963). Stirring Motions in Stablystratified Airstreams Induced by Flow over Mountains. R.A.E. Symposium, 16th November 1961, on Atmospheric Turbulence and its relation to Aircraft. H.M.S.O. [2]
- SHATTUCK, R. D. (1961). Sound Pressures and Correlations of Noise on the Fuselage of a Jet Aircraft in Flight. N.A.S.A. TN D-1086. [2]
- SHEPPARD, P. A. (1963). The Incidence of Atmospheric Turbulence. R.A.E. Symposium, 16th November 1961, on Atmospheric Turbulence and its relation to Aircraft. [2]
- SILSBY, N. S. (1955). Statistical Measurements of Contact Conditions of 478 Transport-Airplane Landings during Routine Daytime Operations. N.A.C.A. Report 1214. [7]
- SILSBY, N. S. and HARRIN, E. N. (1955a). Statistical Measurements of Landing-Contact Conditions of a Heavy Bomber. N.A.C.A. RM L55E03. [7]
- SILSBY, N. S. and HARRIN, E. N. (1955b). Landing Conditions for Large Airplanes in Routine Operations. N.A.C.A. RM L55E18c. [7]
- SILSBY, N. S. (1956). Statistical Measurements of Landing Contact Conditions of Five Military Airplanes during Routine Daytime Operations. N.A.C.A. RM L56F21a. [7]
- SILSBY, N. S. and LIVINGSTON, S. P. (1959). Statistical Measurements of Contact Conditions of Commercial Transports Landing on Airports at an Altitude of 5300 feet and at Sea Level. N.A.S.A. TN D-147. [7]
- SMITH, F. B. (1961). An Analysis of Vertical Wind Fluctuations at Heights between 500 and 5000 ft. *Quart. J. Roy. Met. Soc.* Vol. 87, No. 372, April 1961. [2]
- SPREITER, J. R. and SACKS, A. H. (1951). The Rolling Up of the Trailing Vortex Sheet and its Effect on the Downwash behind Wings. *J. Aero. Sci.* Vol. 18, No. 1, January 1951. [11]
- SQUIRES, H. B. (1954). The growth of a vortex in turbulent flow. Unpublished Paper A.R.C. No. 16,666. [11]
- STAFF OF LANGLEY AIRWORTHINESS BRANCH (1962). Operational Experiences of Turbine-Powered Commercial Transport Airplanes. N.A.S.A. TN D-1392. [7]
- STICKLE, J. W. and SILSBY, N. S. (1960). An Investigation of Landing-Contact Conditions for a Large Turbojet Transport during Routine Daylight Operations. N.A.S.A. TN D-527. [7]
- STICKLE, J. W. (1961). An Investigation of Landing Contact Conditions for Two Large Turbojet Transports and a Turboprop Transport during Routine Daylight Operations. N.A.S.A. TN D-899. [7]
- SUTHERLAND, L. C. and MORGAN, W. V. (1961). The use of model jets for studying acoustic fields near jet and rocket engines. W.A.D.C.—University of Minnesota Conference on Acoustical Fatigue, W.A.D.C. Technical Report 59-676. [12]
- TAYLOR, G. I. (1938). The spectrum of turbulence. *Proc. Roy. Soc.* Vol. A.164, p. 476. 1938. [2, 9]
- TAYLOR, J. (1950). Design and Use of Counting Accelerometers. A.R.C. R. and M. 2812. [5]
- TAYLOR, J. (1953). Measurement of gust loads in aircraft. *Jour. R.Ae.S.*, February 1953. [10]

- TAYLOR, J. (1956). Fatigue Loading Actions on Transport Aircraft. Institute of Mechanical Engineers, Conference on Fatigue of Metals, September, 1956. [7]
- TAYLOR, J. (1958). General Introduction to Thermal Structures. A.G.A.R.D. Report 206. [8]
- TAYLOR, R. H. (1962). Annual Variation of Flight Loads Recorded on Viscount Aircraft by means of the Fatigue Load Meter. R.A.E. Tech. Note No. Structures 322. [10]
- THOMAS, H. H. B. M. and PRICE, P. (1960). A Contribution to the Theory of Aircraft Response in Rolling Manoeuvres including Inertia Cross-Coupling Effects. R.A.E. Report Aero 2634. [4]
- THOMPSON, W. E. (1958). Measurements and Power Spectra of Runway Roughness at Airports in Countries of the North Atlantic Treaty Organization. N.A.C.A. TN 4303. [3]
- TITUS, E. (1959). Maneuver Load Data from Jet-Trainer Operations. A.S.T.I.A. AD-216 306. [5, 8]
- TITUS, E. (1960). Maneuver Load Data from T-37 Trainer Operations. Wright Air Development Division. TN-60-124. [5, 8]
- TITUS, E. (1961). Maneuver Load Data from F-100 Operations. Aeronautical Systems Division, Wright-Patterson Air Force Base. ASD TR 61-683. [5, 8]
- TOLEFSON, H. B. (1956). Summary of Derived Gust Velocities Obtained from Measurements within Thunderstorms. N.A.C.A. Report 1285. [10]
- USHER, C. V. G. (1953). Analysis of  $V$ - $g$  Records for Canberra B2 Aircraft (November 1951 to July 1952) R.A.E. Tech. Note Structures 117. [5]
- VAHLDIK, A. M. (1961). Maneuver Load Data from F-102A Aircraft. Wright Air Development Division. TN 61-46. [5, 8]
- VAHLDIK, A. M. (1961a). Maneuver Load Data from F-105B Aircraft. Wright-Patterson Air Force Base. ASD TN 61-161. [5, 8]
- VAN DRIEST, E. R. (1952). Turbulent Boundary Layer on a Cone in a Supersonic Flow at Zero Angle of Attack. *J. Aero. Sci.* Vol. 19, No. 1, January 1952, pp. 55-57, 72. [8]
- WALKER, W. G. and COPP, M. R. (1959). Summary of VGH and  $V$ - $g$  Data Obtained from Piston-Engine Transport Airplanes from 1947 to 1958. N.A.S.A. TN D-29. [5, 10]
- WALLACE, C. D. (1961). Structural Flight Loads Data from B-52 Bomber Operations. W.A.D.D. TR-61-655. [5, 8, 11]
- WARD, D. C., JR. (1963a). Maneuver Flight Loads Data from RF-101C Aircraft. Final Report. ASD-TDR-62-923. [5, 8]
- WATSON, G. N. (1944). *Theory of Bessel Functions*. 2nd edition. C.U.P. [9]
- WEIBULL, W. (1961). *Fatigue Testing and Analysis of Results*. Pergamon Press. [13]
- WESTFALL, J. R., MILWITZKY, B., SILSBY, N. S. and DREHER, R. C. (1957). A Summary of Ground-Loads Statistics. N.A.C.A. TN 4008. [7]
- WETMORE, J. W. and REEDER, J. P. (1963). Aircraft Vortex wakes in relation to terminal operations. N.A.S.A. TN D-1777. [11]
- WILKINSON, K. G. (1951). Some Problems of Turbine Transport Operation in Europe. R.Ae.S. Anglo-U.S. Conference, 1951. [2]
- WILKINSON, K. G. and VIVIAN, J. (1953). A Rationalised Fuel Reserve Policy for Medium-range Airline Operations. S.A.E. Paper October 1953. [2]
- WOLFE, M. O. W. (1957). Near Field Jet Noise. A.G.A.R.D. Report 112. [12]
- ZBROZEK, J. K. (1953). Gust Alleviation Factor. A.R.C. R. and M. 2970. [10]
- ZBROZEK, J. K. (1960). The Relationship between the Discrete Gust and Power Spectra Presentations of Atmospheric Turbulence, with a Suggested Model of Low-Altitude Turbulence. A.R.C. R. and M. 3216. [9]
- ZBROZEK, J. K. and RIDLAND, D. M. (1960a). A Measured Power Spectrum of the Vertical Component of Atmospheric Turbulence. A.R.C. C.P.522. [2]

**UNCLASSIFIED**

**UNCLASSIFIED**